Investigating the mitochondrial stress response specific to human dopaminergic neurons : insights into Parkinson's Disease-associated alterations and contribution of long non-coding RNAs

Jana Heneine

Sorbonne Université

Ecole doctorale Cerveau-Cognition-Comportement (ED3C, ED n°158)

Equipe Physiopathologie moléculaire de la maladie de Parkinson

Institut du Cerveau (ICM)

CNRS UMR7225 / INSERM U 1127

Investigating the mitochondrial stress response specific to human dopaminergic neurons: insights into Parkinson's Disease-associated alterations and contribution of long non-coding RNAs

Par Jana HENEINE

Thèse de doctorat de Neurosciences

Co-dirigée par Philippe RAVASSARD et Hélène CHEVAL

Présentée et soutenue publiquement le 20 décembre 2023

Devant un jury composé de :

Mme. Ildem AKERMAN	Maître de Conférence, University of Birmingham	Rapporteur
Mme. Wiep SCHEPER	Maître de Conférence, Vrije Universiteit Amsterdam	Rapporteur
Mme Solange DESAGHER	Directrice de Recherche, CNRS, Institut de Génétique de Montpellier	Examinatrice
Mr Sebastien GAUMER	Professeur des Universités, UVSQ,	Examinateur
Mr Peter VANHOUTTE	Directeur de Recherche, CNRS, IBPS	Président du jury
Mme Hélène CHEVAL	Maître de Conférence, Sorbonne Université	Co-encadrante
Mr Philippe RAVASSARD	Chargé de Recherche, CNRS, ICM	Directeur de thèse

Acknowledgments / Remerciements

First of all, I would like to thank Dr. Ildem Akerman, Dr. Wiep Scheper, Dr. Solange Desagher, Dr. Sebastien Gaumer and Dr. Peter Vanhoutte to have accepted to be part of the jury for this thesis and for giving me invaluable feedback. In particular, thank you to the *rapporteurs* Dr. Akerman and Dr. Scheper who took the time to thoroughly read and evaluate my manuscript.

Je voudrais également remercier Madame Desagher et Monsieur Clément Carré pour avoir accepter de faire partie de mon Comité de Suivi de Thèse et pour tous les échanges instructifs tout au long de cette thèse.

Un grand merci à Philippe et Hélène de m'avoir fait confiance pour porter ce projet. J'ai énormément appris d'avoir travaillé avec vous et je ne vous remercierais jamais assez pour votre soutien et votre implication dans ce travail de thèse. Vous m'avez transmis votre enthousiasme pour la recherche, encouragé à participer à des congrès et permis de développer mon esprit scientifique et critique dans un environnement bienveillant. Philippe, je voudrais te remercier pour ton humanité, ta bonne humeur et tes conseils tout au long. Hélène merci pour ta bienveillance, ton humour, ta rigueur et bien entendu ta patience (je sais que ce n'était pas toujours facile). Merci aussi d'avoir toujours été disponible et d'avoir su me rassurer quand tu voyais clairement que le stress montait. J'ai eu une grande chance d'avoir pu réaliser cette thèse sous votre direction !

Je suis reconnaissante à Olga Corti et Jean Christophe-Corvol de m'avoir accueillie dans l'équipe MPP et pour tous les échanges et conseils enrichissants pendant ma thèse.

Je voudrais remercier Claire d'avoir été ma binôme sur ce projet tout au long de ces cinq dernières années ! Un grand merci pour ton amitié, ta disponibilité et ta bienveillance depuis mon arrivée dans l'équipe. J'ai eu beaucoup de chance d'avoir partagé ce projet avec toi : les moments compliqués et les frustration quotidiennes (l'enfer des cinétiques de stress, cellules qui meurent inexplicablement, Western Blot illisibles etc.), mais surtout les bons moments et les réussites qui ont marqués cette aventure ! J'en garderai un très bon souvenir ; merci pour tout.

Ben, thank you so much for your friendship! I will truly miss our coffee breaks or lunchtime at the cantine talking about music, much better food than what we were having and restaurants we needed to try. But I have no doubt we'll just go have that great food instead now! I'm also grateful for your guidance with experiments and data analysis – you've always made yourself available to help when I came to your desk looking lost. I hope you won't miss too much finding my possessions scattered all over the lab!

Clément, merci pour ton humour, ta joie de vivre et pour tous les pains aux chocolat et desserts tout au long de ma thèse ! Tu auras fortement contribué à mon addiction au sucre mais bon je ne me plains pas du tout. Un grand merci pour ton soutien pendant les bons et les moins bons moments. Tes playlists de culture cellulaire vont me manquer (merci d'avoir contribuer à me faire apprécier le rap français).

Noemi, merci pour ton soutien, ton amitié et ta compassion pendant les pauses café nécessaires à la survie des thésards ! C'était un vrai plaisir de parcourir toutes les étapes la de thèse en ta compagnie. Nous voilà enfin docteures !

Merci Corinne pour ta gentillesse et ta bienveillance tout au long. Je suis reconnaissante pour tout ton travail sur la partie iPS du projet.

Flora et Pat, merci pour votre amitié et vos encouragements depuis le début de ma thèse !

Merci à Helena, Pauline et Christiane pour votre amitié et soutien. J'ai été heureuse d'avoir participé à votre formation pendant vos premiers pas dans le labo et d'avoir pu vous voir vous épanouir dans votre travail et dans l'équipe. Je vous souhaite bon courage pour la suite de vos thèses !

Je suis sincèrement reconnaissante à tous les membres de l'équipe - ceux qui y sont toujours et ceux qui y sont passés - toutes les personnes que j'ai eu la chance de rencontrer et qui ont égayé cette thèse, trop nombreuses pour toutes les citer ! Chloé L, Mélanie, Adeline, Christelle, Ruiyi, Fanny, Louise-Laure, Suzanne, Morwena, Thomas, Linda, Ella, Cédric, Gabin, Spela, Chloé P, Aymeric L, Aymeric B, Armin, Evodie, Che, Nicole, Anh … Merci pour votre accueil chaleureux, votre sympathie et vos encouragements au quotidien ! Je n'aurais pu souhaiter faire partie d'une meilleure équipe pendant ma thèse.

Merci aussi à l'ensemble des personnes que j'ai rencontré à l'ICM, avec lesquelles j'ai travaillé ou non, mais qui ont certainement contribué à faire de cette expérience une aventure chaleureuse et enrichissante : David, Claire, Blandine, Clémentine, Marina, Dominic, Liriopé, Marion, Violetta, Elisa, Delphine, Agnès, Benjamin, Radhia, Marine et tant d'autres.

J'ai la chance d'être entourée d'amis incroyables que ce soit à Paris ou ailleurs. Je voudrais les remercier de tout mon cœur pour leur soutien et amour.

Merci à ma famille à laquelle je dois tout. Mes parents, mon frère et ma soeur m'ont toujours encouragé et soutenu dans toutes les aventures que j'entreprenais. C'est grâce à votre amour et soutien indéfectible que j'ai pu réaliser et conclure cette thèse ! Je suis très fière de vous et je mesure chaque jour la chance que j'ai.

Merci à Nour, ma plus grande « hype girl » ! Je te remercie sincèrement d'avoir toujours été empathique lorsque je venais te raconter qu'une expérience s'était mal passée, de m'avoir demandé comment se portaient mes cellules chaque semaine et de m'avoir envoyé des encouragements les lundis, jour des « grosses manips de stress ». Tu as beaucoup œuvré pour me décharger et me permettre de me concentrer sur cette thèse. Merci pour ta présence joyeuse, rassurante et caring. Hâte pour toutes nos aventures dans cet après-thèse !

Gaétan, thank you for so (too) many things! You've been an incredible supporter through it all, always encouraging me to go further but also reminding me that there was a life outside of the lab (which I often forgot)! You've known how to reassure me when I was down, and to share the joy in the ups – and I'm glad I got to share them with you. Thank you for sticking it out with me and for your patience when I struggled with decision making and planning time off because "what if I needed to be in the lab for an experiment". Can't wait for what's next!

Table of Contents

I. Introduction

1. Parkinson's Disease

1.1. The discovery of Parkinson's Disease

In 1817, the English surgeon James Parkinson published the monograph "An Essay on the Shaking Palsy" and medically described for the first time Parkinson's disease as a neurological disorder (Parkinson, 2002). He presented a small number of patients who exhibited a particular association of symptoms: resting tremor, slowness or sometimes absence of voluntary movements (bradykinesia/akinesia), as well as changes in posture and a festinating gait. However, he reported on "the senses and intellects" of these individuals as being "uninjured".

Fifty years later, at the Salpêtrière hospital, Jean-Martin Charcot described more thoroughly the progression of symptoms observed in patients, particularly the establishment and worsening of bradykinesia over a long period of time before rigidity ensued (Charcot, J.M., 1875). Charcot suggested the name "Parkinson's Disease" for the disease, noting that patients did not necessarily display tremor, thus dismissing the term "Shaking Palsy". A report on 80 patients by William Gowers, delineated important specifics about Parkinson's Disease demographics: he notably recognized that the disease was more prevalent in males (Gowers, 1888).

Anatomical knowledge of Parkinson's Disease (PD) came later, with Edouard Brissaud first associating *substantia nigra* (SN) damage to the disease (Brissaud, Edouard, 1985). He raised this hypothesis by reporting on a specific patient who presented a tumour that partly destroyed the *substantia nigra* and resulted in parkinsonian symptoms on the opposing side of the body. Subsequent work from Konstantin Trétiakoff confirmed this hypothesis by reporting depigmentation of patients' SN, which is now known to be caused by the loss of neuromelanin-containing dopaminergic (DA) neurons (Trétiakoff, 1919).

With the mid 1900s, came the discovery of dopamine as a neurotransmitter essential for motor control (Carlsson, Arvid, Lindqvist, Magit, and Magnusson, Tor, 1957). Not long after, dopamine deficits in both the SN and the striatum were reported in the brain of PD patients, attributing to dopamine its central role in the pathology (Ehringer and Hornykiewicz, 1960) (Ehringer, H. & Hornykiewicz, 1960; Sano, 1960). This precipitated the inception of the first human trials using levodopa (L-DOPA), the natural

precursor of dopamine, to alleviate motor symptoms (Birkmayer and Hornykiewicz 1961, Barbeau 1969; Cotziaset *al.,* 1969; Yahr et al. 1969). Since these initial discoveries, PD research has been progressing rapidly. Nevertheless, our understanding of the disease mechanisms remains limited, and no cure has been found to this day.

1.2. Epidemiology

Parkinson's disease is the second most common neurodegenerative disease, after Alzheimer's disease, and the most common neurodegenerative movement disorder worldwide (Tolosa *et al.*, 2021). More than 10 million people worldwide are affected by Parkinson's Disease (PD), with nearly 1 million diagnosed patients in the United States (Parkinson's Foundation. <parkinson.org>) and more than 200 000 patients in France (Association France Parkinson. at <franceparkinson.fr>). Estimated incidence rates stand at 5 to 346 per 100,000 person/year worldwide (von Campenhausen *et al.*, 2005). PD is a progressive disorder; however, the rate of symptom worsening is variable between individuals and predictions are difficult to make (Armstrong and Okun, 2020). Reduced life expectancy is reported by several studies for PD patients (Driver *et al.*, 2008; Macleod, Taylor and Counsell, 2014; Bäckström *et al.*, 2018) and mortality is strongly correlated with severity of PD symptoms (Forsaa *et al.*, 2010). Causes of death are overall strongly influenced by the disease and common ones include aspiration pneumonia and hip fracture-related complications (Bloem, Okun and Klein, 2021).

1.3. Diagnostic criteria

Parkinson's Disease diagnosis relies on the patient's medical history as well as physical examination (Armstrong and Okun, 2020). Clinically, the patient will be inspected for bradykinesia with resting tremors and/or rigidity (Postuma *et al.*, 2015). Individuals also need to present 2 of the 4 following criteria: (1) rest tremor, (2) good response to dopaminergic replacement therapy such as levodopa, (3) dyskinesia (4) either olfactory loss or cardiac sympathetic denervation on iodine-123-meta-iodobenzylguanidine myocardial scintigraphy (imaging test that investigates decreased function of post-ganglionic sympathetic neurons) (Postuma *et al.*, 2015). A

list of symptoms are checked for in a patient's medical history such as gait changes, decreased facial expression, slowness as well as depression and/or anxiety (Postuma *et al.*, 2015). If a diagnosis is unclear, dopamine transporter single-photon emission computed tomography imaging and magnetic resonance imaging (MRI) may be harnessed to aid in differentiating Parkinson's disease from other parkinsonian syndromes (Armstrong and Okun, 2020).

1.4. Main risk factors

The most important risk factor for PD is ageing: incidence is reported to grow rapidly with age and to peak at about 80 years of age in most studies (Ascherio and Schwarzschild, 2016). Due to the ageing of the global population, the number of diagnosed PD cases is expected to increase dramatically in the next years (Bloem, Okun and Klein, 2021). Nevertheless, the disease does not exclusively affect older people with around 25% of patients presenting an age of onset younger than 65 and 5-10% younger than 50 (Pringsheim *et al.*, 2014). Men present a moderately increased risk for PD with women exhibiting lower prevalence: notably at ages 50 to 59, PD prevalence was of 134 per 100 000 for males and 41 per 100 000 for females worldwide (Pringsheim *et al.*, 2014; Elbaz *et al.*, 2016). Additionally, biological sex appears to influence the clinical presentation of PD (Gillies *et al.*, 2014). Differences between sexes in the risk of developing distinct PD non-motor symptoms have been reported: for example, men seem at greater risk for cognitive decline, whereas women are more likely to report urinary dysfunctions and depression (Nicoletti *et al.*, 2017). These sex-related differences are still largely understudied, and women remain under-represented in PD trials (Tosserams *et al.*, 2018). This is of particular importance as reports show less frequent and delayed access to medical professionals and specialized care for women with PD, who are therefore more prone to be undertreated (Nicoletti *et al.*, 2017).

1.5. Symptomatology of Parkinson's Disease

1.5.1. Motor symptoms

Parkinson's disease is a progressive movement disorder and is characterized by the following cardinal symptoms: tremor at rest, slowness in the initiation or execution of movements (bradykinesia), and rigidity (Armstrong and Okun, 2020). These symptoms are usually asymmetric and are accompanied by postural and gait instability (Balestrino and Schapira, 2020). As the disease progresses, these motor disturbances worsen causing increasing disability, impairment in daily activities, depression, fatigue and reduced quality of life, (Tolosa *et al.*, 2021). Presentation and deterioration rate of these motor features are rather heterogeneous between patients, which induced the notion of PD subtypes (Balestrino and Schapira, 2020). PD heterogeneity and subtypes will be discussed further in part 1.5.3.

1.5.2. Non-motor symptoms and the prodromal phase of PD

Over the years, it has become increasingly clear that non-motor symptoms (NMS) are a key component of PD, and are present in virtually all patients (Schapira, Chaudhuri and Jenner, 2017). A variety of NMS has been reported in PD patients ranging from urinary dysfunction, constipation, depression, hyposmia (loss of smell), rapid eye movement (REM) sleep behavior disorder (RBD), memory loss and hallucinations.

Some NMS precede the onset of motor symptoms during what is called the prodromal phase of the disease (Tolosa *et al.*, 2021). This period varies in length in different individuals and the sequence of symptom appearance is variable. Most commonly, hyposmia, RBD, depression and constipation tend to manifest in the prodromal phase of the disease and can precede motor symptoms and PD diagnosis by several years (Figure 1). As evidence for the occurrence of NMS prior to motor symptoms accumulated, studies began focusing on these abnormalities as potential biomarkers for the disease or as indicators of at higher risk individuals (Schapira, Chaudhuri and Jenner, 2017). RBD is particularly associated with an increased risk of subsequent PD diagnosis: 90% of RBD patients are estimated to subsequently

develop a neurodegenerative disease, most commonly Parkinson's disease (43%) and Dementia with Lewy Bodies (25%) (Galbiati *et al.*, 2019).

As the disease advances into its motor stage, more NMS appear, with cognitive and autonomic functions typically declining with disease progression. In the later stages of the disease, these symptoms overtake the clinical picture with patients exhibiting dementia, hypophonia (weaker speech intensity), declining cognitive functions, incontinence, and sexual dysfunction. These NMS gradually become the main cause for deteriorating quality of life and increased cost of care (Barone, Erro and Picillo, 2017). Notably, cognitive impairment and hallucinations frequently account for hospitalization in advanced PD (Safarpour *et al.*, 2015).

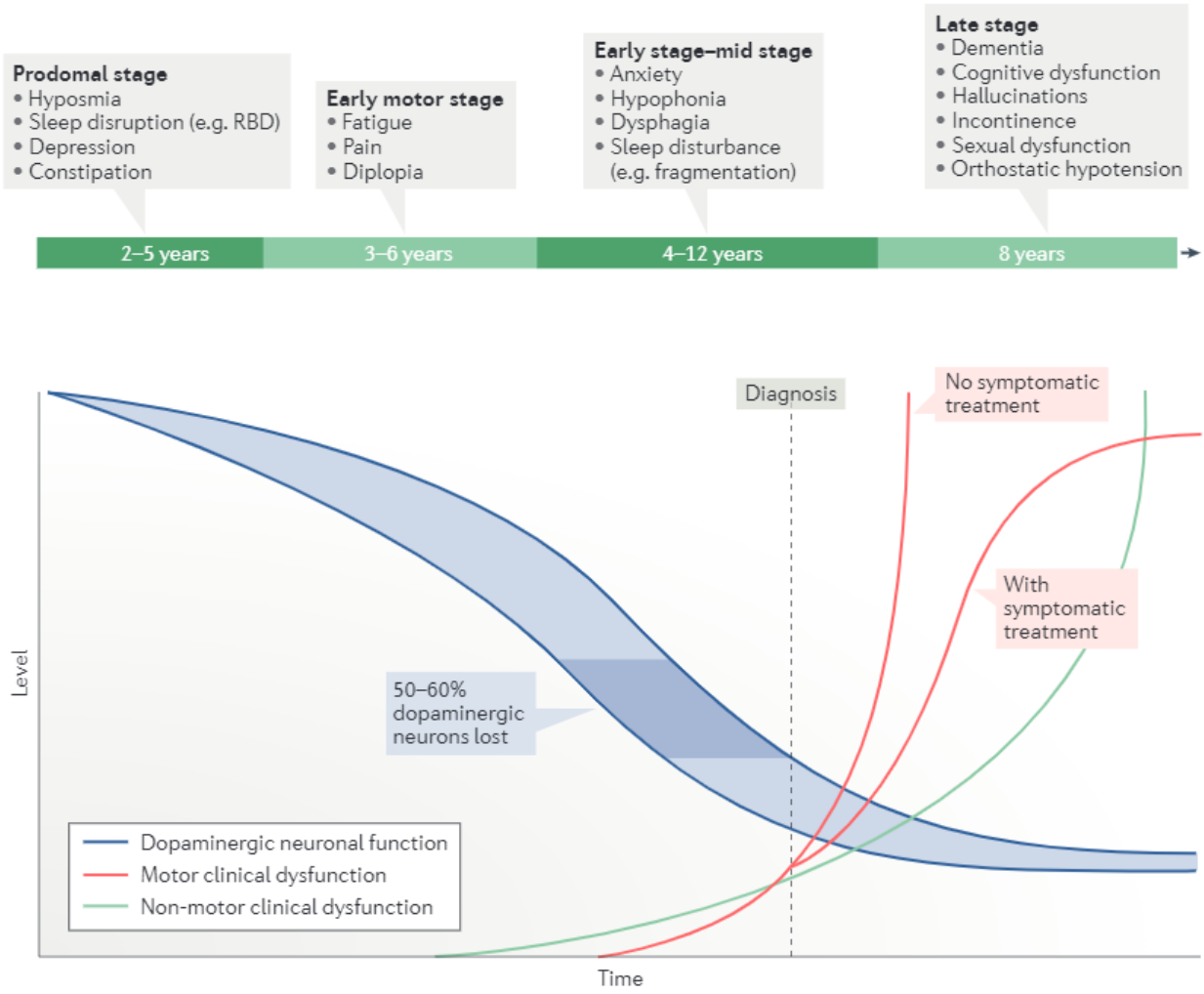

Figure 1. Time courses of the onset of the clinical symptoms of PD *(adapted from Schapira, Chaudhuri, Jenner, 2017). Potential timeline by which the motor and non-motor symptoms of PD may appear.*

1.5.3. Heterogeneity in Parkinson's disease

The significant heterogeneity in age of onset, clinical symptoms and disease progression in PD has become well established (Armstrong and Okun, 2020). This expectedly indicates differences in pathogenic mechanisms and explains discrepancies in treatment responses (Fereshtehnejad *et al.*, 2017). Furthermore, the ever-advancing study of familial forms of PD have revealed that they can differ from classic clinical PD (Tolosa *et al.*, 2021). Consequently, the notion of PD sub-entities has become widely accepted and there has been growing interest in defining these subtypes to improve diagnosis and treatment. First attempts at subtyping PD focused solely on motor symptoms (Thenganatt and Jankovic, 2014). However, recent categorizations propose to integrate both motor and non-motor features of the disease (Fereshtehnejad *et al.*, 2017; Lawton *et al.*, 2018; De Pablo-Fernández *et al.*, 2019).

Parkinson Disease subtypes	Estimated frequency	Clinical presentation	Response of motor symptoms to dopaminergic medication	Disease Progression
Mild motor predominant	49-53%	• Young onset • Mild motor symptoms	Good	Slow
Intermediate	35-39%	• Intermediate age of onset • Moderate motor symptoms • Moderate non-motor symptoms	Moderate to good	Moderate
Diffuse malignant	9-16%	• Variable age of onset • RBD • Mild cognitive impairment • Orthostatic hypotension • Severe motor symptoms • Early gait problems	Resistant	Rapid

Table 1. Proposed Parkinson Disease Subtypes *(adapted from Armstrong and Okun, 2020). Characteristics of commonly proposed PD subtypes based on motor and non-motor symptoms.*

Although a consensus for subtyping has yet to be reached, a prevalent approach distinguishes three groups (Figure 2): mild motor predominant, intermediate, and diffuse malignant PD forms. Mild motor predominant PD is characterized by young onset, usually below ages of 40-50 years, by predominance of rest tremor over other motor symptoms, slower disease progression as well as preserved cognition (Armstrong and Okun, 2020; Tolosa *et al.*, 2021). Younger patients tend to benefit

more dramatically from dopaminergic replacement therapy but consequently, are more at risk to develop motor fluctuations and dyskinesia (Berg *et al.*, 2021). Diffuse malignant PD presents baseline motor symptoms with prominent postural instability and gait disturbances (PIGD) as well as a range of NMS including RBD and mild cognitive impairment (Armstrong and Okun, 2020). Patients exhibit rapid decline of motor function as well as cognition (Simuni *et al.*, 2016). Intermediate forms of PD tend to fall in between the two other subtypes with intermediate age of onset, moderate motor and non-motor symptoms as well as moderate disease progression (Armstrong and Okun, 2020).

As our understanding of the diverse presentations of PD grows, the hope is that diagnosis will become clearer and that counseling will adapt to each individual relating to symptom diversity, disease course and treatment response.

1.6. Etiology: Parkinson's disease as a multifactorial pathology

1.6.1. Genetic factors

PD was long considered to be a sporadic disorder with non-genetic origins. However, 15% of PD cases present family history (15%) and 5-10% are monogenic forms of the disease, following classical Mendelian inheritance patterns (Lesage and Brice, 2009). *SNCA*, encoding α-synuclein, was the first gene to be associated to PD as mutations were reported in a large Italian family and three unrelated families in the nineties (Polymeropoulos *et al.*, 1997). Since then, at least twenty genes were discovered as causes of familial PD (Tolosa *et al.*, 2021). Out of those genes, research appears to have focused more intently on autosomal dominant PD caused by *SNCA*, *LRRK2* and *VPS35*, as well as with autosomal recessive PD caused by *PINK1*, *PRKN* and *DJ-1* (Table 2; Bandres-Ciga *et al.*, 2020). These known monogenic loci, although highly penetrant, only account for 5-10% of cases (Jia, Fellner and Kumar, 2022). However, through genome wide association studies (GWAS), over 90 PD-associated risk loci have been identified (Figure 2; Nalls *et al.*, 2019; Pan *et al.*, 2023). The most robust of those associations were found with *SNCA*, *GBA*, *LRRK2* and *MAPT* (Kalinderi, Bostantjopoulou and Fidani, 2016).

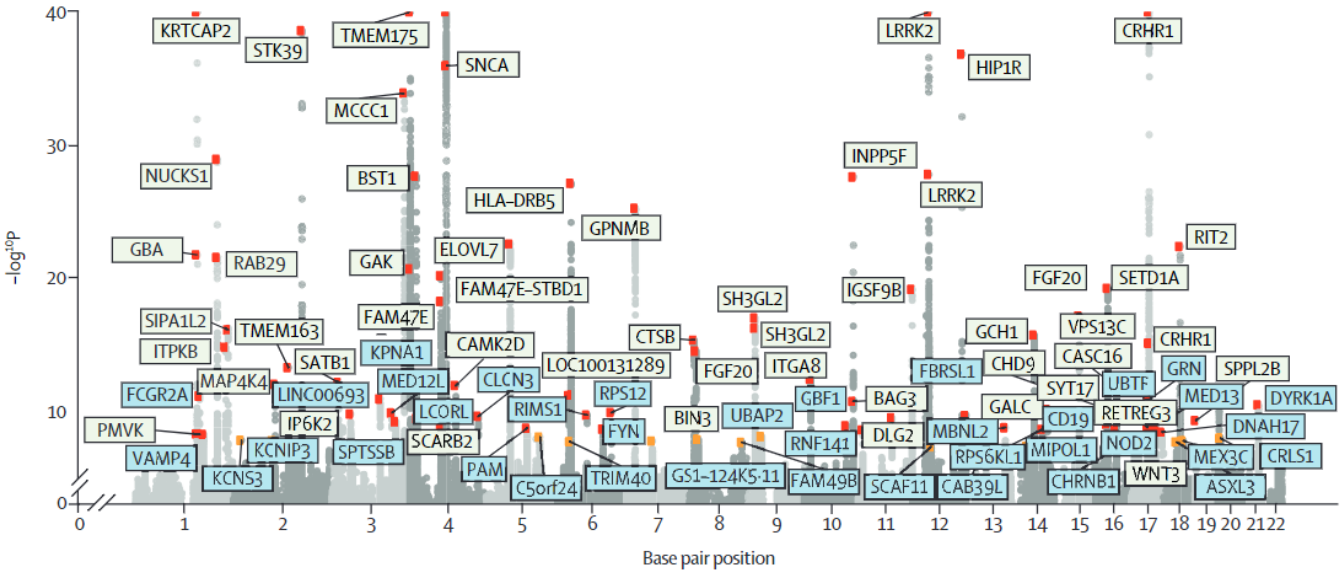

Figure 2. Manhattan plot of significant variant associated with PD and the nearest gene to these variants. *Genes labelled in green are previously identified loci and in blue are novel loci identified by Nalls et al., 2019. –log10 p values were capped at 40. Variant points are color-coded red and orange: orange corresponds to significant variants at p=5×10^{-8} and 5×10^{-9} and red to significant variants at p<5×10–9. The X axis represents the base pair position of variants from smallest to largest per chromosome (1–22), only autosomes were included in this analysis. (Adapted from Nalls et al., 2019)*

Heterogeneity in disease progression, symptoms and age of onset has been reported when comparing familial forms of the disease to sporadic ones and should be taken into account at diagnosis (Table 2). Monogenic PD is usually distinguished by a younger age of onset, particularly below 40 years of age (Berardelli *et al.*, 2013). Furthermore, depending on the disease-causing mutated gene, patients present an important phenotypic diversity. For example, people with *PRKN* and *PINK1* mutations, exhibit a slow progression despite young onset, making early diagnosis difficult (Bloem, Okun and Klein, 2021). These forms of the disease are commonly accompanied by dystonia but rarely dementia. On the other hand, *SNCA* and *GBA*-associated PD are characterized by rapid disease progression and severe cognitive symptoms (Ryan *et al.*, 2019; Tolosa *et al.*, 2021).

Associated gene	Pathogenic mutation(s)	Onset age	Symptom particularities in comparison to sporadic cases	Progression	Frequency
Autosomal Dominant Subtypes					
SNCA (PARK1, PARK4)	Missense (PARK1) Dup/triplication (PARK4)	Early onset	Prominent NMS and early dementia	Rapid	<1%
LRRK2 (PARK8)	Missense	Late onset	Less RBD than seen in classical PD	Slow	1-5% (up to 40% in North African Berber Arab patients)
VPS35 (PARK17)	Missense	Late onset		Slow	<1%
Autosomal Recessive Subtypes					
PARKIN (PARK2)	Missense, loss-of-function, exonic duplication, deletion	Early onset	Common dystonia at onset and frequent dyskinesia	Slow	1-5% (44% of EOPD)
PINK1 (PARK6)	Missense, loss-of-function, exonic duplication, deletion	Early onset	Common dystonia at onset and frequent dyskinesia + common psychiatric symptoms	Slow	2-5%
DJ1 (PARK7)	Missense, loss-of-function, small duplication/deletions	Early onset	Common dystonia at onset and frequent dyskinesia + common psychiatric symptoms	Slow	1%
High-risk gene					
GBA	Missense, loss-of-function, small duplication/deletions	Early onset	Greater dementia risk	Rapid	5-25% of PD patients

Table 2. Most studied genes associated with familial forms of Parkinson's Disease and their characteristics. *EOPD: Early-Onset Parkinson's Disease; PD: Parkinson's Disease, NMS: non-motor symptoms; RBD: Rapid eye movement sleep behavior disorder. (Adapted from Balestrino and Schapira 2020; Tolosa et al., 2021).*

1.6.2. Environmental and behavioral factors

The majority of PD cases appear to be sporadic with unknown etiology. PD appears to be a multifactorial disease with a combination of genetic and environmental risk factors likely to play important roles in causing the disease (Brissaud, Edouard, 1985). Although the "environmentome" – the ensemble of potentially protective or causative environmental factors of an individual – is currently much more complicated

to access and investigate than an individual's genome, several such factors were associated with an altered PD risk.

As previously noted, the biggest risk factor for PD is age, however, the increasingly ageing population does not fully explain the growing number of PD patients in the past few years. Between 1990 and 2016, global age-standardized prevalence rates increased by 21.7% (Dorsey, Elbaz, *et al.*, 2018). It is important to consider that higher prevalence may be partly due to the increasing availability of higher quality studies, better diagnosis awareness, as well as rising life expectancy, which likely contributes to longer disease duration. Nevertheless, robust evidence emerging from epidemiological studies show a significant role for behavioral and environmental factors in disease pathogenesis.

Interestingly, the growing industrialization of the world is suggested to play a role in the increased PD burden. Whilst better health is usually positively associated with socioeconomic level (GBD 2015 SDG Collaborators, 2015), the opposite seems to be true regarding PD with socio-demographic index (Savica *et al.*, 2016). Although the reason for this remains unclear, it is thought to be linked to industrialization consequences, including increased exposure to pesticides, solvents or metals (Pezzoli and Cereda, 2013; Dorsey, Sherer, *et al.*, 2018). For example, case-control studies found approximately a two-fold increase in PD risk associated with exposure to paraquat or maneb/mancozeb (Pezzoli and Cereda, 2013).

Traumatic brain injury (TBI) has also been linked to increased PD risk, most likely due to it possibly causing long-term brain inflammation, mitochondrial dysfunction, increased glutamate release and α-synuclein aggregation in the brain (Marras *et al.*, 2014; Ascherio and Schwarzschild, 2016; Delic *et al.*, 2020). This increased risk was suggested to occur soon after the traumatic brain injury, within 3 to 12 months post-injury, and to diminish over time (Rugbjerg *et al.*, 2008) and even dissipate past 10 years (Fang *et al.*, 2012). However, this is believed to be, at least partially, due to PD symptoms starting years earlier than the official PD diagnosis, with patients already displaying more frequent falls and head trauma (Ascherio and Schwarzschild, 2016). It is therefore difficult to establish whether there might truly be an increase in PD risk following TBI.

On the other hand, some environmental factors have been associated with lower PD risk, most notably tobacco, coffee consumption and the use of non-steroidal anti-inflammatory drugs (NSAIDs) (Ascherio and Schwarzschild, 2016). Several

studies have reported lower PD risk among tobacco smokers and users of smokeless tobacco, with a decreased risk of up to 70% correlated with an increasing duration of smoking (Chen *et al.*, 2010; Thacker *et al.*, 2007; O'Reilly *et al.*, 2005; Hernán *et al.*, 2001). Interestingly, in people who have stopped smoking, the lowered PD risk increases again with time since quitting (Chen *et al.*, 2010). Although criticism has been raised relating to confounding by known PD risk factors and genetic factors, this effect appears confirmed in monozygotic twin studies in which an inverse association between smoking and PD was found (Wirdefeldt *et al.*, 2005; Tanner *et al.*, 2002). One hypothesis to account for this is that there may be a lower nicotine responsiveness in the PD prodromal phase, which may explain why patients diagnosed with PD are less likely to smoke (Ritz *et al.*, 2014). This may mean that the neuroprotective effect of smoking seen in epidemiologic studies is mainly due to reverse causation.

Caffeine consumption was associated with a lower PD risk in several cohorts comparing coffee drinkers to non-coffee drinkers, with some studies showing a more robust effect observed in men than in women, possibly due to interactions between caffeine and postmenopausal hormones (Hu, Gang *et al.*, 2007; Liu *et al.*, 2012). Longitudinal studies have also reported this inverse association between coffee and PD risk. For example, in Finland the relative risk was of 0.40 for individuals consuming 5 cups of coffee per day or more vs. non-drinkers. Relative risk was of 0.26 for individuals drinking 10 or more cups per day vs. non-drinkers (Sääksjärvi *et al.*, 2008; Kachroo, Irizarry and Schwarzschild, 2010). Furthermore, the neuroprotective effect of caffeine has been well studied in mice PD experimental models (Xu *et al.*, 2010; Ascherio and Schwarzschild, 2016). For example, caffeine reduced the dopaminergic neuronal loss induced by chronic exposure to both paraquat and maneb by about 85% (Kachroo, Irizarry and Schwarzschild, 2010). This effect is believed to be due to caffeine's role as an adenosine receptor antagonist and to be mediated by the blockade of adenosine A_{2A}. The evidence for caffeine consumption being neuroprotective is compelling, especially given its well-established safety profile, however, uncertainty remains regarding possible sex-hormone interactions, dose response and the contribution of other coffee components.

Regular users of NSAIDs (≥ 2 times/week) were shown to have a 45% lower PD risk in comparison to non-users in a first prospective study harnessing the Nurses' Health Study and HPFS cohorts (Chen *et al.*, 2003). Later on, this lower PD risk was confirmed by other studies in ibuprofen users specifically but not other NSAIDs, with a

27% reduction in PD risk associated to regular ibuprofen use (Bower *et al.*, 2006; Hernán, Logroscino and García Rodríguez, 2006; Ton *et al.*, 2006; Gao *et al.*, 2011). NSAIDs's anti-inflammatory effect is believed to suppress the important glial response observed in PD, which is thought to participate in the propagation of neurodegeneration (Hirsch and Hunot, 2009; Hirsch, Vyas and Hunot, 2012). However, the correlation between NSAIDs use and lower PD risk is contested as other studies have found no association between NSAIDS and even ibuprofen with PD risk (Ren *et al.*, 2018).

1.7. Pathological hallmarks of Parkinson's Disease

1.7.1. Massive and selective death of dopaminergic neurons

PD is characterized by the massive, selective, and progressive loss of the dopaminergic (DA) neurons of the *substantia nigra pars compacta* (*SNpc*) that innervate the basal ganglia (Figure 3A; Hornykiewicz, 2002; Hall *et al.*, 2014). The loss of these neurons and their projections to the striatum is thought to induce the core motor features of the disease. Dopamine from the *SNpc* acts on two types of striatal GABAergic output neurons termed medium spiny neurons (MSN) that are differentiated by their projection targets (Figure 3B; McGregor and Nelson, 2019):

(1) Direct pathway MSNs (dMSNs) project directly to the basal ganglia output nuclei, the *globus pallidus pars interna* (GPi) and the *substantia nigra pars reticulata* (SNpr) and express G-coupled D1-like dopamine receptors. DMSNs reduce the basal ganglia output (GPi/SNpr), thus alleviating its inhibition of the thalamus and stimulating movement.

(2) Indirect pathway MSNs (iMSNs) project to the basal ganglia output through the globus pallidus pars externa (GPe) and subthalamic nucleus (STN) glutamatergic neurons. They express G-coupled D2-like dopamine receptors and are thus believed to promote basal ganglia output, which inhibits the thalamus and suppresses movement.

The SNpc dopamine regulates those two MSN populations but in opposing ways: it stimulates dMSN activity and represses iMSN activity. Dopamine production thus has the overall effect of promoting movement by inhibiting the GPi and SNpr. In PD, the

loss of SNpc dopamine-producing neurons and consequent depletion of striatal dopamine results in an imbalanced activity of the direct and indirect MSN pathways. Indeed, lack of dopamine increases iMSN activity and suppresses dMSNs leading to greater basal ganglia output, inhibition of the thalamus and motor cortex and suppression of movement (McGregor and Nelson, 2019). Recent studies report that, in early stages of the disease, these pathological alterations are partly compensated by changes in the activity of brain areas that are initially unaffected by PD, such as cortical regions less dependent on the basal ganglia (Michely *et al.*, 2015).

At PD diagnosis, which usually equates to early symptomatic stages of the disease, patient already display loss of 40-60% of DA neurons and up to 80% decline of synaptic function (Mahlknecht, Seppi and Poewe, 2015). This suggests that pathological mechanisms are initiated long before the occurrence of classical motor symptoms and that this prodromal phase of the disease is particularly relevant in the development of disease-modifying treatments.

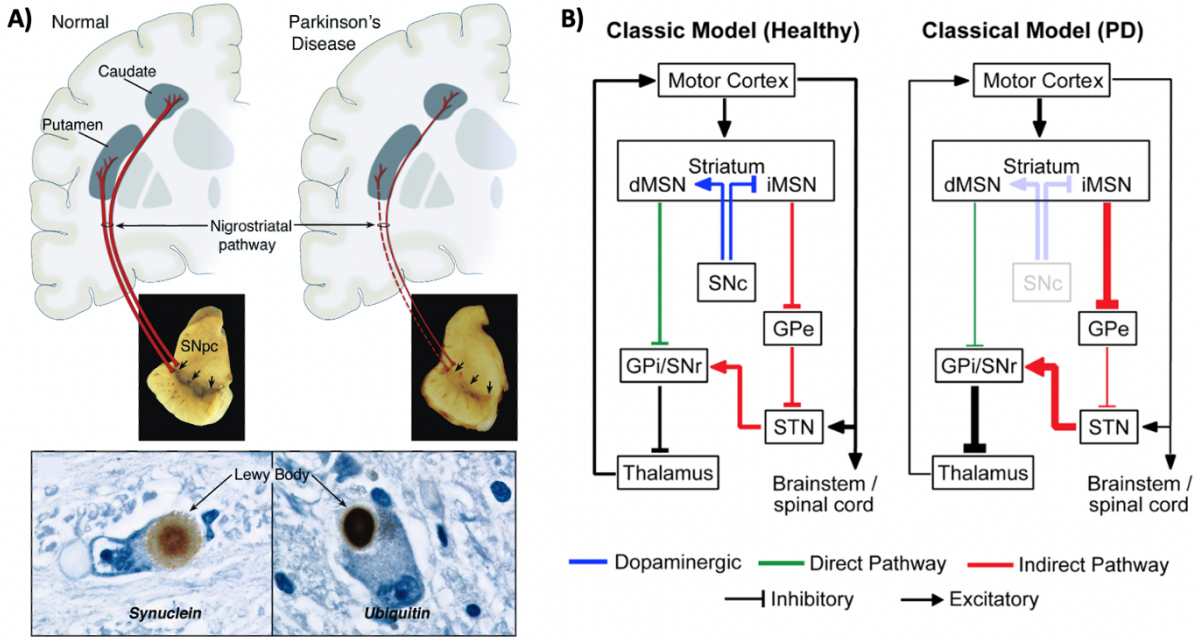

Figure 3. (A) Neuropathology of Parkinson's Disease. *Neuromelanin-expressing dopaminergic neurons of the Substantia Nigra pars compacta (SNpc) that innervate the nigrostriatal pathway are lost in Parkinson's Disease. PD is also characterized by intraneuronal proteinaceous inclusions composed primarily of α-synuclein and called Lewy Bodies (Adapted from Dauer and Przedborski, 2003)* ***(B) Dysfunctions of the basal ganglia circuitry in PD.*** *In a healthy individual (left), dopamine (blueà from the SNc to the striatum activates the direct pathway (green) and inhibits the indirect pathway (red) MSNs. This releases inhibition on the thalamus and cortex and promotes movement. In the PD model (right), loss of SNc dopamine induces hypoactivity of the direct pathway and hyperactivity of the indirect pathway. Consequently, the thalamus and cortex are over-inhibited and movement is suppressed (Adapted and Nelson, 2019)*

1.7.2. Lewy Body pathology

The second neuropathological hallmark of PD is Lewy Body (LB) depositions (Figure 3A). They are intraneuronal proteinaceous and lipid-rich inclusions mainly composed of α-synuclein aggregates (Spillantini *et al.*, 1998). α-synuclein is a presynaptic protein that is abundantly expressed in the brain and is linked to synaptic vesicle trafficking (Maroteaux, Campanelli and Scheller, 1988; George *et al.*, 1995; Iwai *et al.*, 1995; Carnazza *et al.*, 2022). It was discovered to have the propensity to misfold, driven by its hydrophobic central sequence to form insoluble beta-sheet-rich amyloid-like aggregates (Spillantini *et al.*, 1998; Giasson *et al.*, 2001). Proteomic studies have revealed a complex composition for LB with over 300 proteins identified, including α-synuclein-associated proteins and protein implicated in the ubiquitin-proteasome system, responsible for degrading the majority of misfolded or defective cellular proteins (Wakabayashi *et al.*, 2013). Recent advances in correlative light electron microscopy, revealed that a complex mixture of aggregated forms of α-synuclein makes up LB in PD post-mortem brains, in addition to crowding of fragmented organellar and membranous components, including from lysosomes and mitochondria (Shahmoradian *et al.*, 2019). Lewy Bodies are primarily found in the brainstem, cortex and autonomic nervous system in post-mortem brain tissue of Parkinson's disease patients (Tofaris, Goedert and Spillantini, 2017). Interestingly, patterns of LB pathology are linked to distinct diseases called synucleinopathies; for example, LB in oligodendrocytes is the pathological characteristic of Multiple System Atrophy (Spillantini *et al.*, 1998; Tofaris, 2022).

In the early 2000s, Braak and colleagues proposed a sequential model of LB formation and α-synuclein deposition that is, to this day, commonly used as a reference to understand PD (Braak *et al.*, 2003, 2004). This model suggests that the synucleinopathy initiates in the peripheral nervous system (PNS) and gradually gains access to the central nervous system (CNS) through a nasal or gastric route. It also hypothesizes that the aggregates spread between neurons trans-synaptically in a "prion-like" manner. This is in accordance with findings that patients who received transplants of embryonic mesencephalic neurons in their putamen developed Lewy body inclusions in these grafted cells (Kordower *et al.*, 2008; Li *et al.*, 2008). Although the pattern of spreading proposed corresponds well to the onset of different symptoms

during the progression of the disease, this staging system has many limitations as it was reported that only half of PD patients exhibit a matching synucleinopathy pattern (Surmeier, Obeso and Halliday, 2017). Additionally, LB is not systemically present in patients' brains and can be present in healthy individuals' brains, leading to extensive debate regarding the pathogenic role of LB in PD, which will be discussed in part 1.8.1 (Markesbery *et al.*, 2009). Nevertheless, Lewy Body depositions constitute one of the characteristic neuropathological features of PD at post-mortem.

1.7.3. Pathology in other cell types

Accumulating evidence now show that biological alterations due to Parkinson's Disease are not limited to the degeneration of SN DA neurons and the deposition of Lewy Bodies. As mentioned before, LB depositions are found in various part of the brain and not just SN-DA neurons (Braak *et al.*, 2003). Furthermore, it is important to note that more moderate cellular loss has also been reported in other brain regions, although stereological counting data and large sample sizes are lacking (Giguère, Burke Nanni and Trudeau, 2018).

Changes in the cholinergic system have been described in PD. A few studies have reported a 41% average loss of the pedunculopontine nucleus cholinergic neurons, although sample sizes remained small and the death count range was large (Rinne *et al.*, 2008; Karachi *et al.*, 2010; Hepp *et al.*, 2013). Cholinergic neuronal loss was also reported in the dorsal motor nucleus of the vagus with, for instance, 55% cell death reported in 8 patients (5 to 24 years post-diagnosis), exhibiting correlation with disease severity and duration (Gai *et al.*, 1992). Alterations in the nucleus basalis of Meynert were also described by several studies, although the average percentage of cholinergic neuronal loss varied greatly, with up to 72% average cellular death observed (Giguère, Burke Nanni and Trudeau, 2018). Cholinergic neuronal loss, especially Meynert degeneration, was positively correlated by several longitudinal studies with mild cognitive impairment in PD (Schulz *et al.*, 2018; Rong *et al.*, 2021; Wilson, de Natale and Politis, 2021). It was also more prevalent in non-tremor dominant PD subtypes (Karachi *et al.*, 2010).

Overall dopamine levels appear to be decreased by 70-90% in PD patients, particularly in the putamen which exhibited a 98% reduction (Kish, Shannak and Hornykiewicz, 1988; Hornykiewicz, 1998; Kish *et al.*, 2008). Reduced caudate

dopamine marker levels were also reported in PD patients and were associated with visual hallucinations (Kiferle *et al.*, 2014). Furthermore, DA neuronal loss is observed in the ventral tegmental area (VTA), with an average neuronal death in the 40% range that appears linked to disease duration (Damier *et al.*, 1999; Alberico, Cassell and Narayanan, 2015).

Regarding the noradrenergic system, changes in the neuronal population of the *locus coeruleus* have been reported and were even linked to disease duration in two studies (Gai *et al.*, 1991; Bertrand *et al.*, 1997). Examination of post-mortem brains revealed a 63% loss of *locus coeruleus* cells in PD brains (German *et al.*, 1992). Moreover, reduced noradrenaline levels were observed in the striatum and cortical areas (Scatton *et al.*, 1983; Ehringer and Hornykiewicz, 1998). Noradrenaline loss have been associated with depression, anxiety and apathy (Remy *et al.*, 2005).

Whether significant changes in the serotonergic system occur in PD remains debated. Notably, an overall decrease of about 60% in serotonin levels has been described in post-mortem PD brain tissue (Kish *et al.*, 2008). However, reports of changes in the raphe nuclei, source of brain serotonin, are inconsistent with both reduced and increased levels of serotonergic markers and neuronal population being reported in this region (Strecker *et al.*, 2011; Cheshire *et al.*, 2015; Politis and Niccolini, 2015; Qamhawi *et al.*, 2015). Nevertheless, lower serotonin levels have been linked to fatigue in PD (Pavese *et al.*, 2010).

These brain-wide effects observed in PD – other than in the SNpc – are insufficiently documented and lack stereological data. As briefly noted, dysfunctions of these other cell types are linked to a number of non-motor symptoms and even some PD subtypes. It is of great interest to better understand these changes, the symptoms associated to them, and to distinguish these symptoms from *SNpc* dopaminergic-specific ones, as this would lead towards a better understanding and treatment of the pathology.

1.8. Hypotheses surrounding Parkinson's Disease pathological origins

To this day, the pathogenic events causing PD neurodegeneration remain poorly understood, limiting research for disease-modifying treatments. Nevertheless, PD is known to be multifactorial with several cellular mechanisms having been implicated in the pathology (Przedborski, 2017).These processes somehow converge

over a long period of time to ultimately induce the selective loss of DA neurons seen in PD. Two generally held hypothesis regarding the pathological origins and chronology of events leading to the disease are discussed in what follows.

1.8.1. Lewy body pathology

As previously described, LB pathology is a neuropathological hallmark of PD (Henderson, Trojanowski and Lee, 2019). These intraneuronal inclusions are made up of a complex mixture of aggregated α-synuclein forms and of a large number of other proteins and lipids (Shahmoradian *et al.*, 2019). α-synuclein can self-assemble into oligomers and subsequently into amyloid-like fibrils that accumulate in PD (Burré, Sharma and Südhof, 2018). Accumulating evidence suggests that α-synuclein propagates in a prion-like manner whereby aggregates enter cells and promote misfolding and aggregation of soluble proteins, possibly originating in the olfactory bulb or the dorsal motor nucleus of vagus (DMV) and propagating to the SN (Braak *et al.*, 2004; Hawkes, Del Tredici and Braak, 2007; Iljina *et al.*, 2016). Therefore, it was postulated that LB depositions and spreading constituted the toxic component causing the loss of DA neurons and that the spreading of the pathology correlated with the severity of disease.

However, some recent observations are inconsistent with this hypothesis. First, the staging hypothesis was not based on longitudinal data but deduced from comparisons of the LB pathology found in the brains of PD patients and asymptomatic individuals, and association to the severity of the disease (Braak *et al.*, 2004). The asymptomatic individuals exhibiting LB depositions were considered to have not yet developed the disease, however, it is now known that LBs can be found in healthy individuals' brains and in a number of other neurological diseases such as Multiple System Atrophy and Lewy Body Dementia (Markesbery *et al.*, 2009; Dijkstra *et al.*, 2014). LB observed in *post-mortem* samples also did not systematically correlate with disease severity (Parkkinen, Pirttilä and Alafuzoff, 2008; Tofaris, 2022). Furthermore, LB pathology is not always found in regions displaying neuronal loss and can instead be present in areas that do not exhibit any cell death. For example, a study showed neuronal death in the supraoptic nucleus exhibiting no LB inclusions, and no neuronal death in the tuberomammillary nucleus of the hypothalamus displaying abundant LB (Ansorge, Daniel and Pearce, 1997). Moreover, at more biologically pertinent levels,

LB does not seem toxic, as LB can be present for years in some parts of the brains, notably the brainstem, without causing apparent cell death (Markesbery *et al.*, 2009; Surmeier, 2018). These findings challenge the relationship between LB pathology, DA neurodegeneration and PD symptoms.

It is now postulated that LB inclusions are only the tip of the "pathological iceberg" and that perhaps LB are not the toxic entity they were believed to be and are instead part of the end-stage process to dispose of large assemblies of aggregates (Alam *et al.*, 2019). On the other hand, α-synuclein aggregates, not in the form of LB inclusions, are found to be widespread especially in presynaptic neuronal terminals (Kramer and Schulz-Schaeffer, 2007; Burré, 2015). It is now suggested that the toxicity causing neurodegeneration stems from early stages of α-synuclein aggregation, although it is still unknown which forms are most central to the pathogenesis of PD and are damaging to cells (Tofaris, 2022). The kinetics of α-synuclein aggregation and subsequent fibrillization are currently under scrutiny to shed light over this matter. It is now known that a fibrillar aggregate grows by monomer addition, and needs to reach approximately 70 monomers before fibril formation (Sanchez *et al.*, 2021). Interestingly, studies have shown that the *in vitro* fibrillization kinetics of α-synuclein vary between different *SNCA* mutants but that there is common acceleration in the formation of non-fibrillar α-synuclein oligomers, suggesting that this stage is critical to the pathogenesis (Conway *et al.*, 2000; Cremades *et al.*, 2012; Iljina *et al.*, 2016). Indeed, oligomers and not fibrils seem to cause the most severe *substantia nigra* DA neuronal death in animal experiments using lentiviral expression of α-synuclein mutants inducing either oligomer or fibril formation (Winner *et al.*, 2011). However, fibrils seem to be the seeding-competent entity as injection of fibrils in animals drove aggregation and propagation but not injections of oligomers (Peelaerts *et al.*, 2015). It is therefore possible that the fibrils induce the spreading of the pathology and that the oligomers, formed during the increasing assembly of fibrils, are the main toxic species (Cremades *et al.*, 2012; Tofaris, 2022).

Further investigations are required to clarify which form of oligomers are the main toxic component of PD, whether the spreading is dependent on LB, and whether this is all also true in PD patients' brains. Moreover, other questions remain unanswered including: is α-synuclein aggregation and LB pathology in healthy subjects pre-symptomatic, and does it eventually lead to cellular death? Are SN DA neurons more

susceptible to LB pathology? Interestingly, autopsies of PD patients with early-onset genetic forms of PD, such as those associated with *PRKN mutations*, often exhibited DA neurodegeneration without Lewy Body pathology (Poulopoulos, Levy and Alcalay, 2012). Therefore, the exact role of α-synuclein pathology in PD pathogenesis remains widely debated.

1.8.2. Mitochondrial dysfunction as a central component to PD pathogenesis

A central hypothesis in PD research is that mitochondrial dysfunction is the central driver of DA neuronal loss in PD. Several lines of evidence have highlighted the significant role of mitochondria in PD pathogenesis. In the 1970s, individuals taking opioid analogs (MPPP) started displaying severe PD-like motor symptoms (Langston *et al.*, 1983). The drug contained impurities in the form of 1-methyl-4-phenyl-1,2,3,6-tetrahydropyridine (MPTP), a molecule able to cross the BBB where it is converted to the neurotoxic compound 1-methyl-4-phenylpyridinium (MPP+) (Langston *et al.*, 1984; Markey, S.P. *et al.*, 1984). The toxicity of MPP+ resulted in the selective degeneration of the SN DA neurons. This was quickly discovered to be due to the high affinity of the molecule to DA uptake sites, meaning that MPP+ would specifically accumulate within DA neurons (Shen *et al.*, 1985). There, MPP+ concentrated to the mitochondria and reached toxic levels that inhibited complex I of the mitochondrial respiratory chain, suggesting an important link between mitochondrial dysfunction and PD pathology (Ramsay *et al.*, 1986).

It was subsequently shown that the toxin MPP+ and other complex I inhibitors, such as the commonly used pesticide rotenone and the industrial solvent trichloroethylene, caused DA neuronal death in rodent models (Betarbet *et al.*, 2000) and human models (Gash *et al.*, 2008). Based on this, mitochondrial toxins including MPP+ and rotenone, were used to create PD animal models (Gamber, 2016). These models were harnessed to further our understanding of the disease mechanisms and were able to elicit DA neurodegeneration and some associated motor symptoms (Pingale and Gupta, 2020). However, these models remain flawed as they do not fully recapitulate the disease with the absence of LB pathology, the incomplete disease phenotype and even non-specific (rotenone) neurodegeneration.

Following the discovery of MPP+, researchers examined PD patients post-mortem brain tissues and revealed deficiencies in mitochondrial electron transport

chain complex I in SN DA neurons (Schapira *et al.*, 1990; Bindoff *et al.*, 1991). Patients' SN presented significant reduction in the activity of complex I's NADH-ubiquinone reductase denoting a selective deficiency of this complex. These mitochondrial functional deficits were interestingly also observed in other tissues such as platelets and skeletal muscles (Bindoff *et al.*, 1991; Krige *et al.*, 1992; Mann *et al.*, 1992; Taylor *et al.*, 1994). Additionally, significantly high levels of somatic point mutations and deletions in mitochondrial DNA (mtDNA), impacting the proper functioning of the mitochondrial respiratory chain, were reported in *SNpc* DA neurons of late-stage idiopathic PD patients compared to age-matched controls (Bender *et al.*, 2008; Lin *et al.*, 2012; Coxhead *et al.*, 2016). These observations suggest an important role for mitochondrial damage in PD.

Further evidence came through the study of familial monogenic forms of PD, specifically caused by loss-of-function mutations in the genes *PINK1* (*PARK6*) and *PRKN* (*PARK2*) (Kitada *et al.*, 1998; Valente *et al.*, 2004). These genes encode respectively the PTEN induced kinase 1 (PINK1) and the Parkin RBR E3 ubiquitin-protein ligase (PARKIN) that are essential for mitochondrial quality control processes (Quinn *et al.*, 2020). These proteins interact in a key mechanism for the clearance of dysfunctional mitochondria *via* lysosomal degradation, known as mitophagy, with *PINK1* acting upstream of Parkin, which will be described in part 2.2. (Corti, 2019). Mutations in both *PINK1* and *PRKN* were discovered to cause early-onset autosomal recessive forms of PD (Beilina and Cookson, 2016) These mutations impair the protective action of PINK1 and PARKIN and impede the elimination of malfunctioning mitochondria, which could be the cause of the DA neurodegeneration observed in the disease (Quinn *et al.*, 2020).

Other mutations in genes leading to dominant forms of PD have also been associated to mitochondrial dysfunction (Beilina and Cookson, 2016; Borsche *et al.*, 2021). This includes *LRRK2* mutations that were shown to induce increased mitochondrial fragmentations and mitophagy initiation in cortical neurons and in SH-SY5Y cells (Wang *et al.*, 2012; Cherra *et al.*, 2013; Grünewald *et al.*, 2014; Saez-Atienzar *et al.*, 2014; Grünewald, Kumar and Sue, 2019). *VP35* mutants were similarly shown to cause mitochondria hyper-fragmentation in primary DA neuronal and SH-SY5Y cultures, overexpression of mitochondrial E3 ubiquitin ligase-1 (*MUL1*), consequent degradation of the fusion factor *MFN2*, and enhanced turnover of the fission factor DLP1 (Tang *et al.*, 2015; Wang *et al.*, 2016).

Overall, mitochondria impairment is a recurrent aspect of both sporadic and genetic PD forms. This strongly suggests a central role for mitochondrial dysfunction in the pathology. As DA neurons massively and selectively degenerate in PD, the hypothesis is therefore that DA neurons of the SN are particularly susceptible to mitochondrial impairment, leading to bioenergetic crises and eventually neuronal death in PD.

.

1.8.3. Selective vulnerability of DA neurons

One question is fundamental to the pathogenic mechanisms of PD: why would DA neuron be more vulnerable than other cell types to insults such as mitochondrial dysfunction or α-synuclein pathology? Several characteristics specific to DA neurons have been widely hypothesized to be the cause of this.

First, DA neurons are distinguishable from other cell types by their long, unmyelinated and densely branched axons, that exhibit a remarkable number of neurotransmitter release sites - as many as 200,000 vesicular release sites in rodents' SN DA neurons (Matsuda *et al.*, 2009). It has been demonstrated that *SNpc* DA neurons' axons exhibit elevated basal mitochondrial activity and increased oxidative stress due to their extensive arborization, causing a more vulnerable environment (Pacelli *et al.*, 2015). Additionally, it is proposed that these axons exhibit increased expression of α-synuclein, which is mostly a synaptic protein, leading to a higher risk of developing LB pathology (Zharikov *et al.*, 2015).

Secondly, *SNpc* DA neurons display distinctive pacemaking activity, with slow and broad action potentials as well as low intrinsic calcium buffering and cytosolic calcium oscillations (Foehring *et al.*, 2009; Guzman *et al.*, 2010; Morikawa and Paladini, 2011). The slow oscillations particular to *SNpc* DA neurons were suggested to promote calcium entry into mitochondria to meet the higher bioenergetic needs of these highly arborized neurons (Surmeier, 2018). As a result, mitochondria polarization and the production of ROS would be naturally increased in these neurons in comparison to other cell types. These features could mean that *SNpc* DA neurons are generally closer to a bioenergetic "tipping point" that can be more readily triggered by ageing, oxidative stress and mitochondrial dysfunction (Surmeier, 2018).

1.9. Treatment of Parkinson's Disease

1.9.1. Treatments for motor symptoms

To this day, no cure or disease modifying treatments have been uncovered. Therefore, treatment of Parkinson's disease remains symptomatic and mostly targets the dopaminergic pathway to resolve motor symptoms (Armstrong and Okun, 2020). Levodopa (L-DOPA), the natural precursor of dopamine, is the most effective and most harnessed treatment to alleviate motor symptoms (Kalinderi, Bostantjopoulou and Fidani, 2016; Balestrino and Schapira, 2020). L-DOPA crosses the brain-blood barrier (BBB) and is converted into dopamine by the aromatic L-amino acid decarboxylase (AADC/DDC) in the remaining dopaminergic neurons of the *SNpc*. During the first few years of therapy, the clinical response to L-DOPA is at peak efficiency. However, as the disease progresses, patients exhibit reduced response to the drug and present motor fluctuations as well as dyskinesia (Fabbrini and Guerra, 2021). Management of these complications constitutes a challenging issue in PD treatment. Although seemingly less efficient, dopamine agonists and monoamine oxidase-B (MAO-B) inhibitors are also useful treatments for PD motor symptoms and are associated with less complications than L-DOPA (Kalinderi, Bostantjopoulou and Fidani, 2016). These drugs are both used as monotherapy in early phases of PD or in conjunction with L-DOPA. Deep brain stimulation (DBS) is another strategy used to treat advanced PD. It constitutes in administrating chronic, high-frequency direct electrical current on specific targets, most commonly the subthalamic nucleus or the *globus pallidus internus* (Kogan, McGuire and Riley, 2019*)*. DBS was reported as more efficient than pharmacological treatments in improving motor symptoms in advances stage of the disease (Deuschl *et al.*, 2006). Careful patient selection for DBS, based on a range of criteria including age, disease duration and L-DOPA responsiveness, appears to be key for successful treatment (Pal *et al.*, 2015).

1.9.2. Treatments for non-motor symptoms

Management of non-motor symptoms (NMS), whether they are directly caused by the disease itself or are a side effect of dopaminergic replacement therapy, is key to improving patients' quality of life (Barone, Erro and Picillo, 2017). PD-related NMS seem to originate from complex dysfunctions of a multitude of neurotransmitters, and not just dopamine (Armstrong and Okun, 2020). As a result, symptomatic treatments target those other neurotransmitters and include drugs that are already harnessed in the general population for different applications. However, the evidence for these treatments, especially in individuals with PD is largely variable. Example of drugs with convincing evidence of efficacy include antidepressants, such as serotonin and serotonin-noradrenalin reuptake inhibitors (SSRI/SNRI) that often prescribed to treat PD-associated depression and anxiety (Oertel and Schulz, 2016). Furthermore, atomotexine, a noradrenergic reuptake inhibitor, was shown to improve executive dysfunction in patients including impulsivity and risk taking (Oertel and Schulz, 2016). Rivastigmine is a acetylcholinesterase inhibitor that can be efficient in treating PD-related dementia (Arvanitakis, Shah and Bennett, 2019; Espay *et al.*, 2021).

2. Mitochondrial stress response mechanisms

Mitochondrial dysfunction has been established as a central mechanism to PD pathogenesis. Despite the widely held theory that mitochondrial impairment may be the driver to DA neuronal loss in PD, the direct relationship between mitochondrial stress and DA neurodegeneration remains poorly understood.

Mitochondria are multifaceted ubiquitous organelles that are commonly dubbed “the powerhouses of the cell” because of the essential roles they play in numerous cellular processes (Suomalainen and Battersby, 2018; Danese *et al.*, 2021). Most notably, mitochondria are necessary for cellular respiration, a process through which cells transform energy captured from their environment into a usable form: adenosine 5’-triphosphate (ATP). Oxidative phosphorylation or the synthesis of ATP occurs at the inner mitochondrial membrane (IMM), where several complexes make up the Electron Transport Chain (ETC). Other fundamental cellular pathways in which mitochondria play essential roles include calcium homeostasis (Paupe and Prudent, 2018), apoptosis (Bock and Tait, 2020), cell metabolism beyond bioenergetics and metabolic waste management (Spinelli and Haigis, 2018), and lipid synthesis (Mesmin, 2016).

Considering the critical roles played by the mitochondria, disruption of mitochondria bioenergetics may thus severely affect synaptic activity and neuronal survival, likely playing a key role in neurodegeneration (Borsche *et al.*, 2021). To understand whether *SNpc* DA neurons are preferentially vulnerable to such mitochondrial impairment it is crucial to understand which mechanisms are commonly triggered in response to mitochondrial stress. Several signaling pathways have previously been described as activated in response to mitochondrial dysfunction in diverse models and triggered by various stimuli (Kodroń *et al.*, 2021; Patergnani *et al.*, 2021, 2022; Burtscher *et al.*, 2023). These processes begin as protective mechanisms that serve to restore mitochondrial function, but if their activation is persistent or abnormal, it is proposed that they evolve into deleterious responses (**Figure 4**). As the response mechanisms activated by the mitochondria are numerous, selected pathways pertinent to the studies conducted in this thesis will be described in the following section.

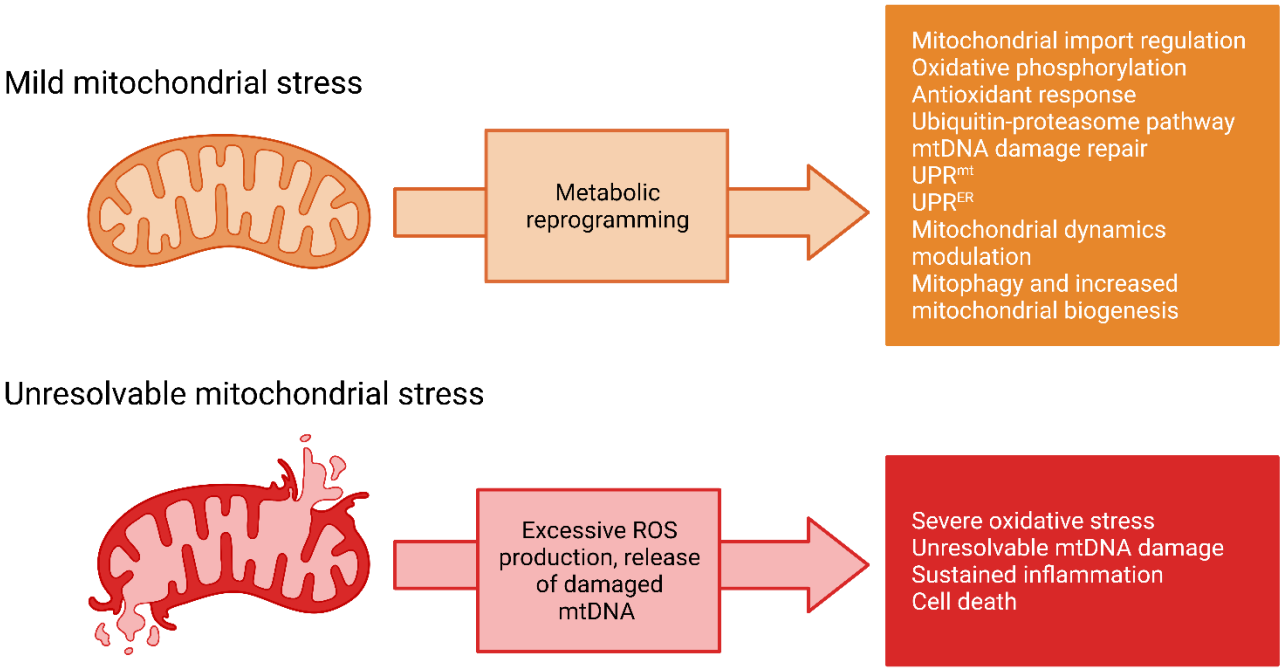

***Figure 4. Overview of mitochondrial stress response mechanisms**. Mild mitochondrial stress in a healthy organism induces beneficial adaptations and metabolic reprogramming allowing for curbing of damage to the mitochondria network and eventual metabolism. A number of compensatory mechanisms may be harnessed to this aim. In contrast, in the case of prolonged and unresolvable mitochondrial stress, adaptation capacity is hindered. This may lead to excessive production of Reactive Oxygen Species inducing severe oxidative stress and to release of damaged mtDNA. This activates the inflammasome, which, when sustained, can result in cell death. (Adapted from Burtscher et al., 2023 and Patergnani et al., 2022).*

2.1. Mitochondrial dynamics

Mitochondria are highly dynamic organelles that undergo constant cycles of fusion and fission to maintain the integrity of the mitochondrial network and ensure distribution and availability to participate in fundamental cellular processes (Yu *et al.*, 2020). The balance between fusion and fission events - mitochondrial dynamics - is essential to several cellular biological processes and is coordinated by a plethora of factors that mainly belong to the family of dynamin-related GTPases (Zhang *et al.*, 2019).

In mammals, mitochondrial fission is mainly regulated by dynamin-related protein-1 (DRP1), which becomes phosphorylated and recruited to the outer mitochondrial membrane (OMM) by adaptors including MiD49, MiD51 (Mitochondrial Dynamics proteins of 49 and 51kDa), mitochondrial fission 1 (Fis1), and Mitochondrial Fission Factor (Mff) (Yu *et al.*, 2020). Once associated to the OMM, DRP1 undergoes

oligomerization into a ring-like structure that constricts the OMM (Lee *et al.*, 2016; Patergnani *et al.*, 2022). Constriction of the membrane induces the recruitment of dynamin-2, which is responsible for finishing the scission process (Tilokani *et al.*, 2018). Fusion events require the fusion of two mitofusin (MFN)-expressing mitochondria's OMMs and then IMMs (Patergnani *et al.*, 2022). Fusion initiates by the tethering of two opposing OMMs through dimerization of their respective MFN proteins (MFN1 and MFN2), leading to the formation of a ring-like structure (Yapa *et al.*, 2021). MFN protein expression is usually activated by de-ubiquitination events that promotes stabilization; otherwise, MFN proteins can be inhibited and degraded *via* phosphorylation (Pyakurel *et al.*, 2015). Secondly, IMM fusion is mediated by dynamin-like GTPase protein optic atrophy 1 (OPA1) and SLC25A46, a member of the mitochondrial solute carrier family SLC25. Alternative splicing and proteolytic cleavage in the mitochondria leads to two isoforms of OPA1: long OPA1 (L-OPA1) and short OPA1 (S-OPA1). The interaction between opposing L-OPA1 is responsible for the tethering and fusion of two IMMs, via OPA1-dependent GTP-hydrolysis (Ge *et al.*, 2020; Liu *et al.*, 2020). However, the role of S-OPA1 is more complex: it appears to also participate in fusion events, particularly allowing for rapid and efficient IMM pore opening during fusion, even though it is sufficient to fully induce this. However, excessive levels of S-OPA1 seem to inhibit fusion and to trigger increased mitochondria fragmentation (Ge *et al.*, 2020; Yu *et al.*, 2020; Patergnani *et al.*, 2022).

Balance between fusion and fission events is essential for quality control of the mitochondrial network, allowing for efficient biogenesis, turnover and distribution of mtDNA. In response to cellular stressors and disease, cellular health maintenance relies on mitochondrial dynamics being able to appropriately redistribute the mitochondrial network depending on cellular needs (Yapa *et al.*, 2021). Fusion can alleviate mitochondrial damage by allowing for the exchange of a multitude of factors between partially dysfunctional mitochondria, including mtDNA, proteins, metabolites and lipids. This can help restore mitochondrial oxidative capacity (W. Yue *et al.*, 2014; Zeng *et al.*, 2021). Fission, on the other hand, helps isolate irreversibly damaged mitochondria, priming them for degradation *via* mitochondrial autophagy or mitophagy

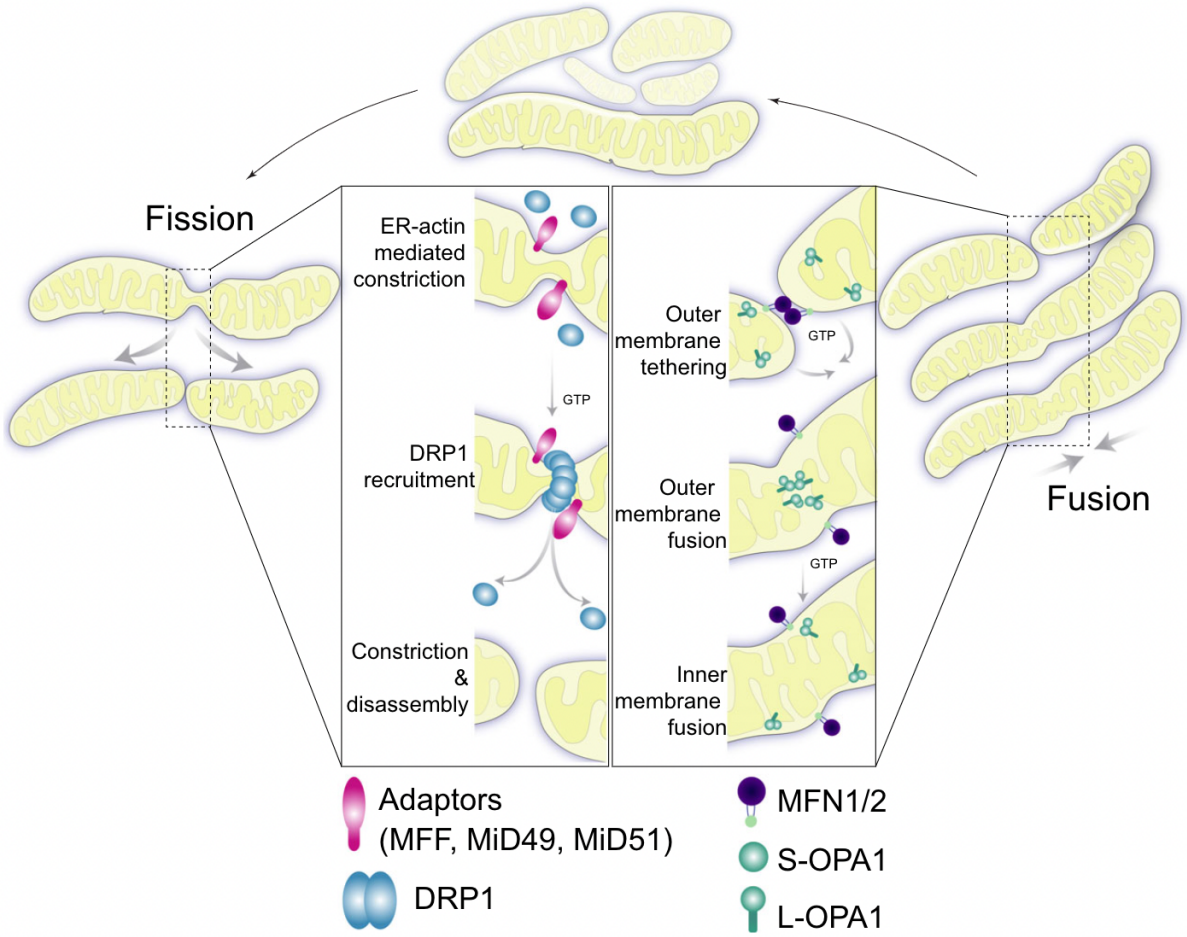

Figure 5. Overview of mitochondrial fission and fusion. *Drp1 is recruited to the site of scission via membrane adaptors. Once there, it undergoes oligomerization into a ring-like structure, constricting the OMM and IMM and driving membrane scission via GTP binding and hydrolysis. Fusion is initiated by the tethering of adjacent mitochondria OMMs via MFN1/2. GTP binding and hydrolysis bring the membranes together. Subsequently, the IMM OPA1 acts in a similar way to induce inner membrane fusion, thereby producing a single mitochondrion. (adapted from Yapa et al., 2021)*

(Westermann, 2010; Liu *et al.*, 2020). Therefore, it is suggested that hyperfusion occurs as a transitory mitochondrial stress response that could alleviate moderate pathological damage to the network, but that persistent stress, induces a switch to hyper-fragmentation in order to clear dysfunctional mitochondria (Patergnani *et al.*, 2022). For example, Lebeau and colleagues observed mitochondria hyperfusion in mouse embryonic fibroblast cells following 6- and 12-hour treatments with the ER stressor thapsigargin, whereas prolonged 24-hour treatment resulted in increased mitochondrial fragmentation (Lebeau *et al.*, 2018).

Mutations in central genes to the mitochondrial dynamics machinery have been implicated in human neurodegenerative diseases, corroborating the importance of these mechanisms to the neural system. For example, mutations in MFN2, essential for OMM fusion, were discovered to cause Charcot-Marie-Tooth Type 2 A disease (Bertholet *et al.*, 2016). Dysfunctional MFN2 and consequently, impaired mitochondrial

fusion, hinders the maintenance of mtDNA integrity, which impacts the proper functioning of the mitochondrial ETC and makes neurons more susceptible to apoptosis. Indeed, patients show a two-fold decrease of total mtDNA copy number in skeletal muscle biopsies compared to healthy individuals (Vielhaber *et al.*, 2013). Furthermore, altered mitochondrial fusion causes inadequate distribution of the mitochondrial network and therefore, inability to satisfy local energetic demands. This was observed in the axons of rat and mice models of Charcot-Marie-Tooth Type 2 A disease, and appeared to drive axonal degeneration (Misko *et al.*, 2012; Franco *et al.*, 2022).

Many studies have reported that the balance between fusion and fission is disrupted in PD, with enhanced mitochondria fragmentation (Heger *et al.*, 2021). The boost in fission was first described in a rat model using mitochondrial toxins rotenone, oligomycin or MPP+ (Barsoum *et al.*, 2006). This was progressively confirmed by a number of studies *using* animal and human cellular PD models presenting mutations in *PRKN*, *VP53* and *LRRK2*, following administration of toxins such as MPP+, rotenone and 6-hydroxydopamine (Gomez-Lazaro *et al.*, 2008; Wang *et al.*, 2011; Su and Qi, 2013; Aboud *et al.*, 2015; Santos *et al.*, 2015; Hanss *et al.*, 2021). More recently, mitochondria hyper-fragmentation and decrease of functionality were observed in PARKIN knockout (KO) iPSC-derived DA neurons, but not in non-dopaminergic neurons, denoting the selective vulnerability of DA neurons (Yokota *et al.*, 2021). This phenotype was associated with decreased expression levels of fusion genes such as *MFN2* (Flippo and Strack, 2017; Hanss *et al.*, 2021) and increased activity of the fission factor DRP1 (Heger *et al.*, 2021). Interestingly, inhibiting DRP1 was able to prevent neuronal death and loss of dopamine release both in a *PINK1*$^{-/-}$ mouse knockout PD model and in a MPTP-caused parkinsonism mouse model (Rappold *et al.*, 2014). This finding reinforces the hypothesis that a surge in mitochondrial fission leading to toxicity and increased neuronal susceptibility to death.

2.2. Mitophagy

An integral process to the maintenance of mitochondrial homeostasis is mitophagy, the selective clearance of damaged or surplus mitochondria by the autophagy machinery (Ashrafi and Schwarz, 2013; Corti, 2019). During this process, impaired mitochondria are engulfed by autophagosomes and then degraded by lysosomes (Bloemberg and Quadrilatero, 2019). Mitophagy is essential for mitochondrial quality control and for proper cell health maintenance. This is the case not only in basal condition but also upon exposure to different stressors, such as oxidative stress or hypoxia (Palikaras, Lionaki and Tavernarakis, 2015; Chen, Kroemer and Kepp, 2020; Patergnani *et al.*, 2022)

In mammals, in different cellular contexts and in diverse pathological situations, several mitophagy mechanisms have been described (Ashrafi and Schwarz, 2013; Chu, 2019). Mitophagy is largely divided into PINK1/PARKIN-dependent or independent mitophagy (Figure 5). Although mitophagy has been extensively studied in recent years, especially the PINK1/PARKIN-mediated pathway, the distinctions between the two types of mitophagy, relating to their mobilization in different tissues and in response to different stressors, remains relatively poorly understood (Wang *et al.*, 2019; Yao *et al.*, 2021). However, some discrepancies have been described, with studies reporting that mitochondrial depolarization and proteotoxicity harness the PINK1/PARKIN-machinery for mitochondrial removal whereas hypoxia (Bellot *et al.*, 2009) and erythroid cell maturation (Sandoval *et al.*, 2008) (for example, seem to mobilize PINK1/PARKIN-independent mechanism. The latter relies on the OMM-localized proteins BCL-2-like-protein (BCL2L13), BNIP3 (BCL2/adenovirus E1B-interacting protein 3), NIX/BNIP3L (BCL2/adenovirus E1B-interacting protein 3-like) and FUNDC1 (FUN14 domain-containing protein 1). These proteins act as mitophagy receptors as they possess LC3-interacting region (LIR) motifs through which they can interact with autophagosomes and trigger mitochondrial degradation (Gatica, Lahiri and Klionsky, 2018; Bloemberg and Quadrilatero, 2019; Zhu *et al.*, 2021).

PINK1/PARKIN-dependent mitophagy is the most studied mitophagy pathway in mammalian cells. PARKIN is an E3 ubiquitin ligase that can regulate the specific ubiquitination of target proteins and cooperate with the Ubiquitin-Proteasome System

for their degradation (Corti, 2019). PTEN-induced kinase 1 or PINK1 is a serine/threonine protein kinase and has a mitochondrial targeting sequence at its N-terminal (Arena and Valente, 2017). Together, PINK1 and PARKIN play an essential role in mitochondrial quality control, by sensing and degrading damaged mitochondria (Quinn *et al.*, 2020). In healthy mitochondria, PINK1 is translocated to the inner mitochondrial membrane (IMM) with the help of outer mitochondrial membrane (OMM) and IMM translocases (respectively TOMM and TIMM) and undergoes proteolysis (Jin *et al.*, 2010, p. 20). In the event of dysfunctional mitochondria and loss of mitochondrial membrane potential, PINK1 becomes stabilized at the OMM where it phosphorylates a pre-existing ubiquitin (Ub) residue at serine 65 (pSer65Ub) (Swatek *et al.*, 2019). This triggers the recruitment of PARKIN to the OMM where it binds to the pSer65Ub and undergoes several conformational changes (Wauer *et al.*, 2015). Following this, its ubiquitin-like domain becomes phosphorylated by PINK1, allowing for the activation of PARKIN at the OMM, where it can harness its E3 activity to enhance ubiquitination of mitochondria surface proteins (Quinn *et al.,* 2020). These newly synthetized Ub chains become the target of PINK1 phosphorylation, resulting in a surge of pSer65 levels, which has become largely viewed as a PINK1/PARKIN-mediated mitophagy marker (Picca *et al.*, 2021). Autophagic receptors such as OPTN, TAX1BP1, NDP52 and P62 are subsequently able to detect and bind the ubiquitinated proteins and start autophagosome formation via interaction with MAP1LC3B/LC3 (Figure 5).

PINK1/PARKIN-dependent mitophagy was initially established in immortalized cultured cell lines and primary rodent neuronal cultures (Ashrafi *et al.*, 2014; Van Laar *et al.*, 2015) and was subsequently also confirmed in human induced pluripotent stem cell (iPSC)-derived dopaminergic neurons (Oh *et al.*, 2017). Indeed, endogenous levels of PINK1 and PARKIN were reported as sufficient to decrease mtDNA levels and increase ubiquitin phosphorylation in response to loss of mitochondrial membrane potential, thus confirming the roles of PINK1 and PARKIN in mitophagy in human dopaminergic neurons (Seibler *et al.*, 2011; Soutar *et al.*, 2018). Additionally, human iPSC-derived DA neurons with loss-of-function PINK1 mutations, displayed inhibited ionophore-induced mitophagy with unresolved reduction of mitochondria membrane potential, further supporting the proposed central role of PINK1 in this type of mitophagy (Bus *et al.*, 2020). Various drugs have been shown to induce PINK1/PARKIN-mediated mitophagy (Georgakopoulos, Wells and Campanella, 2017).

The protonophore carbonyl cyanide m-chlorophenyl hydrazone or CCCP was one of the first drugs harnessed for the study of this mechanism as it causes the depolarization of mitochondria by inhibiting the expression of several ETC proteins (Narendra *et al.*, 2008; Villa *et al.*, 2017). As a result, PARKIN was shown to translocate to depolarized mitochondria and to colocalize with the autophagosome marker LC3, indicating that PARKIN mediates mitophagy (Narendra *et al.*, 2008). Despite being widely used, CCCP, like other protonophores, is known to have several limitations and to be cytotoxic (Georgakopoulos, Wells and Campanella, 2017). Most notably it does not specifically target the mitochondria but has protonophoric activity on other membranes such as the lysosomal membrane, thus producing many off-target effects and high levels of toxicity (Padman *et al.*, 2013). Consequently, other PINK1/PARKIN-mediated mitophagy-inducers are becoming more commonly employed such as the toxin Antimycin A, an ETC complex III inhibitor, often in combination with oligomycin, an ETC complex V inhibitor (Ashrafi *et al.*, 2014; Lazarou *et al.*, 2015; Hsieh *et al.*, 2016; Shaltouki *et al.*, 2018). Indeed, studies found that treatments with these toxins resulted in increased mitochondrial fission as well as reduced mitochondrial motility, and gradually triggered mitochondrial clearance *via* the PINK1/PARKIN axis. Antimycin A alone only achieves a relatively small decrease in mitochondrial membrane potential due to the activation of the compensatory reverse hydrolysis activity of the F_1F_0 -ATP synthase (Ivanes *et al.*, 2014). As a result, it is usually combined with oligomycin, an inhibitor of the the F_1F_0-ATP synthase, which allows for more acute mitochondria depolarization (Lazarou *et al.*, 2015). The use of antimycin A-oligomycin to induce PINK1/PARKIN-dependent mitophagy is appreciated as more physiologically relevant as both toxins are rather selective and accordingly produce less off-target toxic effects and less severe mitochondrial damage (Ashrafi and Schwarz, 2013; Georgakopoulos, Wells and Campanella, 2017).

An accumulating number of studies have highlighted the important role of mitophagy in Parkinson's Disease and other neurodegenerative diseases. One of the first evidence for this was the discovery of mitochondria contained in autophagosomes and marked by activated kinases in the neurons of patients with PD and Lewy Body Dementia (LBD) (Zhu *et al.*, 2003). Moreover, elevated levels of pSer65Ub, denoting increased mitophagy, were reported in postmortem PD patients' brains (Hou *et al.*, 2018).

Since then, disrupted mitophagy was reported in diverse models of toxic-environmental and genetic PD forms. For example, the kinase activity of LRRK2 was found to be inversely correlated with mitophagy levels, with LRRK2 mutations being the most frequent cause for autosomal dominant familial PD (Bonello *et al.*, 2019; Singh *et al.*, 2021). LRRK2 knockout mice exhibited a surge in mitophagy levels, whilst mice DA neurons and microglia and human iPSC-derived DA neurons with the LRRK2 G2019S activation mutation displayed decreased general mitophagy (Hsieh *et al.*, 2016; Singh *et al.*, 2021). Furthermore, treatment with the CNS-penetrant LRRK2 inhibitor GSK3357679A rescued mitophagy in LRRK2 G2019S mice and enhanced it in control mice, supporting the potential role for LRRK2 in regulating mitophagy. Interestingly, both the LRRK2 G2019 mutation and the A53T mutation in SNCA, encoding α-synuclein, were found to impact the initial steps of mitophagy. The effect

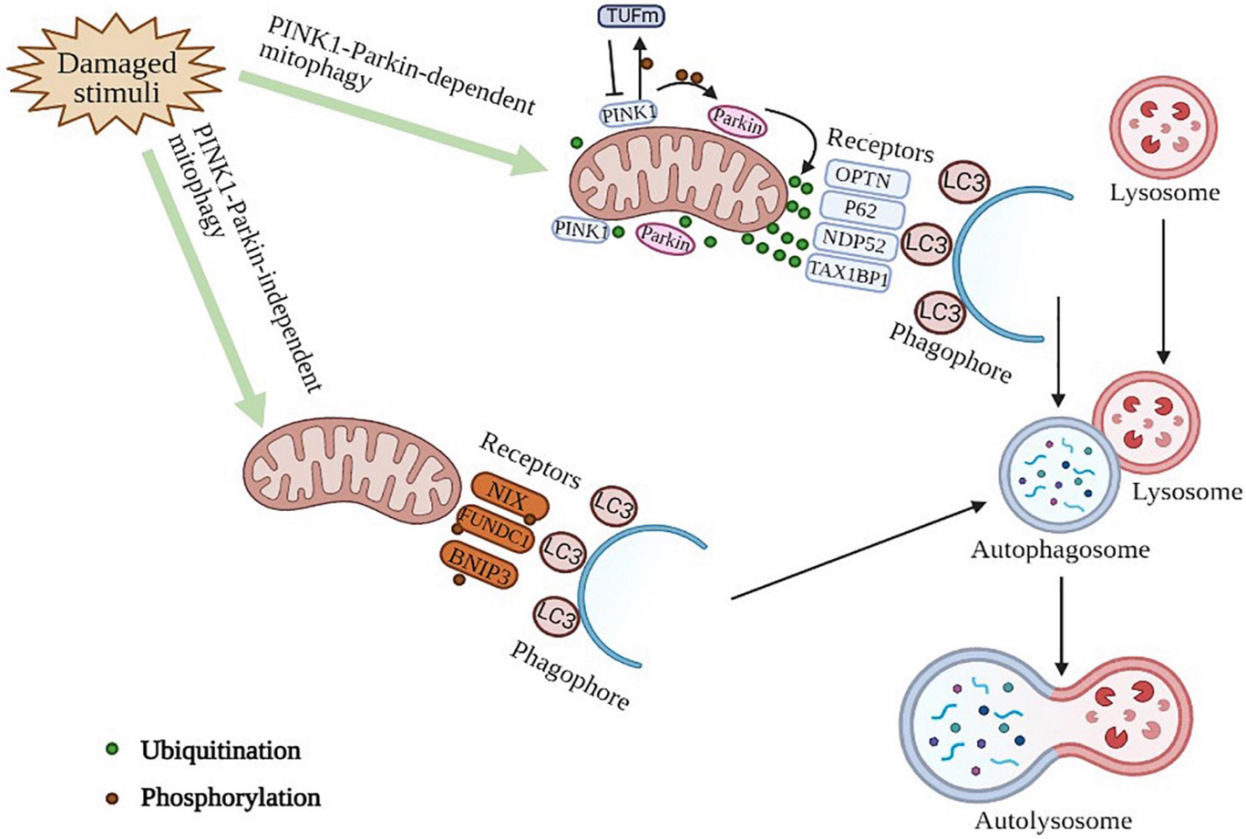

Figure 6. Summary of the molecular mechanisms of PINK1/Parkin-dependent and -independent mitophagy. *(Adapted from* Zhu et al., 2021*).* PINK1 acts as a sensor of mitochondrial damage, upon which it is activated at the OMM. It can, in turn, recruit and activate PARKIN. Subsequently PARKIN can ubiquitynate proteins OMM surface proteins. The autophagic receptors will detect the increasingly ubiquitinated proteins and will trigger the conversion of mitochondria to autophagosome for their clearance by interacting directly with LC3. The PINK1-PARKIN independent mitophagy is mediated by mitophagy receptors: BNIP3, FUNDC1 and NRF1, which can directly interact with LC3 in an ubiquitin-independent manner and can trigger the autophagosome formation.

of such mutations are characterized by the abnormal accumulation on damaged mitochondria's OMM of the protein Miro, a promoter of mitochondrial motility that is usually removed to isolate impaired mitochondria and facilitate mitophagy (Hsieh *et al.*, 2016; Shaltouki *et al.*, 2018). α-synucleinopathy and the aggregation of α-synuclein fibrils was further linked to mitochondrial dysfunction and mitophagy impairment in a number of studies. Seeding cultured primary neurons with preformed α-synuclein fibrils (PFFs) induced the conversion of endogenous α-synuclein into a phosphorylated fibrillar form that can undergo incomplete autophagic degradation to form a neurotoxic non-fibrillar phosphorylated α-synuclein species (Grassi *et al.*, 2018). This form of phosphorylated α-synuclein was shown, by confocal imagery and stimulated emission depletion nanoscopy, to aggregate with mitochondria, depolarize the mitochondrial membrane and cause hyper-fragmentation and mitophagy. Mutations in the gene encoding the lysosomal enzyme GBA, making up the most common genetic PD risk factor, were also linked to mitophagy disruption. Mice heterozygous for the L444P GBA mutation showed significant mitochondrial depolarization, increased total mitochondrial content and increased ROS levels. Using the mitochondrial-target Keima (mt-Keima) reporter system to detect mitochondria fused with lysosomes, it was revealed that the accumulation of damaged mitochondria was due to impaired autophagy delivery of mitochondria to lysosomes. Additionally, protein levels of PARKIN and BNIP3L, regulators of PINK/PARKIN-dependent mitophagy, were significantly decreased, suggesting disruption of mitochondrial priming for autophagic clearance. Corroborating these findings, increased mitochondrial content, oxidative stress and disrupted autophagy were also reportedd in SHSY-5Y cell cultures overexpressing L444P mutated GBA, and in post-mortem brain tissue from PD patients (Li *et al.*, 2019).

Nonetheless, one of the main lines of evidence supporting the importance of mitophagy in PD pathology are the early-onset PD-causing mutations in the mitophagy regulators PINK1 and PARKIN. These loss-of-functions mutations are suggested to impair the initiation of mitophagy, cause the accumulation of damaged mitochondria and thus, increase oxidative stress and drive neuronal loss (Gautier *et al.*, 2016; Puschmann *et al.*, 2017; Scorziello *et al.*, 2020). Studies examining *PINK1-PRKN* mutant drosophila described mitochondrial alterations, locomotive dysfunctions and neuron development deficiencies (Julienne *et al.*, 2017). In contrast, *PINK1* and *PRKN*

knockout mice did not show as acute PD-like neurological deficits, with only mild locomotor dysfunctions triggered by exhaustive exercise and stressed mitochondria, and no significant loss of *SN* DA neurons (Perez and Palmiter, 2005, 2005; Kitada *et al.*, 2007; Sliter *et al.*, 2018). Furthermore, exacerbated mitochondrial dysfunctions caused by crossing a Parkin knockout mice with the Mutator mice – a model that accumulates mutated and impaired mitochondria - triggered significant loss of DA neurons (Pickrell *et al.*, 2015). Compensatory mechanisms may be activated in basal physiological conditions that allow for mitophagy and neuronal homeostasis to be maintained without depending on the PINK1/PARKIN machinery. However, the latter appears indispensable in pathological circumstances, with disruptions to the PINK1/PARKIN axis preventing proper adaptive response to stressors.

Mitochondrial dysfunctions and impaired mitophagy have also been demonstrated in human iPSC-derived DA neurons with *PINK1* and *PRKN* mutations. Indeed, DA neurons with PINK1 loss-of-function mutations displayed inhibited mitophagy initiation and PARKIN stabilization at the OMM when treated with the potassium ionophore valinomycin or with carbonyl cyanide m-chlorophenyl hydrazone (CCCP), which were both shown to induce mitochondrial depolarization and PINK1/PARKIN-dependent mitophagy (Seibler *et al.*, 2011; Rakovic *et al.*, 2019; Bus *et al.*, 2020). Futhermore, *PINK1* mutant neurons had significantly decreased levels of pSer65Ub and of PINK1 kinase activity (Puschmann *et al.*, 2017; Shiba-Fukushima *et al.*, 2017). Mutated *PRKN* was also linked to defective mitophagy in iPSC-derived DA neurons, using the mt-Keima reporter system to detect mitochondria fused with lysosomes (Suzuki *et al.*, 2017). This disruption in mitophagy was only observed in differentiated DA neurons and not in neural progenitors, which was attributed to a metabolic switch that gradually occurs during differentiation whereby cells go from relying on glycolysis to oxidative phosphorylation (Schwartzentruber *et al.*, 2020). Overall, this data confirms the key role mitophagy appears to play in the pathophysiology of PD. Mitophagy has also been reported to regulate another protective mitochondria stress response: the mitochondrial unfolded protein response (UPRmt). This mechanism can be triggered at the same time as mitophagy and they may coordinate to restore mitochondrial homeostasis: mitophagy discards the most severely damaged mitochondria whilst the UPRmt promotes the stabilization and

recovery of salvageable organelles (Pellegrino and Haynes, 2015; Y. Wang *et al.*, 2021).

2.3. The Mitochondrial Unfolded Protein Response

The UPR^{mt} is a transcriptional response to diverse mitochondrial dysfunctions that is reliant on mitochondria-to-nucleus signaling (Schulz and Haynes, 2015). It is generally understood to regulate the proper import, folding and quality control of the mitochondrial proteome by enhancing the expression of mitochondrial chaperones (Pickles, Vigié and Youle, 2018; Anderson and Haynes, 2020). Although the UPR^{mt} was initially characterized in *C. elegans,* it was first identified in mammalian cells when decline in mtDNA levels and misfolded proteins accumulation triggered the production of mitochondrial chaperones and proteases (Martinus *et al.*, 1996; Zhao *et al.*, 2002). Subsequently, more studies in mice and mammalian cell cultures showed that the UPR^{mt} can be induced in response to a range of mitochondrial perturbations, including loss of the mitochondrial aspartyl-tRNA synthetase DARS2 and inhibition of mitochondrial translation (Dogan *et al.*, 2014; Chung *et al.*, 2017), inhibition of the mitochondrial protease LON and the mitochondrial chaperone TRAP1 (Münch and Harper, 2016), and knockdown of mitochondrial ribosomal protein S5 (Mrps5) which causes an imbalance between mitochondrial- and nuclear-encoded OXPHOS proteins (Houtkooper *et al.*, 2013).

Accumulating studies show that three parallel and possibly overlapping UPR^{mt} signaling pathways can be triggered in response to mitochondrial dysfunction (Figure 6). The main and most investigated branch is the ATF5-mediated UPR^{mt}, while the two other arms rely on the mitochondrial NAD+-dependent deacetylase SIRT3 and the hormone receptor Estrogen Receptor alpha (ERα) (Wodrich *et al.*, 2022). The activation of these distinct branches appears to be dependent on the type and location of the mitochondrial stress.

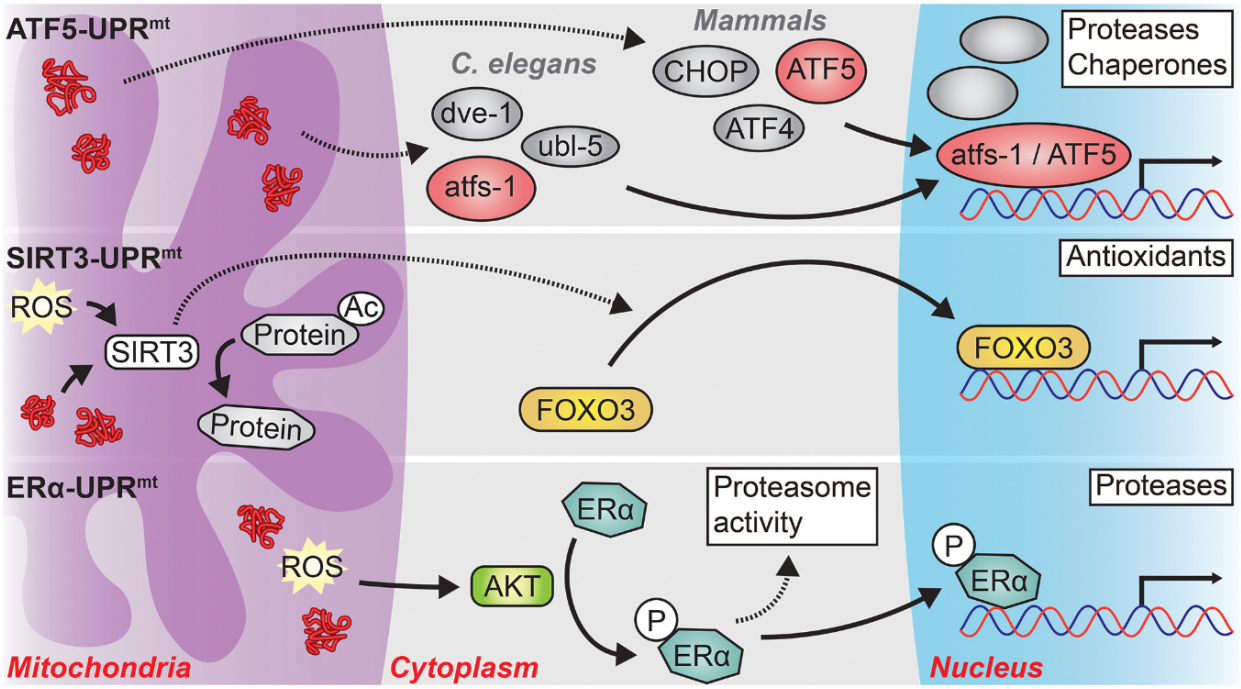

Figure 7. The three arms of the mitochondrial unfolded protein response. *(Adapted from Wodrich et al., 2022). Three branches of the UPR^{mt} have been described as activated in response to mitochondrial damage, depending on the type and location of the stress. ATF5-UPR^{mt}: Mitochondrial matrix misfolded protein accumulation triggers the cytosolic accumulation of ATF5 (mammalian ortholog of ATFS-1 first described in C. elegans). ATF5 translocates to the nucleus and stimulates the expression of proteases and chaperones to rescue mitochondrial health. In mammals, this process is dependent on two transcription factors of the ISR: ATF4 and CHOP, although their exact interaction with ATF5 remains elusive.*
SIRT3-UPR^{mt}: Accumulation of ROS and misfolded proteins in the mitochondrial matrix can activate the mitochondrial NAD+-dependent deacetylase SIRT3. SIRT3 then deacetylates various mitochondrial proteins and triggers the translocation of FOXO3 to the nucleus, where it induces transcription of antioxidants to relieve the mitochondrial oxidative stress.
ERα-UPR^{mt}: Protein stress and ROS in the mitochondrial intermembrane space (IMS) cause the activation of AKT, which, in turn, phosphorylates ERα. ERα is then able to promote proteasome activity but also, by translocating to the nucleus, it acts as a transcription factor, triggering the expression of IMS-specific proteases.
Solid arrows: direct actions; dashed arrows: indirect or unclear mechanisms.

2.3.1. The ATF5-mediated UPR^{mt}

The first and most thoroughly studied UPR^{mt} branch is the ATF5-dependent UPR^{mt}, which is mainly activated in response to the accumulation of unfolded proteins within the mitochondrial matrix (Shpilka and Haynes, 2018). The transcription factor ATF5 contains both a nuclear localization sequence as well as a mitochondrial targeting sequence. In basal conditions, ATF5 is imported into the mitochondria where it is degraded by LONP-1, a mitochondrial matrix protease. Under mitochondrial stress conditions, however, ATF5 undergoes trafficking to the nucleus where it can kickstart the protective transcriptomic UPR^{mt} response and enhance the expression of different factors such as the anti-apoptotic BCL-2 (Dluzen *et al.*, 2011; Fiorese *et al.*, 2016). In

mammals, ATF5 translocation to the nucleus is dependent on CHOP and ATF4, key mediators of the UPR^{ER} as will be described in part 2.4. (Quirós *et al.*, 2017; Shpilka and Haynes, 2018). Although it is still poorly understood how the three factors interact, findings suggest a necessary interaction between ATF5 and the UPR^{ER} for the induction of the UPR^{mt}, whereby the UPR^{ER} activation enhances the expression of ATF5 during mitochondrial dysfunction (Fiorese *et al.*, 2016; Quirós *et al.*, 2017; Melber and Haynes, 2018). Once the UPR^{mt} is activated, a series of translational and epigenetic changes are enacted to reduce the proteotoxic burden and restore mitochondrial function. To achieve this, ATF5, similarly to its *C.elegans* homologue ATFS-1, and ATF4 were shown to bind to a conserved 14-base-pair promoter element, $UPR^{mt}E$ (UPR^{mt} element), in a number of genes to upregulate their expression (Nargund *et al.*, 2015; Fiorese *et al.*, 2016; Quirós *et al.*, 2017). This includes the mitochondrial protease LONP1 and mitochondrial chaperones such as mtHSP70, HSP10 and HSP60, indicating activation of *de novo* protein folding and clearance of misfolded or damaged proteins. Furthermore, the UPR^{mt} and the activation of ATFS-1 appear to promote OXPHOS recovery by limiting the transcription of tricarboxylic acid (TCA) cycle enzyme encoding genes and OXPHOS genes in both the nucleus and the mitochondria, but concurrently induce the expression of glycolysis components (Nargund *et al.*, 2012, 2015). This momentarily relieves the mitochondrial protein folding load by reducing the expression of some of the most highly expressed and hard to process mitochondrial proteins and allowing time for mitochondrial protein homeostasis recovery. On the other hand, the glycolysis surge also benefits mitochondrial recovery by increasing cytosolic ATP production.

2.3.2. The ERα-dependent UPR^{mt}

The Estrogen Receptor alpha (ERα)-mediated arm of the UPR^{mt} appears to be triggered in response to proteotoxic stress and accumulating ROS within the mitochondrial inner membrane space (IMS). The kinase AKT becomes activated by phosphorylation and can, in turn, phosphorylate ERα on serine 167 (Papa and Germain, 2011). Consequently, ERα stimulates the cytosolic ubiquitin-proteasome system, with a reported significant surge in the trypsin-like activity of the proteasome and more moderate increase in chymotrypsin-like and caspase-like activities. This

allows for the degradation of misfolded proteins and reduces proteotoxic stress in the IMS. ERα also translocates to the nucleus to enhance transcription of the IMS-specific protease htrA serine peptidase 2 (*HTRA2*) as well as the transcription factor NRF1, essential for mitochondrial biogenesis and the expression of mitochondrial respiratory chain genes. Interestingly, loss-of-function mutations in *HTRA2* were linked to PD, providing an important link between the UPR^{mt} and PD pathophysiology (Strauss *et al.*, 2005; Ross *et al.*, 2008). This ERα-mediated UPR^{mt} branch thus appears to induce a cytoprotective response by promoting IMS protein quality control processes and by enhancing genes required to rescue mitochondria integrity. It has been reported that disruption to the ERα-UPR^{mt} could lead to the eventual activation of the ATF5-UPR^{mt}, suggesting that the IMS protein stress may spillover into the mitochondrial matrix to induce ATF5-UPR^{mt} (Papa and Germain, 2011).

2.3.3. The SIRT3-mediated UPR^{mt}

The third UPR^{mt} branch is dependent on the mitochondrial NAD+-dependent deacetylase SIRT3 and the forkhead transcription factor FOXO3 (Papa and Germain, 2014). Protein stress and accumulation of ROS in the mitochondrial matrix can activate SIRT3, which can then deacetylate a number of mitochondrial proteins. This includes OXPHOS components, as well as factors of the TCA cycle, amino acid metabolism and fatty acid oxidation, suggesting that SIRT3 enacts a metabolic shift to promote mitochondrial recovery (Hebert *et al.*, 2013; Marcus and Andrabi, 2018). SIRT3 appears to participate in preventing FOXO3 degradation by mediating its deacetylation although it remains unclear how this is done exactly (Zhang, Ma and Feng, 2020). In the nucleus, FOXO3 can induce transcriptional changes to promote expression of antioxidants as a way to reduce mitochondrial oxidative stress (Marcus and Andrabi, 2018).

Although ATF5-UPR^{mt} and SIRT3-UPR^{mt} overlap in that they are both triggered by proteotoxic stress within the mitochondrial matrix, studies report distinct pattern of activation for these two branches. For example, the activation of the transcription factor CHOP is necessary for the activation ATF5-UPR^{mt} but does not seem required for SIRT-UPR^{mt} (Papa and Germain, 2014). Furthermore, increased ROS levels *via*

inhibition of the mitochondrial ETC complex I and III, upregulate SIRT3 and FOXO3, demonstrating that oxidative stress is sufficient to activate SIRT-UPR^{mt}. It has been suggested that SIRT3-UPR^{mt} and ATF5-UPR^{mt} function in a consecutive matter, with SIRT3 being first activated by the sole increase in ROS within the mitochondrial matrix, and ATF5 being stimulated later, when ROS levels are too high or persist for too long, causing protein damage and aggregation (Wodrich *et al.*, 2022).

2.3.4. Link between the UPR^{mt,} aging and PD

Enhanced activation of the UPR^{mt} has been linked to ageing in *C. elegans,* with a progressive increase of mitochondrial chaperones and proteases expression levels, such as hsp-6 and hsp-60, throughout lifespan (Sheng *et al.*, 2021; Zhang *et al.*, 2021). Activation of the UPR^{mt} has been positively correlated with longevity in both *C. elegans* and mice, suggesting that UPR^{mt} induction with age– especially SIRT3-UPR^{mt} and ATF5-UPR^{mt} – is protective and allows for extended lifespan (Ozkurede and Miller, 2019; Zhang *et al.*, 2021). However, this characteristic remains largely debated and requires further investigation to fully comprehend the UPR^{mt}'s link and possibly beneficial effect on age, especially as age is the biggest risk factor for neurodegenerative diseases such as PD (Wodrich *et al.*, 2022).

PD, similarly to other NDD, is characterized by the accumulation and aggregation of misfolded proteins. This drove the scientific community to start examining the potential pathophysiological role of the UPR, both from the mitochondria and from the endoplasmic reticulum, which will be described in part 2.4. Post-mortem brain tissue from PD patients have shown increased levels of UPR^{mt} factors such as HSP60, although more comprehensive analysis of UPR^{mt} markers' expression in such post-mortem tissue are needed to confirm this (Pimenta de Castro *et al.*, 2012). Nevertheless, many studies have demonstrated that PD-causing toxins and genetic mutations induce UPR^{mt} activation (Pellegrino and Haynes, 2015; Bloem, Okun and Klein, 2021). Treatment with MPP+ resulted in increased levels of UPR^{mt}-related chaperones (HSPA9 and HSPE1) and proteases (YME1L1 and CLPP) in human SH-SY5Y cell cultures (Cai *et al.*, 2020). Interestingly, enhanced UPR^{mt} activity with overexpression of ATF5 mitigated cell death in MPP+-treated human cells (Hu, Liu and

Qi, 2021). In iPSC-derived DA neurons, overexpression of the UPR^{mt} mitochondrial protease CLPP suppressed the accumulation of pathogenic α-synuclein phosphorylation and reduced oxidative stress (Hu *et al.*, 2019). In comparison, iPSC-derived DA neurons from PD patient cell lines carrying the α-synuclein A53T mutation, exhibit selective decrease in CLPP expression, also seen in PD patient postmortem brains, which causes an overload in misfolded proteins. This induced detrimental sustained activation of the UPR^{mt}, with α-synuclein seemingly accumulating in mitochondria and triggering the UPR^{mt} directly, inducing heightened oxidative stress and neurotoxicity. This deleterious effect of prolonged UPR^{mt} activation was also seen in *C.elegans* PD-models with the α-synuclein variants A53T and A30P (Martinez et al., 2017) suggesting abnormal neurotoxic UPR^{mt} overactivation in PD. It is important to add that strong evidence for a significant role for the UPR^{mt} is the discovery of PD patients with mutations in HTRA2, a main actor in Erα-UPR^{mt} (Unal Gulsuner *et al.*, 2014). Altogether, our current knowledge of the UPR^{mt} reveals two facets to this mechanism, with an overall beneficial effect under many circumstances, but a detrimental one when chronically activated.

2.4. The Integrated Stress Response

The integrated stress response (ISR) is an evolutionary conserved response to diverse external perturbations causing cellular stress (Pakos-Zebrucka *et al.*, 2016). The main aim of this response is to shut down global protein translation and permit the translation of selective mRNAs, encoding proteins necessary for the cellular stress response. Central to the ISR is the phosphorylation of the eukaryotic translation initiation factor 2 (eIF2α). Four kinases are known to phosphorylate eIF2α in response to various intra- or extra-cellular stimuli: heme-deficiency activated HRI, viral infection-triggered PKR, endoplasmic reticulum protein folding stress-induced PERK and amino acid deprivation-activated GCN2 (Bond *et al.*, 2020; Bilen *et al.*, 2022; Zhang *et al.*, 2022). eIF2α phosphorylation induces a transient attenuation of general translation to block further accumulation of newly synthesized proteins in the impaired ER and momentarily allow cells to save energy and nutrients whilst the stress damage is resolved (Kaufman, 2002; Ron and Walter, 2007). eIF2α is essential for the assembly of the 43S preinitiation ribosomal complex and thus for translation initiation.

Consequently, eIF2α phosphorylation inhibits its action, reduces 43S preinitiation complex assembly and shuts down overall translation (Hinnebusch, Ivanov and Sonenberg, 2016; Young and Wek, 2016). This global protein synthesis reduction is accompanied by selective translation of privileged mRNA transcripts that escape p-eIF2α repression (Andreev *et al.*, 2015). These transcripts were shown to contain upstream open reading frames (uORFs), which are initiation codons found in the 5'-untranslated regions. Usually, when these uORFs are detected and translated, they promote ribosome dissociation from the mRNA preventing translation of their downstream coding region. However, during cellular stress, the uORFs are bypassed by scanning ribosomes, allowing for increased translation of their downstream coding sequence (Young and Wek, 2016). Amongst the transcripts harboring uORFs and being preferentially translated, are the main UPR^{mt} regulator ATF5 and the key UPR^{ER} factors ATF4 and COP (DDIT3) as described below (Vattem and Wek, 2004; Watatani *et al.*, 2008; Palam, Baird and Wek, 2011).

2.5. The unfolded protein response from the endoplasmic reticulum

The endoplasmic reticulum (ER), like the mitochondria, is critical for the maintenance of cellular protein homeostasis due to its significant role in protein synthesis and folding. As a result, it is also equipped with specialized molecular machinery to rapidly sense and resolve proteotoxic stress. These mechanisms constitute the unfolded protein response from the endoplasmic reticulum (UPR^{ER}). Various stimuli, including hypoxia, nutrient deprivation, calcium or redox imbalance, or translation defects, can induce misfolded protein accumulation within the ER lumen, disturbing the ER homeostasis and triggering the UPR^{ER} (Wang and Kaufman, 2016). Furthermore, it has been reported that mitochondrial dysfunctions can also lead to misfolded protein burden in the ER and activation of the UPR^{ER}, suggesting its contribution to the mitochondrial stress response. Indeed, Quirós and colleagues showed that treating mammalian cell cultures with four mitochondrial stressors, doxycycline, actinonin, FCCP and maneb - that respectively block mitochondrial translation, disrupt oxidative phosphorylation, decrease mitochondrial membrane potential, and block mitochondrial protein import - activated the integrated stress response (ISR) mainly regulated by ATF4 (Quirós *et al.*, 2017).

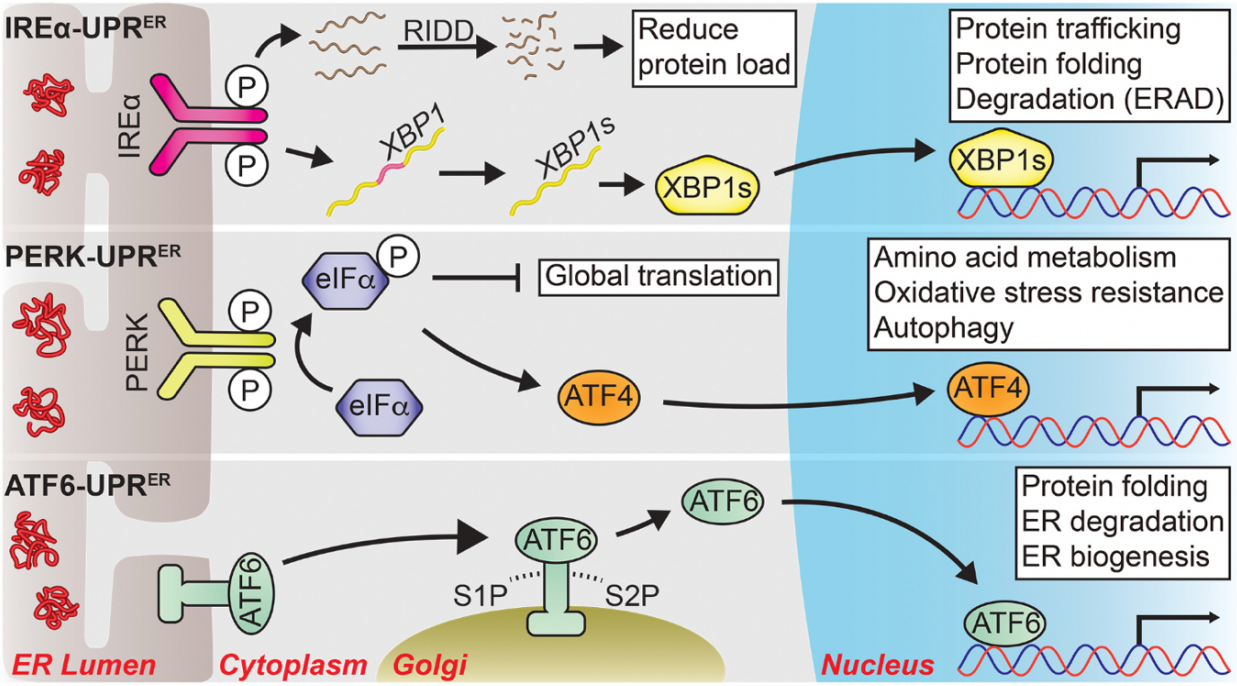

Figure 8. The main branches of the endoplasmic reticulum unfolded protein response. *(Adapted from* Wodrich et al., 2022*). ER stress triggers the activation of the UPR^{ER} made up of three distinct branches.*
IRE1α-UPR^{ER}: IRE1α is activated by dimerization and autophosphorylation. It can then cleave a group of mRNAs and miRNAs and mediate their degradation through IRE1-dependent decay (RIDD), to reduce the ER protein folding burden. IRE1α also activates XBP1 by splicing its encoding mRNA. XBP1s acts as a strong transcription factor that upregulates expression of protein quality control genes.
PERK-UPR^{ER}: PERK is also activated by dimerization and autophosphorylation. It can then phosphorylate eiF2α to suppress global translation and permit translation of selected transcripts, a process called the integrated stress response (ISR). The key transcription factor ATF4 is selectively translated and translocates to the nucleus to drive expression of genes involved in oxidative stress resistance, autophagy and amino acid metabolism.
ATF6-UPR^{ER}: upon stress and dissociation from BiP, ATF6 relocates to the Golgi body where it is cleaved by site-1-protease (S1P) and site-2-protease (S2P) into its transcriptionally active form, ATF6p50. It can then upregulate expression of protein folding enzymes as well as proteins involved in ER protein quality control.
Solid arrows: direct actions; dashed arrows: indirect or unclear mechanisms.

The first role of the UPR^{ER} is to sense stress and then to resolve the homeostatic disruption. To this aim, it triggers three coordinated but distinct pathways that stimulate parallel transcriptional and translational responses: the inositol-requiring enzyme 1 α (IRE1α)-, protein kinase RNA-like endoplasmic reticulum kinase (PERK)- and activating transcription factor 6 (ATF6)-mediated UPR^{ER} (Figure 7). These proteins all comprise a luminal stress-sensing domain within the ER that is bound by the ER chaperone Binding-Immunoglobulin Protein (BiP) to keep them silent under basal conditions (M. Wang & Kaufman, 2016). In the occurrence of ER stress, BiP dissociates from IRE1α, PERK and ATF6 to interact with misfolded proteins within the

ER, inducing activation of the UPR^{ER} signaling pathway (Hetz et al., 2020). The outcome of the UPR^{ER} is highly dependent on the severity and length of the proteotoxic stress: early UPR^{ER} effects are generally reported as a cytoprotective adaptive response, whereas prolonged unresolved stress triggers a switch to a cytotoxic response, with the PERK- and IRE1-arms coordinating to induce apoptosis (Chang et al., 2018; Fink et al., 2018).

2.5.1. PERK-mediated UPR^{ER}

ER proteotoxic stress stimulates the activation of the kinase PERK, *via* its dissociation from BiP, which allows it to undergo dimerization and autophosphorylation. Once it is activated, PERK can phosphorylate eIF2α at serine 51 as previously described (Hetz, Zhang and Kaufman, 2020). *ATF4* and *CHOP*, main effectors of the PERK-mediated UPR^{ER}, are amongst the genes that bypass the inhibition of general translation upon stress. The resulting ATF4 protein subsequently translocates to the nucleus to enact a cytoprotective response by inducing the transcription of genes implicated in antioxidant, amino acid metabolism and autophagy mechanisms (Lu, Harding and Ron, 2004; Vattem and Wek, 2004). Essential autophagy genes, such as MAP1LC3B and ATG5 that are involved in autophagosome biogenesis, were upregulated in an ATF4-dependent manner in response to ER stress, hypoxia and amino acid deprivation (Rzymski *et al.*, 2010; B'chir *et al.*, 2013; Deegan *et al.*, 2015). Increasing autophagic flux enables enhanced recycling of cytoplasmic components as well as ATP levels maintenance, which help the cell recover from the stress-induced damage. NRF2 (NFE2L2), a critical regulator of the antioxidant response was also shown to be transcriptionally upregulated by ATF4 following UPR^{ER} activation in mammalian cells (Sarcinelli *et al.*, 2020). NRF2 binds to the antioxidant response element (ARE) in the promoter of antioxidant enzyme encoding-genes and enhances their expression, including NAD(P)H:quinone oxidoreductase 1, TXN and ROS-detoxifying enzymes such glutathione peroxidase 2 (GPX2, Tonelli, Chio and Tuveson, 2018).

If the ER stress is persistent, a switch in the UPR^{ER} promotes apoptosis through interaction with downstream transcription factor C/EBP homologous protein (CHOP) (Quirós *et al.*, 2017). ATF4 also establishes a feedback loop to

dephosphorylate eIF2α and restore normal translation once ER stress is resolved, by upregulating the protein phosphatase 1 (PP1) regulatory subunit (GADD34) (Harding et al., 2003).

2.5.2. IRE1-regulated UPR^{ER}

First characterized in yeast, the IRE1/XBP1-mediated UPR^{ER} is the most conserved branch of the UPR^{ER} and was found to be required for yeast lifespan extension and stress resistance (Labunskyy *et al.*, 2014). IRE1 is a type 1 ER transmembrane protein kinase/endoribonuclease. Upon misfolded protein accumulation in the ER, IRE1α is freed from BiP, and is activated *via* dimerization and autophosphorylation (Zhou *et al.*, 2006). Active IRE1 was found to modulate unconventional splicing of the mRNA encoding for the powerful transcription factor X-box-binding protein 1 (XBP1), by excising a 26-nucleotide intron in metazoans, shifting the translational open reading frame (Yoshida *et al.*, 2001; Calfon *et al.*, 2002). Active spliced XBP1 (XBP1s) can then translocate to the nucleus and upregulate the expression of protein folding enzymes (PDIA6), ER molecular chaperones (DNAJC3, DNAJB9, DNAJB11 and PDIA3), and ER-associated protein degradation (ERAD) components (EDEM1, HERPUD1 and HRD1) to resolve ER stress (Hwang and Qi, 2018; Hetz, Zhang and Kaufman, 2020). Independently of XBP1, IRE1 initiates a process called regulated IRE1-dependent decay (RIDD), by which it cleaves selected mRNAs and miRNAs to induce their degradation (Maurel *et al.*, 2014). RIDD is believed to reduce the amount of mRNA to be translated and then folded in the ER, attenuating the ER protein burden. However, it was also found that sustained IRE1 activation triggered the decay of a number of microRNAs (miR17, miR34a, miR96 and miR125b), that are responsible for inhibiting the protease and apoptotic-initiator Caspase-2 (Upton *et al.*, 2012). Therefore, persistent IRE1α-UPR also seems to become cytotoxic and to promote apoptosis. The IRE1-UPR^{ER} was reported to also activate TRAF2 and JNK, implicated in autophagy and inflammation (Urano *et al.*, 2000; Sozen *et al.*, 2020; Liang *et al.*, 2022).

2.5.3. *ATF6-mediated UPR^{ER}*

Once liberated by BiP upon ER stress, the full length ATF6 (ATF6p90) protein translocates from the ER to the Golgi apparatus. There, it is sequentially cleaved by two proteases, S1P and S2P, to produce a final fragment containing a basic leucine zipper (bZIP) transcription factor 'ATF6p50' (Haze *et al.*, 1999; Ye *et al.*, 2000). ATF6p50 can then transit to the nucleus and stimulate the expression of ER chaperones and enzymes involved in protein folding and trafficking such as DNAJB11 and DNAJB9 (Wu *et al.*, 2007; Bommiasamy *et al.*, 2009). ATF6p50's and XBP1s' actions overlap to a certain degree, most probably to regulate the transcriptional output as a response to ER stress. This appears to occur *via* the formation of XBP1s/ATF6p50 heterodimers that promote crosstalk and co-regulation of gene transcription (Yamamoto *et al.*, 2007; Shoulders *et al.*, 2013).

2.5.4. *Interplay between the three UPR^{ER} branches*

Overall, the UPR^{ER} coordinates a response to ER proteotoxicity that aims to relieve ER stress and facilitate cell survival. However, as previously noted, sustained unresolved stress and thus prolonged activation of the UPR^{ER}, can induce pro-apoptotic signaling from both the PERK- and IRE1α branches. The three arms of the UPR^{ER} act in coordination with each other and reports suggest a chronology to their respective activation, although the evidence remains contradictive and lacking. Some studies suggest the branches reliant on ATF6 and IRE1α are rapidly activated upon ER stress and can be attenuated with time, through elusive mechanisms. In this scenario, PERK-mediated UPR^{ER} would follow the first two pathways and be mainly activated under chronic stress (Rutkowski *et al.*, 2006; Lin *et al.*, 2007; Wang and Kaufman, 2016). However, it has also been suggested that PERK mediates the immediate adaptive response to ER stress (Ron and Walter, 2007; Hetz, Zhang and Kaufman, 2020). Therefore, the chronology of UPR^{ER} branches activation remains to be properly elucidated.

2.5.5. Links between the UPR^{ER}, aging and PD

Many studies have linked changes in the UPR^{ER} to aging, with initial studies showing a weakening in the UPR^{ER} response with age in *C.elegans* (Ben-Zvi, Miller and Morimoto, 2009; Taylor and Dillin, 2013). This was confirmed in the aged mouse brain, where sleep deprivation-mediated activation of the UPR^{ER} was diminished (Naidoo *et al.*, 2011). More recently, senescent human lung fibroblast cultures were shown to retain the capacity to sense stress properly but to be unable to efficiently coordinate an appropriate transcriptional response *via* the UPR^{ER} (Sabath *et al.*, 2020). Therefore, the capacity to trigger the UPR^{ER} appears to decline with age, suggesting that restoring UPR^{ER} functionality could improve lifespan. Several studies in *C. elegans* have revealed an important role for IRE1α and XBP1 in promoting longer lifespan *via* interaction with daf-16 (FOXO3 ortholog in worms) to upregulate ER stress resistance factors (Henis-Korenblit *et al.*, 2010). IRE1α was also shown to contribute to lifespan extension, whereby dietary restriction promoted ERAD activity and improved proteostasis with age in *C. elegans* (Matai *et al.*, 2019). Regarding the PERK-mediated UPR^{ER}, acute activation of the pathway-maintained homeostasis and was cytoprotective, whereas chronic PERK activation shortened lifespan through gut dysplasia (Wang *et al.*, 2015). Moreover, reducing PERK activity in aging mice was favorable, with age-related memory and neuronal excitability decline being rescued (Sharma *et al.*, 2018). Interestingly, suppressing PERK did not always have beneficial effects depending on the cell type: PERK deletion specifically in mouse DA neurons provoked motor and cognitive consequences, due to the dysregulation of dopamine release and of *de novo* translation (Longo *et al.*, 2021).

The contribution of the UPR^{ER} has become of increased interest in the study of neurodegenerative diseases (Hughes and Mallucci, 2019; van Ziel and Scheper, 2020). Hoozemans and colleague were the first to show that the UPR^{ER} is modulated in PD, reporting increased protein levels of p-PERK and p-eIF2α in *SNpc* DA neurons of human postmortem tissue from PD patients, in comparison to age-matched controls (Hoozemans *et al.*, 2007). Large increase in the levels of BiP and p-PERK were also detected in the cingulate gyrus and parietal cortex in postmortem brain tissue of patients with dementia with Lewy bodies and Parkinson's disease dementia, when compared to Alzheimer's disease patients and age-matched controls (Baek *et al.*,

2016). Interestingly, BiP levels were significantly correlated with α-syn pathology in the cingulate gyrus. However, a more recent study reported an increased in mRNA but not protein levels of BiP in several brain regions of patients with PD, including the cingulate gyrus (Baek *et al.*, 2019). UPR^{ER} dysregulation in PD was further evidenced by the account of reduced protein expression of BiP and ATF4 and increased CHOP levels in *SNpc* postmortem tissue from PD patients (Selvaraj *et al.*, 2012; Esteves and Cardoso, 2020). Additionally, elevated p-IRE1α levels were detected in neurons containing high α-syn levels or Lewy Bodies in patients' postmortem tissue (Heman-Ackah *et al.*, 2017). Moreover, α-syn aggregates were shown as accumulated in ER microsome fractions of human PD brain tissue, suggesting a direct relationship between α-syn and activation of the UPR^{ER} (Colla *et al.*, 2012). Altogether this data presents solid evidence that dysregulated UPR^{ER} is associated with PD and with α-syn pathology.

In vitro and *in vivo* animal PD model studies treated with neurotoxins corroborated the previous findings. Treatment with rotenone provoked the induction of a pro-apoptotic response reliant on IRE1α and Caspase-12 in a rat model (Tong *et al.*, 2016). MPTP mice PD model showed increased mRNA levels of BiP and CHOP (Selvaraj *et al.*, 2012), and intracerebral MPP+ injections in rabbit induced ATF6 activation in the *SNpc* (Ghribi *et al.*, 2003). BiP, CHOP and Caspase-12 proteins were also overexpressed in rats treated with 6-OHDA in the SN and corpus striatum regions (Cai *et al.*, 2016).

More recently, data collected in iPSC-derived neurons also confirm the implication of the UPR^{ER} in PD pathophysiology. Cortical neurons derived from iPSC containing a triplication in the SNCA gene presented activation of the IRE1α-XBP1 branch of the UPR^{ER} (Heman-Ackah *et al.*, 2017). DA-neuron derived from cell lines from three unrelated PD patients heterozygous for the GBA-N370S mutation also showed upregulation of BiP and IRE1α (Fernandes *et al.*, 2016).

The role of the IRE1α-UPR^{ER} in PD pathophysiology has been particularly investigated compared to the other two branches. A neuroprotective role for XBP1s against DA neuron loss was reported in MPP+-treated and 6-OHDA-treated PD mice models (Sado *et al.*, 2009; Valdés *et al.*, 2014). On the other hand, IRE1α induction drove JNK- and autophagy-mediated neurodegeneration in *Drosophila* presenting overexpression of wild type or missense α-syn mutant (Carreras-Sureda *et al.*, 2019;

Yan *et al.*, 2019). Diminished IRE1α expression resulted in reduced neuronal loss. Based on this data, the XBP1s-mediated response, downstream of IRE1α, could have a cytoprotective effect in PD pathology, whilst XBP1-independent IRE1 signaling appears to be deleterious.

The PERK- and ATF6-mediated branches of the UPR^{ER} have been less well examined in the context of PD pathogenesis. Nevertheless, deletion of the pro-apoptotic effector CHOP, downstream of PERK, was protective against DA neuronal death in 6-OHDA-treated mice but in MPTP-treated mice, suggesting a variable role for CHOP dependent on the toxic stimulus (Silva *et al.*, 2005). The PERK-UPR^{ER} could thus be a cytotoxic stress response in dopaminergic neurons. On the other hand, ATF6 overexpression following MPP+ treatment, activated astrocytes and upregulated ER chaperones and ERAD factors to protect DA neurons from apoptosis (Egawa *et al.*, 2011; Hashida *et al.*, 2012). Vidal and colleagues recently showed that viral-mediated delivery of an XBP1/ATF6 protein heterodimer, thus activating the UPR^{ER}, appeared to enhance α-syn aggregates degradation in an *in vivo* PD mouse model and favors DA neuronal survival following 6-OHDA treatment (Vidal *et al.*, 2021). This suggests a potential neuroprotective role in PD mediated by XBP1s in interaction with ATF6.

2.5.6. Interactions between the ER and mitochondria at mitochondrial-associated ER membranes

A growing body of evidence reports that mitochondria are widely associated with the ER. Interactions between the two organelles occur, most importantly, through their membrane structures *via* physical contact points named mitochondria-associated ER membranes or MAMs (Xia *et al.*, 2019; Yang *et al.*, 2020). At these locations the membranes of the two structures are very close but do not fuse, allowing both organelles to retain their biological integrity. Electron and fluorescence microscopy have shown that the mitochondria and the ER may interact within a distance of about 10-20 nm (Csordás *et al.*, 2006; Giacomello and Pellegrini, 2016). The MAM contact points remain relatively stable, even when the ER and mitochondria move along the cytoskeleton. MAMs allow for the ER and mitochondria to coordinate a range of biological functions, including calcium signaling, apoptosis regulation, ER stress response and inflammation (Xia *et al.*, 2019). Under basal conditions, MAMs are

essential for lipid synthesis and trafficking as well as calcium transfer from the ER to mitochondria, essential for regulating mitochondrial dynamics and biogenesis (Marchi, Patergnani and Pinton, 2014). Upon exposure to difference stressors, MAMs are implicated in distinct processes. For instance, ER stress causes the accumulation of misfolded proteins in the ER. As a result, the ER triggers the UPR through which novel protein synthesis is blocked and molecular chaperones are induced to assist in protein folding. Such chaperones consume large amounts of ATP. To meet these energetic demands, contact area between the ER and mitochondria are increased to facilitate the passage of ATP from mitochondria to the ER and of calcium from the ER to the mitochondria (Bravo *et al.*, 2012; van Vliet and Agostinis, 2018). Interestingly, the presence of the UPR^{ER} main actor PERK in MAMs has been reported by several studies (Kato *et al.*, 2020; Fan and Jordan, 2022). MAM-residing PERK appears to play a role in mediating apoptosis upon severe oxidative stress. Indeed, the absence of PERK reduced ER stress-induced apoptosis as a result of less MAM formation and dysfunctional ROS signal transmission to mitochondria (Verfaillie *et al.*, 2012; Liu *et al.*, 2013). IRE1 was also localized to MAMs in several studies and was reported to operate as a scaffold in MAMs and determined the distribution of inositom-1,4,5-triphosphate receptors in these contact points (Carreras-Sureda *et al.*, 2019). In this study, IRE1 deficiency impacted mitochondrial physiology and metabolism in basal conditions. Interestingly, this function was independent of the UPR. Furthermore, mTOR signaling was shown to modulate IRE1 availability and activation at MAMs (Sanchez-Alvarez, del Pozo and Bakal, 2017). This mechanism was suggested to tightly regulate activation of IRE1 following UPR^{ER} engagement to prevent the cytotoxicity its sustained activity would cause. In line with this, IRE1 was shown to operate as part of the UPR^{ER} in MAMs, whereby it translocated to MAM upon ER stress and activated XBP1 in a cytoprotective manner (Riaz *et al.*, 2020). There is less data regarding ATF6 activity at the MAM, although it was reported that ATF6 activation conferred longevity in *C.elegans* by regulating ER calcium release to the mitochondria *via* the inositol triphosphate receptor (Burkewitz *et al.*, 2020). Our understanding of the interactions between mitochondria and the ER at MAMs and their role in cellular health is lacking. However, these bridges between the two organelles have revealed how important communication between them is crucial for cell survival and proper functioning of a number of essential physiological and stress response processes.

3. Long non-coding RNAs

3.1. Non-coding RNA: from junk DNA to essential regulatory elements

Historically, genomic research has predominantly focused on protein-coding genes (PCG) and their encoded proteins. In 2001, the human genome was first sequenced (International Human Genome Sequencing Consortium, Nature, 2001) and surprisingly revealed that protein-coding exons only made up less than 2% of the genome. Furthermore, with recent advances in high throughput sequencing technology, it is now accepted that a large part - more than 75% - of the genome is transcribed (Djebali *et al.*, 2012). The non-coding part of the human genome was initially dismissed and regarded as non-functional “junk DNA” or transcriptional “noise”. Accumulating evidence has however shown that it can encode diverse functional non-coding RNAs (ncRNA), that play essential roles in various biological processes, mainly by regulating gene expression at the transcriptional and post-transcriptional levels (Palazzo and Lee, 2015).

Interestingly, there appears to be a strong correlation between the proportion of ncRNAs and the complexity of an organism, here defined as cellular diversity, whereas the number of PCGs seems to be rather similar across a large variety of species (Figure 8; Liu, Mattick and Taft, 2013). This feature of ncRNAs suggests they are at least partly functional and may play an intriguing role in bestowing this cellular complexity of organisms. As a result, the notion of RNA, simply as an intermediate between DNA and protein, has become obsolete, expanding the field of genomic and transcriptomic analysis to further identify and examine ncRNAs that could be central to numerous fundamental biological processes.

This non-coding transcriptome comprises several classes of RNAs that have more or less defined roles in critical cellular processes. They include transfer RNAs (tRNAs) and ribosomal RNAs (rRNAs), involved in mRNA translation; small nuclear RNAs (snRNAs) that participate in messenger RNA (mRNA) splicing; and microRNAs that are known to regulate gene expression post-transcriptionally. The most abundant class of these ncRNAs, albeit still poorly understood, has attracted growing interest in biomedical research as they appear to be versatile regulators of many cellular processes: long non-coding RNAs.

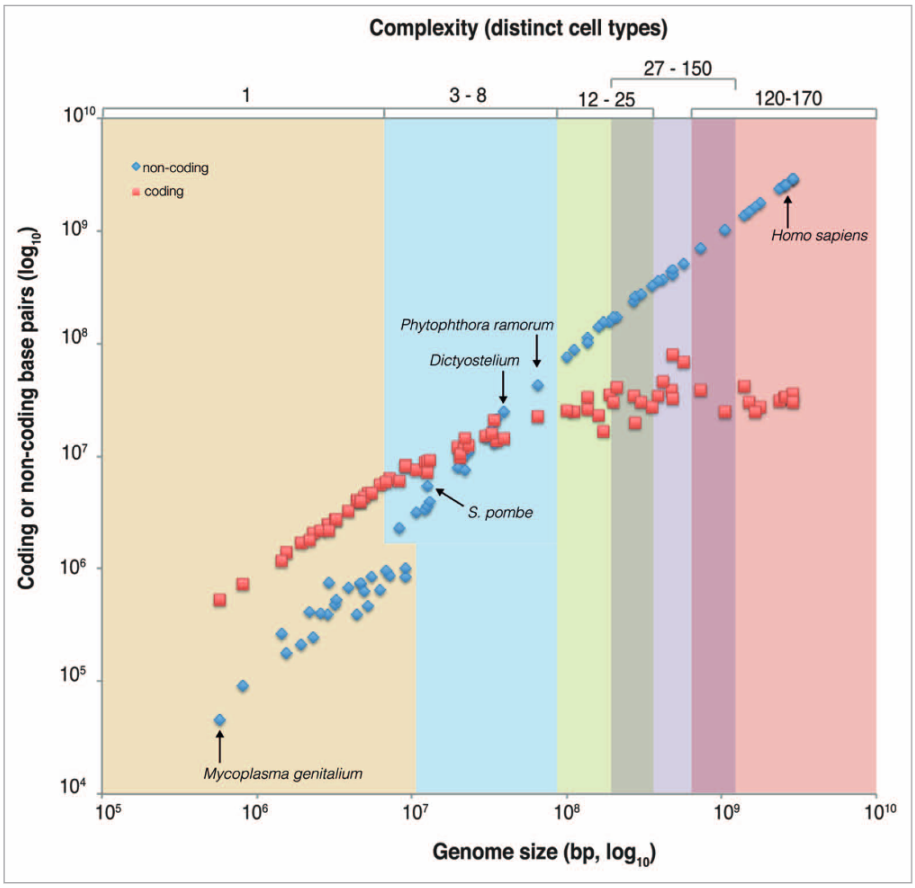

Figure 9. Relationship between biological complexity and genome composition. *Every organism is plotted as a pair of data points: a blue point for the total non-protein coding bases, and a red point for the total protein-coding sequence bases, which cumulate to give the total genome size (x-axis). The complexity of the genome is calculated based on the distinct cell types previously identified for each organism. The total non-protein-coding bases increase exponentially with the complexity of the organism whereas, the total protein-coding sequence is asymptotic, with the intersection between both happening among simple multicellular organisms. (Adapted from Liu, Mattick and Taft, 2013).*

3.2. Long non-coding RNAs: definition

Long non-coding RNAs (lncRNAs) are primarily defined by exclusion criteria: they are transcripts greater than 200 nucleotides in length and have no predicted protein coding potential. Many computational approaches, such as CPAT (Coding Potential Assessment tool), CPC2 (Coding Potential Calculator 2), CNIT (Coding-Non-Coding Identifying Tool), and RNAsamba, are used to predict a transcript's coding potential that are mainly reliant on identifying RNA sequence features (Li, Zhang and Liu, 2020; Chowdhary, Satagopam and Schneider, 2021). This includes open reading frame (ORF) length, integrity and isoelectric point, poly(A) enrichment, as well as the Fickett TESTCODE score and the hexamer score (Kang *et al.*, 2017a; Guo *et al.*, 2019). The Fickett score is used to assess the preference and composition frequency of each base in codons of the full length transcript, and the hexamer score takes into account the combination frequency of six adjoining bases in the transcript (Fickett and Tung, 1992; Wang *et al.*, 2013a). It is important to note that generally ORFs longer

than 100 codons are classified as coding transcripts, although this is not a definite cutoff as some exceptions were found: for example the lncRNAs XIST and H19 were shown to have longer ORFs (Jalali *et al.*, 2015; Chowdhary, Satagopam and Schneider, 2021).

The 200 base pair size cutoff allows to differentiate lncRNAs from a range of smaller non-coding elements such as tRNAs, snRNAs, snoRNAs and microRNAs (miRNAs). It also means that they make up a large and heterogeneous group of ncRNAs. Many databases compiling these elements in the human genome exist, with differing criteria, including:

- NONCODEV6, which indicates 173,112 lncRNA transcripts identified in the human genome (Zhao *et al.*, 2021).
- The LINCipedia version 5.2 database, which presently contains 127,802 human lncRNA transcripts (Volders *et al.*, 2019).
- The more stringent GENCODE database, which currently holds 56,357 human lncRNA transcripts (version 44, July 2023; gencodegenes.org).

The difference in the number of transcripts between these databases is related to the number of isoforms that they reference. Due to the complexity of lncRNA alternative splicing, as well as alternative promoters and polyadenylation sites, an important number of isoforms are reconstructed for each lncRNA. NONCODE and LINCipedia compile these more comprehensively, while GENCODE, based on transcript structure by relying on expressed sequence tags (EST) and cDNA data, contains fewer but rather accurate isoforms (Iyer *et al.*, 2015; Kanitz *et al.*, 2015; Ulitsky, 2016).

High throughput sequencing revealed that lncRNAs share many similarities with mRNA transcripts. Indeed, a large number seem to be transcribed by RNA Polymerase II (RNA Pol II) (Guttman *et al.*, 2009). However, a study used α-amanitin, a specific RNA Pol II inhibitor, and interestingly found that some lncRNAs were still transcribed with 10% being upregulated (Nakaya *et al.*, 2007). This suggests that these transcripts can also be synthesized by RNA Polymerase III or single polypeptide nuclear RNA polymerase IV. LncRNAs are also often found to be 5'-capped (Guttman *et al.*, 2009), polyadenylated and to go through alternative splicing, although less efficiently than mRNA (Ulitsky and Bartel, 2013; Melé *et al.*, 2017). As such, a single lncRNA gene locus can give rise to one or several transcripts that can contain one or multiple differentially spliced exons.

An increasing number of lncRNAs are found to play important roles in a range of biological processes as an accumulating number of studies investigate different lncRNAs. This includes transcripts implicated in cell pluripotency and differentiation (Sherstyuk, Medvedev and Zakian, 2018), programmed cell death (Jiang *et al.*, 2016), mitochondrial respiration and mitophagy (S.-H. Wang *et al.*, 2021). As lncRNAs appear to be involved in essential cellular functions, it can be expected that their changed expression could cause dysfunctions at many levels and participate in the physiopathology of many diseases. In line with this, it is well-documented that numerous lncRNAs have their expression levels altered in response to different stressors such as oxidative stress (Giannakakis *et al.*, 2015) and in a variety of disorders (Statello *et al.*, 2021), including neurodegenerative and other neurological disorders (Aliperti, Skonieczna and Cerase, 2021), cancers (Chi *et al.*, 2019) and cardiovascular disease (Poller *et al.*, 2018; Monteiro *et al.*, 2019). Such arguments have strengthened the notion of lncRNAs as physiologically relevant elements and as important molecular actors to study in the context of various biological processes and disorders.

Nevertheless, the functionality of a large number of lncRNAs remains unknown. Consequently, it is still debated how many lncRNAs are functional or are transcription by-products, as proof of function is lacking for most lncRNAs. A certain level of “junk” RNA can be expected given our knowledge of evolution: random mutations and the displacement of a few base pairs may result in the formation of transcription start sites and transcription factor binding sites (Palazzo and Lee, 2015). As a result, a sequence may become randomly transcribed and if it is not deleterious to the organism, may be tolerated by natural selection and retained.

3.3. LncRNA proposed classifications

The abundance of lncRNAs and their heterogeneity relative to their genomic origins, biogenesis and potential modes of action called for ways to categorize these elements.

3.3.1. Classification by genomic organization

Our limited but ever-growing understanding of lncRNAs mean that we still do not have clear knowledge of their sequence-structure-function relationship. In consequence, they are often annotated by their genomic organization, that is, their location relative to the closest PCG (Figure 10). Many such categories have been defined in literature; here we applied the classification devised by the Lncipedia database as follows:

- If the lncRNA overlaps a PCG on the same strand: the lncRNA is intronic if there is no overlap with protein-coding exons, otherwise the lncRNA is sense overlapping.
- If the lncRNA overlaps a PGC on the opposite strand, it is an antisense lncRNA.
- If the lncRNA does not overlap any protein coding gene: it is bidirectional if the transcription start site of the PGC is within 1kb of the lncRNA transcriptional start site. Otherwise, the lncRNA is intergenic.

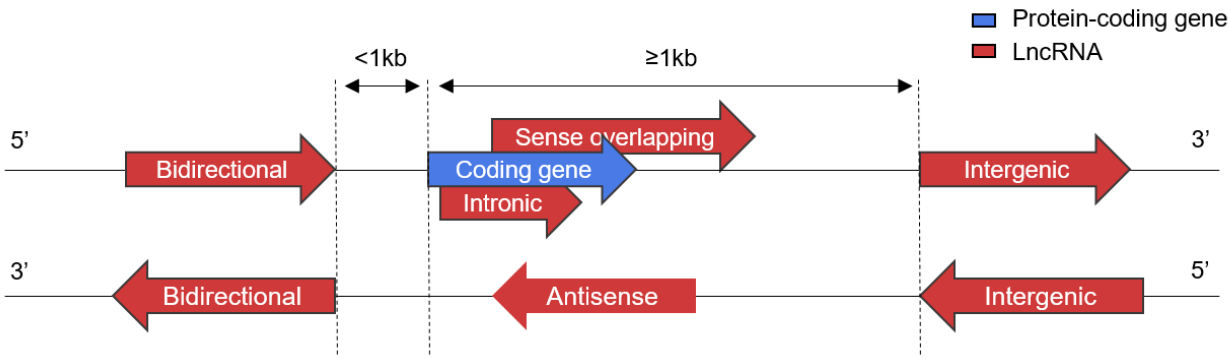

Figure 10. Classification of long non-coding RNAs based on their location relative to the nearest protein-coding gene. *The protein-coding gene is in blue whereas the lncRNAs are in red.*

3.3.2. Classification by length

As described earlier, lncRNAs are defined and differentiated from other ncRNAs by their length: they have to be at least 200 bp long. However, this bottom-line cutoff does not exclude that lncRNAs may have highly varying lengths. Some lncRNAs, dubbed macro lncRNAs or very long intergenic lncRNAs (vlncRNAs) have been described as longer than 10 kb (Kornienko *et al.*, 2013).

3.4. LncRNAs show highly specific expression patterns

3.4.1. Tissue and cell-type specificity

Despite the previously described similarities with PCGs, lncRNAs are present at lower levels overall and exhibit distinct expression patterns (Djebali *et al.*, 2012; Morán, Akerman, van de Bunt, *et al.*, 2012; Ulitsky and Bartel, 2013). They notably appear to be more tissue- and cell-type specific than PGCs, with a growing number of studies differentiating between:

- a minority of ubiquitously expressed (UE) lncRNAs that display higher expression levels overall, such as MALAT1, TUG1, NEAT1, XIST, HOTAIR and many others (Bhan and Mandal, 2015; Zhang, Hamblin and Yin, 2017; Lin *et al.*, 2018; C. Guo *et al.*, 2020; W. Wang *et al.*, 2021; Monroy-Eklund *et al.*, 2022).
- a majority of tissue-specific (TS) lncRNAs that are often selectively expressed in distinct cell-types and subcellular structures (Morán, Akerman, van de Bunt, *et al.*, 2012; Deveson *et al.*, 2017; Jarroux, Morillon and Pinskaya, 2017; Gendron *et al.*, 2019; de Goede *et al.*, 2021)

Strikingly, the brain and the testis were found to be particularly rich sources of specifically expressed lncRNAs (Derrien *et al.*, 2012; Washietl, Kellis and Garber, 2014; Ward *et al.*, 2015; de Goede *et al.*, 2021). Within the brain, significantly different transcriptome patterns were uncovered for white and grey matter, mainly at the level of lncRNAs, which could underlie the distinct identity and functions of each region (Mills *et al.*, 2013). This variability across tissues is believed to arise from their distinctive cell-type populations and to be even more so dependent on the cell type identity. In the human neocortex, single RNA-seq analysis highlighted that although lncRNAs

commonly exhibited low expression in bulk tissues, many were abundantly present when looking at individual cell-types (Liu *et al.*, 2016).

Many other transcriptomic studies confirmed a high tissue-specificity for lncRNAs. A study identified 1128 lncRNAs in human islet cells by RNA-seq and realigned them with 16 human non-pancreatic RNAs-seq datasets to find approximately 43% that were never annotated before and therefore likely to be islet-specific (Morán, Akerman, van de Bunt, *et al.*, 2012). Moreover, this specificity was confirmed by RT-qPCR for 12 lncRNAs.

Cabili and colleagues collected RNA-seq data from 24 human tissues and cell lines to generate a human lncRNA catalogue (Cabili *et al.*, 2011). 4273 lncRNAs were identified and annotated. To assess tissue specificity, this study attributed an entropy-based score to each lncRNA by quantifying the similarity between a lncRNA's expression pattern across tissues and another predefined pattern corresponding to the event that a transcript is only expressed in one tissue. 78% of lncRNAs were tissue-specific in comparison to about 19% of PCGs. These results were not simply due to poorly expressed lncRNAs being difficult to detect in some tissues and were well-reflected in 35% of the more highly expressed transcripts.

Moreover, our team assembled the lncRNA repertoire of E14.5 mice ventral mesencephalic dopaminergic (DA) neurons and found that 72.6% were novel transcripts that had never been previously identified, suggesting strong cell-type specificity (Gendron *et al.*, 2019). Comparing DA neurons with ventral hindbrain serotonergic (5-HT) neurons that develop from adjacent neuroepithelial regions specified by the same combination of morphogenes (SHH and FGF8), it was shown that only 165 out of 2060 total lncRNAs identified in both cell types were commonly expressed. The remaining transcripts were specific to DA (767 lncRNAs or 82.3%) or 5-HT neurons (1128 lncRNAs or 87%), confirming the strong relationship between cell type identity and lncRNAs' expression. In comparison, 55.5% of DA neuron-specific and 59.4% of 5-HT neuron-specific mRNAs were identified. This study did not exclude monoexonic lncRNAs that had clear ATAC-seq signal overlapping their transcription start site (73.1% of novel lncRNAs and 16.9% of previously annotated lncRNAs), which means that the observed cell-specificity and number of newly discovered lncRNAs could be partly due to a bias linked to the lack of annotation of monoexonic lncRNAs. However, this doesn't rebut the large number of cell-specific lncRNAs that were

identified using the same criteria for both cell types and the fact that these single exon transcripts are still specific to the cell type.

3.4.2. Temporal specificity

Furthermore, lncRNAs' expression appears not only spatially dependent but also temporally, with expression levels varying throughout development and adulthood indicating a potential timing-specific biological role (Ward *et al.*, 2015; Jarroux, Morillon and Pinskaya, 2017). In macaques, high throughput sequencing identified a large number of spatial-temporal lncRNAs that were selectively expressed in 1 of 4 tissues (brain, colon, liver and lung) but also in 1 of 3 developmental stages (Li *et al.*, 2015, p. 20). Genome-wide transcriptional analysis in the human brain also revealed that the specific expression of lncRNAs across several brain regions was developmentally regulated, with the most distinctive lncRNAs expression patterns found in the cerebellar cortex (Zhang, Hamblin and Yin, 2017). Interestingly, this study highlights the dramatical alterations of the lncRNA transcriptome during fetal development, in contrast to its seemingly much more stable state after birth and until late adulthood.

The observed specific expression patterns of lncRNA and the consistency in this specificity across different models are strong arguments in favor of their functional relevance as potential biomarkers and regulatory elements defining the complexity of various tissues, cell-types as well as developmental stages. Some have argued that only the abundant and thus ubiquitously expressed lncRNAs were likely to be of importance regarding cellular biological function as low expression may not be compatible with a potent input. However, certain functions may not require high expression, such as a lncRNA acting as a scaffold to regulate chromosomal architecture or would require high expression only at specific sites and timings, which could be difficult to accurately detect (Palazzo and Lee, 2015). This suggests that highly expressed lncRNAs could contribute to biological processes shared between diverse cell types, such as proliferation or regulation of alternative splicing (Zhang, Hamblin and Yin, 2017), while the more specifically expressed lncRNAs, would contribute to processes linked to specific cell type or tissue identity, such as phenotypic and functional variations (Jarroux, Morillon and Pinskaya, 2017). Furthermore, the low expression of lncRNAs may be due to the use of bulk transcriptomic analysis. Single cell transcriptomics have reported that some lncRNAs usually displaying low

expression in bulk tissue analysis, were strongly expressed in individual cells (Liu *et al.*, 2016; Deveson *et al.*, 2017).

3.5. LncRNAs show rapid sequence turnover and several conservation levels

Functional exploration of non-coding elements has mainly relied on studying evolutionarily conserved patterns within transcripts' genes, RNA sequences as well as interaction partners. Comparative analysis of genes across species are thus harnessed to infer functional relevance of novel elements (Diederichs, 2014; Palazzo and Lee, 2015; Ulitsky, 2016). This paradigm was essential to study miRNAs, predict their targets and their potential function (Bartel, 2009; Auyeung *et al.*, 2013). In the past two decades, the genomes of a number of species have been deeply sequenced, which allowed for more thorough comparison of annotated lncRNAs across these species (Ulitsky, 2016). A conspicuous feature of lncRNAs emerged from such analysis: most of them display poor primary sequence conservation in comparison to PCGs and other ncRNAs, suggesting greater species-specificity. Despite this rapid evolutionary turnover, lncRNAs are not evolutionarily neutral and appear more conserved than introns or random intergenic sequences (Ulitsky and Bartel, 2013; Ransohoff, Wei and Khavari, 2018). On the other hand, lncRNA exons evolve at a faster pace than coding exons or untranslated regions of PCGs (UTR). This makes orthology analysis very challenging in lncRNAs, impeding the search for functional transcripts. Nevertheless, some focal points have emerged from the ever-increasing number of multi-species lncRNAs studies, that are addressed in the following subsections.

3.5.1. A minority of lncRNAs show evolutionary sequence and splicing conservation

A subset of lncRNAs is still found to be highly conserved across various species, although this remains a small minority. Mapping of the mouse genome found homologous lncRNAs for about 13.26% of annotated lncRNAs in humans (Yue *et al.*, 2014). Even when focusing on a specific tissue, similar results are obtained: only 60% of lncRNAs identified in the mouse liver were homologous to lncRNAs annotated in rat liver, and 27% were homologous to human liver lncRNAs (Kutter *et al.*, 2012).

Additionally, few lncRNAs conserve their exon-intron architecture: about 20% of splicing events in human lncRNAs are maintained outside of primates (Washietl, Kellis and Garber, 2014). One of the most studied lncRNAs metastasis-associated lung adenocarcinoma transcript 1 (MALAT1), is one of the few strongly expressed and remarkably conserved lncRNAs in species ranging from humans to zebrafish and is known to be involved in a number of important cellular processes including pre-mRNA alternative splicing (Zhang, Hamblin and Yin, 2017). This lncRNAs exhibits a 3'-end triple-helical tertiary structure that folds onto itself to protect the transcript from exonuclease-mediated decay (Monroy-Eklund *et al.*, 2022).

3.5.2. Highly conserved lncRNAs exhibit shorter alignable sequences than mRNAs

Interestingly, only short patches of the highly evolutionarily preserved lncRNAs' primary sequences seem to be conserved among homologous transcripts (Ulitsky, 2016). These alignable stretches are approximately five times shorter than those found in PCGs, with roughly 20% of a lncRNA's sequence being homologous in the human and mouse genomes (Hezroni *et al.*, 2015). Therefore, the subset of highly conserved lncRNAs seem subjected to weaker evolutionary constraints than PCGs. These conserved patches present a significant bias towards the 5'-end promoter regions of those lncRNAs, suggesting sequence-specific functions could arise from the 5'-end (Kretz *et al.*, 2013; Hezroni *et al.*, 2015). On the other hand, the 3'-end exhibits an overall faster sequence turnover, potentially contributing to more species-selective functions. The conservation of such short sequence patches also raises the hypothesis that lncRNA function may rely on shorter elements that do not require specific surrounding sequences to be effective (Ulitsky, 2016). A proposed example for such function, is lncRNAs that may act as competing endogenous RNAs (ceRNAs) and whose sequence only needs to contain a short binding site for miRNAs or RNA-binding proteins. It is also suggested that the conserved location of these lncRNAs may be important for their functions, and they would most likely regulate gene expression around their loci. An example of a lncRNA with short conserved sequence but differing exon-intron structure is the lnc-ONECUT1, that is located downstream of the gene ONECUT1 in both the human, mouse and other vertebrates' genomes as reported by the Encyclopedia of DNA Elements or ENCODE project (ENCODE Project

Consortium, 2012; Ulitsky, 2016; Luo *et al.*, 2020). Few splice sites are conserved in such a lncRNA.

3.5.3. LncRNA conservation displays several dimensions/levels

With the increase in lncRNA studies, the need for new paradigms of conservation, that do not just rely on sequence comparison analysis, became more and more apparent. Apart from primary sequence conservation patterns as previously described, secondary structure conservation has also been investigated. Selective constraints enforced on structure and not primary sequence could explain the evolutionary poor sequence conservation of lncRNAs. LncRNAs do fold into secondary structures that appear stable in many cases, however no significant correlation was found between primary sequence conservation and the amount of secondary structure of a lncRNA (Managadze *et al.*, 2011; Spitale *et al.*, 2015).

Examples of lncRNAs that act through conserved structural elements includes the previously described MALAT1 (Zhang, Hamblin and Yin, 2017), but also other well-studied lncRNAs such as NEAT1, a transcript essential for paraspeckle formation and highly structurally organized within the paraspeckle, which will be described further in part 3.7.2 (Lin *et al.*, 2018). Both these lncRNAs contain triplex elements, which consist of three strands of RNA, two forming a Watson-Crick duplex and the third interacting with the duplex's major groove to form Hoogsteen and reverse Hoogsteen hydrogen bonds (Wilusz *et al.*, 2012; Devi *et al.*, 2015; Wang, Li and Huang, 2020). MALAT1 and NEAT1 lack poly(A)-tails at their 3'-end and are instead stabilized by this triple helical structure that allows for their abundant transcription. MALAT1 and NEAT1's 3'-end triplex elements were also shown to act as a translational enhancer in a study using HeLa cells although it is still unsure how this capacity plays a role in these lncRNAs' functions (Wilusz *et al.*, 2012). One hypothesis is that these lncRNAs interact with translational machinery through this triple helix elements and act as sponges to keep the machinery away from specific mRNAs. A more recent study by McCown and colleagues examined 53 MALAT1 homologs from a number of human cell lines including HEK293, HeLa, and HepG2 cells and identified a larger evolutionary conserved core consisting of numerous helices and containing the established triplex element (McCown *et al.*, 2019). This core mediates some of the well described MALAT1-protein interactions, such as the binding of TDP-43, a protein playing critical

role in frontotemporal dementia and amyotrophic lateral sclerosis (Guo *et al.*, 2015; Ratti and Buratti, 2016).

Overall, associating function to specific secondary structures remains difficult in most cases and there is still little evidence of evolutionary selection of specific structures except for certain lncRNAs (Ulitsky, 2016; Szcześniak *et al.*, 2021). The use of structure-based homology has however already proven to be useful and will surely grow with our knowledge of these non-coding elements. Indeed, this technique was harnessed to identify homologues of roX lncRNAs, a transcript central to chromosome X dosage in male *Drosophila*, in various Drosophila species across about 40 million years of evolution (Quinn *et al.*, 2016).

Several studies have highlighted positional conservation of lncRNAs, based on hypothesis that in some cases, transcription of a lncRNA locus may be of greater importance than the RNA product itself (Kornienko *et al.*, 2013; Statello *et al.*, 2021). Such a situation would require the lncRNA locus to be conserved as well as short splicing motifs to permit transcription elongation, but not the bulk of the lncRNA sequence. A number of syntenic lncRNAs have been discovered across distant species: such transcripts are found in the same chromosomal region and in the same relative orientation to surrounding PCG orthologues, but do not necessarily display alignable sequences (Hezroni *et al.*, 2015; Mohammadin *et al.*, 2015). Strikingly, numerous lncRNAs annotated in humans were found to have their position and sequence conserved in various mammals, but only had their locus conserved and not their sequence in more distant species. Such findings emphasize the importance of considering synteny when analyzing lncRNAs' evolution and function, but also reiterate the species-specificity of lncRNAs. However, identifying syntologous lncRNAs remains difficult as it relies on having access to high-quality annotations for all the species of interest, which are not always available.

A lot of unanswered questions remain regarding the conservation of lncRNAs across different species and what this would mean regarding their potential functions. Ulitsky proposed a paradigm of lncRNA conservation that summarizes well the possibilities previously explored (Figure 10; Ulitsky, 2016). To conclude on this part, it is important to note the significant lesser evolutionary retainment of lncRNAs compared to mRNA, making them particularly pertinent to study in species-specific contexts. Continued exploration of the different conservation models for these ncRNAs, that we

are only beginning to unravel, will also be crucial in expanding our knowledge of lncRNA functionality.

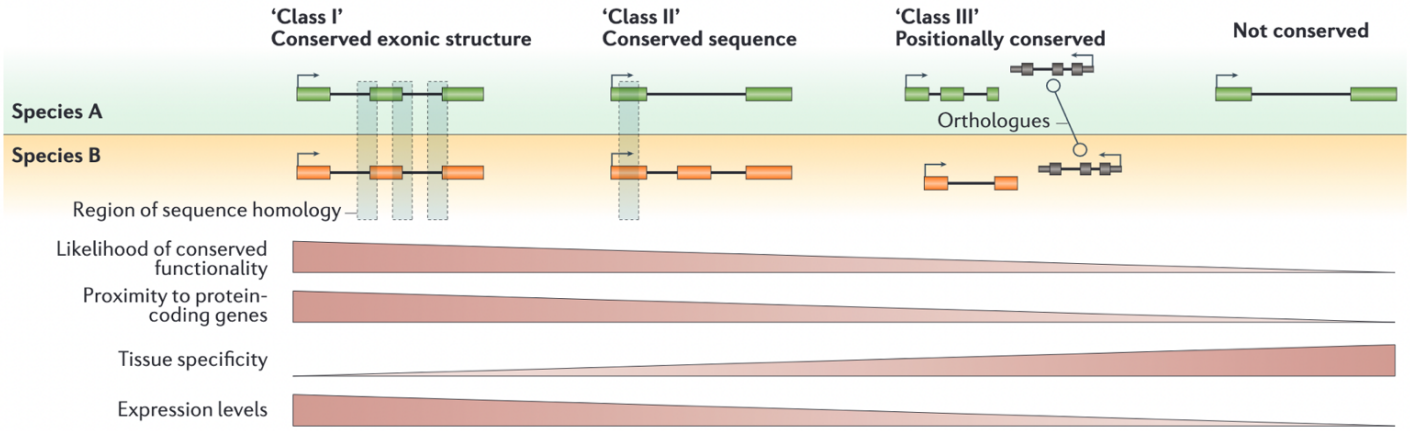

Figure 11. LncRNA sequence conservation classes. *(Adapted from Ulitsky, 2016). Proposed groups of lncRNAs displaying sequence conservation across species. Class I: transcripts with conserved exonic structure between two species; class II: conserved sequence between species; class III: transcripts that are positionally conserved in two species but not sequence conserved. Class I transcripts are more likely of conserving function amongst species, to be close to PCGs and to have higher expression levels. In contrast, class III and not conserved lncRNAs are more likely to be tissue specific.*

3.6. LncRNAs display overall higher nuclear retention but are also present in the cytoplasm

mRNA is known to be processed in the nucleus and trafficked to the cytoplasm, where transcripts are distributed amongst different subcellular compartments depending on their function (Bridges, Daulagala and Kourtidis, 2021). In contrast, lncRNAs appear more abundant in the nucleus although a number of cytoplasmic lncRNAs have also been annotated (Derrien *et al.*, 2012; Zuckerman and Ulitsky, 2019). Some of these transcripts are exclusively nuclear or cytoplasmic whilst others are present in both (Djebali *et al.*, 2012). Nuclear retention elements have been found in the sequence of some transcripts, as well as repeat elements that favor nuclear residency; however, this is not the case for most nuclear lncRNAs (Lubelsky and Ulitsky, 2018; Shukla *et al.*, 2018). Nevertheless, this increased nuclear retention in comparison to mRNA was investigated and found to be due to a greater instability of nuclear lncRNAs (Clark *et al.*, 2012) and to correlate with slow nuclear export or heightened cytoplasmic degradation due in part to inefficient splicing of lncRNAs (Bahar Halpern *et al.*, 2015; Zuckerman and Ulitsky, 2019). Many scenarios were proposed to be the cause for this, including chromatin sequestration of lncRNAs,

inhibiting its proper processing, insufficient spliceosome binding capacity, and degradation of improperly spliced transcripts before their arrival to the nuclear pore (Zuckerman and Ulitsky, 2019). Consequently, lncRNAs' export to the cytoplasm correlates strongly with more efficient splicing. It was also found to rely on the nuclear RNA export factor 1 (NXF1) that is usually favored in the case of long, A/U-rich transcripts containing one or few exons, as are many lncRNAs (Zuckerman *et al.*, 2020). Once in the cytoplasm, the transcripts can be assigned to distinct organelles – such as the mitochondria (Rackham *et al.*, 2011; Dong *et al.*, 2017) - or bind to RNA-binding proteins (RBPs) within the cytoplasm, although our understanding of those processes remains limited (Statello *et al.*, 2021).

The subcellular localization of lncRNAs seems to be key in defining their biological roles. In accordance with this, environmental stresses or infections are able to alter lncRNA localization and to provoke trafficking of a transcript to a particular cellular compartment, such as in response to oxidative stress (Giannakakis *et al.*, 2015; Jarroux, Morillon and Pinskaya, 2017). For instance, the well-studied nuclear-transcribed lncRNA MALAT1 was found aberrantly translocated to the mitochondria in hepatocellular carcinoma (HepG2) cells, whereas it is largely located to the nucleus in healthy liver cells (Zhao *et al.*, 2019). Although its exact function remains elusive, MALAT1 seems to be involved in nuclear-mitochondria crosstalk, essential for cellular homeostasis, and to play a role in regulating mitochondrial metabolism as knockdown of this lncRNA disrupted ATP production. MALAT1 has also been implicated in translation modulation by promoting mRNA circularization and recruitment of translation initiation factors (Marzluff, 2012) or by enhancing mTOR-mediated translation (Malakar *et al.*, 2019).

3.7. LncRNAs regulate gene expression through diverse modes of action

It has become well-documented that numerous lncRNAs are involved in essential cellular processes, primarily by regulating gene expression. Although this regulatory potential is undeniably diverse and should be studied in a case-by-case situations, lncRNAs' regulatory mechanisms can be cautiously examined at several levels. One way of viewing lncRNAs' function is to investigate their point of action

relative to their transcription site (Gil and Ulitsky, 2020). As such, two types of transcripts are identified:

- ***Cis*-acting lncRNAs:** these lncRNAs exert their functions at or nearby their site of transcription. Their action is thus dependent on their loci.
- ***Trans*-acting lncRNAs**: they are transcribed and processed, and then leave their initial site of transcription to exert their function elsewhere. Their final destination - within the nucleus or cytoplasm – is not dependent on their initial transcription site. As such, lncRNAs from this group could be transcribed from another genomic location without any impact on their function, and their loss of function can be rescued by supplanting them from exogenous locations.

Within these two large groups of lncRNAs, different modes of actions have been described that will be subsequently summarized.

3.7.1. Cis-acting lncRNAs

A considerable number of currently known lncRNAs are implied to act in *cis,* as they were found tethered to the chromatin by RNA Pol II around their site of transcription and near active genes they potentially act upon (Werner *et al.*, 2017). Indeed, chromatin-associated lncRNAs were identified by carrying out nuclear fractionation of HEK293 cells, separating soluble and loosely bound components from the obtained chromatin pellet, and by performing RNA-seq on both extracts. Strikingly, 57% of the total lncRNAs were found to be chromatin-enriched, in contrast to 16% of total mRNAs (Werner and Ruthenburg, 2015). It is often suggested that action in cis is favored for lncRNAs due to their overall low expression: export to the cytoplasm would dilute the transcripts too much to allow for plausible function (Gil and Ulitsky, 2020). This mode of action also goes hand in hand with syntenic lncRNA conservation, where the locus rather than the sequence presents strong evolutionary constraint.

Several *cis*-acting transcripts have been well-characterized in the past decade, adding to our understanding of potential lncRNA functions in *cis*. First, it is important to cautiously distinguish the lncRNA's main functional feature to understand its mode of action and biological role: the DNA sequence of the lncRNA (making the transcript itself dispensable), the RNA transcript itself, or the process of transcription or splicing (Latos *et al.*, 2012; Paralkar *et al.*, 2016; Gil and Ulitsky, 2020).

(a) The lncRNA transcript is responsible for regulation neighboring genes' expression

In this case, lncRNAs exhibit the capacity to alter adjacent PCGs expression by recruiting regulatory factors, and to facilitate or block their binding or function at specific DNA loci (Kopp and Mendell, 2018). These lncRNAs operate at a close proximity to their target PCG by localizing to a preformed chromatin loop, which ensure rapid alterations of gene expression (Gil and Ulitsky, 2020). Both activating and repressive lncRNAs have been described as recruiting chromatin modifiers in this manner and targeting them to the PCG's promoter region to enhance or suppress transcription (Quinn and Chang, 2016).

For example, the lncRNA *UMLILO* is essential for the activation of multiple neighboring chemokine genes in mice monocytes. In response to the activation of tumor necrosis factor, it can recruit and bind the WDR5-MLL complex, made up of the RNA-binding adapter protein WDR5 that recognizes H3K4 methylation and the methyltransferase MLL. Through this complex, it induces the deposition of histone 3 lysine 4 trimethylation (H3K4me3) activation epigenetic chromatin activation marks at the target promoters, thus stimulating the chemokines' expression (Fanucchi *et al.*, 2019). The lncRNA PLUTO was shown to facilitate interactions between an enhancer cluster and the key β cell transcription factor *PDX1*, thus controlling *PDX1* transcription (Akerman *et al.*, 2017). PLUTO knockdown reduced the contacts between PDX1 and the upstream enhancers, showing that transcription of PDX1 is reliant on PLUTO-mediated contacts with then enhancer cluster.

The lncRNA *ANRIL* is an example of a repressive transcript that suppresses gene expression in cis through interaction with a chromatin modifier: it was shown to recruit the polycomb repressive complex 1 (PRC1) to the promoters of the adjacent CDKN2A and CDKN2B genes in melanoma and prostate epithelium cells (Pasmant *et al.*, 2007; Yap *et al.*, 2010). As a result, PRC1 inhibits the expression of CDKN2A and CDKN2B, which are well-studied tumor suppressors that participate in apoptosis, proliferation, senescence as well as ageing (Kong, Hsieh and Alonso, 2018).

Furthermore, some lncRNAs – both repressive and activating - were shown to act as decoys and bind regulatory factors as a way to sequester them from the promoters of their target PGCs. For instance, lncPRESS1 is a p53-regulated lncRNA that can

sequester the deacetylase sirtuin 6 (SIRT6), which usually suppresses several genes essential for pluripotency and is thus involved in triggering differentiation (Jain *et al.*, 2016). By inhibiting SIRT6's action in human embryonic stem cells (hESCs), lncPRESS1maintains the cells in their pluripotent state.

(b) Gene regulation in cis relies on the act of transcription and/or splicing of the lncRNA

Local gene regulation can sometimes depend entirely on the transcription through a lncRNA locus and the transcript processing, independently of the final lncRNA product.One suggested mechanism is that the transcription through the lncRNA gene impacts the surrounding chromatin and can thus modulate the interactions and expression of neighboring PGCs (Gil and Ulitsky, 2020). This can be related to the recruitment of chromatin-modifying complexes during Pol II-mediated transcription elongation and the ensuing epigenetic modifications at or around the locus (Sims, Belotserkovskaya and Reinberg, 2004). Another possibility is that transcription of the lncRNA locus induces changes in chromatin folding and thus can favor different DNA interactions (Heinz *et al.*, 2018; Hsieh *et al.*, 2020). For example, transcription of the lncRNA *BLUSTR* (or *linc1319*) was found to have an activating effect on the adjacent *SFMBT2* gene in mouse embryonic stem cells (Engreitz *et al.*, 2016). This effect was not dependent on the DNA sequence of *BLUSTR,* as was demonstrated by sequential deletions of the lnRNA's exons and introns but appeared linked to the proper transcription of the locus. Indeed, hindering BLUSTR transcription or splicing, such as by promoter deletion or insertion of additional polyA signals, resulted in reduced H3K4me3 and increased histone 3 lysine 27 trimethylation (H3K27me3) at the SFMBT2 promoter and reduced RNA Pol II occupancy at the locus. Consequently, SFMBT2 expression was significantly lowered.

Alternatively, some repressive lncRNAs were found to function *via* transcriptional interference, by overlapping transcriptional units of target PGCs. Such is the case with the lncRNA *AIRN:* it is transcribed from a locus that overlaps in the antisense direction the promoter of the mammalian imprinted gene *IGFR2*. As a result, when AIRN is transcribed and thus, when antisense transcription through the IGFR2 promoter occurs, IGFR2 is silenced by transcriptional interference (Latos *et al.*, 2012).

Some lncRNAs act through the presence of functional elements within their sequence that can regulate the expression of nearby PCGs (Statello *et al.*, 2021). Most notably, a group of lncRNAs are transcribed from sequences comprising active enhancers and are dubbed enhancer-lncRNAs or e-lncRNAs (Paralkar *et al.*, 2016; Statello *et al.*, 2021). The hypothesis is that these transcripts could mediate the activity of the enhancers within their sequences, and that transcription of the lncRNA at least partly contribute to activating the underlying enhancer (Gil and Ulitsky, 2020). One such lncRNA is *BENDR* whose transcription was shown to activate enhancer elements in its sequence that in turn modulate the expression of nearby gene *BEND4* in mouse embryonic stem cells (Engreitz *et al.*, 2016). Interestingly, deleting the BENDR promoter inhibited binding of Pol II at the target gene promoter, but the insertion of early poly(A) signals in the lncRNA sequence thus terminating transcription prematurely, did not.

e-lncRNAs may also regulate enhancer availability by ensuring adequate spatial interactions between the enhancer and its target PGCs (Werner *et al.*, 2017; Schertzer *et al.*, 2019). Indeed, some e-lncRNAs were found to recruit proteins involved in the formation and maintenance of active chromatin loops, such as the Mediator complex through which contacts between the lncRNA loci and the adjacent gene are facilitated (Lai *et al.*, 2013). For instance, the lncRNA *SWINGN*, transcribed from an enhancer, was reported to bind SMARCB1 with high affinity in human fibroblasts, and to promote its binding at specific loci to promote gene activation (Grossi *et al.*, 2020). SMARCB1 contains SWI/SNF complexes which are ATP-dependent chromatin remodelers important for the maintenance of chromatin architecture, gene expression, and in the activation of enhancers (Alver *et al.*, 2017). In particular SWI/SNF complexes partake in the process of oncogene-induced senescence (Lenain *et al.*, 2017). Interestingly, SWINGN was shown to interact with SMARCB1 exclusively in proliferating and not in senescence conditions, and to mediate the activation of pro-oncogenic genes by promoting SMARCB1 binding (Grossi *et al.*, 2020).

Repressive lncRNAs can also overlap with enhancers and exhibit enhancer-dependent action, through a process named enhancer competition (Gil and Ulitsky, 2020). An example of this lies in the e-lncRNA *PVT1* that is adjacent to the essential proliferation actor MYC. The promoters of both *PVT1* and *MYC* compete to bind an enhancer that originates from the lncRNA sequence (Cho *et al.*, 2018). Consequently, silencing the PVT1 promoter enhances the activity of MYC and boosts cellular

proliferation, suggesting an important role for the lncRNA in the switch to cellular differentiation.

The importance of cis-acting lncRNA regulatory networks is becoming increasingly evident (Statello et al. 2021): in many cases, multiple cooperating lncRNAs rather than a single lncRNAs' action seem responsible for regulating proximal gene expression. Transcripts that collaborate to modulate a gene can also do so *via* different mechanisms of action that are either transcript dependent or independent (Gil and Ulitsky, 2020). For instance, the lncRNAs PWR1 and ICR1 found in yeast cooperate to regulate the cell surface protein Flo11 (Bumgarner *et al.*, 2009). ICR1 is located on the same strand as FLO11 and can repress its expression through transcriptional interference. PWR1 overlaps ICR1 and can similarly repress ICR1 expression through transcriptional interference. The expression of these two lncRNAs is mediated by two transcription factors: Flo8 and Sfl1, which competitively bind to the vicinity of the FLO11 promoter to determine which lncRNA is expressed (Bumgarner *et al.*, 2012).

3.7.2. Trans-acting lncRNAs

Although a majority of characterized lncRNAs have regulatory roles in *cis*, more and more transcripts are found to operate at a location distant to their transcription site and thus, to act in *trans*. These studies have allowed to distinguish three ways in which lncRNAs can function in *trans*:

(a) Trans-acting lncRNAs can modulate chromatin activity and gene expression at distant loci

A number of lncRNAs were found to regulate gene expression and to alter chromatin environment at a remote location. They can also recruit and interact with chromatin modifying factors at a target gene's promoter region in *trans* and either activate or repress its expression. Interestingly, some of these transcripts are able to function both in *cis* and in *trans.* For example, the lncRNA *ANRIL* is able to modulate the expression of several PGCs in *trans*, as well as its previously mentioned function in *cis. ANRIL* was shown in HEK 293 cells to target gene promoters containing Alu motifs across the genome, where it binds and recruits polycomb proteins resulting in altered expression levels (Holdt *et al.*, 2013).

Furthermore, *trans*-acting transcripts were found to influence chromatin accessibility by forming hybrid DNA-RNA structures such as chromatin R loops, in the same way as *cis*-acting lncRNAs (Statello *et al.*, 2021). Auxin-regulated promoter loop (APOLO) is a lncRNA that, in response to auxin, is able to bind distant target PGCs' promoters that contain specific motifs and to generate R-loops as studied in Columbia-0 plants (Ariel *et al.*, 2020). Through the formation of these structures, APOLO lifts the inhibition of these genes usually applied by Polycomb factor like heterochromatin protein 1 (LHP1) and enables targeted gene expression.

(b) Through trans-regulatory and scaffolding functions, lncRNAs can shape nuclear organization

It was found that lncRNAs could participate in shaping nuclear structure and composition *via* their scaffolding potential, thus inherently modulating nuclear transcription. Several studies found lncRNAs that play critical roles in the assembly of nuclear condensates. These condensates are membraneless compartments that consist of micron-scale RNA-protein concentrates and are involved in various biomolecular processes (Banani *et al.*, 2017). One type of such condensates are paraspeckles that have been linked to an overall cellular stress response and to potentially partake in cellular homeostasis maintenance (West *et al.*, 2016; McCluggage and Fox, 2021). They appear to control gene expression and nuclear retention of target RNAs, in response to stressors. Paraspeckles formation was shown to be dependent on the lncRNA nuclear enriched abundant transcript 1 (*NEAT1*) (Clemson *et al.*, 2009). Interestingly, NEAT1 presents two available isoforms of different lengths and only one – NEAT1 *long* – can act as a paraspeckle building scaffold (Sasaki *et al.*, 2007; Sunwoo *et al.*, 2009). The middle region of NEAT1 *long* was discovered, using the human HAP1 cell line, to enclose two subdomains that are able to recruit NONO and SFPQ, two paraspeckle core proteins (Yamazaki *et al.*, 2018). This initiates the formation of paraspeckles *via* liquid-liquid phase separation, although it remains elusive how NEAT1 is assembled into the core, spherical paraspeckles.

Another well studied lncRNA that is essential to the functioning of a type of nuclear condensates is *MALAT1*. MALAT1 is drafted to nuclear speckles, which are compartments that concentrate fundamental splicing components, and facilitates localization at and interaction with nascent pre-mRNA (Hutchinson *et al.*, 2007;

Engreitz *et al.*, 2014). Depleting MALAT1 induces defects in nuclear speckles but does not block their formation (Fei *et al.*, 2017).

On top of their ability to operate as scaffolds for proteins and RNAs, trans-acting lncRNAs are also capable of functioning as scaffolds for chromosomes and thus control the architecture of specific nuclear domains. The lncRNA *Functional Intergenic Repeating RNA Element* (*FIRRE)* lncRNA originates from the X chromosome and is able to spatially bring into proximity at least five trans-chromosomal loci (Hacisuleyman *et al.*, 2014). This co-localization of chromosomal loci is lost following FIRRE deletion but is at least partially rescued by expression of transgenic *FIRRE* RNA, highlighting the trans-acting mechanism of this lncRNA (Lewandowski *et al.*, 2019).

(c) Trans-acting lncRNAs are able to bind and modulate proteins

A number of lncRNAs were shown to directly interact with proteins by binding to specific sequence motifs (Statello *et al.*, 2021). Such a capacity can be used to modulate splicing events and thus, alter the mRNA processing and translation (Romero-Barrios *et al.*, 2018). One mechanism harnessed by lncRNAs to achieve this is to sequester essential splicing factors. This is done by small nucleolar RNA-related lncRNAs (sno-lncRNAs) that enclose small nucleolar RNAs (snoRNAs) at each end of their sequence and that can therefore fine tune the availability of splicing elements (Yin *et al*. 2012). Additionally, some lncRNAs are able to enact post-transcriptional modifications upon splicing proteins to regulate their activity (West *et al.*, 2014) and others were described as forming RNA-RNA duplexes with pre-mRNA to limit spliceosome access or to recruit splicing factors (Romero-Barrios *et al.*, 2018).

Other lncRNAs appear to fold into distinct structures that can interact with and modulate the behavior of proteins. *FOXD3* antisense transcript 1 (*FAST*) is an abundant transcript in human embryonic stem cells (hESCs) and is essential for WNT signaling and pluripotency maintenance. Through the formation of stem-loops, FAST is able to block the interaction of β-TrCP with phosphorylated β-cathenin, suppressing the former's degradation and allowing it to translocate to the nucleus (C.-J. Guo *et al.*, 2020). There, β-cathenin promotes the expression of several WNT-dependent genes, essential to pluripotency maintenance.

(d) LncRNAs can act in *trans* by binding with other RNA molecules

Some trans-acting lncRNAs were described to bind to other RNAs through base-pairing interactions to carry out their function. An important and abundant group of such lncRNAs is named competing endogenous RNAs (ceRNAs) and is able to regulate miRNA activity. Their sequences contain miRNA recognition elements (MREs) through which they act as miRNAs "sponges" and can therefore modulate their availability (Salmena *et al.*, 2011; Kartha and Subramanian, 2014). For example, the muscle-specific *lincMD1* dictates the onset of muscle differentiation through its activity as a miRNA sponge (Cesana *et al.*, 2011). Upon myoblast differentiation, *lincMD1* is upregulated and can increasingly sequester miR-133 and miR-135. This action alleviates the repressive effect of the miRNAs on two genes, *MAML1* and *MEF2C*, which are known to activate muscle-specific gene expression. Another known ceRNA is *MIAT* who was initially discovered as associated with myocardial infarction (Ishii *et al.*, 2006) but has since been linked to a variety of diseases such as schizophrenia (Rao *et al.*, 2015), and thyroid cancer progression (Guo *et al.*, 2021). MIAT is described to function as a ceRNA network that regulates the availability of several identified miRNAs, through which is seems to play an essential role in maintaining cell proliferation and migration (Guo *et al.*, 2021).

Other trans-acting lncRNAs that base pair to RNAs regulate specific signaling pathways by recruiting essential proteins (Statello *et al.*, 2021). For example, several lncRNAs were discovered to transactivate Staufen-mediated mRNAs decay (Gong and Maquat, 2011). This process is usually carried out by the protein STAU1 that binds to the 3'-UTRs of mRNAs to be degraded. LncRNAs containing Alu elements can form duplexes with the mRNAs' 3'-UTR sequence and recruit STAU1, hence promoting their degradation. Interestingly, another lncRNA can recruit STAU1 for different purposes. *TINCR*, a lncRNA involved in human epidermal differentiation, was revealed to bind to a variety of mRNA involved in differentiation and to promote their stabilization and expression via the recruitment of STAU1 (Kretz *et al.*, 2013).

As such, trans-acting lncRNAs' role as powerful post-transcriptional regulators is becoming more and more appreciated.

3.8. LncRNAs are implicated in a range of neuropathophysiological processes

Through their previously described regulatory functions, lncRNAs' essential roles in numerous of biological processes is increasingly recognized. A number of transcripts were described as implicated in cell differentiation (Fatica and Bozzoni, 2014; Sherstyuk, Medvedev and Zakian, 2018), cell proliferation (Zhang, Hamblin and Yin, 2017), immune system function (Chen, Satpathy and Chang, 2017) , CNS development (Sauvageau *et al.*, 2013; Briggs *et al.*, 2015) and many more critical physiological pathways. As such, dysfunctions of these powerful regulators are suggested to contribute to many diseases, including neurological disorders (Aliperti, Skonieczna and Cerase, 2021).

Numerous lncRNAs have been identified in and associated to the nervous system (Briggs *et al.*, 2015; Clark and Blackshaw, 2017; Wei *et al.*, 2018; Salvatori, Biscarini and Morlando, 2020). However, the next section will focus on lncRNAs studied in the context of neurodegenerative disorders. In fact, several lncRNAs were identified as deregulated in the context of neurodegenerative disorders and were suggested to participate in distinct pathological processes(Zhou *et al.*, 2021). As a result, there is increased effort to evaluate the potential of such lncRNAs as disease biomarkers (Zhang, He and Bian, 2021). It is also interesting to note that through Genome Wide Association studies (GWAS), many single nucleotide polymorphisms associated to human pathologies were identified in non-coding regions of the genome including lncRNAs (Altshuler, Daly and Lander, 2008; Brodie, Azaria and Ofran, 2016; Nalls *et al.*, 2019). This suggests a role for them as risk factors for those diseases.

Many such lncRNAs have been associated to a range of diseases notably incuding neurodegenerative diseases. For instance, 249 lncRNAs were identified in the hippocampus of APP/PS1 (Amyloid precursor protein/Presenilin 1) transgenic mice with Alzheimer's disease (AD), out of which 99 were downregulated in comparison to control mice and 150 upregulated, suggesting a potential role for them in the pathology (Fang *et al.*, 2017). One of those lncRNAs named BACE1-AS1, antisense to the gene encoding the β-secretase BACE1, was similarly upregulated in AD patients in comparison to controls (Faghihi *et al.*, 2008). Interestingly, BACE1-AS1 was shown to drive higher levels of amyloid beta$_{1-42}$ (Aβ_{1-42}), the main component of the AD

pathological hallmark amyloid plaques, *via* the modulation of BACE1 translation in a post-transcriptional feed-forward mechanism. Indeed, downregulating the expression of BACE1-AS1 using siRNA silencing in SH-SY5Y neuroblastoma cells decreased BACE1 expression as well as $A\beta_{1-42}$ levels (Liu *et al.*, 2014). Moreover, knockdown of BACE1-AS1 in an amyloid precursor protein (APP)-overproduction mice model, inhibited BACE1 and APP production and ameliorated the mice's memory and learning ability (Zhang *et al.*, 2018). Overall, these findings suggest an important role for BACE1-AS1 in AD-driven neurotoxicity.

Likewise, accumulating studies have discovered lncRNAs that exhibit altered expression in a PD context – either in cellular or animal models of the disease or in PD patients' postmortem brain tissues – meaning that they may be key PD-specific markers and that they may serve as diagnostic biomarkers for the disease (Kraus *et al.*, 2017; Kuo *et al.*, 2021). Accumulating evidence shows that some of these lncRNAs participate in essential physiopathological processes of the disease, we present the most robustly studied of these lncRNAs in Table 3 (Lyu, Bai and Qin, 2019).

A few lncRNAs have been associated to PD-linked neuroinflammation including NEAT1 and HOTAIR (Zhang, He and Bian, 2021). For instance, NEAT1 was discovered to be upregulated in an MPP+-treated mouse model and in MPP^+-treated SK-N-SH cells (Yan *et al.*, 2018; Liu, Li and Zhao, 2020). Knockdown of NEAT1 expression in the SK-N-SH model suppressed MPP+-induced inflammation, cytotoxicity and apoptosis, through acting as a molecular sponge of miR-212-5p and thus alleviating the latter's repressive effect on RAB3IP, that is reported as involved in PD progression (Liu, Li and Zhao, 2020). The lncRNA HOTAIR was also shown to modulate RAB3IP expression via sponging of miR-126-5p in MPP^+-induced SH-SY5Y cells (Lin *et al.*, 2019). Notably, knocking down HOTAIR and RAB3IP and overexpressing miR-126-5p significantly promoted cell proliferation and reduced apoptosis.

NEAT1 was also found to enhance MPTP-driven autophagy by inhibiting PINK1 degradation and thus, stabilizing its expression (Yan *et al.*, 2018). Consequently, NEAT1 knockdown suppressed autophagy and relieved neuronal injury. SNHG1 is another lncRNA that has been linked to autophagy in PD and is upregulated in PD patients' brain tissue and in MPP^+-treated mice (Qian *et al.*, 2019). Downregulation of SNHG1 enhanced autophagy and reduced MPP^+-induced cell death while SNHG1

overexpression exacerbated cytotoxicity by modulating the PTEN/AKT/mTOR axis through sponging and sequestering of miR-153-3p.

Some lncRNAs have been associated to apoptosis regulation in PD. LincRNA-p21 is a transcript that has been described as a transcriptional repressor that is activated by p53, can associate with repressive complex and modulate their localization so as to inhibit the expression of specific genes (Huarte *et al.*, 2010). Therefore, p53 is suggested to enact its regulation of apoptosis; through the modulation of such repressive lncRNA. LincRNA-p21 was reported as upregulated in 30 brain specimen derived from PD patients (Kraus *et al.*, 2017). Overexpression of lincRNA-p21 in MPP^+-treated SH-SY5Y cells lead to it sponging miR-1277, indirectly enhancing the expression of α-synuclein and inducing apoptosis. MALAT1 was similarly shown to partake in α-synuclein regulation: its overexpression increased α-synuclein levels through the inhibition of miR-129 expression in PD-mouse models, and consequently promoted apoptosis. The lncRNA UCA1 also appears to modulate α-synuclein expression. It was discovered to be upregulated in the brain tissue of a PD-mouse model as well as in MPP^+-treated SH-SY5Y cells and thus was suggested to participate in the pathology mechanisms (Lu *et al.*, 2018). Further investigation revealed that overexpressing UCA1 significantly upregulated α-synuclein mRNA and protein levels. On the other hand, UCA1 knockdown reduced the activity of the apoptosis effector caspase-3 and therefore, MPP^+-caused apoptosis in SH-SY5Y cells.

Another lncRNA of interest that has been linked to PD progression is H19 that appears to be downregulated in MPP^+-induced PD mice model, MPP^+-treated SH-SY5Y neuroblastoma cells and 6-OHDA-treated mice DA neurons (J. Jiang *et al.*, 2020; Zhang, Xia and Lin, 2020). Interestingly, H19 overexpression was found to alleviate apoptosis in these models via its negative regulation of miR-585-3p and miR-301b-3p, that themselves inhibit PIK3R3 and HPRT1 expression respectively. Therefore, targeting this lncRNA could potentially constitute a PD therapeutic strategy. It is important to note that, in a study investigating cardiac metabolic disorders in palmitic acid-treated H9C2 cells (from embryonic heart rat tissue), overexpression of lncRNA H19 was found to inhibit the expression of PINK1/Parkin signaling proteins and to alleviate mitophagy (S.-H. Wang *et al.*, 2021). Through RNA pull-down, mass spectrometry and RNA-binding protein immunoprecipitation assays, it was revealed that H19 was capable of blocking PINK1 translation by obstructing the binding of

eukaryotic translation initiation factor 4A isoform 2 (eIF4A2) to PINK1 mRNA, thus modulating mitophagy. This property has yet to be investigated in PD, where mitochondrial dysfunction and mitophagy play a central pathogenic role. It is noteworthy, that the large majority of lncRNAs studied in the context of PD constitute ubiquitously expressed lncRNAs. As the disease is defined by the selective degeneration of DA neurons, it would be interesting to investigate whether there are lncRNA specifically expressed in these neurons and if they may participate to mechanisms intrinsic to DA neurons.

In recent years, the number of lncRNAs that have become functionally investigated and that have been linked to neurodegenerative diseases and in particularly PD has been steadily growing. This has served to confirm their potent regulatory identity and continues to shed light on many pathological processes. As our understanding of lncRNAs grows, it is expected that they will constitute appealing targets for therapeutic studies and novel potential disease biomarkers.

The Unfolded Protein Response of the Endoplasmic Reticulum orchestrates the cell-specific response of human dopaminergic neurons to mitochondrial stress: from transcriptional programs including long non-coding RNAs to alterations in mitochondrial homeostasis.

Jana Heneine, Claire Colace-Sauty, Christiane Zhu, Benjamin Galet, Justine Guégan, François-Xavier Lejeune, Thomas Garreau, Noemi Asfogo, Corinne Pardanaud-Glavieux, Olga Corti, Philippe Ravassard*s and Hélène Cheval*.

Institut du Cerveau - Paris Brain Institute - ICM, Sorbonne Université, Inserm U1127, CNRS UMR7225, APHP, Hôpital Pitié Salpêtrière, Paris, France

*** Corresponding authors:**

helene.cheval@icm-institute.org

philippe.ravassard@icm-institute.org

Keywords: human dopaminergic neurons, UPR^{ER}, PERK, lncRNAs, mitophagy, mitochondrial DNA biogenesis, translation

Summary: The Unfolded Protein Response of the Endoplasmic Reticulum is induced upon stress in human dopaminergic neurons and modulates mitochondrial homeostasis and transcriptional programs including expression of long non-coding RNAs (lncRNAs). We discovered a lncRNA involved in translation resumption after stress.

Abstract

Mitochondrial dysfunction is thought to be central to the pathophysiology of Parkinson's disease. The preferential vulnerability of dopaminergic (DA) neurons of the *substantia nigra pars compacta* to mitochondrial stress may underlie their massive degeneration and the occurrence of motor symptoms. Using LUHMES-derived DA neurons, we demonstrated that inhibition of the mitochondrial electron transport chain resulted in a severe alteration of mitochondrial turnover, pushing the balance towards mitochondrial loss, a reduction of the maturation status of the DA population and an increased proportion of apoptotic cells. PERK-mediated Unfolded Protein Response of the Endoplasmic Reticulum (UPR^{ER}) emerged as the key coordinator of the stress response, governing the inactivation of the mitochondrial UPR (UPRmt), the initiation of mitophagy and the cell-specific expression of long non-coding RNAs (lncRNAs). Importantly, we discovered novel lncRNAs specifically expressed in human DA neurons upon stress. Among them, we showed that lnc-SLC6A15-5 contributes to the resumption of translation after mitochondrial stress.

Introduction

Parkinson's Disease (PD) is a prevalent neurological disorder characterized by the degeneration of several neuronal subtypes, but affecting predominantly the dopaminergic (DA) neurons of the *substantia nigra pars compacta* (SNpc) (Pacelli *et al*, 2015; Brichta & Greengard, 2014; Pissadaki & Bolam, 2013; Damier *et al*, 1999; Hirsch *et al*, 1988). The progressive and massive DA neuronal loss constitutes a hallmark of the disease, responsible for the major motor symptoms observed in patients, rigidity, bradykinesia and tremor (Dickson *et al*, 2009; Kalia & Lang, 2015). Mitochondrial dysfunction has emerged as a prominent player in PD pathogenesis, marked by several lines of evidence in PD patients and animal models. Defects in mitochondrial complex I activity and mitochondrial DNA homeostasis have been shown in brain tissue from PD patients (Schapira *et al*, 1989; Dölle *et al*, 2016; Borsche *et al*, 2021; Grünewald *et al*, 2019), and exposure to environmental mitochondrial toxins, such as 1-methyl-4-phenyl-1,2,3,6-tetrahydropyridine (MPTP) or rotenone, has been linked to the manifestation of clinical symptoms resembling PD and underlying DA neurodegeneration in the SNpc (Langston *et al*, 1983; Sherer *et al*, 2003a, 2003b). Furthermore, an ever growing number of studies reported changes to mitochondrial biology using various cellular and animal models (Dauer & Przedborski, 2003; Pacelli *et al*, 2015; Bose & Beal, 2016). Importantly, the significance of mitochondrial alterations in the pathophysiology of PD has been emphasized by the discovery of the causal link between mutations in *PRKN* and *PINK1* and autosomal recessive forms of PD (Pickrell & Youle, 2015). *PRKN* and *PINK1* encode the E3 ubiquitin ligase PARKIN and the mitochondrial serine/threonine kinase PINK1, which hold joint pivotal roles in mitochondrial quality control in response to mitochondrial dysfunction (Eldeeb *et al*, 2022; Zhu *et al*, 2013). Altogether, functional changes to mitochondria naturally

accumulating during aging are suspected to lead to a homeostatic imbalance that significantly enhances the vulnerability of DA neurons of the SNpc to cell death compared to other neuronal subtypes. The selective effects of *PRKN* and *PINK1* gene mutations, which sensitize primarily the SNpc DA neurons to cell death, despite being ubiquitously expressed in various cell types, raises intriguing questions about the DA neuron-specific factors contributing to mitochondrial stress vulnerability.

So far, specific molecular signatures defining neuronal cells have been obtained using transcriptomic data focused on protein-coding genes. However, non-coding elements of the genome, such as long non-coding RNAs (lncRNAs), are gaining prominence for their cell-specific regulatory functions, spanning from epigenetic to post-translational levels (Cabili *et al*, 2011; Morán *et al*, 2012; Washietl *et al*, 2014; Ward *et al*, 2015; Jiang *et al*, 2016; Akerman *et al*, 2017; Liu *et al*, 2017; Gendron *et al*, 2019; Seifuddin *et al*, 2020; de Goede *et al*, 2021; Ulitsky & Bartel, 2013; Jarroux *et al*, 2017; Mattick *et al*, 2023). Moreover, most lncRNAs exhibit limited conservation across species and the vast majority of PD-associated single nucleotide polymorphisms (SNPs) fall into non-coding regions with potential regulatory functions (Altshuler *et al*, 2008; Nalls *et al*, 2019). Consequently, lncRNAs, along with their associated molecular mechanisms, emerge as promising candidates for elucidating the specific molecular mechanisms underlying vulnerability to stress and, by extension, the pathophysiology of human diseases associated with the alteration of specific cellular subtypes. Due to their weak inter-species conservation, their relevance takes on an even more significant dimension in the context of pathologies for which animal models do not fully recapitulate the human clinical manifestations, such as PD.

In the context of mitochondrial stress, extensive research has unveiled the central role of the integrated stress response (ISR) in human cells (Krug *et al*, 2014; Quirós *et al*,

2017; Jennings *et al*, 2023; van der Stel *et al*, 2022; Carta *et al*, 2023), leading to the activation of the PERK-mediated Unfolded Protein Response of the Endoplasmic Reticulum (UPR^{ER}). PERK-dependent phosphorylation of EIF2α results in the attenuation of general translation, while allowing for selective translation of stress-associated proteins, such as ATF4, which initiates key transcriptional programs promoting pro-survival or pro-apoptotic responses, depending on the severity and duration of the stress (Wek & Cavener, 2007). However, the extent to which other branches of the UPR^{ER}, mediated by the activation of IRE1 or ATF6, or the UPR^{mt}, are involved in coping with mitochondrial stress is still unclear and highly differ across different cell types and mitochondrial stress conditions (Quirós *et al*, 2017; Cai *et al*, 2020).

In this study, we demonstrate that exposing human DA neurons derived from LUHMES cells (Lotharius *et al*, 2002; Scholz *et al*, 2011) to inhibitors of the electron transport chain prompted the simultaneous activation of all branches of the UPR^{ER}, with a pronounced emphasis on the PERK-UPR^{ER} pathway. This latter pathway contributed to induction of stress-induced mitophagy and inactivation of the UPR^{mt} in neurons. Importantly, we discovered novel lncRNAs expressed in DA neurons specifically during the mitochondrial stress response, downstream of the PERK-mediated UPR^{ER}. Among these stress-induced lncRNAs, *lnc-SLC6A15*, emerged as a regulator of translation resumption that occurs following mitochondrial stress.

Results

Mitochondrial stress induced by the inhibition of the electron transport chain destabilizes mitochondrial turnover in human DA neurons.

To study the effect of mitochondrial stress on human DA neurons, we used DA neurons generated from LUHMES cells (LUnd Human MESencephalic neuronal cell line, immortalized DA progenitors; Lotharius *et al*, 2002; Scholz *et al*, 2011). LUHMES cells differentiate rapidly and homogeneously into DA neurons that can be produced in large numbers, facilitating PD research (Lotharius *et al*, 2002, 2005; Höllerhage *et al*, 2017; Pierce *et al*, 2018). Accordingly, after 6 days of differentiation, 90% of the cells expressed the enzyme tyrosine hydroxylase (TH), essential to the production of dopamine, and 74% co-expressed TH with the DA transporter DAT **(Figure 1a; Figure 2a, b, d)**. At this time point, we treated the neurons for 8 h with the mitochondrial toxins antimycin A and oligomycin, which trigger mitochondrial stress through the inhibition of the complex III and the ATP synthase of the mitochondrial respiratory chain respectively. Importantly, these toxins have been shown to induce PINK1/PARKIN-dependent mitophagy, a mitochondrial quality control mechanism relevant to PD (Lazarou *et al*, 2015; Georgakopoulos *et al*, 2017).To confirm its activation, we assessed the phosphorylation of ubiquitin at Serine 65, a marker of the early phase of this mitophagy program (Kazlauskaite *et al*, 2014; Wauer *et al*, 2015; Ge *et al*, 2020; Picca *et al*, 2021). We observed staining for phosphorylated ubiquitin in around 60% of the neurons as early as 4 h after application of these toxins, compared to 2 to 5% in control conditions (**Figure 1b, c)**. Mitophagy initiation was associated with an alteration of the mitochondrial network reminiscent of mitochondrial fragmentation, as demonstrated by the scattered localization of the mitochondrial import receptor subunit

TOMM20 upon stress compared to the control neurons exhibiting a rather clustered TOMM20 staining (**Figure 1b, d**).

Mitochondrial turnover in physiological conditions as well as under stress relies on the fine balance between mitophagy and mitochondrial biogenesis (Zhu et al., 2013). We therefore investigated *de novo* synthesis of mitochondrial DNA (mtDNA) as a marker of mitochondrial biogenesis by studying the incorporation of the thymidine analog EdU. As mature neurons are post-mitotic cells, EdU integration is expected to be specific to mtDNA (Prole *et al*, 2020). Consistently, we observed co-localization of 90% of the EdU puncta with TOMM20 (**Supplementary Figure 1b-c**) and massive reduction of the EdU signal after treatment of the neurons with 2',3'-dideoxycytidine (ddC), an inhibitor of chain elongation (**Supplementary Figure 1a**). Following 8 h of treatment with mitochondrial toxins, the area occupied by the EdU signal was reduced by half compared to control conditions, and the number of EdU-positive puncta per neuron was decreased by 30%, with no change at earlier time points (**Figure 1e-g**), demonstrating stalled synthesis of mtDNA. Altogether, these results indicate impairment of mitochondrial turnover following stress in DA neurons, with an overall induction of mitophagy and decrease of mitochondrial biogenesis.

Mitochondrial stress alters the maturity and survival rate of human DA neurons

We then examined whether the inhibition of the electron transport chain also affected the identity and survival of LUHMES-derived DA neurons. We observed a tendency towards a reduction in the percentage of DA neurons expressing TH upon stress compared to control conditions (90 % in controls *versus* 77% upon stress; p= 0,0623; **Figure 2a, b**), with an overall decrease in TH signal intensity (**Figure 2c**). Treatment with the mitochondrial toxins also led to a 26% decrease in the percentage of mature

DA neurons expressing both TH and DAT (**Figure 2d**) and in a reduction of DAT signal intensity in DA neurons with residual expression (**Figure 2e**). These results suggest that mitochondrial stress induced an alteration of the DA neurons maturation status. In parallel, we observed that the proportion of DA neurons expressing the pro-apoptotic marker cleaved Caspase 3 (cCASP3) slightly rose from 5% in control conditions to 10% following mitochondrial stress, indicating increase in cell death (**Figure 2f, g**).

Mitochondrial stress leads to the concomitant activation of the three UPR^{ER} branches and inhibition of neuronal development pathways in human DA neurons.

To decipher the signaling pathways induced in DA neurons in response to mitochondrial stress, we investigated the stress-associated alterations of the transcriptome using RNA-seq. Principal component analysis demonstrated that datasets generated from DA neurons treated with mitochondrial toxins or with vehicle (DMSO) alone formed two distinct clusters (**Figure 3a**). Application of mitochondrial stress accounted for nearly 60% of the variance between the samples, as shown at the PC1 level, represented on the x axis. Focusing on protein-coding genes, we identified 12898 unique transcripts, including 772 genes with significant upregulation of expression upon stress and 605 with significant downregulation. Gene ontology analysis on the latter category revealed an enrichment in genes associated with the biological process “Nervous system development” (**Figure 3b**), reminiscent of the significant decrease in mature DA neurons observed following mitochondrial stress (**Figure 2a-e**). In addition, mRNA levels of all the 13 mitochondrial genes encoding sub-units of complexes I, III, IV and V of the electron transport chain (Schon *et al*, 2012), were significantly reduced (**Figure 3c**). Together with the alterations in

mitochondrial DNA synthesis (**Figure 1e-g**), this indicated that mitochondrial genomic programs are strongly impaired in response to the treatment with mitochondrial toxins. In parallel, gene ontology analysis on the 772 protein-genes upregulated upon stress revealed a strong enrichment in genes associated with the Unfolded Protein Response of the endoplasmic reticulum (UPR^{ER}) with the terms “Response to Endoplasmic Reticulum Stress”, “Intrinsic Apoptotic Signaling Pathway in Response to ER Stress” and “Response to Unfolded Protein” (**Figure 3b**). Interestingly, many terms from this analysis also referred to amino acid transport processes, previously shown to be induced via the integrated stress response, in particular the UPR^{ER}-PERK pathway, during ER stress (Harding *et al*, 2003; Han *et al*, 2013; Quirós *et al*, 2017). Several studies have highlighted the role of the UPR^{ER} in response to mitochondrial stress in mammalian cells (Quirós *et al*, 2017; Krug *et al*, 2014; Jennings *et al*, 2023; van der Stel *et al*, 2022; Carta *et al*, 2023), and show a predominant role of the PERK-ATF4 pathway, with no or weak activation of the other UPR^{ER}-associated branches, i.e. IRE1-XBP1 or ATF6 pathways. In contrast, pathway analysis on our datasets revealed concomitant activation of all branches of the UPR^{ER} at the transcriptional level upon stress (**Figure 3d**). To validate this result and assess the activation kinetics of the different UPR^{ER} pathways, we examined mRNA expression of several key players in each pathway at different time points during the treatment with the mitochondrial toxins compared to the control condition (**Figure 3e**). The PERK-EIF2α-mediated UPR^{ER} was strongly activated as early as 2 h into toxin exposure, as shown by the overexpression of *ATF4* mRNA and its target genes, i.e. *ATF3*, *DDIT3*, *TRIB3* and *CHAC1*, which are involved in cell death programs (Han et al., 2013). In parallel, the early overexpression of *NRF2* mRNA indicates that PERK activation upon stress also resulted in induction of the signaling pathway dependent on the antioxidant factor NRF2. We confirmed the

activation of the IRE1-mediated UPR^{ER} upon stress, as demonstrated by the increased expression of *XBP1s*, generated by IRE1-dependent splicing of *XBP1,* as early as 2 h of stress (Park *et al*, 2021), and by the overexpression of XBP1s target gene, *DNAJC3* after 6 h of stress. In contrast, the IRE1-dependent TRAF2-JUNK pathway was not induced. Regarding the ATF6 pathway, we showed an upregulation of its target genes *HSPA5* and *XBP1*, after 30 min and 4 h of stress respectively. Moreover, expression of *EDEM1* and *HERPUD1*, encoding proteins involved in ER-associated degradation (ERAD) and associated with both IRE1- and ATF6-mediated UPR^{ER} pathways (Adachi *et al*, 2008; Park *et al*, 2021), was increased from 2 to 4 h of treatment with the mitochondrial toxins. Of note, PERK, IRE1 and ATF6 activities are known to be regulated by post-translational modifications upon stress, allowing for the induction of a rapid response and explaining the absence of early transcriptional changes for these genes upon stress. However, we observed that *ATF6* and *PERK* mRNA expression was upregulated at 4 h and 8 h of stress respectively, suggesting adaptations in the stress response across time. As expected with the activation of PERK (Han *et al*, 2013), there was a 2,6 fold increase in the phosphorylation of EIF2α upon stress (**Figure 3f**), indicating attenuation of general translation. Interestingly, none of the branches of the mitochondrial UPR (UPR^{mt}) appeared to be involved in the stress response at the investigated time points (**Figure 3e**), as previously shown (Quirós *et al*, 2017). Except for the up-regulation of the ATF4-target gene *ATF5*, expression of the associated chaperones *YME1L1*, *LONP1* and *CLPP* was unchanged or even decreased upon stress (**Figure 3e**, lower panel). Similarly, there was no change or a tendency towards reduced expression for key genes of the SIRT3 UPR^{mt} pathway (i.e. *FOXO3* and *SIRT3*) and *NRF1*, a target gene of the ERα-mediated UPR^{mt}. As a whole, we established that mitochondrial stress in human DA neurons triggered transcriptional

programs responsible for loss of neuronal identity and activation of the PERK-, IRE1 and ATF6-mediated UPR^{ER}, leading to an engagement towards apoptosis.

The transcriptional response of human DA neurons to mitochondrial stress appears to rely primarily on the PERK-mediated UPR^{ER}.

We investigated further the regulation processes involved in the response of DA neurons to mitochondrial stress by studying changes in chromatin accessibility using ATAC-seq. This technology allows for the detection of potential active regulatory regions, such as promoters, enhancers, repressors etc. We identified 39720 peaks, reflecting regions of open chromatin, present in the 3 datasets obtained from the control cultures of DA neurons, and 39 375 peaks in the 4 datasets from DA neurons subjected to mitochondrial stress. We found 1327 regions more accessible and 2667 regions less accessible upon stress compared to control conditions (**Supplementary Figure 2a**). Most changes were observed in intragenic and intergenic regions, accounting for 85% and 63% of the regions respectively, with increased or in most cases decreased accessibility. In contrast to these latter categories, the number of promoter-associated regions with increased accessibility rose following mitochondrial stress. In line with the transcriptomic analyses, gene ontology enrichment analyses performed on the genes associated with these promoter regions confirmed the activation of transcriptional programs upon mitochondrial stress, in particular the engagement in the apoptotic pathway downstream of ER stress (**Supplementary Figure 2b**) and the alteration of neuronal identity (**Supplementary Figure 2c**). Similarly, extending this analysis to all the regions with increased accessibility upon stress, we found enrichment in regions associated with gene regulation, stress response and apoptosis, whereas less accessible regions following stress were

associated with cell-cell adhesion processes and nervous system development (**Supplementary Figure 2d**). To pinpoint key transcription factors involved in these genomic stress responses, we cross-referenced our data with ChiP-seq datasets and determined whether the identified stress-associated chromatin regions had already been experimentally shown to bind specific transcription factors (**Figure 2g**). Thus, regions found to be more accessible upon mitochondrial stress were significantly associated with ATF4, ATF3 as well as MYC, whereas regions with reduced accessibility were associated with transcription factors involved in neurodevelopment, such as NEUROD1 and NEUROG2.

Altogether, analysis of transcription factors binding sites within open chromatin regions suggested a predominant role for the PERK-EIF2a-ATF4 pathway in the mitochondrial stress response of DA neurons.

PERK-mediated UPR^{ER} contributes to the regulation of mitochondrial turnover and the inhibition of the UPR^{mt} in human DA neurons exposed to mitochondrial stress.

Given the highlighted prevailing contribution of the PERK-ATF4 UPR^{ER} pathway in the stress response of LUHMES-derived DA neurons and the close connection between the ER and mitochondria (Senft & Ronai, 2015), we assessed the direct involvement of this pathway in the observed mitochondrial alterations (**Figure 2**). To this end, we used the selective synthetic inhibitor GSK2606414 (compound 7-methyl-5-(1-{[3-(trifluoromethyl)phenyl]acetyl}-2,3-dihydro-1*H*-indol-5-yl)-7*H*-pyrrolo[2,3-d]pyrimidin-4-amine) to inhibit PERK (Axten *et al*, 2012; Mercado *et al*, 2018; Gundu *et al*, 2022) and examined the effects of this inhibition on mitophagy, mitochondrial biogenesis and the regulation of the UPR^{mt} upon stress. We first verified the expected effect of

GSK2606414 on ATF4 expression following stress. As anticipated, in cells exposed to the mitochondrial toxins, there was a significant increase in ATF4 protein levels from 4 h to 8 h of treatment; this effect was similar to that of tunicamycin, an N-glycosylation inhibitor known to activate ER stress and the UPR^{ER} (**Figure 4a, b**). Addition of GSK2606414 to the medium significantly attenuated this response, reducing ATF4 protein levels in stressed cells to levels comparable to those in control cells. In addition, GSK2606414 inhibited the transcriptional induction of the ATF4 target gene *ATF3* following mitochondrial stress, confirming its overall inhibitory effect on the PERK-ATF4 pathway (**Figure 4c**).

We next tested whether PERK inactivation could modulate stress-induced mitophagy (**Figure 4d, e; Supplementary Figure 3**). In the absence of antimycin A and oligomycin, there was no impact of GSK2606414 treatment on the number of neurons expressing PSer65-Ub. In contrast, application of GSK2606414 in stress conditions resulted in a notable decrease in the percentage of neurons expressing PSer65-Ub at all time points examined (from 60-65% with toxins only, to 38% with toxins and GSK2606414), demonstrating that induction of mitophagy upon mitochondrial stress was modulated by the PERK-ATF4 UPR^{ER}. Strikingly, analysis of TOMM20 expression by immunofluorescence revealed that PERK inhibition by GSK2606414 resulted in a disorganization of the mitochondrial network in control conditions that was similar to that caused by mitochondrial stress (**Figure 4d, f; Supplementary Figure 3**). Adding GSK2606414 in stress conditions, however, did not trigger any changes in the spatial distribution of TOMM20 compared to the conditions with the toxins only or with GSK only. Moreover, GSK2606414 led to a strong alteration of mitochondrial biogenesis in control conditions (**Figure 4g, h**), as evaluated by the incorporation of EdU into de novo synthesized mtDNA molecules in control conditions or upon 8h of stress.

Assessment of the number of EdU-positive puncta or the area of EdU+ signal per neuron revealed that PERK inactivation triggered a significant decrease in mitochondrial biogenesis in control conditions (90%) that was more drastic than that caused by treatment with the mitochondrial toxins only (60%); in contrast, GSK2606414 had no effect on mitochondrial biogenesis following stress. Thus, PERK-mediated UPR^{ER} appears to play a key role in maintaining the integrity of the mitochondrial network under basal conditions and in promoting mitophagy induction upon mitochondrial stress.

We then sought to determine whether the UPR^{ER} was responsible for attenuating the UPR^{mt} during mitochondrial stress (**Figure 4i**). We investigated mRNA expression of genes involved in the three UPR^{mt} branches and found that inhibition of PERK by GSK2606414 abolished or significantly reduced the stress-induced downregulation of *SIRT3* and the mitochondrial chaperones *CLPP*, *LONP1* and *YME1L1*, compared to control conditions. These results demonstrate a role for PERK in the inactivation of the ATF5- and SIRT3-mediated UPR^{mt} within 8 h of mitochondrial stress. In contrast, exposure to GSK2606414 reduced *NRF1* expression in control conditions from 30 min on, whereas it had no effect upon stress. In human DA neurons, PERK-mediated UPR^{ER} thus participates in regulating basal expression of *NRF1*, a key actor of the ERα-mediated UPR^{MT} response.

Mitochondrial stress regulates the expression of LncRNAs in human DA neurons.

One of the hypotheses raised to explain why midbrain DA neurons are more prone to degenerate in PD than other neuronal populations is that they may be particularly vulnerable to mitochondrial stress. In this context, we paid particular attention to lncRNAs, which constitute potent cell- and species-specific genomic regulators,

speculating that they would be pivotal actors of the mitochondrial stress response specific to human DA neurons. From our transcriptomic data, we identified 1177 genes encoding lncRNAs expressed in human DA neurons (**Figure 5**). Amongst these non-coding elements, 23% had not been sequenced and annotated before and were therefore absent in existing databases (i.e. not annotated, **Figure 5a**). Using a categorization system based on their position relative to their closest protein-coding genes, we found that the majority of these lncRNAs were antisense overlapping (47%), intergenic (26%), bidirectional (12%) or sense overlapping (14%). Since most lncRNAs have not been functionally assessed yet, we estimated their putative functions considering their high probability to act in cis (Gil & Ulitsky, 2020) and thereby regulate their closest genes on the genome. Gene Ontology analysis on their adjacent protein-coding genes (**Figure 5b**) overall revealed a major enrichment in lncRNAs close to, and therefore potentially regulating, genes implicated in the regulation of transcription, highlighting the contribution of such elements in the regulation of genomic programs. We also found enrichments in genes involved in the regulation of developmental processes, telomere maintenance, or cytoplasmic translation. Among the 1177 lncRNAs, 336 were specifically expressed in the control condition and 159 only upon mitochondrial stress (**Figure 5c**). Interestingly, many lncRNAs with reduced expression or switched off upon stress were adjacent to protein-coding genes implicated in the regulation of transcription (**Figure 5d**), whereas many lncRNAs upregulated or specifically expressed under mitochondrial stress were at the vicinity of protein-coding genes involved in amino acid transport and regulation of nuclear division (**Figure 5d**). Furthermore, the proportion of novel, non-annotated lncRNAs, reached 28% within the stress-specific group, a proportion higher than among the control-specific lncRNAs (19%) or the lncRNAs expressed in both conditions (23%).

Given the increasing number of existing and accessible RNA-sequencing data, this high percentage of newly discovered lncRNAs suggests a possible selective involvement in the response of human DA neurons to mitochondrial stress. Focusing on their closest protein-coding genes, we found an enrichment in terms associated with biological processes related to amino acid transport, as well as translation (**Figure 5e**). Thus, our data suggest that lncRNAs expressed upon mitochondrial stress contribute to the regulation of two major steps of the stress response of human DA neurons, as shown in **Figure 3b,d,f**. We next investigated whether lncRNAs expressed in DA neurons could be regulated by the transcription factors ATF3 and ATF4, which are the main mediators of the PERK UPR^{ER} (**Figure 5f**). Using available ChiP-seq datasets (Epanchintsev *et al*, 2017; Davis *et al*, 2018), we identified 571 putative binding loci for ATF3 and 202 for ATF4 within the promoters of 49% and 17% of the identified lncRNAs respectively. In both cases, we found that half of the potential target lncRNAs were regulated upon stress, around 40% of which were downregulated and 10% upregulated. The high proportion of lncRNAs potentially targeted for ATF3-dependent transcription, supports a preeminent role for the PERK-ATF4-mediated UPR^{ER} in the regulation of lncRNAs in human DA neurons exposed to mitochondrial stress. We selected lncRNAs of interest for further validation based on their expression profile upon stress, the function of their closest protein-coding genes and the presence of PD-associated single nucleotide polymorphisms (**Table 1**). We confirmed their expression profile by RT-qPCR and explored their regulation by the PERK-mediated UPR^{ER} using the inhibitor GSK2606414 (**Figure 5g**). In line with our previous results, expression of most lncRNAs was affected by PERK inhibition: GSK2606414 suppressed the stress-related downregulation of selected lncRNAs potentially involved in the generation and development of neurons (*lnc-TTC29*, *lnc-SLAIN1-11*, *lnc-MNAT1-2*, *ZNF778-DT*,

MIR4697HG) and the upregulation of most of the selected lncRNAs associated with possible roles in the regulation of translation and the stress response (*lnc-SLC6A15, VLDLR-AS1, VPS11-DT, lnc-FKRP, SNHG1, TMEM161B-DT*). However, few lncRNAs were also regulated by GSK2606414 at basal level compared to control conditions (either downregulated, such as *FBXL19-AS1* and *NIPBL-DT*; or upregulated, such as *lnc-SLCA15-5* and *VPS11-DT*). Altogether, these results converge towards an implication of lncRNAs in the response of human DA neurons to mitochondrial stress, with a notable role in the regulation of translation mediated by the UPR^{ER}.

The lncRNA *lnc-SLC6A15-5* specifically expressed in DA neurons regulates the resumption of translation following mitochondrial stress.

We specifically focused on *lnc-SLC6A15-5*, a lncRNA selectively expressed upon mitochondrial stress (**Figure 6a**) and adjacent to the protein-coding genes *TMTC2*, involved in ER calcium homeostasis, and to *SLC6A15*, encoding a neutral amino acid transporter linked to depression, including in PD patients (Kohli *et al*, 2011; Zheng *et al*, 2017). Interestingly, *lnc-SLC6A15-5* was amongst the lncRNAs regulated by the PERK-mediated UPR^{ER} pathway at the basal level and following stress (**Figure 5g**). This lncRNA has been recently annotated (*ENSG00000289309*), but we identified 3 novel isoforms exclusively expressed in DA neurons exposed to mitochondrial stress (**Figure 6a, b**). These isoforms share the first 2 exons and the same transcription start site (TSS), at which level we observed an ATAC-seq peak that was significantly higher in the stress condition compared to control, suggesting the presence of an active promoter. The longest transcript possesses 5 exons, whereas the shortest isoforms display 3 and 4 exons respectively. Two additional annotated isoforms that were not sequenced in our datasets, *ENST00000689302.1* and *ENST00000688936.2*, have

exons 2, 3 and 4 in common with the isoforms identified in our study, but have different TSS and first exon, not associated with an ATAC-seq peak. Similarly, another annotated lncRNA, *ENSG00000288941,* shared its last exon with the longest isoform detected here, but was not expressed in our datasets. Therefore, our newly annotated isoforms of *lnc-SLC6A15-5* may be specific to human DA neurons subjected to mitochondrial stress. To characterize further this lncRNA, we determined its subcellular localization using cellular fractionation, with *MALAT1* and *MT-ND2* as marker RNAs of the nucleus and the cytoplasm respectively and found that 65% of it was localized to the nucleus, whether or not the neurons were exposed to mitochondrial toxins (**Figure 6c).** We then sought to determine whether *lnc-SLC6A15-5* contributed to the major events of the mitochondrial stress response observed in human DA neurons: the alteration of the DA maturation status, the induction of mitophagy, the decrease in the de novo synthesis of mitochondrial DNA and the inhibition of general translation. We first used CRISPR inhibition technology coupled with viral vector delivery to knockdown this lncRNA. LUHMES cells transduced with a vector expressing either a single guide RNA targeting *lnc-SLC6A15-5* (sgRNA *lnc-SLC6A15-5)* or a sgRNA with no target (sgRNA NEG) were FACS-purified to generate homogeneous cell pools expressing each of these sgRNAs and differentiated into DA neurons. CRISPR inactivation led to an 85% decrease in *lnc-SLC6A15-5* expression upon stress compared to sgRNA NEG (**Supplementary Figure 4a**). Knock-down of *lnc-SLC6A15-5* had no effect on DA neuron identity or maturity, nor on induction of mitophagy or de novo synthesis of mitochondrial DNA at 8 h of stress (**Supplementary Figure 4b-g**). To investigate this lncRNA's involvement in the regulation of translation following exposure to mitochondrial stress, we analyzed the incorporation of the puromycin analog O-propargyl-puromycin (OPP) into newly synthesized proteins in DA neurons with or

without *lnc-SLC6A15-5* knockdown. As expected, mitochondrial stress applied for 8 h resulted in significant attenuation of translation compared to control conditions, as shown by the 81% decrease of the OPP signal (**Supplementary Figure 5a**), and in a significant increase of EIF2α phosphorylation (**Supplementary Figure 5b**). These effects were however independent of the changes in *lnc-SLC6A15-5* expression. We speculated that *lnc-SLC6A15-5* could be involved in the pro-survival response mediated by the resumption of translation after a stress. We therefore analyzed OPP incorporation 30 minutes after washing out the mitochondrial toxins from the culture medium to promote recovery of translation. There was no difference in levels of *lnc-SLC6A15-5* expression in the 30 minutes recovery condition compared to the mitochondrial stress condition without recovery (**Figure 7a,** NEG). Moreover, the knock-down approach reduced *lnc-SLC6A15-5* to about 15% of control levels in both conditions (**Figure 7a,** KD-Lnc-SLC6A15-5). Following wash out of the toxins from DA neurons treated with sgRNA NEG, there was a significant increase in the number of OPP puncta and intensity of OPP signal per neuron, indicating ongoing translational resumption (**Figure 7b-d, and Supplementary Figure 5**). This process was significantly slowed down in cells in which *lnc-SLC6A15-5* was knocked-down, as indicated by the reduction in OPP puncta and OPP signal intensity per neuron following removal of the toxins. These results suggest that *lnc-SLC6A15-5* contributes to a pro-survival response *via* the restoration of general translation. In this context, we explored the possibility that *lnc-SLC6A15-5* exerts this effect through inactivation of EIF2α (**Supplementary Figure 5c**) but did not detect any changes to the ratio between the phosphorylated form of EIF2α and total EIF2α levels following *lnc-SLC6A15-5* silencing. The UPR^{ER} triggers general translation attenuation not only *via* EIF2α but also through inhibition of mTOR. We therefore investigated the possible effect of *lnc-*

SLC6A15-5 on genes involved in the regulation of general translation *via* mTOR (**Figure 7e**, **Supplementary Figure 5d**). *SESN2* is a potent inhibitor of mTOR and a PERK-ATF4 target gene (Brüning *et al*, 2013; Garaeva *et al*, 2016). We found it to be overexpressed after stress in the KD-Lnc-SLC6A15 conditions compared to NEG *lnc-SLC6A15-5*, whether or not the toxins were washed out, indicating that it is regulated by *lnc-SLC6A15-5* under mitochondrial stress. Moreover, in the KD-Lnc-SLC6A15 condition, *SESN2* expression tended to increase more strongly following wash out of the toxins than in cells kept in presence of the toxins (p=0,09). Altogether, these results suggest that *lnc-SLC6A15-5* downregulated *SESN2* upon mitochondrial stress in human DA neurons, allowing for faster translation recovery once the stress signal becomes resolved. In parallel, we explored the role of *lnc-SLC6A15-5* in the regulation of genes encoding various amino-acid transporters (SLC1A3, SLC1A5, SLC3A2, SLC7A5) also known to be PERK-ATF4 target genes (Brüning *et al*, 2013; Han *et al*, 2013; Garaeva *et al*, 2016) and to contribute to mTOR activation (Zhuang *et al*, 2019). All these genes were found to be overexpressed following *lnc-SLC6A15-5* downregulation in cells exposed to mitochondrial toxins (**Figure 7e**), indicating a role of this lncRNA in their inhibition under conditions of mitochondrial stress. Strikingly, *SESN2* and the amino acid transporters regulated by *lnc-SLC6A15-5* are known PERK-ATF4 target genes (Brüning *et al*, 2013; Han *et al*, 2013; Garaeva *et al*, 2016), and are upregulated upon activation of the PERK-mediated UPR^{ER} (**Figure 3**~~)~~. Altogether, these results suggest that *lnc-SLC6A15-5* function counteracts ATF4-mediated transcription during mitochondrial stress. Accordingly, examining *ATF3* expression, we found it to be higher when a 30 minutes recovery from the toxin-induced stress was allowed in comparison to the full 8h of stress, in the condition of *lnc-SLC6A15-5* knock-down only (**Figure 7e**). This indicates an inhibitory effect of *lnc-*

SLC6A15-5 on *ATF3* expression during translation resumption after stress. Overall, *lnc-SLC6A15-5* appears to contribute to a pro-survival response associated with attenuation of PERK-ATF4-mediated UPR^{ER} and resumption of translation.

Discussion

We conducted a comprehensive study to decipher and tie altogether the cellular and molecular mechanisms underlying the response of human DA neurons to mitochondrial stress. We demonstrated the central role of the PERK-mediated UPR^{ER} in orchestrating cell-specific transcriptional programs upon stress, notably through the regulation of lncRNAs expression. Interestingly, PERK activation led to the inactivation of the UPR^{mt} and contributed to the maintenance of mitochondrial integrity and turnover following exposure to mitochondrial toxins. Importantly, we identified a stress-specific lncRNA, *lnc-SLC6A15-5*, which regulated the resumption of translation after mitochondrial stress, by modulating expression of ATF4 target genes involved in the regulation of mTOR activity.

Our work showed that inhibition of the electron transport chain by mitochondrial toxins triggered the concomitant activation of the 3 branches of the UPR^{ER} in human DA neurons, mediated by PERK, IRE1 and ATF6. However, the PERK-EIF2a-ATF4 pathway appeared to play a predominant role in the stress response, as its pharmacological inhibition resulted in alterations at the transcriptional and cellular levels that counteracted this response. While there is a consensus regarding the importance of ATF4 in the mitochondrial stress response in mammalian cells, the involvement of the other branches of the UPR^{ER} or UPR^{mt} remains unclear. The fact that many crosstalks have been uncovered between the PERK-, IRE1- and ATF6-mediated UPR^{ER} (Walter *et al*, 2018; Brewer, 2014) makes the analysis of the contribution of each pathway in the stress response more complex. Indeed, PERK-ATF4 involvement could mask activation of other pathways that share common target genes. Moreover, despite the use of cellular models with homogeneous cell populations, such as LUHMES cells, stress responses differ depending on the cell

types, the activating stimuli, or the duration and intensity of the mitochondrial stress signal (Lamech & Haynes, 2015; Ko *et al*, 2020). This is particularly noteworthy regarding the activation of the UPR^{mt}, which has been observed more frequently, but not systematically, after longer stressor applications (Houtkooper *et al*, 2013; Krug *et al*, 2014; Monti *et al*, 2015; Quirós *et al*, 2017; Cai *et al*, 2020), or using stressors leading to localized alterations, such as mitochondrial protein folding stress (Münch & Harper, 2016; Uoselis *et al*, 2023). In our study, we found that the UPR^{mt} was inactivated following 8 h of treatment with the chosen mitochondrial toxins, and remarkably this effect was directly attributable to the PERK-UPR^{ER}. We cannot exclude that we only observed the first steps of a multiphasic stress response in which UPR^{mt} would be induced at later time points. However, our results suggest that the 8 h stress protocol brought the cells to a crossroad where pro-survival, protective and pro-apoptotic pathways were co-activated, but ultimately leaning towards commitment to cell death, as indicated by the increase in apoptotic neurons observed in our conditions and the predominant activation of the PERK-UPR^{ER} with upregulation of the pro-apoptotic factors CHOP, CHAC1 and TRIB3.

At the cellular level, we have shown that the PERK-UPR^{ER} also contributes to the regulation of mitochondrial turnover upon mitochondrial stress in human DA neurons, since its inactivation by the PERK-specific pharmacological inhibitor GSK2606414 significantly reduced the proportion of DA neurons with ongoing mitophagy. Such direct implication of PERK activation in the induction of mitophagy has been sparsely documented so far and only been described following exposure to chromium (Dlamini *et al*, 2021) or ER stress (Zhang *et al*, 2014), through the transcriptional activation of *PRKN* expression by ATF4 (Zhang *et al*, 2014; Bouman *et al*, 2011). In contrast, ATF4 appeared to restrain the induction of mitophagy following

mitochondrial protein folding stress (Uoselis *et al*, 2023). In our study, *PRKN* was not regulated transcriptionally upon stress, suggesting that modulation of mitophagy by PERK-ATF4 could be channeled through another mechanism.

In contrast, activation of PERK was not found to contribute to the changes in mitochondrial biogenesis, monitored upon stress in terms of newly synthesized mitochondrial DNA. However, using the inhibitor GSK2606414, we showed that PERK pathway activity was necessary in basal conditions for the maintenance of the mitochondrial network and for the biogenesis of mitochondrial DNA, in line with the literature (Muñoz *et al*, 2013; Mesbah Moosavi & Hood, 2017; Kato *et al*, 2020; Sassano *et al*, 2023). Remarkably, these studies revealed that PERK involvement was independent of the UPR. In parallel, ATF6 has also been linked to mitochondrial biogenesis, namely through its regulation by PGC1α (Wu *et al*, 2011; Misra *et al*, 2013). In our conditions, involvement of PERK was demonstrated *via* its pharmacological inactivation, which completely shut down mitochondrial DNA biogenesis. However, we cannot rule out crosstalk between PERK- and ATF6-mediated pathways, with PERK being the primary sensor.

To assess the intrinsic features governing the cell-specificity of the response of human DA neurons to mitochondrial stress, we focused on lncRNAs. Expression of such molecules only depends on transcription, and therefore they can be rapidly mobilized in the context of the cellular response to stress. In addition, their regulatory functions in crucial cellular processes, such as cell growth, proliferation, apoptosis or translation, as well as their species- and cell-specificity, constitute strong arguments for a role of lncRNAs in adapting stress responses to the particularities of each cellular subtypes. LncRNAs have been shown to participate to regulatory pathways associated with p53, mTOR and eIF2 (Scholda *et al*, 2023). A growing number of studies have

explored the contribution of lncRNAs to ER stress response (Quan *et al*, 2018; Li *et al*, 2023), and very often in the context of pathologies such as cancers, leading to the identification of disease-related molecular signatures (Zhang *et al*, 2023; Chen *et al*, 2022; Shen *et al*, 2023). However, most of these investigations focused on single lncRNAs, many of which directly regulate components of the UPR^{ER} (Brookheart *et al*, 2009; Yang *et al*, 2015; Bhattacharyya & Vrati, 2015; Su *et al*, 2016; Wu *et al*, 2020; Martinez-Amaro *et al*, 2023). In line with this, we have discovered novel isoforms of a lncRNA, *lnc-SLC6A15-5*, with probable roles in the resumption of translation once the mitochondrial stress is resolved. Interestingly *lnc-SLC6A15-5* appeared to contribute to the regulation of the UPR^{ER}, as it exerted its action on the transcription of ATF4 target genes that encode mTOR modulators. *Lnc-SLC6A15-5* was upregulated by the UPR^{ER} upon stress, overall suggesting that it could be part of a feedback loop to dampen the UPR^{ER} once the stress is over.

So far, genome-wide studies investigating lncRNAs in the context of PD relied on existing databases, and most of them were performed on brain tissue or blood samples from patients or animal models (Xin & Liu, 2021). Such approaches bring important information regarding lncRNAs as potential biomarkers of the disease, however they have limited potential for the discovery of cell-specific lncRNAs and their functions (Liu *et al*, 2017; Mattick *et al*, 2023). Thus, the vast majority of the lncRNAs investigated in PD are ubiquitously expressed and also known for their implication in other diseases, including MALAT1, NEAT1, H19, lncRNA-p21 or SNHG1 for instance (Kraus *et al*, 2017; Yan *et al*, 2018; Qian *et al*, 2019; Liu *et al*, 2020; Zhang *et al*, 2020; Xin & Liu, 2021; Zhang *et al*, 2022). Using a method allowing for the discovery of novel transcripts, we have established the exhaustive repertoire of lncRNAs expressed in mature human LUHMES-derived DA neurons in basal conditions and following

mitochondrial stress. This study lays the foundations for the detailed investigation of the role of lncRNAs in key steps of the DA-specific response to mitochondrial stress and, more generally, in the pathophysiology of PD, characterized by the degeneration of these neurons.

Materials and Methods

LUHMES cell culture and differentiation

LUHMES cells were grown in proliferation medium containing Advanced Dulbecco's Modified Eagle Medium (DMEM)/F12, 1% N-2 supplement, 1% penicillin/streptomycin (P/S), L-Glutamine (2 mM, Life Technologies), and human basic fibroblast growth factor (FGF, 40 ng/mL, R&D Systems). Cells were maintained at 37°C in a humidified atmosphere containing 5% CO_2, passaged using 0.05% trypsin (Gibco) and plated at a density of 2.3 x 10^4 cells/cm^2. Plastic cell culture flasks and multi-well plates were coated with poly-L-ornithine (pLO, 50 µg/mL), fibronectin bovine plasma (1 µg/mL, Sigma-Aldrich) and 1% P/S, and incubated overnight at 37°C. After removing the coating solution, culture flasks were washed twice with water before cell seeding.

For differentiation, LUHMES cells were plated at a cell density of 5 x 10^4 cells/cm^2 in proliferation medium. After 24 h (day 0 of differentiation), proliferation medium was replaced by differentiation medium consisting of Advanced DMEM/F12, 1% N-2 supplement, 1% P/S, L-Glutamine (2 mM), dibutyryl cyclic AMP (cAMP, 1 mM, Sigma-Aldrich), recombinant human growth-derived neurotrophic factor (GDNF, 2 ng/mL, Peprotech) and tetracycline (1 µg/mL, Sigma-Aldrich). On day 2 of differentiation, LUHMES cells were seeded into pre-coated culture plates at a cell density of 1x 10^5 cells/cm^2. The following day, differentiation medium was changed.

Mitochondrial Stress

LUHMES-derived DA neurons (day 6 of differentiation) were treated with a combination of antimycin A (25 µM, Sigma-Aldrich), and oligomycin (10µM, Sigma-Aldrich). Stock solutions of these toxins, at 2 mg/mL and 25 mg/mL respectively, were dissolved in dimethyl sulfoxide (DMSO). After treatment, neurons were collected or fixed for

subsequent analysis. For controls experiments, DMSO was added to the samples without mitochondrial toxins.

PERK-UPR^{ER} inhibition

For experiments investigating the contribution of the PERK-mediated UPR^{ER} to the stress response, cells were incubated with GSK2606414 (25µM, Selleckchem), simultaneously to the incubation with mitochondrial toxins or with DMSO for the control experiments.

Immunofluorescence

Glass coverslips were added to the 4-well plates and pre-coated with pLO and fibronectin, overnight at 37°C. Next, laminin (5 µg/mL, Life technologies) was added to the coating medium at 37°C for 1 h, before cell seeding. After culture and treatments, cells were fixed for 15 min in 4% paraformaldehyde prepared in PBS 1X. Immunofluorescent labelling was performed as described previously (Gendron *et al*, 2019). The primary and secondary antibodies used are described in Supplementary Table S1. Nuclei were labelled with DAPI DNA stain.

Image acquisition were performed on either SP8 inverted confocal microscope (Leica) with a 40x or 63x oil immersion objective or AxioScan Z1 (Zeiss) with a x20 objective.

Mitochondrial biogenesis assay

Replication of mitochondrial DNA (mtDNA) was monitored using the Click-iT Plus EdU Cell Proliferation Kit for Imaging (Salic & Mitchison, 2008) (Invitrogen) according to manufacturer's instructions. Briefly, EdU was added at a final concentration of 10 µM to the differentiation medium, and incubated for 2, 4, and 8 h at 37°C, or only 8 h when

cells were treated with GSK2606414. Then, neurons were fixed in 4% PFA for 15 min at room temperature, followed by permeabilization with PBS-Triton 0.2% supplemented with 4% goat serum overnight at 4°C. The following day, after washes, cells were incubated for 30 min at room temperature in the dark with the Click-iT Plus reaction cocktail readily prepared according to the manufacturer's instructions. In the EdU control experiments, neurons were pretreated for 4 h with 2',3'-dideoxycytidine (ddC, 100 µM). This was followed by cotreatment of ddC and EdU for 4 h or 24 h of incubation. As ddC was dissolved in DMSO, controls experiments were supplemented with an equal DMSO volume. For control experiments regarding mitochondrial stress, DMSO was added to the samples without mitochondrial toxins.

Translation assay

Protein synthesis was assessed using the Click-iT Plus OPP Alexa Fluor 647 Protein Synthesis Assay Kit (Invitrogen) according to manufacturer's guidelines. Cells were incubated in fresh medium containing O-propargyl-puromycin (OPP, 20 µM) for 30 min at 37°C. For this experiment, two conditions were tested: 8 h stress or DMSO for which the OPP-supplemented medium also contained mitochondrial toxins or DMSO, and 7h30 stress/DMSO followed by 30 min of recovery for which the OPP-supplemented medium was free of toxins or DMSO. After 30 min of incubation, cells were fixed using 4% PFA for 15 min at room temperature and, after washes in PBS1X, stored at 4°C overnight in PBS1X. The following day, cells were permeabilized in PBS-Triton 0.5% for 15 min and were then incubated for 30 min at room temperature in the dark with freshly made Click-iT OPP reaction cocktail as per manufacturer's instructions. Cells were then washed with the Click-iT Reaction Rinse Buffer before proceeding with immunofluorescence and DAPI staining.

RNA extraction

Total RNAs were purified from LUHMES cells using a RNeasy Minikit (Qiagen) following manufacturer's instructions. RNAs were further treated with DNAse I (Roche) for 20 min at room temperature to prevent genomic DNA contamination. RNA quantification was determined either by spectrophotometry (Nanodrop 2000c, THERMO Scientific) prior to RT-qPCR or using a High Sensitivity RNA ScreenTAPE analyzer (Agilent technologies) for RNA-seq. In the latter case, the RNA integrity number (RIN) was used to determine RNA quality for all tested samples. RNA was stored at −80 °C until reverse transcription or RNA-seq.

For subcellular localization, Trizol reagent (Life technologies) was used following manufacturer's instructions for RNA extraction.

Subcellular fractionation

A minimum of 10 million of cells was used for subcellular fractionation. LUHMES cells were enzymatically dissociated by using 0.05% trypsin, centrifuged, and washed once with PBS. The cell pool was divided in two parts, the first part for total RNA extraction directly lysed with Trizol reagent (Life technologies) and -80°C frozen, and the second part for fractionation. Subcellular fractionation was performed as described by Gagnon et al. (Gagnon *et al*, 2014). Briefly, cells were lysed with hypotonic buffer (10 mM Tris-HCl [pH 7.5], 10mM NaCl, 3mM $MgCl_2$, 0.3% NP-40, 10% Glycerol) supplemented of 100U RNase-OUT and DTT (10mM) during 10 min on ice. Intact nuclei were separated of cytosol fraction by centrifugation 3 min at 1000g at 4°C. Then, the supernatant was recovered (cytosol fraction), and RNA were precipitated with 150mM Na_2Ac [pH 5.5], 95% EtOH supplemented with DT40 (10µg), 1 h at -20°C. During this time, the pellet

was washed in hypotonic buffer (see above) before lysed by Trizol reagent supplemented with DT40 (10µg) and then frozen at -80°C.

Real time quantitative RT-PCR (RT-qPCR)

Up to 800 ng total RNAs were used to generate a first cDNA strand (Superscript II reverse transcriptase, THERMO Fisher Scientific) with random hexamers as indicated by the manufacturer. qPCR experiments were realized on the Light Cycler 384 real-time PCR system (Roche); with SYBER green detection (Roche). The comparative method of relative quantification ($2^{-\Delta\Delta CT}$) was used to calculate the expression levels of each target gene and human TBP mRNA was used to normalize the expression of all samples. The list of primers used is provided in the Supplementary table S2.

Western blotting

Cells were differentiated and re-plated in T75 flasks. At day 6 of the differentiation, cells were scraped from the plate and lysed in 1× Ripa buffer (Sigma-Aldrich) supplemented with 1× protease and phosphatase inhibitor cocktail (ThermoFisher Scientific). The lysate was centrifuged at 13 500 rpm for 5 min at 4 °C, and the supernatant was collected. Protein concentration was measured using a BCA kit (Pierce). Each sample (15 µg) was boiled for 5 min and applied on NuPAGE 4%–12% Bis-Tris Gel (Biorad). The gel was transferred onto a nitrocellulose membrane. The membranes were incubated with primary antibodies at 4°C overnight followed by secondary antibody for 1 h at room temperature. Membranes were scanned and analyzed using Chemidoc Touch Imaging system (Biorad). The list of antibodies used for western Blotting are presented in Supplementary Table S1.

Image processing and analysis

For experiments investigating mitophagy induction, the slides were digitized using the AxioScan Z1 (Zeiss) with a x20 objective and acquired using the ZEN software. The resulting files were exported and whole slide image were processed on QuPath, an open-source machine learning software (Bankhead *et al*, 2017). The total number of cells on each image was obtained by counting the DAPI stained nuclei. Following cell detection, the QuPath algorithm was able to quantify the number of cells labeled with markers of interest by setting specific intensity thresholds. For experiments investigating mitophagy, mitochondrial biogenesis and protein synthesis, images were acquired with the Leica TCS SP8 Digital LightSheet inverted confocal microscope with a x40 or x63 oil objective, using the LAS (Leica Application Suite) X acquisition software and processed with the ImageJ software available at https://imagej.nih.gov/ij/ (Schneider *et al*, 2012). A threshold was set to select the signal of interest, then different parameters were analyzed including the area and intensity of our signal of interest (here, EdU and OPP). For punctiform signals, as provided by EdU and OPP, the number of puncta per neuron (and puncta colocalization with TOMM20 for EdU) was also quantified using the spot detection and colocalization ImageJ plugin ComDet v.0.5.5. Regarding the analysis of the mitochondrial marker TOMM20 labeling, the area occupied by clusters of mitochondria (defined as the area of TOMM20+ clusters) was also measured using the subcellular detection tool from QuPath software.

DNA lentiviral constructs for CRISPR inhibition and activation

Loss of function was performed with CRISPR inhibition technology (CRISPRi). LV_U6-empty_EF-1α-KRAB-dCas9-T2A-TagEGFP backbone vector was kindly provided by Jorge FERRER's Lab (Imperial College London). The sgRNA targeting *lnc-SLC6A15-*

5 (KD), or the control sgRNA (sgNEG - targeting the human AAVS1 locus), were cloned into BsmBI sites of LV backbone vectors. The KD sgRNA was designed 35pb after *lnc-SLC6A15-5* transcription start site (TSS) using a bulge-allowed quick guide-RNA designer for CRISPR/Cas derived RGENs (http://www.rgenome.net/cas-designer/). All sgRNA sequences used in this study are presented in Supplementary Table S3.

Lentiviral vector production

Lentiviral vector stocks were produced as previously described (Scharfmann *et al*, 2008). Briefly, HEK 293T cells were transfected by the p8.9 packaging plasmid (ΔVprΔVifΔVpuΔNef) (2), the pHCMV-G that encoded the VSV glycoprotein-G (Zufferey *et al*, 1997) and the pTRIP ΔU3 recombinant lentiviral vector. The supernatants were treated with DNAse I (Roche Diagnostic) prior to their ultracentrifugation, and the resultant pellets were re-suspended in PBS, aliquoted, and then frozen at -80°C until use. The amount of p24 capsid protein was quantified by the HIV-1 p24 antigen ELISA (Beckman Coulter). All transductions were normalized relative to p24 capsid protein quantification.

Fluorescence-activated cell sorting (FACS)

For CRISPRi experiments, KD-lnc-SLC6A15-5 or control (NEG) cells are both expressing GFP and were purified using cell sorting. Cells were enzymatically dissociated by using 0.05% trypsin, centrifuged, washed once with PBS and filtered (50 µm filter) prior to cell sorting. GFP+ cells were purified using a S3 Biorad cell sorter. Cell suspensions from LUHMES non-transduced were used to adjust background fluorescence.

RNA-sequencing (RNA-seq)

4 independent LUHMES cell differentiations were treated or not with mitochondrial toxins. 500 ng of total RNA were used from Control (n=4) and stressed (n=4) DA neurons to prepare stranded RNAseq libraries following manufacturer's recommendations using KAPA mRNA hyperprep (Roche Diagnostic). Each final library was quantified and qualified with 2200 Tapestation (Agilent). Final samples of pooled library preparation were sequenced on NextSeq500 with High Output Kit cartridge at 2x150M reads/sample.

Assay for Transposase-Accessible Chromatin (ATAC-seq)

For each sample, 70 000 cells collected and centrifuged at 500 g, at 4 °C during 20 min. Cells were resuspended in 25 µL of lysis buffer (10 mM Tris-HCl pH 7.4, 10 mM NaCl, 3 mM $MgCl_2$-$6H_2O$, 0.1% IGEPAL CA-630) during 30 min at 4 °C. Then, after centrifugation at 500 g, at 4 °C during 30 min the nuclear pellet was treated by Tn5 transposase. The pellet was resuspended in 25 µl of 12.5 µl 2x TN buffer; 2 µl of Tn5; 10.5 µl d'H_2O and incubated at 37 °C for 1 h. Next, 5 µl of clean-up buffer (900 mM NaCl, 300 mM EDTA) were added to transposase treated nuclei, followed by 2 µl of 5% SDS and 2 µl of 20mg/ml Proteinase K, and incubated for 30 min at 40 °C. DNA samples were then purified twice using 68 µl of AMPure-XP beads (Beckman Coulter_A63881) and next eluted in 13 µl of buffer EB (Qiagen Cat No./ID: 19086). Amplification and size selection of ATAC-seq libraries were performed according to Grbesa et al. (2017 PMID: 29155775) using Nextera XT Index kit (Illumina-15055293). Extracted DNA concentration was measured by 2200 Tapestation (Agilent

Technologies). Final samples of pooled library preparation were sequenced on Novaseq6000 with SP-100 cartridge at 100M reads/sample.

RNAseq analysis and de novo annotation of lncRNAs

The analysis of lncRNA expressions from Next-Generation Sequencing (NGS) data involved a comprehensive pipeline of sequential steps. Initially, raw FASTQ files underwent quality assessment using FastQC v0.11.8, followed by Trimmomatic v0.39 trimming to remove low-quality trailing bases, adapters, and reads shorter than 50 bases. Cleaned reads were then aligned to the hg38 human reference genome using HISAT2 v2.2.1 (Kim *et al*, 2019), resulting in ordered BAM files generated through Samtools v1.11 (Danecek *et al*, 2021). Subsequent transcript assembly and abundance estimation were performed using StringTie v2.1.4 (Pertea *et al*, 2015), followed by the merging of transcript annotations from all samples into a unified catalog using StringTie merge. Expression levels of transcripts were quantified through StringTie FPKM normalization. Comparative analysis against Gencode v44 and LNCipedia v5.2 reference catalogs was carried out using GffCompare v0.11.2 (Pertea & Pertea, 2020), with transcript annotations categorized as "known" or "unknown" based on class codes. Coding potential prediction was executed using CPC2 v1.0.1 (Kang *et al*, 2017), CPAT v3.0.3 (Wang *et al*, 2013) and CNIT (Guo *et al*, 2019). Annotations were enriched with details about nearest protein-coding genes and LNCipedia classification. The catalog underwent successive filtration, including removal of low-expression transcripts, retention of non-coding transcripts predicted by multiple tools, and elimination of short transcripts with lengths below 200 bases. Additionally mono-exonic transcripts not present in Gencode or LNCipedia were retained only if an ATAC-seq peak was present within 100 bases from the transcription

start site (TSS). The remaining transcripts were filtered according to specific gene/transcript types from Gencode. The filtered catalog was then merged with the Gencode catalog, appending transcripts that did not exactly match the reference. This updated catalog was quantified with STAR v2.7 (Dobin *et al*, 2013) using original FASTQ files. Resulting FPKM counts were integrated into the filtered catalog, which underwent consolidation into a gene-centric format, retaining annotations solely for the most highly expressed transcript per gene. This comprehensive pipeline facilitated the detailed analysis of lncRNA expressions and provided valuable insights into their roles and functions. Normalization and differential analysis for protein-coding or non-coding genes were performed with the DESeq2 package.

ATAC-seq data processing

Steps for quality control were identical to those used for RNA-seq data treatment (Trimmomatic, FastQC). Reads with a length below 50 bp have been removed in further analysis. Paired-end reads were mapped to the human genome (build hg38) with Bowtie2. Duplicate reads were discarded with the Picard tools. Peaks were called using the MACS2 program with the option callpeak. Individual peak annotations were obtained with the R software version 3.5.1 (R Development Core Team, 2018) using the ChIPseeker R package (v1.20). Consensus peak was obtained using the DiffBind R package (v2.12).

Pathway enrichment analysis and transcription factor motifs search

Enrichr web tool (https://maayanlab.cloud/Enrichr/) was used to perform gene ontology (GO) and pathway enrichment analysis of gene lists with the GO Biological Processes

2023 and Reactome 2022 databases (Chen *et al*, 2013; Kuleshov *et al*, 2016; Xie *et al*, 2021; Gillespie *et al*, 2022). Cistrome Data Browser toolkit (http://dbtoolkit.cistrome.org) and Cistrome-GO were used to identify transcription factors with binding sites significantly overlapping promoters of lncRNAs or ATAC-seq-detected open chromatin regions, and to perform functional enrichment analysis from the results obtained (Zheng *et al*, 2019; Mei *et al*, 2017; Li *et al*, 2019).

Data availability

Raw sequence reads from RNA-seq and ATAC-seq are available from GEO under accession number GSE (in progress).

Statistics

For evaluation of TH, DAT and cCASP3 staining as well as P-eIF2α/eIF2α protein levels in 8 h control and stress conditions, statistical analyses were performed using paired Student's *t* tests. For mitochondrial DNA synthesis, mitophagy and protein synthesis experiments, two-way analysis of variance ANOVA tests were applied, followed by post-hoc Tukey's multiple comparison test. All these tests were carried out using GraphPad 9.1.2.

Regarding kinetic experiments evaluating RNA expression of UPR^{ER} and UPR^{mt} factors as well as of candidate lncRNAs, group differences and evolutions of expression values were investigated using linear mixed-effects models (LMMs) by fitting one model per gene of interest. In each model, the factor variables Condition (four levels for Control and Stress with or without the GSK2606414 treatment), Time (30, 120, 240, 360, and 480 minutes) and their interaction term were regarded as fixed effects, while a random (intercept) effect was used to account for values obtained from

the same differentiation experiments. All LLMs were fitted using the lmer function of the lme4 R package (v1.1-34) (Bates *et al*, 2015) with R version 4.3.1 (R Development Core Team, 2023). For each gene, the significance of the main and interaction effects of Condition and Time was assessed by Type II Wald Chi-square tests using the function Anova of the car R package (v3.1-2). For post hoc pairwise comparisons, all conditions were compared at each time point using the emmeans R package (v1.8.8) with the Tukey's method for multiple testing. Prior to modeling, a log-transformation (log(x+0.1)) was applied to expression data in order to better meet the the LMM assumptions of normality and homoscedasticity of residuals. The same analysis was performed on the RT-qPCR results looking at the RNA expression of multiple targets in the 7h30 with 30 minutes recovery or 8 h control or stress conditions. All the test results were graphically reported as heatmaps generated with the ComplexHeatmap R package (v.2.16.0).

Supplemental material

Results from additional experiments are shown in Supplementary Figures 1 to 5:

Supplementary Figure 1 shows the incorporation of EdU in mtDNA in DA neurons as mean to follow mitochondrial biogenesis. Supplementary Figure 2 shows the number of ATAC-seq peaks defining chromatin regions with altered accessibility upon 8 h of mitochondrial stress, as well as Gene Ontology enrichment analyses performed on genes associated with these regions. Supplementary Figure 3 shows the effect of GSK2606414 on the initiation of mitophagy (marked by the expression of Phospho-Serine 65 ubiquitin) following 4 and 6 h of mitochondrial stress, compared to control conditions. Supplementary Figure 4 shows the effect of the inhibition of Lnc-SLC6A15-5 expression in the number of mature DA neurons (TH and DAT expression *via*

immunofluorescence), initiation of mitophagy (Phospho-Serine 65 ubiquitin expression) and mitochondrial biogenesis (Edu integration into mtDNA) upon 8 h of stress. Supplementary Figure 5 shows the effect of the inhibition of Lnc-SLC6A15-5 expression on the expression of molecular actors involved in the regulation of translation, at the protein level (EIF2α and phospho-EIF2α) or mRNA level (DDIT4, SYNCRIP, MTOR, RPS6KB1, RPS6, EIF4EBP1 and EIF4EBP2), following 8 h of stress, or 7h30 of stress and 30 min of recovery. Supplementary tables 1, 2 and 3 recapitulate the lists of antibodies, primer sequences and sgRNA sequences used in this study.

References

Adachi Y, Yamamoto K, Okada T, Yoshida H, Harada A & Mori K (2008) ATF6 is a transcription factor specializing in the regulation of quality control proteins in the endoplasmic reticulum. *Cell Struct Funct* 33: 75–89

Akerman I, Tu Z, Beucher A, Rolando DMY, Sauty-Colace C, Benazra M, Nakic N, Yang J, Wang H, Pasquali L, *et al* (2017) Human Pancreatic β Cell lncRNAs Control Cell-Specific Regulatory Networks. *Cell Metab* 25: 400–411

Altshuler D, Daly MJ & Lander ES (2008) Genetic mapping in human disease. *Science* 322: 881–888

Axten JM, Medina JR, Feng Y, Shu A, Romeril SP, Grant SW, Li WHH, Heerding DA, Minthorn E, Mencken T, *et al* (2012) Discovery of 7-methyl-5-(1-{[3-(trifluoromethyl)phenyl]acetyl}-2,3-dihydro-1H-indol-5-yl)-7H-pyrrolo[2,3-d]pyrimidin-4-amine (GSK2606414), a potent and selective first-in-class inhibitor of protein kinase R (PKR)-like endoplasmic reticulum kinase (PERK). *J Med Chem* 55: 7193–7207

Bankhead P, Loughrey MB, Fernández JA, Dombrowski Y, McArt DG, Dunne PD, McQuaid S, Gray RT, Murray LJ, Coleman HG, *et al* (2017) QuPath: Open source software for digital pathology image analysis. *Sci Rep* 7: 16878

Bates D, Mächler M, Bolker B & Walker S (2015) Fitting Linear Mixed-Effects Models Using lme4. *Journal of Statistical Software* 67: 1–48

Bhattacharyya S & Vrati S (2015) The Malat1 long non-coding RNA is upregulated by signalling through the PERK axis of unfolded protein response during flavivirus infection. *Sci Rep* 5: 17794

Borsche M, Pereira SL, Klein C & Grünewald A (2021) Mitochondria and Parkinson's Disease: Clinical, Molecular, and Translational Aspects. *JPD* 11: 45–60

Bose A & Beal MF (2016) Mitochondrial dysfunction in Parkinson's disease. *J Neurochem* 139 Suppl 1: 216–231

Bouman L, Schlierf A, Lutz AK, Shan J, Deinlein A, Kast J, Galehdar Z, Palmisano V, Patenge N, Berg D, *et al* (2011) Parkin is transcriptionally regulated by ATF4: evidence for an interconnection between mitochondrial stress and ER stress. *Cell Death Differ* 18: 769–782

Brewer JW (2014) Regulatory crosstalk within the mammalian unfolded protein response. *Cell Mol Life Sci* 71: 1067–1079

Brichta L & Greengard P (2014) Molecular determinants of selective dopaminergic vulnerability in Parkinson's disease: an update. *Front Neuroanat* 8: 152

Brookheart RT, Michel CI, Listenberger LL, Ory DS & Schaffer JE (2009) The non-coding RNA gadd7 is a regulator of lipid-induced oxidative and endoplasmic reticulum stress. *J Biol Chem* 284: 7446–7454

Brüning A, Rahmeh M & Friese K (2013) Nelfinavir and bortezomib inhibit mTOR activity via ATF4-mediated sestrin-2 regulation. *Mol Oncol* 7: 1012–1018

Cabili MN, Trapnell C, Goff L, Koziol M, Tazon-Vega B, Regev A & Rinn JL (2011) Integrative annotation of human large intergenic noncoding RNAs reveals global properties and specific subclasses. *Genes Dev* 25: 1915–1927

Cai Y, Shen H, Weng H, Wang Y, Cai G, Chen X & Ye Q (2020) Overexpression of PGC-1α influences the mitochondrial unfolded protein response (mtUPR) induced by MPP+ in human SH-SY5Y neuroblastoma cells. *Sci Rep* 10: 10444

Carta G, van der Stel W, Scuric EWJ, Capinha L, Delp J, Bennekou SH, Forsby A, Walker P, Leist M, van de Water B, *et al* (2023) Transcriptional landscape of mitochondrial electron transport chain inhibition in renal cells. *Cell Biol Toxicol*

Chen EY, Tan CM, Kou Y, Duan Q, Wang Z, Meirelles GV, Clark NR & Ma'ayan A (2013) Enrichr: interactive and collaborative HTML5 gene list enrichment analysis tool. *BMC Bioinformatics* 14: 128

Chen J, Shen L & Yang Y (2022) Endoplasmic reticulum stress related lncRNA signature predicts the prognosis and immune response evaluation of uterine corpus endometrial carcinoma. *Front Oncol* 12: 1064223

Damier P, Hirsch EC, Agid Y & Graybiel AM (1999) The substantia nigra of the human brain. II. Patterns of loss of dopamine-containing neurons in Parkinson's disease. *Brain* 122 (Pt 8): 1437–1448

Danecek P, Bonfield JK, Liddle J, Marshall J, Ohan V, Pollard MO, Whitwham A, Keane T, McCarthy SA, Davies RM, *et al* (2021) Twelve years of SAMtools and BCFtools. *Gigascience* 10: giab008

Dauer W & Przedborski S (2003) Parkinson's disease: mechanisms and models. *Neuron* 39: 889–909

Davis CA, Hitz BC, Sloan CA, Chan ET, Davidson JM, Gabdank I, Hilton JA, Jain K, Baymuradov UK, Narayanan AK, *et al* (2018) The Encyclopedia of DNA elements (ENCODE): data portal update. *Nucleic Acids Res* 46: D794–D801

Dickson DW, Braak H, Duda JE, Duyckaerts C, Gasser T, Halliday GM, Hardy J, Leverenz JB, Del Tredici K, Wszolek ZK, *et al* (2009) Neuropathological assessment of Parkinson's disease: refining the diagnostic criteria. *Lancet Neurol* 8: 1150–1157

Dlamini MB, Gao Z, Hasenbilige null, Jiang L, Geng C, Li Q, Shi X, Liu Y & Cao J (2021) The crosstalk between mitochondrial dysfunction and endoplasmic reticulum stress promoted ATF4-mediated mitophagy induced by hexavalent chromium. *Environ Toxicol* 36: 1162–1172

Dobin A, Davis CA, Schlesinger F, Drenkow J, Zaleski C, Jha S, Batut P, Chaisson M & Gingeras TR (2013) STAR: ultrafast universal RNA-seq aligner. *Bioinformatics* 29: 15–21

Dölle C, Flønes I, Nido GS, Miletic H, Osuagwu N, Kristoffersen S, Lilleng PK, Larsen JP, Tysnes O-B, Haugarvoll K, *et al* (2016) Defective mitochondrial DNA homeostasis in the substantia nigra in Parkinson disease. *Nat Commun* 7: 13548

Eldeeb MA, Thomas RA, Ragheb MA, Fallahi A & Fon EA (2022) Mitochondrial quality control in health and in Parkinson's disease. *Physiol Rev* 102: 1721–1755

Epanchintsev A, Costanzo F, Rauschendorf M-A, Caputo M, Ye T, Donnio L-M, Proietti-de-Santis L, Coin F, Laugel V & Egly J-M (2017) Cockayne's Syndrome A and B Proteins Regulate Transcription Arrest after Genotoxic Stress by Promoting ATF3 Degradation. *Mol Cell* 68: 1054-1066.e6

Gagnon KT, Li L, Janowski BA & Corey DR (2014) Analysis of nuclear RNA interference in human cells by subcellular fractionation and Argonaute loading. *Nat Protoc* 9: 2045–2060

Garaeva AA, Kovaleva IE, Chumakov PM & Evstafieva AG (2016) Mitochondrial dysfunction induces SESN2 gene expression through Activating Transcription Factor 4. *Cell Cycle* 15: 64–71

Ge P, Dawson VL & Dawson TM (2020) PINK1 and Parkin mitochondrial quality control: a source of regional vulnerability in Parkinson's disease. *Mol Neurodegener* 15: 20

Gendron J, Colace-Sauty C, Beaume N, Cartonnet H, Guegan J, Ulveling D, Pardanaud-Glavieux C, Moszer I, Cheval H & Ravassard P (2019) Long non-coding RNA repertoire and open chromatin regions constitute midbrain dopaminergic neuron - specific molecular signatures. *Sci Rep* 9: 1409

Georgakopoulos ND, Wells G & Campanella M (2017) The pharmacological regulation of cellular mitophagy. *Nat Chem Biol* 13: 136–146

Gil N & Ulitsky I (2020) Regulation of gene expression by cis-acting long non-coding RNAs. *Nat Rev Genet* 21: 102–117

Gillespie M, Jassal B, Stephan R, Milacic M, Rothfels K, Senff-Ribeiro A, Griss J, Sevilla C, Matthews L, Gong C, *et al* (2022) The reactome pathway knowledgebase 2022. *Nucleic Acids Res* 50: D687–D692

de Goede OM, Nachun DC, Ferraro NM, Gloudemans MJ, Rao AS, Smail C, Eulalio TY, Aguet F, Ng B, Xu J, *et al* (2021) Population-scale tissue transcriptomics maps long non-coding RNAs to complex disease. *Cell* 184: 2633-2648.e19

Grünewald A, Kumar KR & Sue CM (2019) New insights into the complex role of mitochondria in Parkinson's disease. *Progress in Neurobiology* 177: 73–93

Gundu C, Arruri VK, Sherkhane B, Khatri DK & Singh SB (2022) GSK2606414 attenuates PERK/p-eIF2α/ATF4/CHOP axis and augments mitochondrial function to mitigate high glucose induced neurotoxicity in N2A cells. *Curr Res Pharmacol Drug Discov* 3: 100087

Guo J-C, Fang S-S, Wu Y, Zhang J-H, Chen Y, Liu J, Wu B, Wu J-R, Li E-M, Xu L-Y, *et al* (2019) CNIT: a fast and accurate web tool for identifying protein-coding and long non-coding transcripts based on intrinsic sequence composition. *Nucleic Acids Research* 47: W516–W522

Han J, Back SH, Hur J, Lin Y-H, Gildersleeve R, Shan J, Yuan CL, Krokowski D, Wang S, Hatzoglou M, *et al* (2013) ER-stress-induced transcriptional regulation increases protein synthesis leading to cell death. *Nat Cell Biol* 15: 481–490

Harding HP, Zhang Y, Zeng H, Novoa I, Lu PD, Calfon M, Sadri N, Yun C, Popko B, Paules R, *et al* (2003) An integrated stress response regulates amino acid metabolism and resistance to oxidative stress. *Mol Cell* 11: 619–633

Hirsch E, Graybiel AM & Agid YA (1988) Melanized dopaminergic neurons are differentially susceptible to degeneration in Parkinson's disease. *Nature* 334: 345–348

Höllerhage M, Moebius C, Melms J, Chiu W-H, Goebel JN, Chakroun T, Koeglsperger T, Oertel WH, Rösler TW, Bickle M, *et al* (2017) Protective efficacy of phosphodiesterase-1 inhibition against alpha-synuclein toxicity revealed by compound screening in LUHMES cells. *Sci Rep* 7: 11469

Houtkooper RH, Mouchiroud L, Ryu D, Moullan N, Katsyuba E, Knott G, Williams RW & Auwerx J (2013) Mitonuclear protein imbalance as a conserved longevity mechanism. *Nature* 497: 451–457

Jarroux J, Morillon A & Pinskaya M (2017) History, Discovery, and Classification of lncRNAs. *Adv Exp Med Biol* 1008: 1–46

Jennings P, Carta G, Singh P, da Costa Pereira D, Feher A, Dinnyes A, Exner TE & Wilmes A (2023) Capturing time-dependent activation of genes and stress-response pathways using transcriptomics in iPSC-derived renal proximal tubule cells. *Cell Biol Toxicol* 39: 1773–1793

Jiang C, Li Y, Zhao Z, Lu J, Chen H, Ding N, Wang G, Xu J & Li X (2016) Identifying and functionally characterizing tissue-specific and ubiquitously expressed human lncRNAs. *Oncotarget* 7: 7120–7133

Kalia LV & Lang AE (2015) Parkinson's disease. *Lancet* 386: 896–912

Kang Y-J, Yang D-C, Kong L, Hou M, Meng Y-Q, Wei L & Gao G (2017) CPC2: a fast and accurate coding potential calculator based on sequence intrinsic features. *Nucleic Acids Res* 45: W12–W16

Kato H, Okabe K, Miyake M, Hattori K, Fukaya T, Tanimoto K, Beini S, Mizuguchi M, Torii S, Arakawa S, *et al* (2020) ER-resident sensor PERK is essential for mitochondrial thermogenesis in brown adipose tissue. *Life Sci Alliance* 3: e201900576

Kazlauskaite A, Kondapalli C, Gourlay R, Campbell DG, Ritorto MS, Hofmann K, Alessi DR, Knebel A, Trost M & Muqit MMK (2014) Parkin is activated by PINK1-dependent phosphorylation of ubiquitin at Ser65. *Biochem J* 460: 127–139

Kim D, Paggi JM, Park C, Bennett C & Salzberg SL (2019) Graph-based genome alignment and genotyping with HISAT2 and HISAT-genotype. *Nat Biotechnol* 37: 907–915

Ko KR, Tam NW, Teixeira AG & Frampton JP (2020) SH-SY5Y and LUHMES cells display differential sensitivity to MPP+, tunicamycin, and epoxomicin in 2D and 3D cell culture. *Biotechnol Prog* 36: e2942

Kohli MA, Lucae S, Saemann PG, Schmidt MV, Demirkan A, Hek K, Czamara D, Alexander M, Salyakina D, Ripke S, *et al* (2011) The neuronal transporter gene SLC6A15 confers risk to major depression. *Neuron* 70: 252–265

Kraus TFJ, Haider M, Spanner J, Steinmaurer M, Dietinger V & Kretzschmar HA (2017) Altered Long Noncoding RNA Expression Precedes the Course of Parkinson's Disease-a Preliminary Report. *Mol Neurobiol* 54: 2869–2877

Krug AK, Gutbier S, Zhao L, Pöltl D, Kullmann C, Ivanova V, Förster S, Jagtap S, Meiser J, Leparc G, *et al* (2014) Transcriptional and metabolic adaptation of human neurons to the mitochondrial toxicant MPP(+). *Cell Death Dis* 5: e1222

Kuleshov MV, Jones MR, Rouillard AD, Fernandez NF, Duan Q, Wang Z, Koplev S, Jenkins SL, Jagodnik KM, Lachmann A, *et al* (2016) Enrichr: a comprehensive gene set enrichment analysis web server 2016 update. *Nucleic Acids Res* 44: W90-97

Lamech LT & Haynes CM (2015) The unpredictability of prolonged activation of stress response pathways. *J Cell Biol* 209: 781–787

Langston JW, Ballard P, Tetrud JW & Irwin I (1983) Chronic Parkinsonism in humans due to a product of meperidine-analog synthesis. *Science* 219: 979–980

Lazarou M, Sliter DA, Kane LA, Sarraf SA, Wang C, Burman JL, Sideris DP, Fogel AI & Youle RJ (2015) The ubiquitin kinase PINK1 recruits autophagy receptors to induce mitophagy. *Nature* 524: 309–314

Li S, Wan C, Zheng R, Fan J, Dong X, Meyer CA & Liu XS (2019) Cistrome-GO: a web server for functional enrichment analysis of transcription factor ChIP-seq peaks. *Nucleic Acids Res* 47: W206–W211

Li X, Li J, Shan G & Wang X (2023) Identification of long non-coding RNA and circular RNA associated networks in cellular stress responses. *Front Genet* 14: 1097571

Liu R, Li F & Zhao W (2020) Long noncoding RNA NEAT1 knockdown inhibits MPP+-induced apoptosis, inflammation and cytotoxicity in SK-N-SH cells by regulating miR-212-5p/RAB3IP axis. *Neurosci Lett* 731: 135060

Liu SJ, Horlbeck MA, Cho SW, Birk HS, Malatesta M, He D, Attenello FJ, Villalta JE, Cho MY, Chen Y, *et al* (2017) CRISPRi-based genome-scale identification of functional long noncoding RNA loci in human cells. *Science* 355: aah7111

Lotharius J, Barg S, Wiekop P, Lundberg C, Raymon HK & Brundin P (2002) Effect of mutant alpha-synuclein on dopamine homeostasis in a new human mesencephalic cell line. *J Biol Chem* 277: 38884–38894

Lotharius J, Falsig J, van Beek J, Payne S, Dringen R, Brundin P & Leist M (2005) Progressive degeneration of human mesencephalic neuron-derived cells triggered by dopamine-dependent oxidative stress is dependent on the mixed-lineage kinase pathway. *J Neurosci* 25: 6329–6342

Martinez-Amaro FJ, Garcia-Padilla C, Franco D & Daimi H (2023) LncRNAs and CircRNAs in Endoplasmic Reticulum Stress: A Promising Target for Cardiovascular Disease? *Int J Mol Sci* 24: 9888

Mattick JS, Amaral PP, Carninci P, Carpenter S, Chang HY, Chen L-L, Chen R, Dean C, Dinger ME, Fitzgerald KA, *et al* (2023) Long non-coding RNAs: definitions, functions, challenges and recommendations. *Nat Rev Mol Cell Biol* 24: 430–447

Mei S, Qin Q, Wu Q, Sun H, Zheng R, Zang C, Zhu M, Wu J, Shi X, Taing L, *et al* (2017) Cistrome Data Browser: a data portal for ChIP-Seq and chromatin accessibility data in human and mouse. *Nucleic Acids Res* 45: D658–D662

Mercado G, Castillo V, Soto P, López N, Axten JM, Sardi SP, Hoozemans JJM & Hetz C (2018) Targeting PERK signaling with the small molecule GSK2606414 prevents neurodegeneration in a model of Parkinson's disease. *Neurobiol Dis* 112: 136–148

Mesbah Moosavi ZS & Hood DA (2017) The unfolded protein response in relation to mitochondrial biogenesis in skeletal muscle cells. *Am J Physiol Cell Physiol* 312: C583–C594

Misra J, Kim D-K, Choi W, Koo S-H, Lee C-H, Back S-H, Kaufman RJ & Choi H-S (2013) Transcriptional cross talk between orphan nuclear receptor ERRγ and transmembrane transcription factor ATF6α coordinates endoplasmic reticulum stress response. *Nucleic Acids Res* 41: 6960–6974

Monti C, Bondi H, Urbani A, Fasano M & Alberio T (2015) Systems biology analysis of the proteomic alterations induced by MPP(+), a Parkinson's disease-related mitochondrial toxin. *Front Cell Neurosci* 9: 14

Morán I, Akerman I, van de Bunt M, Xie R, Benazra M, Nammo T, Arnes L, Nakić N, García-Hurtado J, Rodríguez-Seguí S, *et al* (2012) Human β cell transcriptome analysis uncovers lncRNAs that are tissue-specific, dynamically regulated, and abnormally expressed in type 2 diabetes. *Cell Metab* 16: 435–448

Münch C & Harper JW (2016) Mitochondrial unfolded protein response controls matrix pre-RNA processing and translation. *Nature* 534: 710–713

Muñoz JP, Ivanova S, Sánchez-Wandelmer J, Martínez-Cristóbal P, Noguera E, Sancho A, Díaz-Ramos A, Hernández-Alvarez MI, Sebastián D, Mauvezin C, *et al* (2013) Mfn2 modulates the UPR and mitochondrial function via repression of PERK. *EMBO J* 32: 2348–2361

Nalls MA, Blauwendraat C, Vallerga CL, Heilbron K, Bandres-Ciga S, Chang D, Tan M, Kia DA, Noyce AJ, Xue A, *et al* (2019) Identification of novel risk loci, causal insights, and heritable risk for Parkinson's disease: a meta-analysis of genome-wide association studies. *Lancet Neurol* 18: 1091–1102

Pacelli C, Giguère N, Bourque M-J, Lévesque M, Slack RS & Trudeau L-É (2015) Elevated Mitochondrial Bioenergetics and Axonal Arborization Size Are Key Contributors to the Vulnerability of Dopamine Neurons. *Curr Biol* 25: 2349–2360

Park S-M, Kang T-I & So J-S (2021) Roles of XBP1s in Transcriptional Regulation of Target Genes. *Biomedicines* 9: 791

Pertea G & Pertea M (2020) GFF Utilities: GffRead and GffCompare. *F1000Res* 9: ISCB Comm J-304

Pertea M, Pertea GM, Antonescu CM, Chang T-C, Mendell JT & Salzberg SL (2015) StringTie enables improved reconstruction of a transcriptome from RNA-seq reads. *Nat Biotechnol* 33: 290–295

Picca A, Guerra F, Calvani R, Romano R, Coelho-Júnior HJ, Bucci C & Marzetti E (2021) Mitochondrial Dysfunction, Protein Misfolding and Neuroinflammation in Parkinson's Disease: Roads to Biomarker Discovery. *Biomolecules* 11: 1508

Pickrell AM & Youle RJ (2015) The roles of PINK1, parkin, and mitochondrial fidelity in Parkinson's disease. *Neuron* 85: 257–273

Pierce SE, Tyson T, Booms A, Prahl J & Coetzee GA (2018) Parkinson's disease genetic risk in a midbrain neuronal cell line. *Neurobiol Dis* 114: 53–64

Pissadaki EK & Bolam JP (2013) The energy cost of action potential propagation in dopamine neurons: clues to susceptibility in Parkinson's disease. *Front Comput Neurosci* 7: 13

Prole DL, Chinnery PF & Jones NS (2020) Visualizing, quantifying, and manipulating mitochondrial DNA in vivo. *Journal of Biological Chemistry* 295: 17588–17601

Qian C, Ye Y, Mao H, Yao L, Sun X, Wang B, Zhang H, Xie L, Zhang H, Zhang Y, *et al* (2019) Downregulated lncRNA-SNHG1 enhances autophagy and prevents cell death through the miR-221/222 /p27/mTOR pathway in Parkinson's disease. *Exp Cell Res* 384: 111614

Quan H, Fan Q, Li C, Wang Y-Y & Wang L (2018) The transcriptional profiles and functional implications of long non-coding RNAs in the unfolded protein response. *Sci Rep* 8: 4981

Quirós PM, Prado MA, Zamboni N, D'Amico D, Williams RW, Finley D, Gygi SP & Auwerx J (2017) Multi-omics analysis identifies ATF4 as a key regulator of the mitochondrial stress response in mammals. *J Cell Biol* 216: 2027–2045

Salic A & Mitchison TJ (2008) A chemical method for fast and sensitive detection of DNA synthesis in vivo. *Proc Natl Acad Sci U S A* 105: 2415–2420

Sassano ML, van Vliet AR, Vervoort E, Van Eygen S, Van den Haute C, Pavie B, Roels J, Swinnen JV, Spinazzi M, Moens L, *et al* (2023) PERK recruits E-Syt1 at ER-mitochondria contacts for mitochondrial lipid transport and respiration. *J Cell Biol* 222: e202206008

Schapira AH, Cooper JM, Dexter D, Jenner P, Clark JB & Marsden CD (1989) Mitochondrial complex I deficiency in Parkinson's disease. *Lancet* 1: 1269

Scharfmann R, Xiao X, Heimberg H, Mallet J & Ravassard P (2008) Beta cells within single human islets originate from multiple progenitors. *PLoS One* 3: e3559

Schneider CA, Rasband WS & Eliceiri KW (2012) NIH Image to ImageJ: 25 years of image analysis. *Nat Methods* 9: 671–675

Scholda J, Nguyen TTA & Kopp F (2023) Long noncoding RNAs as versatile molecular regulators of cellular stress response and homeostasis. *Hum Genet*

Scholz D, Pöltl D, Genewsky A, Weng M, Waldmann T, Schildknecht S & Leist M (2011) Rapid, complete and large-scale generation of post-mitotic neurons from the human LUHMES cell line. *J Neurochem* 119: 957–971

Schon EA, DiMauro S & Hirano M (2012) Human mitochondrial DNA: roles of inherited and somatic mutations. *Nat Rev Genet* 13: 878–890

Seifuddin F, Singh K, Suresh A, Judy JT, Chen Y-C, Chaitankar V, Tunc I, Ruan X, Li P, Chen Y, *et al* (2020) lncRNAKB, a knowledgebase of tissue-specific functional annotation and trait association of long noncoding RNA. *Sci Data* 7: 326

Senft D & Ronai ZA (2015) UPR, autophagy, and mitochondria crosstalk underlies the ER stress response. *Trends Biochem Sci* 40: 141–148

Shen X, Wu S, Yang Z & Zhu C (2023) Establishment of an endoplasmic reticulum stress-associated lncRNAs model to predict prognosis and immunological characteristics in hepatocellular carcinoma. *PLoS One* 18: e0287724

Sherer TB, Betarbet R, Testa CM, Seo BB, Richardson JR, Kim JH, Miller GW, Yagi T, Matsuno-Yagi A & Greenamyre JT (2003a) Mechanism of toxicity in rotenone models of Parkinson's disease. *J Neurosci* 23: 10756–10764

Sherer TB, Kim JH, Betarbet R & Greenamyre JT (2003b) Subcutaneous rotenone exposure causes highly selective dopaminergic degeneration and alpha-synuclein aggregation. *Exp Neurol* 179: 9–16

van der Stel W, Yang H, Vrijenhoek NG, Schimming JP, Callegaro G, Carta G, Darici S, Delp J, Forsby A, White A, *et al* (2022) Mapping the cellular response to electron transport chain inhibitors reveals selective signaling networks triggered by mitochondrial perturbation. *Arch Toxicol* 96: 259–285

Su S, Liu J, He K, Zhang M, Feng C, Peng F, Li B & Xia X (2016) Overexpression of the long noncoding RNA TUG1 protects against cold-induced injury of mouse livers by inhibiting apoptosis and inflammation. *FEBS J* 283: 1261–1274

Ulitsky I & Bartel DP (2013) lincRNAs: genomics, evolution, and mechanisms. *Cell* 154: 26–46

Uoselis L, Lindblom R, Lam WK, Küng CJ, Skulsuppaisarn M, Khuu G, Nguyen TN, Rudler DL, Filipovska A, Schittenhelm RB, *et al* (2023) Temporal landscape of mitochondrial proteostasis governed by the UPRmt. *Sci Adv* 9: eadh8228

Walter F, O'Brien A, Concannon CG, Düssmann H & Prehn JHM (2018) ER stress signaling has an activating transcription factor 6α (ATF6)-dependent 'off-switch'. *J Biol Chem* 293: 18270–18284

Wang L, Park HJ, Dasari S, Wang S, Kocher J-P & Li W (2013) CPAT: Coding-Potential Assessment Tool using an alignment-free logistic regression model. *Nucleic Acids Res* 41: e74

Ward M, McEwan C, Mills JD & Janitz M (2015) Conservation and tissue-specific transcription patterns of long noncoding RNAs. *J Hum Transcr* 1: 2–9

Washietl S, Kellis M & Garber M (2014) Evolutionary dynamics and tissue specificity of human long noncoding RNAs in six mammals. *Genome Res* 24: 616–628

Wauer T, Simicek M, Schubert A & Komander D (2015) Mechanism of phospho-ubiquitin-induced PARKIN activation. *Nature* 524: 370–374

Wek RC & Cavener DR (2007) Translational control and the unfolded protein response. *Antioxid Redox Signal* 9: 2357–2371

Wu J, Ruas JL, Estall JL, Rasbach KA, Choi JH, Ye L, Boström P, Tyra HM, Crawford RW, Campbell KP, *et al* (2011) The unfolded protein response mediates adaptation to exercise in skeletal muscle through a PGC-1α/ATF6α complex. *Cell Metab* 13: 160–169

Wu M-Z, Fu T, Chen J-X, Lin Y-Y, Yang J-E & Zhuang S-M (2020) LncRNA GOLGA2P10 is induced by PERK/ATF4/CHOP signaling and protects tumor cells from ER stress-induced apoptosis by regulating Bcl-2 family members. *Cell Death Dis* 11: 276

Xie Z, Bailey A, Kuleshov MV, Clarke DJB, Evangelista JE, Jenkins SL, Lachmann A, Wojciechowicz ML, Kropiwnicki E, Jagodnik KM, *et al* (2021) Gene Set Knowledge Discovery with Enrichr. *Curr Protoc* 1: e90

Xin C & Liu J (2021) Long Non-coding RNAs in Parkinson's Disease. *Neurochem Res* 46: 1031–1042

Yan W, Chen Z-Y, Chen J-Q & Chen H-M (2018) LncRNA NEAT1 promotes autophagy in MPTP-induced Parkinson's disease through stabilizing PINK1 protein. *Biochem Biophys Res Commun* 496: 1019–1024

Yang N, Fu Y, Zhang H, Sima H, Zhu N & Yang G (2015) LincRNA-p21 activates endoplasmic reticulum stress and inhibits hepatocellular carcinoma. *Oncotarget* 6: 28151–28163

Zhang H, Feng H, Yu T, Zhang M, Liu Z, Ma L & Liu H (2023) Construction of an oxidative stress-related lncRNAs signature to predict prognosis and the immune response in gastric cancer. *Sci Rep* 13: 8822

Zhang H, Liu X, Liu Y, Liu J, Gong X, Li G & Tang M (2022) Crosstalk between regulatory non-coding RNAs and oxidative stress in Parkinson's disease. *Front Aging Neurosci* 14: 975248

Zhang X, Yuan Y, Jiang L, Zhang J, Gao J, Shen Z, Zheng Y, Deng T, Yan H, Li W, *et al* (2014) Endoplasmic reticulum stress induced by tunicamycin and thapsigargin protects against transient ischemic brain injury: Involvement of PARK2-dependent mitophagy. *Autophagy* 10: 1801–1813

Zhang Y, Xia Q & Lin J (2020) LncRNA H19 Attenuates Apoptosis in MPTP-Induced Parkinson's Disease Through Regulating miR-585-3p/PIK3R3. *Neurochem Res* 45: 1700–1710

Zheng J, Yang X, Zhao Q, Tian S, Huang H, Chen Y & Xu Y (2017) Association between gene polymorphism and depression in Parkinson's disease: A case-control study. *J Neurol Sci* 375: 231–234

Zheng R, Wan C, Mei S, Qin Q, Wu Q, Sun H, Chen C-H, Brown M, Zhang X, Meyer CA, *et al* (2019) Cistrome Data Browser: expanded datasets and new tools for gene regulatory analysis. *Nucleic Acids Res* 47: D729–D735

Zhu J, Wang KZQ & Chu CT (2013) After the banquet: mitochondrial biogenesis, mitophagy, and cell survival. *Autophagy* 9: 1663–1676

Zhuang Y, Wang X-X, He J, He S & Yin Y (2019) Recent advances in understanding of amino acid signaling to mTORC1 activation. *Front Biosci (Landmark Ed)* 24: 971–982

Zufferey R, Nagy D, Mandel RJ, Naldini L & Trono D (1997) Multiply attenuated lentiviral vector achieves efficient gene delivery in vivo. *Nat Biotechnol* 15: 871–875

Data availability statement

The GEO accession number for RNA-seq and ATAC-seq reported in this paper is:

All other data are available in the manuscript or supplemental materials.

Acknowledgments

The authors would like to thank the iVECTOR core facility of the Paris Brain Institute for technical assistance in producing all lentiviral vectors, the Genotyping and Sequencing Platform of the Paris Brain Institute for technical assistance in performing RNA-seq, and ATAC-seq. We thank Jorge Ferrer (Imperial College London) for sharing the CRISPRi lentiviral vector.

This work was supported by the foundation de France, France Parkinson, Edmond & Lily Safra foundation and the Institut Hospitalo-Universitaire de Neurosciences Translationnelles de Paris, A-ICM, Investissements d'Avenir ANR-10-IAIHU-06. Jana Heneine received funding from the Ministère de la Recherche et de l'Enseignement Supérieur and from the Fondation de la recherche Médicale (FRM, 4th year PhD program). The authors declare no competing financial interests.

Authors contribution

JH performed most of the experiments. CCS and CPG helped with cell culture. CCS helped with RT-qPCR experiments, designed the lentiviral constructions for the knock-down experiments, transfected and FACS-purified the homogeneous cell pools containing the viral constructions. CZ et NA helped with the immunofluorescence experiments to investigate mitochondrial turnover, and BG helped for the image analyses from immunofluorescence experiments. JG, FXL and TG contributed to the bioinformatics and statistical analyses. OC helped with the conception of the study. JH,

PR and HC conceived the study, designed the experiments, analyzed the data and wrote the manuscript. All authors read, checked and suggested modifications to the manuscript.

Figure legends

Figure 1. Inhibition of the mitochondrial electron transport chain induces mitophagy and a decrease in mitochondrial biogenesis in DA neurons. (a) TH (green) and DAT (red) expression, assessed by immunofluorescence on LUHMES cells differentiated for 6 days. **(b)** Phospho-Serine 65 ubiquitin (red), TOMM20 (green) and MAP2 (grey) expression in DA neurons treated with DMSO (Control) or after exposition to mitochondrial toxins for 4 h, 6 h and 8 h (Stress), observed by immunofluorescence. **(c)** Percentage of phospho-Serine65 ubiquitin-positive neurons in control conditions and following 4 h, 6 h or 8 h of mitochondrial stress (Two-way ANOVA with Tukey's multiple comparisons test). **(d)** Area (in μm^2) of the TOMM20-positive cluster in neurons in control conditions and following 4 h, 6 h or 8 h of mitochondrial stress (Mixed-effects analysis withTukey's multiple comparisons test). **(e)** MAP2 (grey) and TOMM20 (red) expression assessed by immunofluorescence and EdU (green) detection in control conditions or following mitochondrial stress for 2 h, 4 h or 8 h. **(a, b and e)** Nuclei were stained using DAPI (blue). For each low magnification photograph, areas indicated by dotted lines are zoomed and presented on the right panel. **(f)** Area comprising EdU signal (in μm^2) per neuron in control conditions or following mitochondrial stress for 2 h, 4 h or 8 h (Mixed-effects analysis and Bonferroni's multiple comparisons test). **(g)** Number of EdU-positive puncta per neuron in control conditions and upon a 2 h-, 4 h- or 8 h-stress (Mixed-effects analysis and Bonferroni's multiple comparisons test). **(c, d, f and g)** Each dot represents the data obtained from 3 independent differentiation experiments. The bar represents the mean of the 3 values, and the error bars show standard error of the mean. *p-value ≤ 0,05, **** p-value ≤ 0,0001

Figure 2. Mitochondrial stress leads to loss of mature dopaminergic marker and cell death. **(a)** TH (green) and DAT (red) expression, assessed by immunofluorescence on DA neurons in control conditions or upon 8 h mitochondrial stress. Quantification of the **(b)** percentage of TH^+ cells (two-tailed paired t-test) **(c)** mean TH signal intensity per TH^+ cell (two-tailed paired t-test), **(d)** percentage of TH^+ DAT^+ cells (two-tailed paired t-test) and **(e)** mean DAT signal intensity per TH^+ DAT^+ cell (two-tailed paired t-test) in both control and stress (8 h) conditions. **(f)** TH (green) and cleaved CASP3 (cCASP3, red) expression, assessed by immunofluorescence on DA neurons in control conditions or upon 8 h-mitochondrial stress. **(a and f)** Nuclei were stained using DAPI (blue). For each low magnification photograph, areas indicated by dotted lines are zoomed and presented on the right panel. **(g)** Quantification of the percentage of TH^+ cells that exhibited $cCASP3^+$ staining in both control and stress conditions (two-tailed paired t-test). **(b, c, d, e and g)** Each dot represents the data obtained from 3 independent differentiation experiments. The bar represents the mean of the 3 values, and the error bars show standard error of the mean. *p-value ≤ 0,05, **p-value ≤ 0,01.

Figure 3. Mitochondrial stress triggers the Unfolded Protein Response of the Endoplasmic Reticulum (UPR^{ER}) and inactivates neuronal development pathways. RNAseq datasets analysis were performed from 4 independent LUHMES cell differentiation experiments in control (DMSO) or stress conditions (oligomycin and antimycin) **(a)** Principal Component Analysis (PCA) of RNA-seq datasets from DA neurons in control (blue) or stress conditions (green). **(b)** Gene ontology analysis (Biological Process 2023, Enrichr) performed on protein-coding genes with upregulated (green) or downregulated (blue) expression after 8 h of mitochondrial

stress compared to control conditions. **(c)** mRNA expression in FPKM of mitochondrial protein-coding genes in control or stress conditions using the RNA-seq datasets (Control, blue; Stress, green). The bar represents the mean of the 4 values per condition (Control, Stress), and the error bars show standard error of the mean (DESeq2 differential analysis). **(d)** Pathway analysis (Reactome 2022, Enrichr) performed on protein-coding genes with upregulated expression after 8 h of mitochondrial stress compared to control conditions. **(e)** Heatmaps representing mRNA expression by RT-qPCR of genes encoding main actors of the three branches of the UPR^{ER} and of the UPR^{mt} at different time points (30 min, 2 h, 4 h, 6 h and 8 h) during mitochondrial stress, compared to control conditions (Two-way ANOVA with Tukey multiple comparisons test). mRNA expression was normalized relatively to *TBP* mRNA expression. Data are represented in Log_2(Fold change Stress/Control) for 3 independent experiments. **(f)** EIF2α, phosphorylated EIF2α (P-EIF2α) and vinculin expression assessed by western blot in control conditions and upon mitochondrial stress (8 h). Quantification of the P-EIF2α/EIF2α ratio in control conditions and upon mitochondrial stress (8 h) from 3 independent differentiation experiments represented by 3 dots (two-tailed paired t-test). The bar represents the mean of the 3 values, and the error bars show standard error of the mean. **(g)** Transcription factors with binding regions (established by publicly available ChIPseq datasets) showing a significant overlap with open chromatin regions associated with altered accessibility upon stress and determined by ATACseq on DA neurons (Cistrome DB). *p-value ≤ 0,05; **p-value ≤ 0,01; ***p-value ≤ 0,001; **** p-value ≤ 0,0001.

Figure 4. PERK-mediated UPR^{ER} regulates mitophagy and the UPR^{mt} upon stress, as well as the mitochondrial integrity and biogenesis at a basal level. (a) ATF4 and vinculin expression assessed by western blot in control conditions (DMSO only) and upon mitochondrial stress (antimycin A and oligomycin), in the presence or absence of GSK2606414, at different time points of stress (0 h, 30 min, 2 h, 4 h, 6 h and 8 h). Tunicamycin was used as a positive control for the activation of the PERK pathway. **(b)** Quantification of ATF4 protein expression (normalized to vinculin) in control conditions and upon mitochondrial stress, in the presence or absence of GSK2606414, at different time points of stress (0 h, 30 min, 2 h, 4 h, 6 h and 8 h). Data were normalized to the condition Control 0 h that was present in each gel (Two-way ANOVA with Tukey multiple comparisons test). **(c)** Quantification of *ATF3* mRNA expression assessed by RT-qPCR in control conditions and upon mitochondrial stress, in the presence or absence of GSK2606414, at different time points of stress (0 h, 30 min, 2 h, 4 h, 6 h and 8 h). mRNA expression was normalized relatively to *TBP* mRNA expression. **(d)** Phospho-Serine 65 ubiquitin (red), TOMM20 (green) and MAP2 (grey) expression in DA neurons treated with DMSO (Control) or after exposure to mitochondrial toxins for 8 h (Stress), in the presence or absence of GSK2606414, observed by immunofluorescence. **(e)** Percentage of phospho-Serine65 ubiquitin-positive neurons in control conditions and following 4 h, 6 h or 8 h of mitochondrial stress, in the presence or absence of GSK2606414 (Two-way ANOVA with Tukey multiple comparisons test). Data obtained in absence of GSK2606414 are shown in Figure 1b,c. **(f)** Area (in μm^2) of the TOMM20-positive cluster in neurons measured in control conditions and after 4 h, 6 h or 8 h of mitochondrial stress, in the presence or absence of GSK2606414 (Mixed-effects analysis with Tukey multiple comparisons test). Data obtained in absence of GSK2606414 are shown in Figure 1b,d. **(b, c, e and**

f) Data from 3 independent differentiation experiments, represented by 3 dots, were used. The bar represents the mean of the 3 values, and the error bars show standard error of the mean. **(g)** MAP2 (grey) and TOMM20 (red) expression assessed by immunofluorescence and EdU (green) detection in control conditions or following mitochondrial stress for 8 h, in the presence or absence of GSK2606414 (Two-way ANOVA with Tukey multiple comparisons test). **(d and g)** Nuclei were stained using DAPI (blue). For each low magnification photograph, areas indicated by dotted lines are zoomed and presented on the right panel. **(h)** Area comprising EdU signal (in μm^2) per neuron and number of EdU-positive puncta per neuron in control conditions or following mitochondrial stress for 8 h (Two-way ANOVA with Tukey's multiple comparisons test). Data were obtained from 4 independent differentiation experiments. Each dot represents the mean area containing the EdU signal or the number of EdU puncta for one experiment of differentiation. The bar represents the mean of the 4 values, and the error bars show standard error of the mean. **(i)** Heatmap representing mRNA expression by RT-qPCR of genes encoding main actors of the UPR^{mt} at different time points (30 min, 2 h, 4 h, 6 h and 8 h) of mitochondrial stress, in the presence or absence of GSK2606414, compared to control conditions (DMSO only) at each time point. Data are represented in Log_2(Fold change compared to Control) for 3 independent experiments (Type II Wald Chi-square tests ANOVA function with Tukey's multiple comparisons test). mRNA expression was normalized relatively to *TBP* mRNA expression. *p-value ≤ 0,05; **p-value ≤ 0,01; ***p-value ≤ 0,001; **** p-value ≤ 0,0001

Figure 5. Mitochondrial stress response in human DA neurons includes the regulation of lncRNAs orchestrated by the PERK-mediated UPR^{ER}. (a) Number of annotated and non-annotated lncRNAs depending on their genomic loci.

n=4 RNA-seq datasets for DA neurons in control conditions; n=4 RNA-seq datasets for DA neurons submitted to a 8 h long mitochondrial stress. **(b)** Gene Ontology Analysis (Biological Process 2023, Enrichr) performed on the neighbouring protein-coding genes to all lncRNAs expressed in DA neurons, independent of the conditions (Control and Stress). **(c)** Venn diagram of overlap of lncRNAs expressed in control conditions and upon 8 h of mitochondrial stress. Percentages of lncRNAs expressed specifically in each condition are shown. **(d)** Gene Ontology Analysis (Biological Process 2023, Enrichr) performed on the neighbouring protein-coding genes to lncRNAs with altered expression upon stress (upregulated in green, downregulated in blue) compared to control conditions. **(e)** Gene Ontology Analysis (Biological Process 2023, Enrichr) performed on the neighbouring protein-coding genes to non-annotated lncRNAs specifically expressed upon stress. **(f)** Number of lncRNAs with promoters containing binding sites for ATF3 and ATF4 (determined by publicly available ChiP-Seq datasets) and categorized according to their expression profile upon stress compared to control conditions. **(g)** Heatmap representing RNA expression by RT-qPCR of genes encoding candidate lncRNAs (described in Table 1) at different time points (30 min, 2 h, 4 h, 6 h and 8 h) during mitochondrial stress, in the presence or absence of GSK2606414, compared to control conditions (DMSO only) at each time point. Data are represented in Log_2(Fold change compared to Control) for 3 independent experiments (Two-way ANOVA with Tukey multiple comparisons test). RNA expression was normalized relatively to *TBP* mRNA expression. *p-value ≤ 0,05; **p-value ≤ 0,01; ***p-value ≤ 0,001

Figure 6. Newly identified *lnc-SLC6A15-5* is specifically expressed upon mitochondrial stress in DA neurons. (a) Schematics of the locus of *lnc-SLC6A15-5*.

ATAC-seq peaks are depicted in black, reads from RNA-seq are in blue for the control condition, green for the stress condition. The scales represent reads per million (RPM). **(b)** RNA expression in FPKM of the 3 isoforms of *lnc-SLC6A15-5* in control (blue) or stress (green) conditions using the RNA-seq datasets (Control, n=4; Stress 8h, n=4). The bar represents the mean of the 4 values per condition (Control, Stress), and the error bars show standard error of the mean (DESeq2 differential analysis). Of note, transcripts are considered as expressed if their expression is higher than 1 FPKM in at least one sample and different from 0 in the 3 others. **(c)** Relative abundance of *lnc-SLC6A15-5*, assessed by RT-qPCR, in the nuclear or cytoplasmic fractions, in comparison with the nuclear RNA marker *MALAT1* and cytoplasmic RNA marker *MT-ND2*. Two independent experiments were used.

Figure 7. *lnc-SLC6A15-5* contributes to the resumption of translation following mitochondrial stress.

(a-e) Four different experimental conditions were used. Control (blue) and stress (green) conditions were performed either for 8 h (plain bars) or for 7h30 followed by 30 min recovery (hatched bars).

(a) *Lnc-SLC6A15-5* expression, assessed by RT-qPCR, in DA neurons transduced by lentiviral vectors carrying *dCAS9-KRAB* and sgRNAs either targeting lnc-SLC6A15-5 (KD *lnc-SLC6A15-5*) or a non-human sequence (NEG), in the 4 experimental conditions. RNA expression was normalized relatively to *TBP* mRNA expression. Data from 3 independent differentiation experiments, represented by 3 dots, were used. The bar represents the mean of the 3 values, and the error bars show standard error of the mean (Two-way ANOVA with Tukey's multiple comparison test). **(b)** Detection of OPP (grey) in DA neurons expressing normal (NEG) or reduced levels (KD) of *lnc-SLC6A15-*

5, in control or stress conditions for 7 h 30 min followed by 30 min recovery. Nuclei were stained using DAPI (blue). **(c)** OPP signal intensity in DA neurons (TH in control or stress conditions for 7 h 30 min followed by 30 min recovery (Two-way ANOVA with Tukey's multiple comparison test). Data were obtained from 3 independent differentiation experiments. Each dot represents the percentage of the OPP intensity in DA neurons for one experiment of differentiation. **(d)** Number of OPP puncta per DA neuron, in control or stress conditions for 7 h 30 min followed by 30 min recovery (Two-way ANOVA with Tukey's multiple comparison test). Data were obtained from 3 independent differentiation experiments. Each dot represents the number of OPP puncta per neuron per imaging field (n=4-6 per condition, per experiment). **(c and d)** The bar represents the mean of the values, and the error bars show standard error of the mean. **(e)** *SESN2, SLC1A3, SLC1A5, SLC3A2, SLC7A5 and ATF3* mRNA expression, assessed by RT-qPCR, in DA neurons expressing normal (NEG) or reduced levels (KD) of *lnc-SLC6A15-5*, in the 4 experimental conditions (Type II Wald Chi-square tests ANOVA function with Tukey's multiple comparisons test). mRNA expression was normalized relatively to *TBP* mRNA expression. Data from 3 independent differentiation experiments, represented by 3 dots, were used. The bar represents the mean of the 3 values, and the error bars show standard error of the mean. *p-value ≤ 0,05; **p-value ≤ 0,01; ***p-value ≤ 0,001; **** p-value ≤ 0,0001

Table 1. Description of the selected lncRNAs. For each lncRNA presented in Figure 5g, the locus, classification depending on their genomic locus, closest coding-genes, presence of PD-associated single nucleotide polymorphism and presence of ATF3 or ATF4 binding sites at their promoter are provided.

Table 1

Category	Name	Locus	Classification	Closest protein-coding gene	Intersecting with PD-linked SNP	Promoter associated to ATF3	Promoter associated to ATF4
Upregulated in stress and associated to translation regulation and stress response	**Lnc-SLC6A15**	chr12: 83456731-84128270	Intergenic	SLC6A15; TMTC2		Yes	
	VLDLR-AS1	chr9: 2503280-2621386	antisense overlapping	VLDLR		Yes	Yes
	VPS11-DT	chr11: 119067374-119067698	bidirectional	VPS11		Yes	Yes
	lnc-FKRP	chr19: 46787815-46789039	antisense overlapping	SLC1A5		Yes	
	SNHG1	chr11: 62851991-62855460	bidirectional	SLC3A2		Yes	Yes
	SNHG5	chr6: 85676990-85678736	intergenic	SYNCRIP; HTR1E		Yes	Yes
	TMEM161B-DT	chr5: 88268938-88436684	bidirectional	TMEM161B; MEF2C		Yes	Yes
Downregulated and associated to PD-linked SNP	lnc-PSMC3IP-3	chr17: 42545451-42557693	antisense overlapping	HSD17B1	x		
	MIR4697HG	chr11: 133896438-133901601	intergenic	IGSF9B; SPATA19	x		
	FBXL19-AS1	chr16: 30919319-30923269	antisense overlapping	FBXL19	x	Yes	Yes
Downregulated in stress and associated to neuron generation	NIPBL-DT	chr5: 36871364-36876700	bidirectional	NIPBL		Yes	
	ZNF778-DT	chr16: 89215211-89217653	bidirectional	ZNF778		Yes	Yes
	Lnc-MNAT1-2	chr14: 60657073-60659096	antisense overlapping	SIX1		Yes	
	lnc-TTC29	chr4: 146628898-146638145	bidirectional	POU4F2		Yes	
	lnc-SLAIN1-11	chr13: 78596129-78599619	antisense overlapping	POU4F1		Yes	

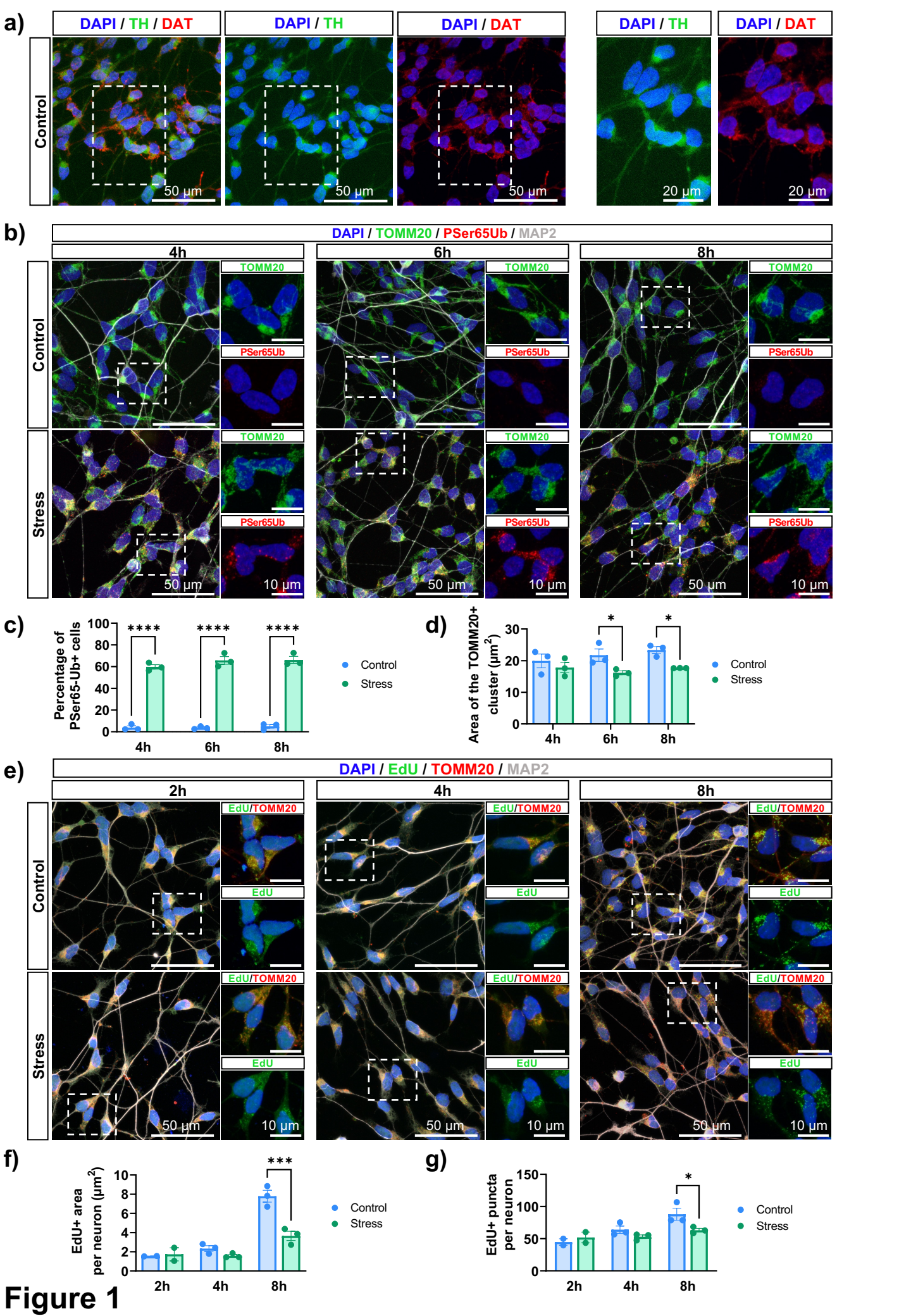
a)
DAPI / TH / DAT
DAPI / TH
DAPI / DAT
DAPI / TH
DAPI / DAT
Control
50 µm
50 µm
50 µm
20 µm
20 µm
b)
DAPI / TOMM20 / PSer65Ub / MAP2
4h
6h
8h
Control
Stress
TOMM20
PSer65Ub
50 µm
10 µm
c)
Percentage of PSer65-Ub+ cells
****
Control
Stress
4h
6h
8h
d)
Area of the TOMM20+ cluster (µm²)
*
Control
Stress
4h
6h
8h
e)
DAPI / EdU / TOMM20 / MAP2
2h
4h
8h
Control
Stress
EdU/TOMM20
EdU
50 µm
10 µm
f)
EdU+ area per neuron (µm²)
***
Control
Stress
2h
4h
8h
g)
EdU+ puncta per neuron
*
Control
Stress
2h
4h
8h

Figure 1

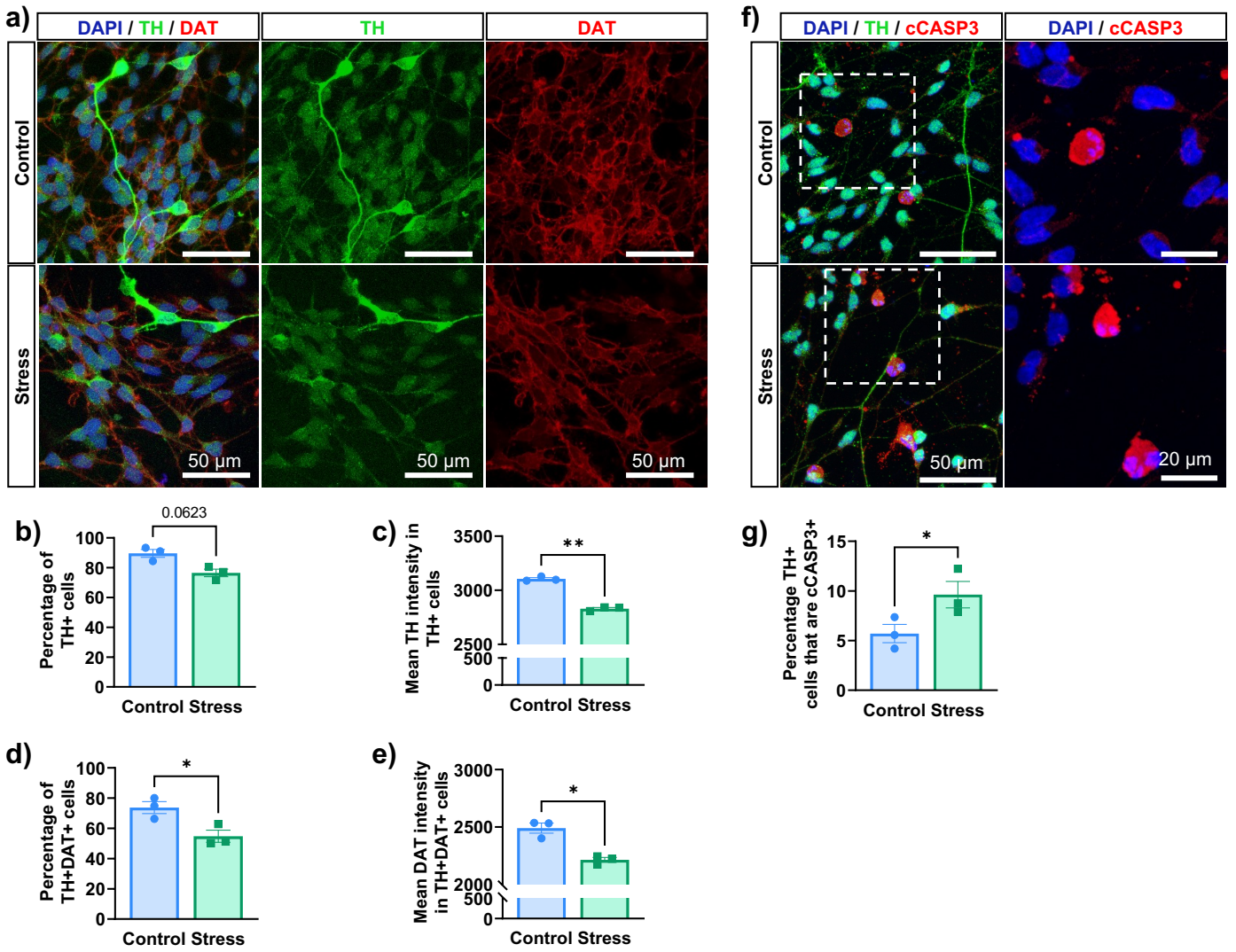
a)
DAPI / TH / DAT
TH
DAT
Control
Stress
50 µm
50 µm
50 µm
f)
DAPI / TH / cCASP3
DAPI / cCASP3
Control
Stress
50 µm
20 µm
b)
0.0623
Percentage of TH+ cells
100
80
60
40
20
0
Control Stress
c)
Mean TH intensity in TH+ cells
3500
3000
2500
500
0
**
Control Stress
g)
Percentage TH+ cells that are cCASP3+
15
10
5
0
*
Control Stress
d)
Percentage of TH+DAT+ cells
100
80
60
40
20
0
*
Control Stress
e)
Mean DAT intensity in TH+DAT+ cells
3000
2500
2000
500
0
*
Control Stress

Figure 2

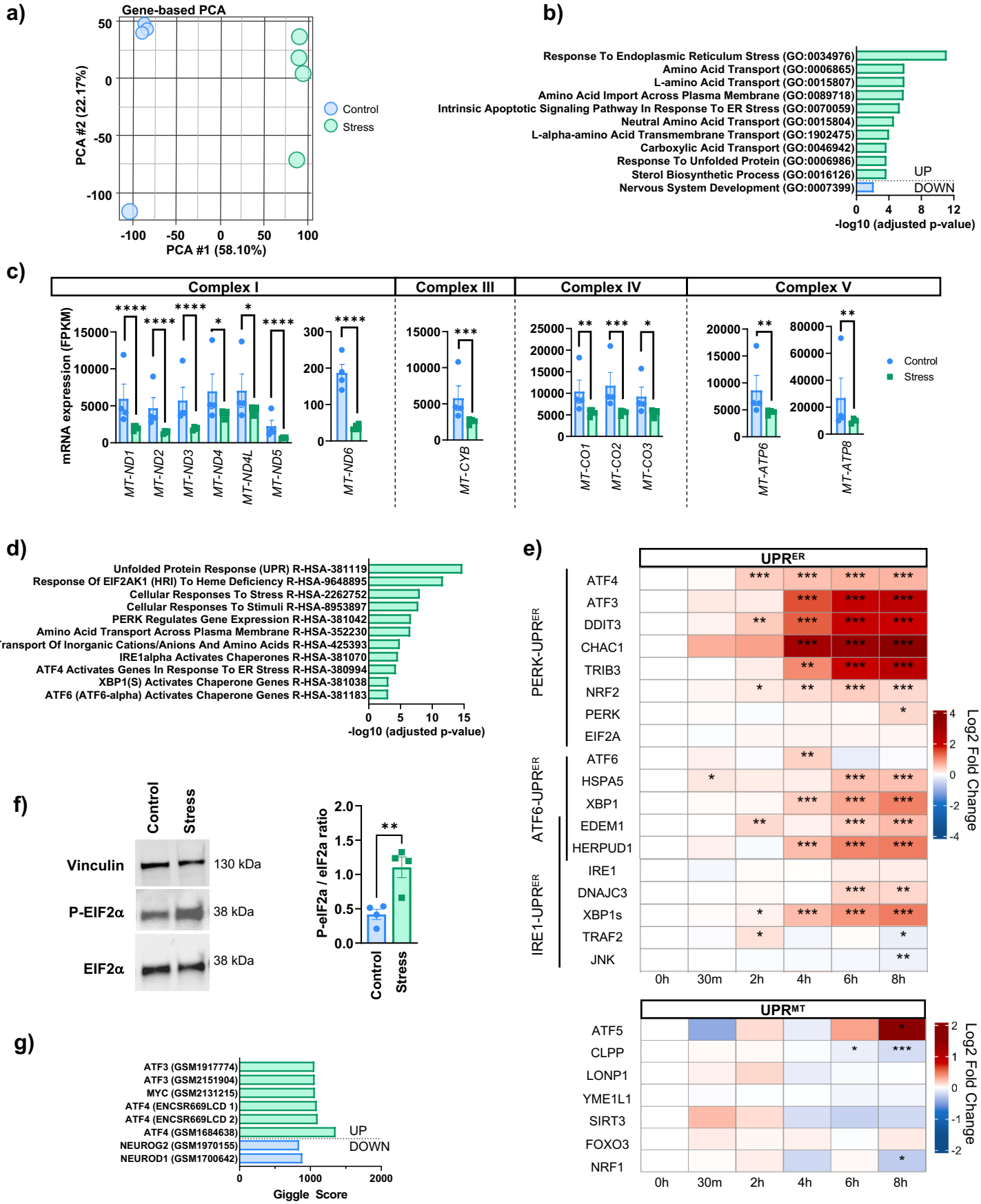
a)
Gene-based PCA
PCA #2 (22.17%)
PCA #1 (58.10%)
Control
Stress
b)
Response To Endoplasmic Reticulum Stress (GO:0034976)
Amino Acid Transport (GO:0006865)
L-amino Acid Transport (GO:0015807)
Amino Acid Import Across Plasma Membrane (GO:0089718)
Intrinsic Apoptotic Signaling Pathway In Response To ER Stress (GO:0070059)
Neutral Amino Acid Transport (GO:0015804)
L-alpha-amino Acid Transmembrane Transport (GO:1902475)
Carboxylic Acid Transport (GO:0046942)
Response To Unfolded Protein (GO:0006986)
Sterol Biosynthetic Process (GO:0016126)
Nervous System Development (GO:0007399)
UP
DOWN
-log10 (adjusted p-value)
c)
Complex I
Complex III
Complex IV
Complex V
mRNA expression (FPKM)
MT-ND1
MT-ND2
MT-ND3
MT-ND4
MT-ND4L
MT-ND5
MT-ND6
MT-CYB
MT-CO1
MT-CO2
MT-CO3
MT-ATP6
MT-ATP8
Control
Stress
d)
Unfolded Protein Response (UPR) R-HSA-381119
Response Of EIF2AK1 (HRI) To Heme Deficiency R-HSA-9648895
Cellular Responses To Stress R-HSA-2262752
Cellular Responses To Stimuli R-HSA-8953897
PERK Regulates Gene Expression R-HSA-381042
Amino Acid Transport Across Plasma Membrane R-HSA-352230
Transport Of Inorganic Cations/Anions And Amino Acids R-HSA-425393
IRE1alpha Activates Chaperones R-HSA-381070
ATF4 Activates Genes In Response To ER Stress R-HSA-380994
XBP1(S) Activates Chaperone Genes R-HSA-381038
ATF6 (ATF6-alpha) Activates Chaperone Genes R-HSA-381183
-log10 (adjusted p-value)
e)
UPR^ER
PERK-UPR^ER
ATF6-UPR^ER
IRE1-UPR^ER
ATF4
ATF3
DDIT3
CHAC1
TRIB3
NRF2
PERK
EIF2A
ATF6
HSPA5
XBP1
EDEM1
HERPUD1
IRE1
DNAJC3
XBP1s
TRAF2
JNK
0h
30m
2h
4h
6h
8h
Log2 Fold Change
UPR^MT
ATF5
CLPP
LONP1
YME1L1
SIRT3
FOXO3
NRF1
f)
Control
Stress
Vinculin
130 kDa
P-EIF2α
38 kDa
EIF2α
38 kDa
P-eIF2a / eIF2a ratio
g)
ATF3 (GSM1917774)
ATF3 (GSM2151904)
MYC (GSM2131215)
ATF4 (ENCSR669LCD 1)
ATF4 (ENCSR669LCD 2)
ATF4 (GSM1684638)
NEUROG2 (GSM1970155)
NEUROD1 (GSM1700642)
UP
DOWN
Giggle Score

Figure 3

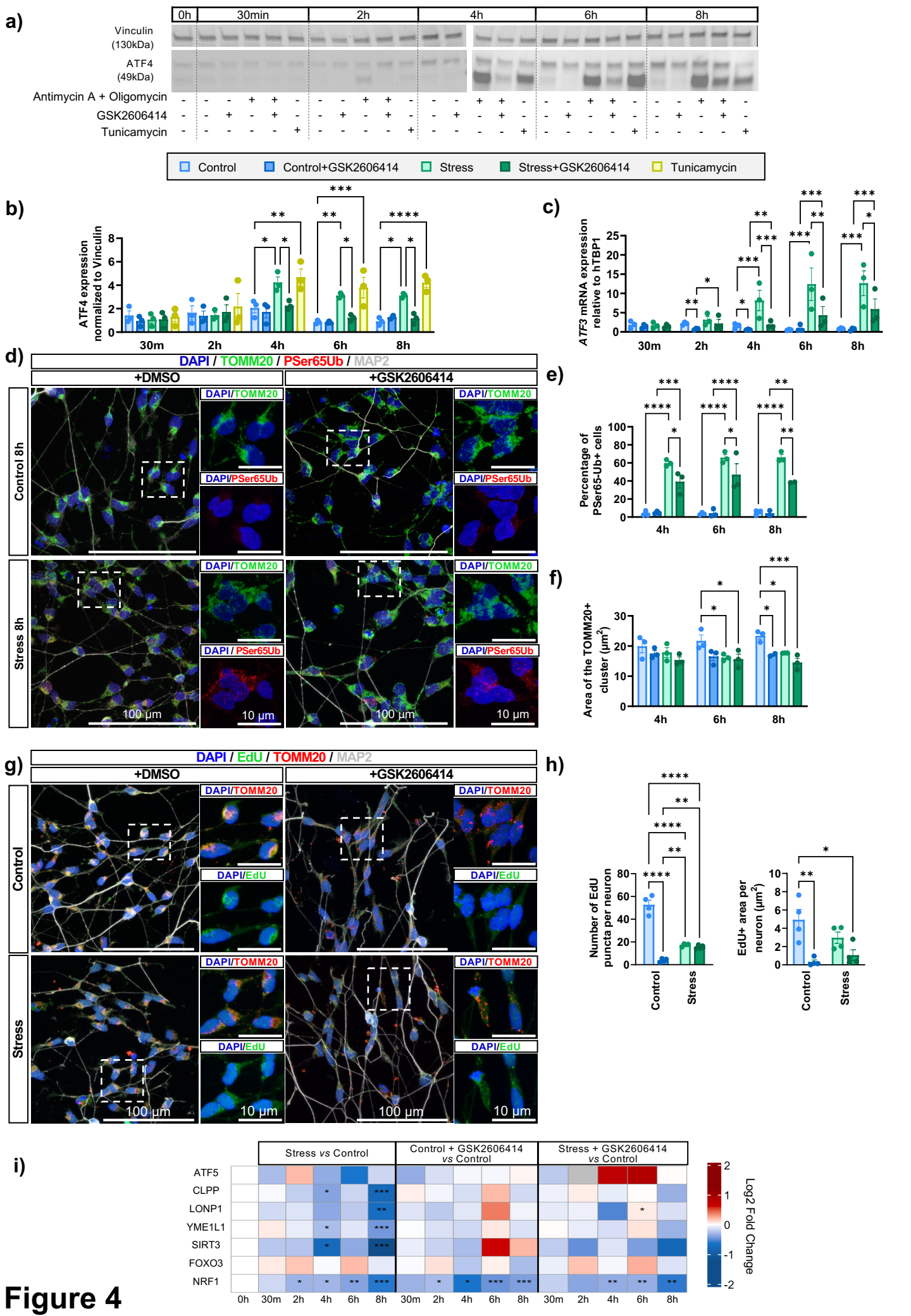
a)
0h
30min
2h
4h
6h
8h
Vinculin (130kDa)
ATF4 (49kDa)
Antimycin A + Oligomycin
GSK2606414
Tunicamycin
Control
Control+GSK2606414
Stress
Stress+GSK2606414
Tunicamycin
b)
ATF4 expression normalized to Vinculin
30m
2h
4h
6h
8h
c)
ATF3 mRNA expression relative to hTBP1
d)
DAPI / TOMM20 / PSer65Ub / MAP2
+DMSO
+GSK2606414
Control 8h
Stress 8h
DAPI/TOMM20
DAPI/PSer65Ub
100 µm
10 µm
e)
Percentage of PSer65-Ub+ cells
f)
Area of the TOMM20+ cluster (µm²)
g)
DAPI / EdU / TOMM20 / MAP2
Control
Stress
DAPI/EdU
h)
Number of EdU puncta per neuron
EdU+ area per neuron (µm²)
i)
Stress vs Control
Control + GSK2606414 vs Control
Stress + GSK2606414 vs Control
ATF5
CLPP
LONP1
YME1L1
SIRT3
FOXO3
NRF1
Log2 Fold Change

Figure 4

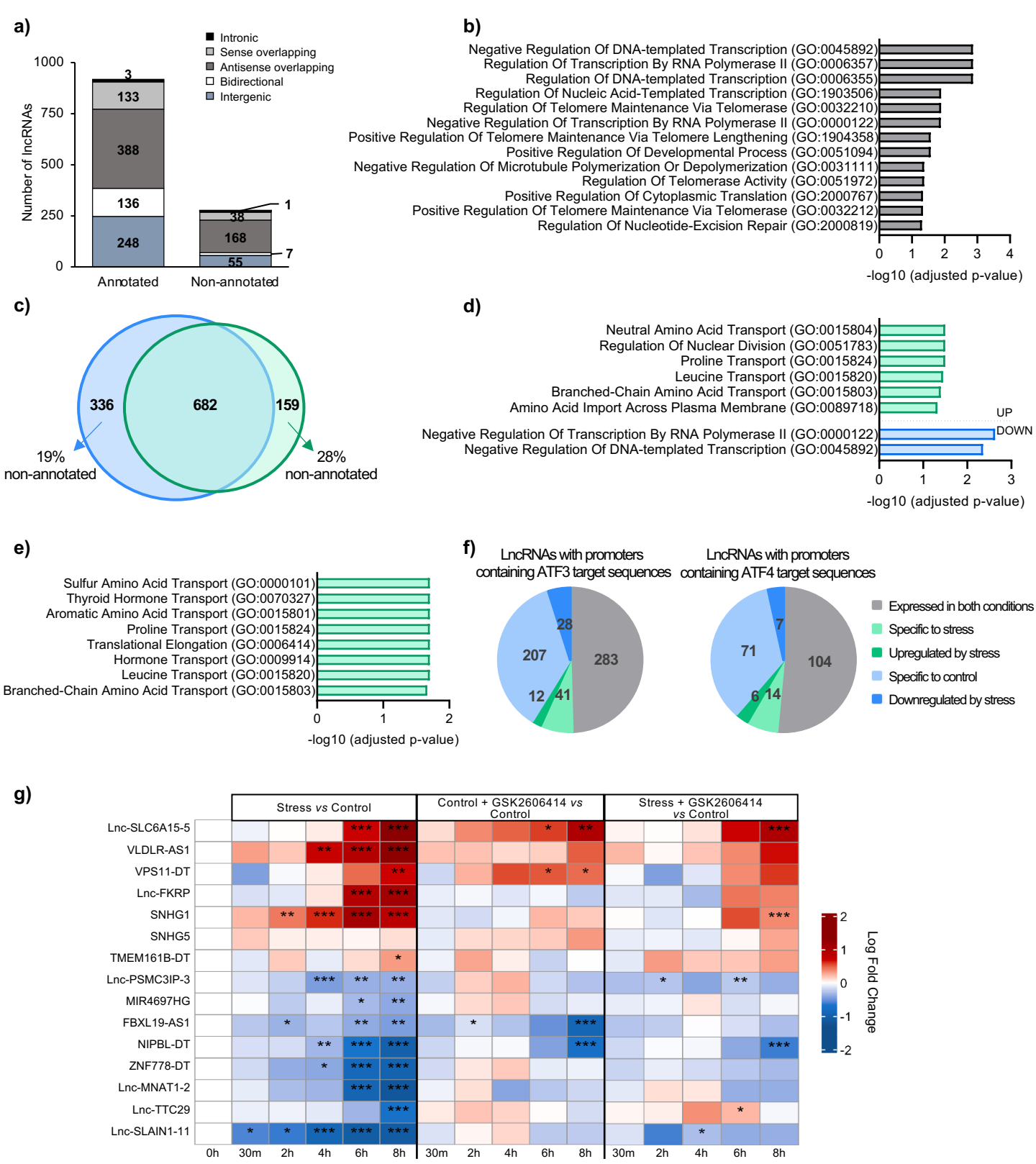
a)
Intronic
Sense overlapping
Antisense overlapping
Bidirectional
Intergenic
Number of lncRNAs
1000
750
500
250
0
3
133
388
136
248
38
168
55
1
7
Annotated
Non-annotated
b)
Negative Regulation Of DNA-templated Transcription (GO:0045892)
Regulation Of Transcription By RNA Polymerase II (GO:0006357)
Regulation Of DNA-templated Transcription (GO:0006355)
Regulation Of Nucleic Acid-Templated Transcription (GO:1903506)
Regulation Of Telomere Maintenance Via Telomerase (GO:0032210)
Negative Regulation Of Transcription By RNA Polymerase II (GO:0000122)
Positive Regulation Of Telomere Maintenance Via Telomere Lengthening (GO:1904358)
Positive Regulation Of Developmental Process (GO:0051094)
Negative Regulation Of Microtubule Polymerization Or Depolymerization (GO:0031111)
Regulation Of Telomerase Activity (GO:0051972)
Positive Regulation Of Cytoplasmic Translation (GO:2000767)
Positive Regulation Of Telomere Maintenance Via Telomerase (GO:0032212)
Regulation Of Nucleotide-Excision Repair (GO:2000819)
0 1 2 3 4
-log10 (adjusted p-value)
c)
336
682
159
19%
non-annotated
28%
non-annotated
d)
Neutral Amino Acid Transport (GO:0015804)
Regulation Of Nuclear Division (GO:0051783)
Proline Transport (GO:0015824)
Leucine Transport (GO:0015820)
Branched-Chain Amino Acid Transport (GO:0015803)
Amino Acid Import Across Plasma Membrane (GO:0089718)
UP
DOWN
Negative Regulation Of Transcription By RNA Polymerase II (GO:0000122)
Negative Regulation Of DNA-templated Transcription (GO:0045892)
0 1 2 3
-log10 (adjusted p-value)
e)
Sulfur Amino Acid Transport (GO:0000101)
Thyroid Hormone Transport (GO:0070327)
Aromatic Amino Acid Transport (GO:0015801)
Proline Transport (GO:0015824)
Translational Elongation (GO:0006414)
Hormone Transport (GO:0009914)
Leucine Transport (GO:0015820)
Branched-Chain Amino Acid Transport (GO:0015803)
0 1 2
-log10 (adjusted p-value)
f)
LncRNAs with promoters containing ATF3 target sequences
28
207
283
12
41
LncRNAs with promoters containing ATF4 target sequences
7
71
104
6
14
Expressed in both conditions
Specific to stress
Upregulated by stress
Specific to control
Downregulated by stress
g)
Stress vs Control
Control + GSK2606414 vs Control
Stress + GSK2606414 vs Control
Lnc-SLC6A15-5
VLDLR-AS1
VPS11-DT
Lnc-FKRP
SNHG1
SNHG5
TMEM161B-DT
Lnc-PSMC3IP-3
MIR4697HG
FBXL19-AS1
NIPBL-DT
ZNF778-DT
Lnc-MNAT1-2
Lnc-TTC29
Lnc-SLAIN1-11
0h 30m 2h 4h 6h 8h 30m 2h 4h 6h 8h 30m 2h 4h 6h 8h
2
1
0
-1
-2
Log Fold Change

Figure 5

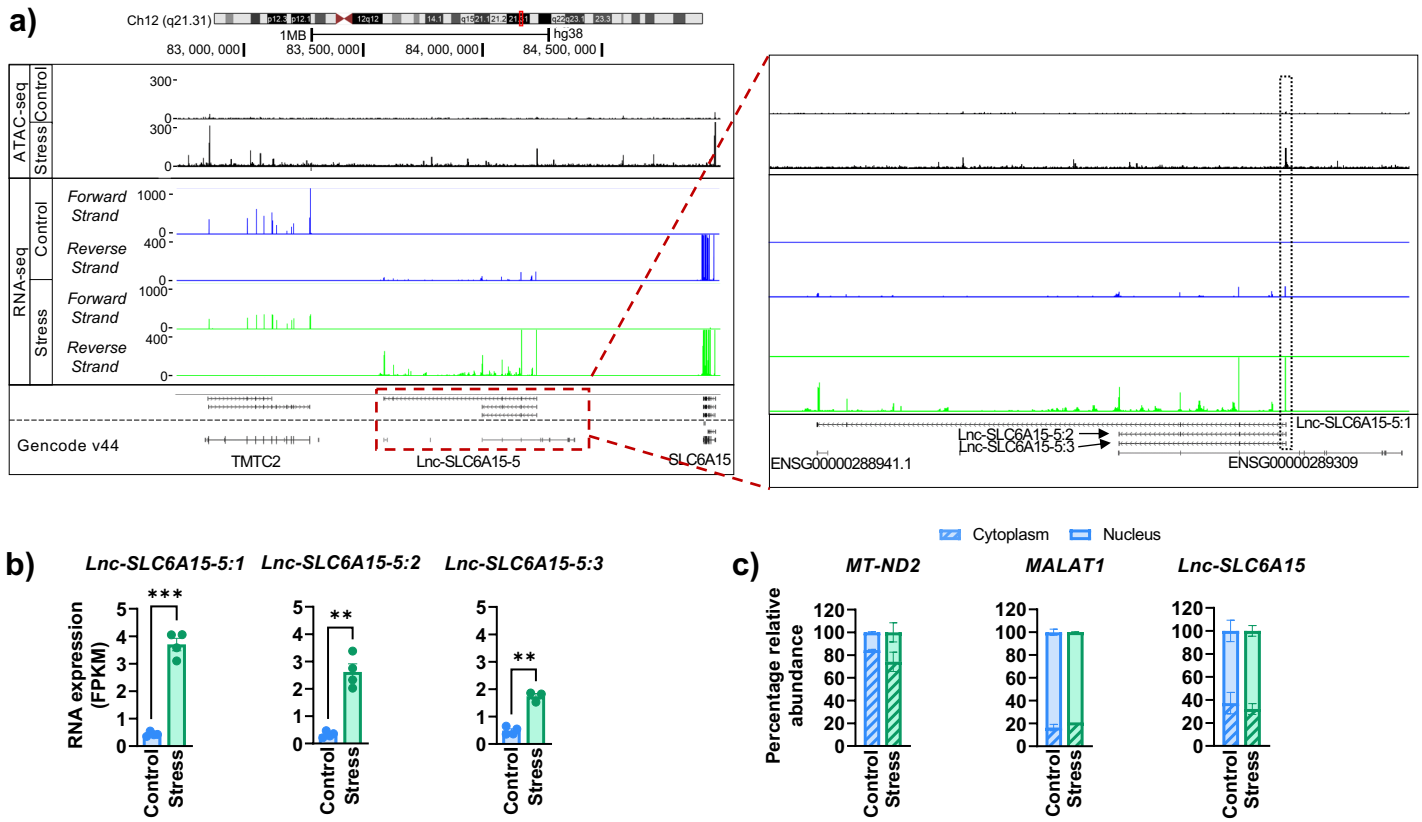
a)
Ch12 (q21.31)
1MB
hg38
83, 000, 000
83, 500, 000
84, 000, 000
84, 500, 000
ATAC-seq
Control
Stress
RNA-seq
Forward Strand
Reverse Strand
Gencode v44
TMTC2
Lnc-SLC6A15-5
SLC6A15
Lnc-SLC6A15-5:1
Lnc-SLC6A15-5:2
Lnc-SLC6A15-5:3
ENSG00000288941.1
ENSG00000289309

b)
Lnc-SLC6A15-5:1
Lnc-SLC6A15-5:2
Lnc-SLC6A15-5:3
RNA expression (FPKM)
Control
Stress
c)
Cytoplasm
Nucleus
MT-ND2
MALAT1
Lnc-SLC6A15
Percentage relative abundance

Figure 6

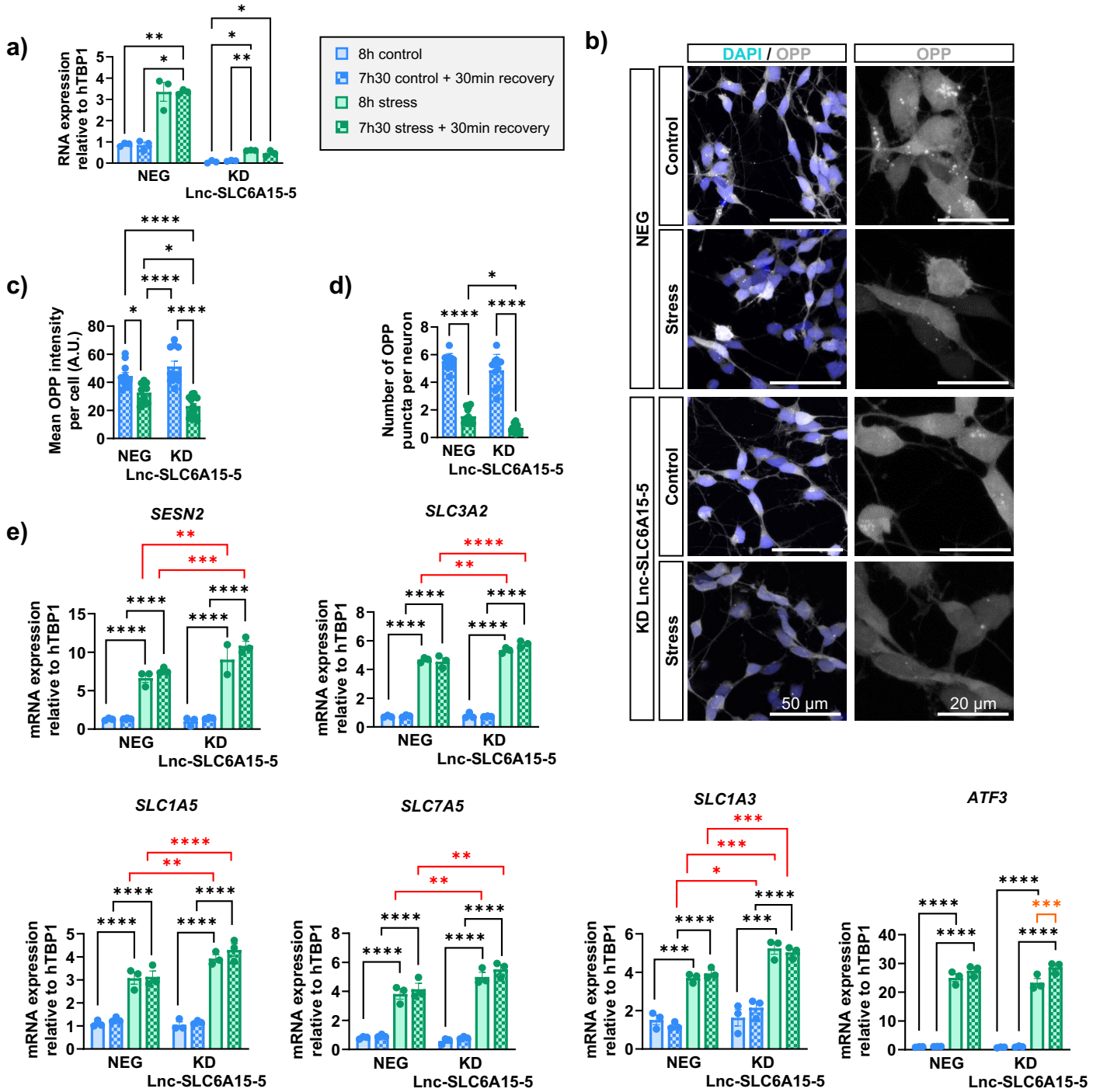
a)
RNA expression relative to hTBP1
NEG
KD
Lnc-SLC6A15-5
8h control
7h30 control + 30min recovery
8h stress
7h30 stress + 30min recovery
b)
DAPI / OPP
OPP
NEG
KD Lnc-SLC6A15-5
Control
Stress
50 µm
20 µm
c)
Mean OPP intensity per cell (A.U.)
d)
Number of OPP puncta per neuron
e)
SESN2
SLC3A2
SLC1A5
SLC7A5
SLC1A3
ATF3
mRNA expression relative to hTBP1

Figure 7

Supplementary data

Supplementary table S1

Primary antibodies for Immunostaining				
Antigen	**Supplier**	**Reference**	**Host**	**Dilution**
CASPASE 3 (Cleaved)	Cell Signaling Technology	9661	Rabbit	1/500
DAT	Millipore	mab369	Rat	1/400
TH	Millipore	ab152	Rabbit	1/400
Phospho Ser65 Ubiquitin	Cell Signaling Technology	N-70973S	Rabbit	1/500
TOMM20	Abcam	ab56783	Mouse	1/1000
MAP2	Abcam	ab5392	Chicken	1/2500

Primary antibodies for Western blotting				
Antigen	**Supplier**	**Reference**	**Host**	**Dilution**
ATF4 (D4B8)	Cell Signaling	11815S	Rabbit	1/1000
Phospho-EIF2α (Ser51)	Cell Signaling	3398S	Rabbit	1/1000
EIF2α (D7D3)	Cell Signaling	5324S	Rabbit	1/1000
Vinculin	Invitrogen	MA5-11690	Mouse	1/1000

Secondary antibodies				
Antigen	**Supplier**	**Reference**	**Host**	**Dilution**
Alexa Fluor Anti-Rabbit 555	Thermo Fisher Scientific	A21428	Goat	1/1000
Alexa Fluor Anti-Rat 555	Thermo Fisher Scientific	A21434	Goat	1/1000
Alexa Fluor Anti-Rabbit 488	Thermo Fisher Scientific	A11070	Goat	1/1000
Alexa Fluor Anti-Rabbit Cy3	Thermo Fisher Scientific	A10520	Goat	1/1000
Alexa Fluor Anti-Mouse 488	Thermo Fisher Scientific	A11029	Goat	1/1000
Alexa Fluor Anti-Mouse 555	Thermo Fisher Scientific	A21422	Goat	1/1000
Alexa Fluor Anti-Chicken 647	Thermo Fisher Scientific	A21449	Goat	1/1000
Peroxidase AffiniPure Anti-Rabbit	Jackson	115-035-144	Goat	1/10000
Peroxidase AffiniPure Anti-Mouse	Jackson	115-035-003	Goat	1/20000

Supplementary table S2

Gene	Forward Primer	Reverse Primer
TBP	TGCACAGGAGCCAAGAGTGAA	CACATCACAGCTCCCCACCA
PERK	AGAGAGAGGAGCGTGTGTCT	TCCTGGTCCATTGCAGTCAC
EIF2A	GTTGCAACAGCTTATAGACCCC	GACAGTGTTTCGTGGTGTGC
ATF4	TCCTCGATTCCAGCAAAGCA	CCAATCTGTCCCGGAGAAGG
ATF3	CCTTTCATCTTCTTCAGGGGCT	AGGAAGAGCTGAGGTTTGCC
DDIT3	CATGTTAAAGATGAGCGGGTGG	TGGATCAGTCTGGAAAAGCACA
CHAC1	CGCTGTGGATTTTCGGGTAC	TTGCTTACCTGCTCCCCTTG
TRIB3	GTGTCGCTTTGTCTTCGCTG	CTGCCTTGCCCGAGTATGAG
NRF2	GAGCAAGTTTGGGAGGAGCT	GGTTGGGGTCTTCTGTGGAG
TRAF2	CATACCCGCCATCTTCTCCC	TCATTCGGGCCCTTCATCAC
JNK	ATGAAGCTCTCCAACACCCG	GCCATTGATCACTGCTGCAC
ATF6	TTCAGTCTCGTCTCCTCGGT	ATCTTCCTTCAGTGGCTCCG
HSPA5	GACAAGAAGGAGGACGTGGG	GCATCGCCAATCAGACGTTC
EDEM1	ATATGGTGCCCTCCCTGAGA	AGAAGCTCTCCATCCGGTCT
HERPUD1	TTCCATTTAGACCGAGGCCG	GAGGTGGTTGGGGTCTTCAG
XBP1	CGGAAGCCAAGGGGAATGAAGT	TGCAGAGGTGCACGTAGTCTGAGT
XBP1 s	CGGAAGCCAAGGGGAATGAAGT	ATACCGCCAGAATCCATGGGGAGA
IRE1	CTGGAGCCTAGAGAAGCAGC	GGGACAGTGATGTTCTCCCG
DNAJC3	ACCTGACAATGTGAATGCCCT	TGGAAGTTATCTGGGTGCCAC
ATF5	GGATGGCTCGTAGACTATGGG	CGCTCAGTCATCCAGTCAGA
CLPP	ATGACATCTACTCGCGGCTG	TTGCAGGAAGAGGAGCTGTG
LONP1	TGATCAACGTGTCGGGCTAC	CTTGGCCTTGCTCTCATCCA
YME1L1	GGAGCCACAAACTTCCCAGA	AAGCCAACAGTACCTCGAGC
SIRT3	CGTTGTGAAGCCCGACATTG	AAGTCCCGGTTGATGAGCAG
FOXO3	TGGTTTGAACGTGGGGAACT	GCTGGGTTAGGAAAATGGCG
NRF1	TCAGCAAACGCAAACACAGG	GTGACCGTGGTTGGCAATTC
lnc-SLC6A15-5	GCAATGCTAGGCTCCTGACA	TATCCTCCCCGGGTTACTCG
VLDLR-AS1	TACTTGCAGTTTCCAGGGGC	CACGTACGGCTTCTTTCTTGC
VPS11-DT	TGCCGGATGTGACTGTAACT	CCCTCATCTTGATCTCCCGG
lnc-FKRP	GAGTTTCTCTGGGTGGGACG	CAGCCCTCAGTGTCCAAGAC
SNHG1	CGTTGGAACCGAAGAGAGCT	CTGTAACGCTGGCTTTGCAT
SNHG5	CACAGTGGAGCAGCTCTGAA	GGCTACTCGTCCACACTCAG
TMEM161B-DT	TCTAAAGCAACTTCCGTGGGT	GCTGTTCGTCCCCTCACAAA
lnc-PSMC3IP-3	ACATCCAGCTGCAACCTCTC	TGTATGCCACGTTGAGGGAC
MIR4697HG	GGAAAAGGCTCTGTCGTGGA	GAAGTGTGTGTGCAGGCTTG
FBXL19-AS1	GGCTGTCCCCTCTATCCTCA	GGTGGAGAAGTGAGATGGGC
NIPBL-DT	CGCTGGACAAGGCTGGAATA	TAGCGCACTGGTACACACAC
ZNF778-DT	TGTCTGAACATCACGCCGAA	TGGTCTTGGCTCCTACGGTA
lnc-MNAT1-2	TCTTGCCTTTCCATGAGCGT	GGCAGAGGTGGATGGAGATG
lnc-TTC29	GGAAAGGGGAGTGTTCACGT	ATGGCTCCTGATAACTGCGG
lnc-SLAIN1-11	CGTGGCGCTAAGACTGAGAT	CCTTTCCCACCCCATTCGAA
SESN2	TCTCCTCCTTCGTGTTTGGC	GGCTCTCTGACTTCTCCAGC

SLC3A2	TGGTCCCAGTGGCGGATATA	CTACGGGGATGAGATTGGCC
SLC1A5	CTCCTTGATCCTGGCTGTGG	GGGCAGCTCACTCTTCACTT
SLC7A5	TTCTTCAACTGGCTCTGCGT	GAGACGGCGATCAGGAAGAG
SLC1A3	ACATGAAGGAACAGGGGCAG	GGAGTGGCAAGACGATGACT
DDIT4	GGTTCGCACACCCATTCAAG	CCAAAGGCTAGGCATGGTGA
SYNCRIP	TGGGAAACTGGAACGAGTGAA	TGATCTGGTGGCTTGGCAAA
mTOR	AGCTCTTCGGCCTGGTTAAC	CTTCTCCCTGTAGTCCCGGA
RPS6KB1	ACTTCTGGCTCGAAAGGTGG	TGTTCGTGGGCTGCCAATAA
RPS6	GCCCCAAAAGAGCTAGCAGA	GCAGGACACGTGGAGTAACA
EIF4EBP1	CCTTCCAGTGATGAGCCCC	GTGTTCACGAAGAGGAGGGG
EIF4EBP2	GGATCGTCGCAATTCTCCCA	GCCAAATCAGGTGCACACAA

Supplementary table S3

	primer1	primer2
sgNEG	caccgTCCCCTCCACCCCACAGTG	aaacCACTGTGGGGTGGAGGGGAc
sgRNA targetting lnc-SLC6A15-5	caccgCTTTCTCTGGCTGGTAGCGA	aaacTCGCTACCAGCCAGAGAAAGc

Supplementary Figure 1. (a) Detection of incorporated EdU (green) in DA neurons after incubation with EdU for 4 h or 24 h in the presence or absence of ddC. The right panels are zoomed areas from the left panels, indicated by dotted squares. **(b)** TOMM20 (red) expression assessed by immunofluorescence and EdU (green) detection in control conditions or following mitochondrial stress for 8 h. **(a, b)** Nuclei were stained using DAPI (blue). **(c)** Percentage of EdU-positive puncta co-localized with TOMM20 per neuron in control conditions and upon a 2 h-, 4 h- or 8 h-stress. Data were obtained from 3 independent differentiation experiments. Each dot represents the percentage of EdU puncta TOMM20 positive for one experiment of differentiation. The bar represents the mean of the 3 values, and the error bars show standard error of the mean.

Supplementary Figure 2. (a) Number of ATAC-seq peaks altered upon a 8 h long stress and defining chromatin regions with decreased or increased accessibility, depending on their genomic loci. **(b)** Gene ontology analysis (Biological Process 2023,

Cistrome DB) performed on ATAC-seq peaks linked to promoters and displaying increased accessibility upon 8 h of stress compared to control conditions. **(c)** Gene ontology analysis (Cellular Component 2023, Cistrome DB) performed on ATAC-seq peaks linked to promoters and displaying decreased accessibility upon 8 h of stress compared to control conditions. **(d)** Gene ontology analysis (Biological Process 2023, Cistrome DB) performed on all ATAC-seq peaks displaying altered accessibility (increased in green, decreased in blue) upon 8 h of stress compared to control conditions.

Supplementary Figure 3. Phospho-Serine 65 ubiquitin (red), TOMM20 (green) and MAP2 (grey) expression in DA neurons treated with DMSO (Control) or after exposition to mitochondrial toxins for 4 h and 6 h (Stress), in the presence or absence of GSK2606414, observed by immunofluorescence. Nuclei were stained using DAPI (blue). For each time point, the right panels are zoomed areas from the left panels, indicated by dotted squares.

Supplementary Figure 4. (a) *Lnc-SLC6A15-5* expression, assessed by RT-qPCR, in DA neurons transduced by lentiviral vectors carrying *dCAS9-KRAB* and sgRNAs either targeting *lnc-SLC6A15-5* (KD *lnc-SLC6A15-5*) or a non-human sequence (NEG), in control conditions or following 8 h of mitochondrial stress (Two-way ANOVA with Tukey's multiple comparison test). RNA expression was normalized relatively to *TBP* mRNA expression. Data from 3 independent differentiation experiments, represented by 3 dots, were used. The bar represents the mean of the 3 values, and the error bars show standard error of the mean . **(b)** TH (green) and DAT (red) expression, assessed by immunofluorescence on DA neurons expressing normal (NEG) or reduced levels

(KD) of *lnc-SLC6A15-5* in control conditions or upon 8 h mitochondrial stress . **(c)** Graphs show quantification of the percentage of TH^+ cells and TH^+ DAT^+ cells in both control and stress (8 h) condition (Two-way ANOVA with Tukey's multiple comparison test; no significant p-values found). **(d)** Phospho-Serine 65 ubiquitin (red), TOMM20 (green) expression in DA neurons expressing normal (NEG) or reduced levels (KD) of lnc-SLC6A15-5 and treated with DMSO (Control) or after 8 h long exposition to mitochondrial toxins (Stress), observed by immunofluorescence. **(e)** The graph represents the percentage of phospho-Serine65 ubiquitin-positive neurons in DA neurons expressing normal (NEG) or reduced levels (KD) of *lnc-SLC6A15-5*, in control conditions and following 8 h of mitochondrial stress (Two-way ANOVA with Tukey's multiple comparison test). **(f)** TOMM20 (red) and MAP2 (grey) expression assessed by immunofluorescence and EdU (green) detection in DA neurons expressing normal (NEG) or reduced levels (KD) of *lnc-SLC6A15-5* and treated with DMSO (Control) or after a 8 h long exposition to mitochondrial toxins (Stress). **(g)** Percentage of EdU-positive puncta in DA neurons expressing normal (NEG) or reduced levels (KD) of *lnc-SLC6A15-5*, in control conditions and following 8 h of mitochondrial stress (Two-way ANOVA with Tukey's multiple comparison test). **(b, d, f)** Nuclei were stained using DAPI (blue). The right panels are zoomed areas from the left panels, indicated by dotted squares. **(c, e, g)** Data were obtained from 3 independent differentiation experiments, represented by 3 dots. The bar represents the mean of the 3 values, and the error bars show standard error of the mean. *p-value ≤ 0,05; **p-value ≤ 0,01 ns p-value

Supplementary Figure 5. (a) Detection of OPP (grey) in DA neurons expressing normal (NEG) or reduced levels (KD) of *lnc-SLC6A15-5*, in control conditions or

following 8 h of mitochondrial stress. Nuclei were stained using DAPI (blue). The graph displays the mean intensity of the OPP signal per TH^+ neurons, in control conditions or following 8 h of mitochondrial stress (Two-way ANOVA with Tukey's multiple comparison test). Data were obtained from 2 independent differentiation experiments. Each dot represents the mean intensity of the OPP signal in DA neurons for one experiment of differentiation. The bar represents the mean of the 2 values, and the error bars show standard error of the mean. **(b)** EIF2α, phosphorylated EIF2α (P-EIF2α) and Vinculin expression, assessed by Western Blot, in DA neurons expressing normal (NEG) or reduced levels (KD) of *lnc-SLC6A15-5*, under 4 different experimental settings. Quantification of the P-EIF2α/EIF2α ratio in DA neurons expressing normal (NEG) or reduced levels (KD) of *lnc-SLC6A15-5,* in control conditions and upon mitochondrial stress (8 h) from 2 independent differentiation experiments represented by 2 dots. The bar represents the mean of the 2 values, and the error bars show standard error of the mean. **(c)** Control (blue) and stress (green) conditions were performed either during 8 h (plain bars) or during 7h30 followed by 30 min recovery (hatched bars). *DDIT4, SYNCRIP, MTOR, RPS6KB1, RPS6, EIF4EBP1 and EIF4EBP2* mRNA expression, assessed by RT-qPCR, in DA neurons expressing normal (NEG) or reduced levels (KD) of *lnc-SLC6A15-5*, in the 4 experimental conditions (Type II Wald Chi-square tests ANOVA function with Tukey's multiple comparisons test). mRNA expression was normalized relatively to *TBP* mRNA expression. Data from 3 independent differentiation experiments, represented by 3 dots, were used. The bar represents the mean of the 3 values, and the error bars show standard error of the mean. *p-value ≤ 0,05; **p-value ≤ 0,01; ***p-value ≤ 0,001; **** p-value ≤ 0,0001.

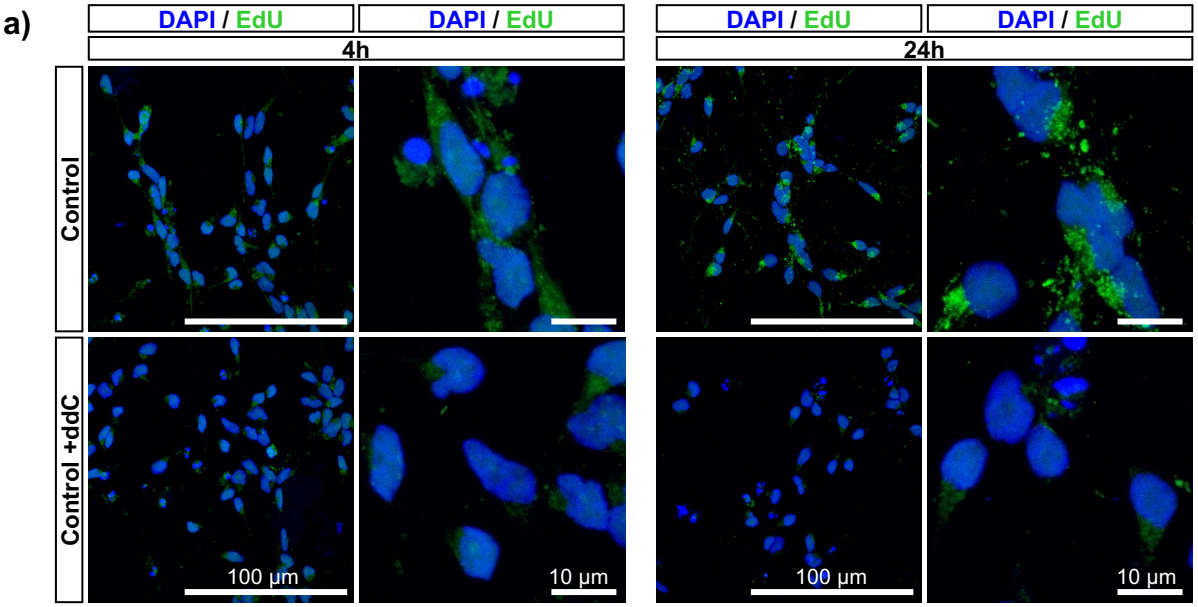

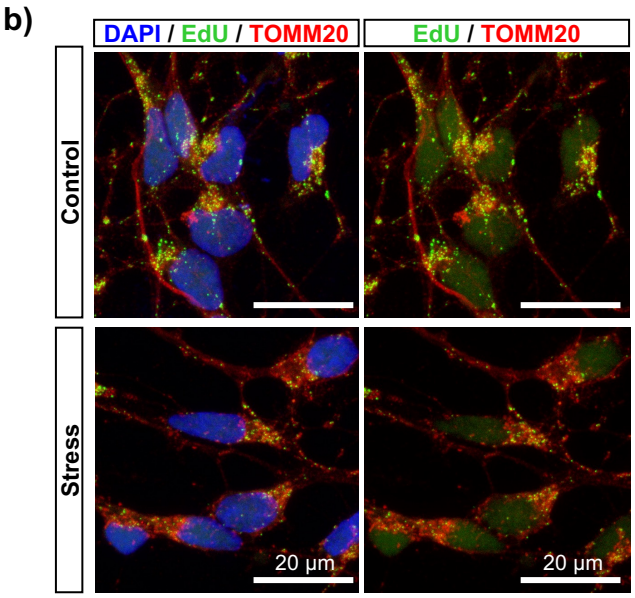

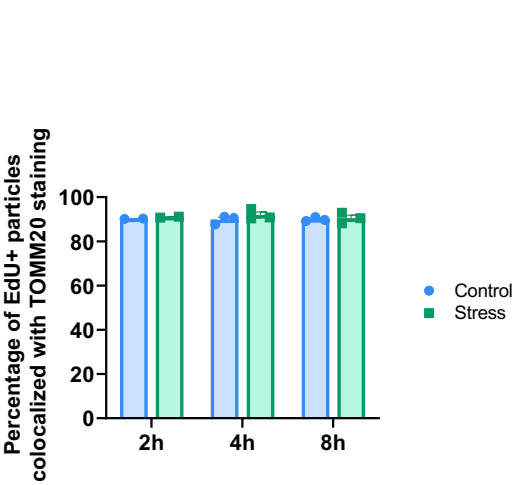

Supplementary Figure 1

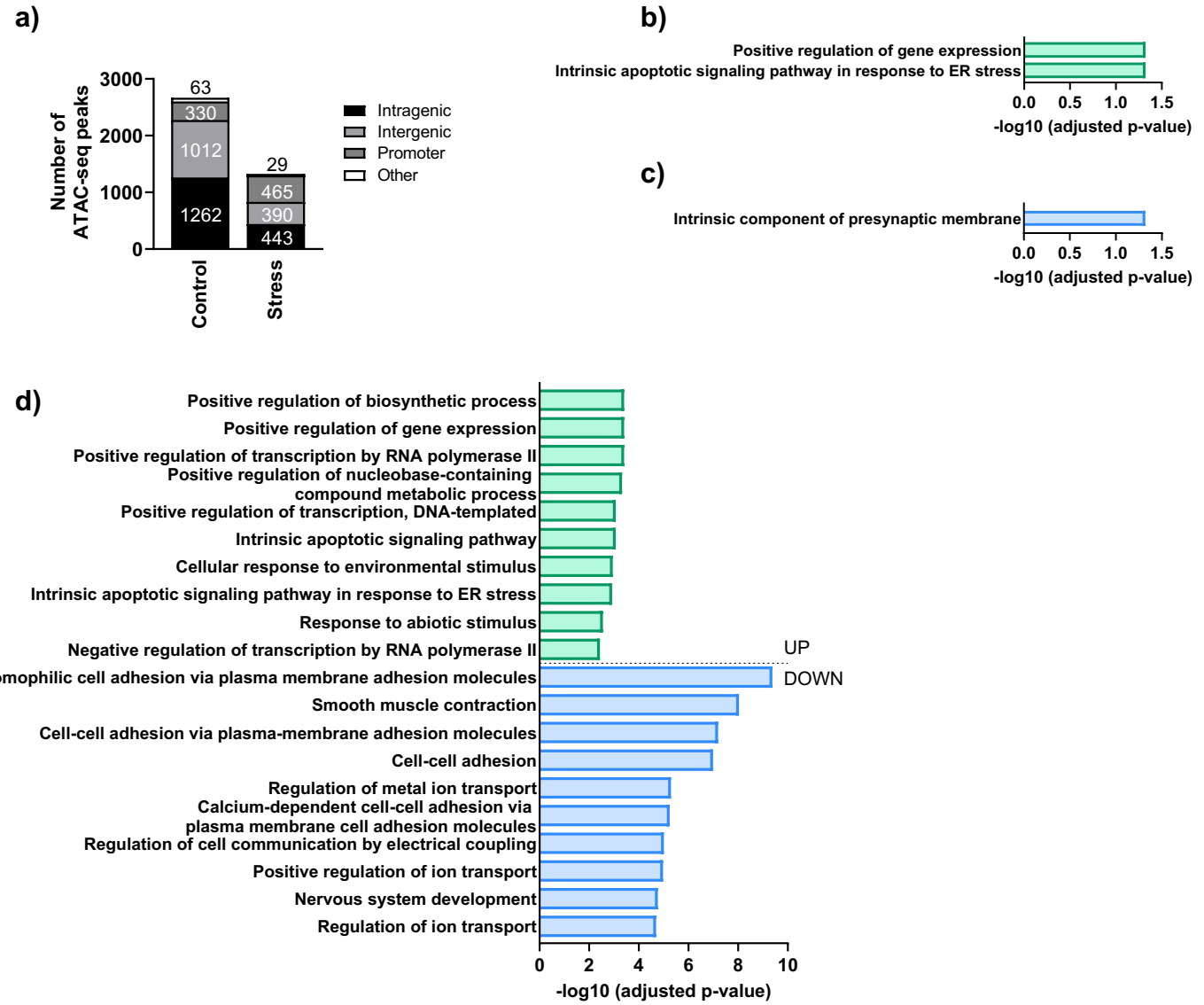

Supplementary Figure 2

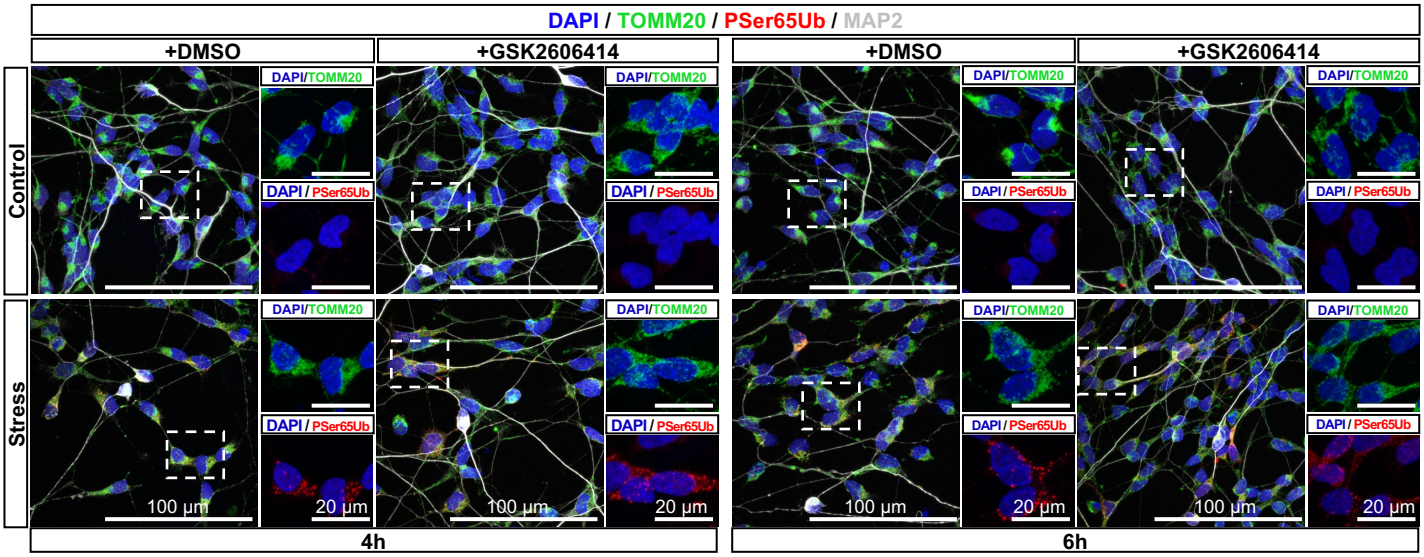

Supplementary Figure 3

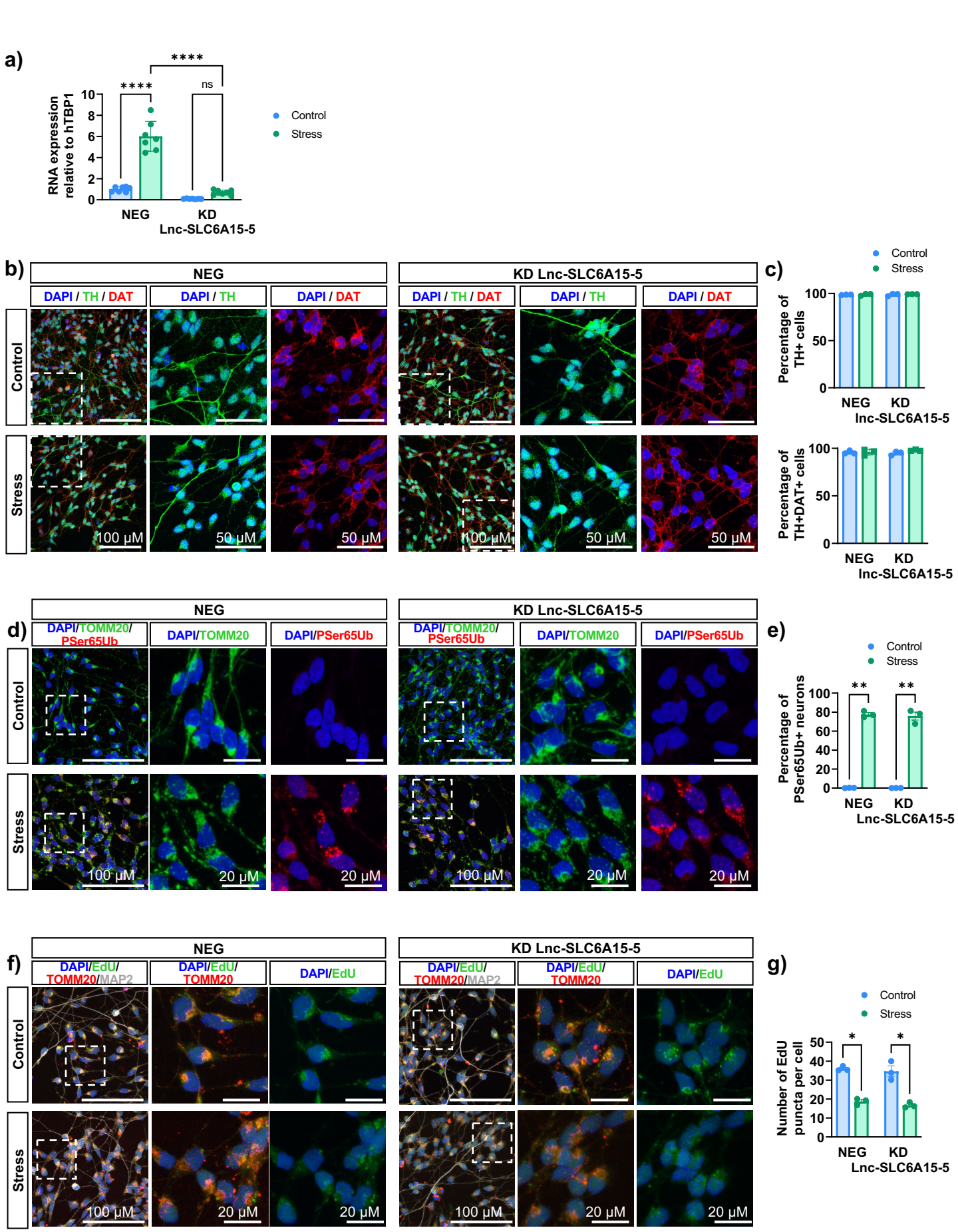

Supplementary Figure 4

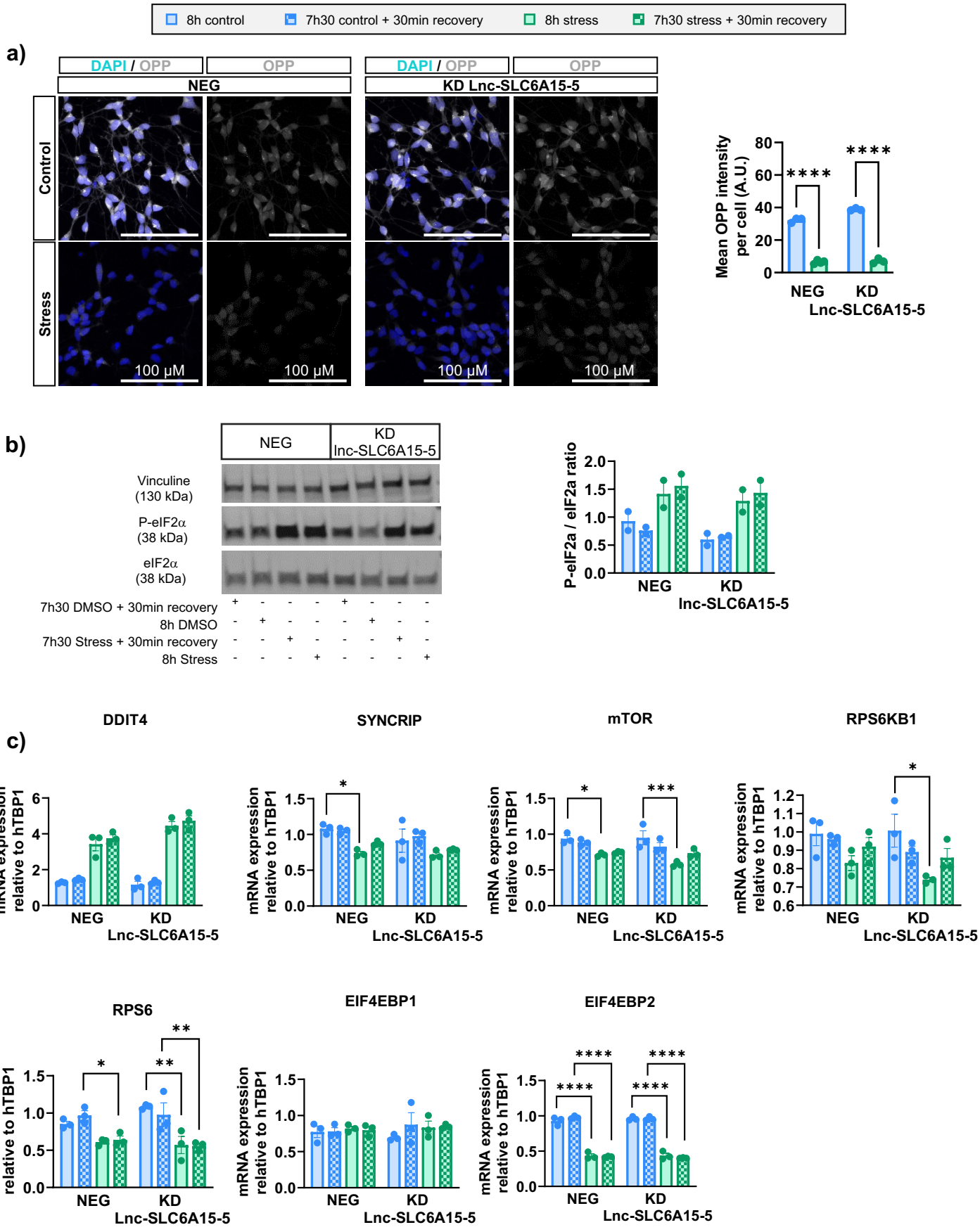

Supplementary Figure 5

IV. Study 2

Transcriptomic study of the PD-associated defects in the mitochondrial stress response of human DA neurons

1. Introduction

PD is defined by the drastic and selective loss of DA neurons of the *SNpc* (Balestrino and Schapira, 2020; Bloem, Okun and Klein, 2021) . This directly causes the hallmark motor symptoms of the disease: rigidity, bradykinesia and tremor. The molecular mechanisms governing this selective vulnerability of DA neurons in PD are still widely unknown, yet they are of crucial importance to understand the aetiology of the disease. Extensive evidence have determined mitochondrial dysfunction as a key component of PD pathophysiology (Bose and Beal, 2016; Borsche *et al.*, 2021; Gao *et al.*, 2022). Most notably, mutations in *PINK1* and *PRKN*, encoding critical regulators of mitochondrial quality control processes, cause autosomic recessive familial forms of PD (Deng, Wang and Jankovic, 2018; Bandres-Ciga *et al.*, 2020; O'Callaghan, Hardy and Plun-Favreau, 2023). These genes respectively encode the mitochondrial serine/threonine kinase PINK1 and the E3 ubiquitin ligase PARKIN and modulate mitophagy, the selective clearance of dysfunctional or unnecessary mitophagy (Corti, 2019; Barazzuol *et al.*, 2020).. Therefore, mutations in *PINK1* and *PRKN*, interfere with the maintenance of mitochondrial homeostasis. Although PINK1 and PARKIN are ubiquitously expressed in neuronal and non-neuronal cells, mutations in these genes lead to the preferential and drastic degeneration of DA neurons. DA neurons exhibit increased vulnerability to mitochondrial damage and a prominent hypothesis in PD research is that this causes the selective DA degeneration in the disease. Therefore, understanding the intrinsic genomic elements that make human DA neurons more susceptible than other cell subtypes to mitochondrial stress is pivotal to fully grasp PD pathophysiology. As of yet, the search for specific molecular signatures defining specific neuronal cells, have been obtained using transcriptomic data focusing on the protein-coding genome. However, there is increasing interest in the study of non-coding elements of the genome, notably lncRNAs, which were reported to display much greater cell specificity than protein-coding genes (Li *et al.*, 2015; Ward *et al.*, 2015; Deveson *et al.*, 2017; Gendron *et al.*, 2019). Growing evidence reveals that lncRNA are potent genomic regulators that are involved in essential developmental and cellular processes, as well as in a number of diseases (DiStefano, 2018; Kopp, 2019; Gil and Ulitsky, 2020; Aliperti, Skonieczna and Cerase, 2021). Furthermore, the majority of PD-associated SNPs fall into non-coding genomic regions, including in lncRNA sequences (Altshuler, Daly and Lander, 2008; Nalls *et al.*, 2019). LncRNAs

are therefore strong research candidates for the study of cell type-specific mechanisms involved in human pathophysiology, such as PD.

In the first project detailed in this thesis, we harnessed the LUHMES immortalized ventral mesencephalic precursor cells to efficiently and rapidly produce a pure population of DA neurons (Lotharius and Brundin, 2002; Lotharius, 2005). This allowed for a DA neuron-targeted analysis, which is key to the study of DA-specific elements, especially in the case of the highly cell-type specific lncRNAs. From this analysis, we were able to determine the mitochondrial stress response in a homogeneous DA neuron population. In the current study, we now want to assess whether this mitochondrial stress response is altered in a PD context, in particular linked to *PRKN* mutations. To this aim, we used induced pluripotent stem cells (iPSC) originating from PD patients carrying *PRKN* mutations. Many studies have investigated the stress response of PD cellular models, notably iPSC-derived DA neurons, although the large majority using targeted approach and exploring specific pathways (Shaltouki *et al.*, 2015; Chung *et al.*, 2016; Avazzadeh *et al.*, 2021). We set out to reproduce the unbiased approach used in the first project, based on high throughput sequencing (RNA-seq data) to explore the cellular mitochondrial stress response, with a particular focus on lncRNAs.

In the homogeneous DA neuronal population, derived from LUHMES cells, we have observed robust UPR^{ER} activation upon mitochondrial stress. Interestingly, several lines of evidence have linked PARKIN, ER stress and UPR^{ER} control. Indeed, PARKIN was first linked to ER stress as it was found to have a protective effect against UPR^{ER}-mediated apoptosis upon ER proteotoxic stress (Imai, Soda and Takahashi, 2000; Imai *et al.*, 2001). Studies subsequently determined that *PRKN* was transcriptionally regulated by ATF4 (Bouman *et al.*, 2011). PARKIN's protective effect against neuronal death in PC12 neuronal cultures treated with the mitochondrial toxin MPP+, was dependent on ATF4 maintaining PARKIN expression levels (Sun *et al.*, 2013). These observations suggest a functional association between PARKIN, mitochondrial dysfunction, and ER stress. Furthermore, PARKIN-deficient drosophila exhibit an activation of PERK-UPR^{ER} in basal conditions, and inhibition of PERK with GSK2606414 was neuroprotective (Celardo *et al.*, 2016). This points to a direct contribution of PARKIN to UPR^{ER} modulation. However, the most studied UPR^{ER} branch in a PD context remains the IRE1-mediated UPR^{ER}, although it is predominantly studied in candidate approach, investigating specific mechanisms (Yang *et al.*, 2009;

Jiao *et al.*, 2017; Costa *et al.*, 2020). However, little data is available in the context of *PRKN* mutation, even less in iPSC-derived neurons (Sison *et al.*, 2018). Cortical neurons differentiated from an iPSC line with a triplication in the *SNCA* gene, exhibited significant activation of the IRE1-UPR^{ER} (Heman-Ackah *et al.*, 2017; Zambon *et al.*, 2019). This was also the case in iPS-derived DA neurons originating from three patients with *GBA* mutations (Fernandes *et al.*, 2016; Schöndorf *et al.*, 2018). The LUHMES-derived DA neurons also displayed inactivation of the UPR^{mt}. Few studies have explored the role of the UPR^{mt} in PD, and none in a *PRKN* mutant model. Nevertheless, *PINK1* mutation in *C.elegans* activated ATFS-1 (equivalent to human ATF5-dependent UPR^{mt}, which promoted DA neuron survival (Cooper *et al.*, 2017). *SNCA* mutant *C.elegans* also were able to trigger the UPR^{mt}, although its sustained activation was neurotoxic (Martinez *et al.*, 2017).

2. Material and Methods

iPS cell culture and differentiation

IPS cells were differentiated using a ventral midbrain-directed protocol inspired by the work of Kirkeby and colleagues (Kirkeby *et al.*, 2017) and mimicking the stages of embryonic development leading to the formation of the ventral midbrain. During the first nine days of differentiation, neural induction was achieved by double SMAD inhibition using SB and Noggin, and ventralization was induced by the addition of SHH and CHIR99021 to the growth medium. From day 9 and until day 17 of differentiation, FGF8b was added to the growth medium, to direct the differentiation towards the mesencephalic fate. Trophic factors BDNF, GDNF and TGFB3 were added to the medium from day 10 until the end of the differentiation at day 40, so as to promote cell survival.

Six cell lines were used in this study: two cell lines originating from two compound heterozygous PRKN mutant PD patients, two cell lines derived from healthy individuals including one that was related to one of the PD patients and was heterozygous for one of the PRKN mutations, two *PRKN* KO isogenic cell lines produced through CRISPR-Cas9 technology-induced mutations. These isogenic cells were produced by our team. The guide RNAs harnessed for this targeted the catalytic site of PARKIN located on exon 2. The absence of additional mutations in these cell lines was verified by sequencing. The *PRKN* mutations were evaluated by a structural biochemist team that confirmed the resulting PARKIN loss-of-function. The characteristics and mutations present in each cell line are described in **Table 1**.

Mitochondrial Stress

Differentiated iPSC were treated at day forty with a combination of antimycin A (25 µM, Sigma-Aldrich), and oligomycin (10µM, Sigma-Aldrich). Stock solutions of these toxins, at 2 mg/mL and 25 mg/mL respectively, were dissolved in dimethyl sulfoxide (DMSO). After treatment, cells were collected or fixed for subsequent analysis. For controls experiments, DMSO was added to the samples without mitochondrial toxins.

RNA extraction

Total RNAs were purified from iPS cells using the RNeasy Minikit (Qiagen) as per manufacturer's instructions. To prevent genomic DNA contamination, RNAs were then treated with DNAse I (Roche) for 20 min at room temperature.. Quantification of obtained RNA was determined using a High Sensitivity RNA ScreenTAPE analyzer (Agilent technologies). The RNA integrity number (RIN) was used to determine RNA quality for all tested samples. RNA was stored at −80 °C until RNA-seq.

RNA-sequencing (RNA-seq)

For each cell line, i.e. originating from the two healthy individuals, the two patients and the two *PRKN* KO isogenic cells, 4 independent differentiation were treated or not with mitochondrial toxins. 200 ng of total RNA were used from Control (n=4) and stressed (n=4) cells to prepare stranded RNAseq libraries as per manufacturer's recommendations using KAPA mRNA hyperprep (Roche Diagnostic). Each final library was quantified and qualified with 2200 Tapestation (Agilent). Final samples of pooled library preparation were sequenced on NextSeq500 with High Output Kit cartridge at 2x150M reads/sample.

RNAseq analysis and de novo annotation of lncRNAs

The analysis of lncRNA expressions from Next-Generation Sequencing (NGS) data involved a extensive pipeline of sequential steps. First, raw FASTQ files underwent quality assessment using FastQC v0.11.8, followed by Trimmomatic v0.39 trimming to discard low-quality trailing bases, adapters, and reads shorter than 50 bases. Cleaned reads were then aligned to the hg38 human reference genome using HISAT2 v2.2.1 (Kim *et al.*, 2019), resulting in ordered BAM files generated through Samtools v1.11 (Danecek *et al.*, 2021). Subsequent transcript assembly and abundance estimation were performed using StringTie v2.1.4 (Pertea *et al.*, 2015), followed by the merging of transcript annotations from all samples into a unified catalog using StringTie merge. Expression levels of transcripts were quantified through StringTie TPM (transcript per million) normalization. Comparative analysis against Gencode v44 and LNCipedia v5.2 reference catalogs was carried out using GffCompare v0.11.2 (Pertea and Pertea, 2020), with transcript annotations categorized as "known" or "unknown" based on class codes. Coding potential prediction was executed using CPC2 v1.0.1 (Kang *et al.*, 2017b), CPAT v3.0.3 (Wang

et al., 2013b), PLEK (Li, Zhang and Zhou, 2014) and RNAsamba (Camargo *et al.*, 2020). Annotations were enriched with details about nearest protein-coding genes and LNCipedia classification. The catalog underwent successive filtration, including removal of low-expression transcripts, retention of non-coding transcripts predicted by multiple tools, and elimination of short transcripts with lengths below 200 bases. The remaining transcripts were filtered according to specific gene/transcript types from Gencode. The filtered catalog was then merged with the Gencode catalog, appending transcripts that did not exactly match the reference. This updated catalog was quantified with STAR v2.7 (Dobin *et al.*, 2013) using original FASTQ files. Resulting TPM counts were integrated into the filtered catalog, which underwent consolidation into a gene-centric format, retaining annotations solely for the most highly expressed transcript per gene. This comprehensive pipeline facilitated the detailed analysis of lncRNA expressions and provided valuable insights into their roles and functions.

Pathway enrichment and gene ontology analysis

Enrichr tool was used to perform pathway enrichment on gene lists, harnessing the GO Biological Processes 2023, Reactome 2022 and KEGG 2021 Human databases (Chen et al., 2013; Kuleshov et al., 2016; Xie et al., 2021; Gillespie et al., 2022; Kanehisa et al., 2023).

3. Results

3.1. The ventral midbrain-directed differentiation protocol efficiently generated TH-positive dopaminergic neurons.

Our team has set up a protocol for differentiating human induced pluripotent stem cells (hiPSC) into DA neurons, based on the work of Kirkeby and colleagues (2017, PMID:28094017). It is centered around the activation of the ventralizing factor Sonic Hedgehog (SHH), the inhibition of dorsalization *via* the BMP pathway using factors such as Noggin and SB431542 and the use of ventral mesencephalic DA neuronal specification factor Fibroblast growth factor 8 (FGF8) (Kriks et al., 2011; Chambers et al., 2009). This forty-day long protocol has been progressively adapted in our team to ameliorate the production of differentiated and mature DA neurons in a healthy individual-derived cell line first (Healthy individual 2). It has then been extended to and validated in our other cell lines that are described in the table below (**Table 4**).

Name	Abbreviation	Mutation in *PRKN*	Donor
Healthy individual 1	HI 1	No mutation	58-year-old woman
Healthy individual 2	HI 2	*PRKN* heterozygous deletion ex8-9	38-year-old man brother of P1
PRKN KO isogenic line 1	KO 1	*PRKN* compound heterozygous (del CAC/del C)	Originating from HI2 line
PRKN KO isogenic line 2	KO 2	*PRKN* compound heterozygous (ins CTGGGAAA/del CCACT)	Originating from HI2 line
Patient 1	P 1	*PRKN* compound heterozygous (del ex8-9/R42P)	46-year-old woman sister of HI2
Patient 2	P 2	*PRKN* compound heterozygous (del ex 2 /c.255 del A)	45-year-old woman

Table 4. Induced Pluripotent Stem cell lines used in the study. *We had access to six cell lines: two were derived from two healthy individuals, one presenting no mutation and one carrying a heterozygous ex8-9 deletion of PRKN; two from patients each carrying different PRKN compound heterozygous mutations, and finally two isogenic cell lines originating from the Healthy Individual 2 cell line in which PRKN knockout (KO) was induced.*

To assess whether this differentiation protocol resulted in the generation of DA neurons and in potential changes in the context of *PRKN* deficiency, we performed

immunofluorescence staining for the L-dopa producing enzyme Tyrosine Hydroxylase (TH) at day 40 of differentiation on cells originating from healthy individual-derived, patient-derived and *PRKN* KO isogenic iPS cell lines (**Figure 12**). All three groups displayed a percentage of TH-positive neurons neighboring 10%, confirming DA neuron generation. For this experiment, less patient samples were available for staining than for the other groups; it will therefore be important to reproduce the immunostaining on additional samples.

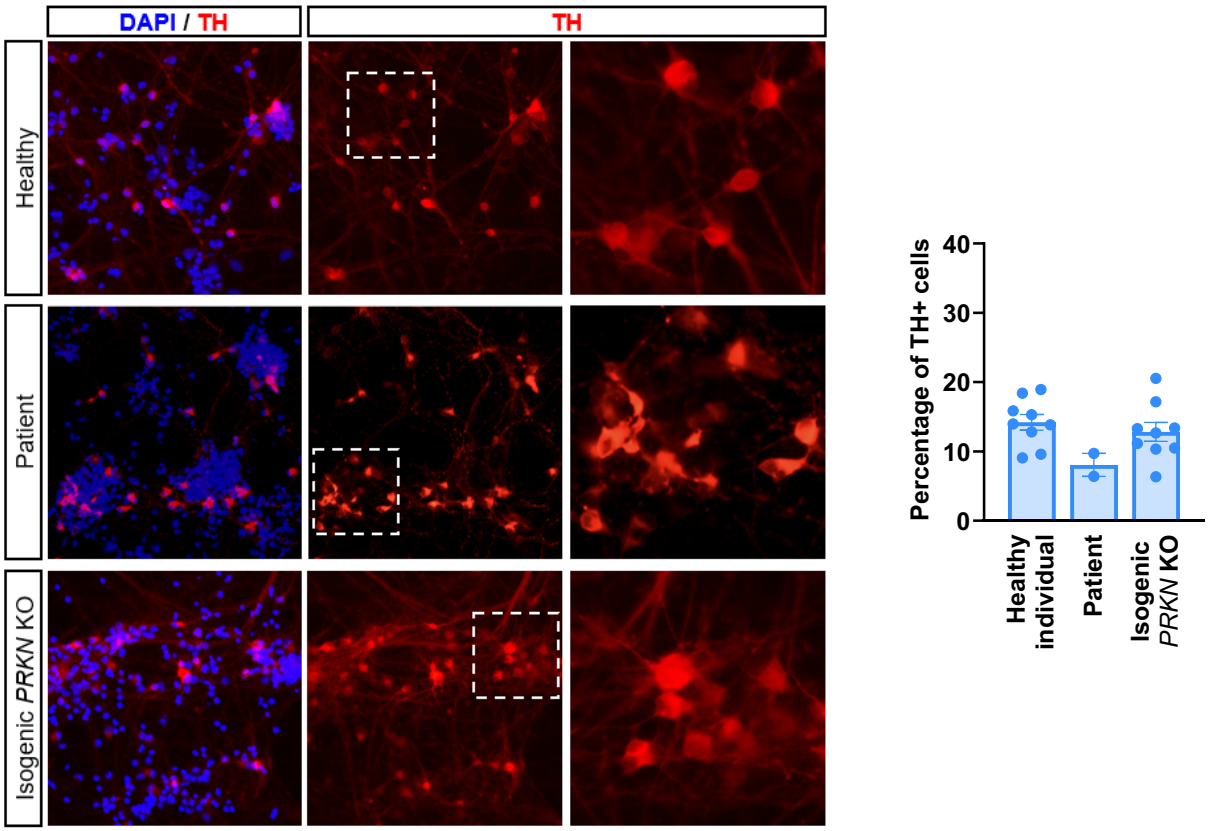

Figure 12. Immunofluorescence staining for TH in healthy, patient-derived and PRKN KO isogenic-derived cells at 40 days of differentiation. *Staining for DAPI shown in blue and for TH in red. Zoomed field showed as the last image for each condition is framed in the middle wide field. The graph represents the percentage of TH-positively stained cells in the overall population. Each dot represents the percentage of TH-stained cell per imaging field (healthy individual n=9; patient n=2; isogenic PRKN KO n=9). The bar represents the mean value with the standard error of the mean.*

3.2. The differentiated cells display coherent transcriptomic signatures consistent with ventral midbrain development.

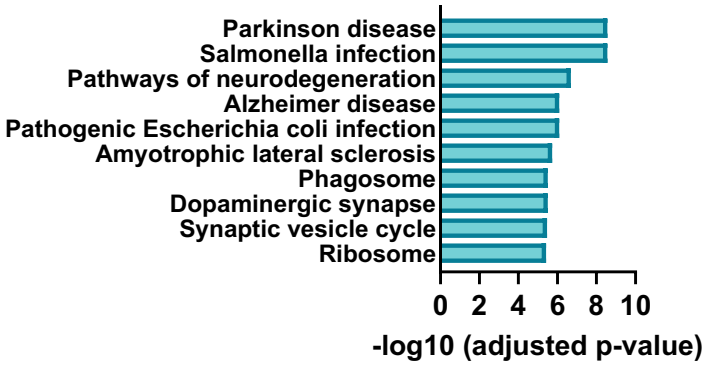

Figure 13. Pathway enrichment analysis (KEGG 2021 Human) on the top 2% most expressed genes from the RNA-seq data obtained from two healthy individual-derived differentiated cells. *Here the graph is showing only the first 10 terms that appeared significantly enriched (360 genes).*

To further validate our differentiation protocol, we investigated the transcriptomic profile of the differentiated cells originating from the healthy individuals using RNA-seq. Using pathway enrichment analysis on the 2% most expressed genes in these cells, we found an enrichment in genes involved in "Parkinson's Disease", "Pathways of Neurodegeneration, "Alzheimer's Disease", "Dopaminergic Synapse" and "Synaptic vesicle cycle" according to the KEGG 2021 Human database (**Figure 13**). Gene ontology analysis also indicated an enrichment in genes involved in "neuronal projection morphogenesis", "axogenesis" and "*Subtantia Nigra* development" (**Figure 14**). Altogether, these observations suggest that the protocol efficiently guided the differentiation towards the neuronal and more specifically, ventral midbrain fate. Alternative pathways in which the highly expressed genes may be implicated, were

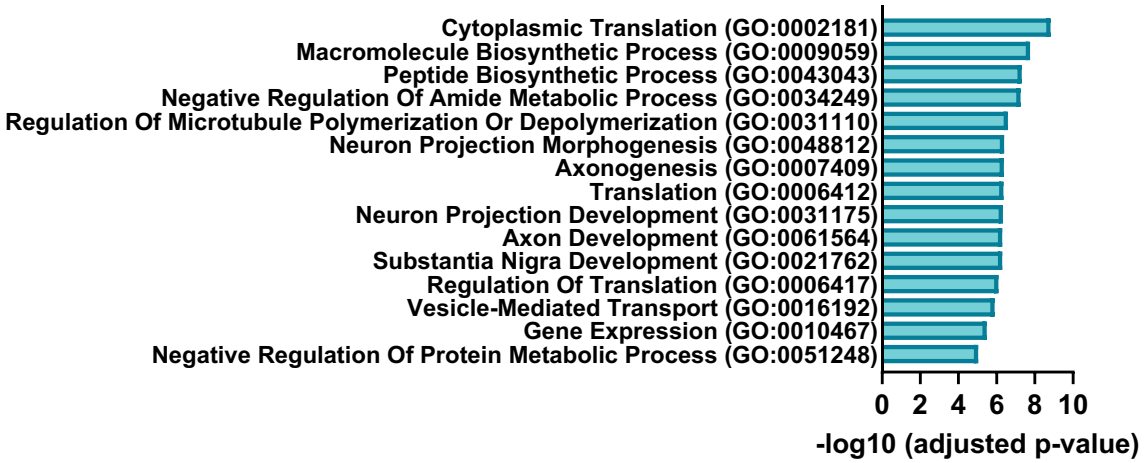

Figure 14. Gene Ontology analysis (Biological Process 2023) on the top 2% most expressed genes from the RNA-seq data obtained from two healthy individual-derived differentiated cell pools. Here showing only the first 15 terms that appeared significantly enriched (360 genes).

related to developmental processes including microtubule polymerization or depolymerization as well as cytoplasmic translation.

We then wanted to investigate more precisely the different cellular populations within the differentiated cell pool. To this end, we assessed the expression level of neuronal and glial cell type-specific markers in the datasets stemming from the two healthy individual derived-iPSC cells (**Figure 15**). The two cell lines expressed markers of the different cellular subtypes in a similar manner. We observed the expression of immature neuronal markers *DCX* and *SOX2*, as well as of mature neuronal markers *MAP2*, *PSD95* and *NeuN*, confirming the successful generation of a neuronal population. Strong expression of the dopamine transporter *VMAT2*, dopamine receptor *DRD2* and ventral midbrain-specific potassium channel *GIRK2* (Reyes *et al.*, 2012), point towards a DA neuron-directed differentiation.

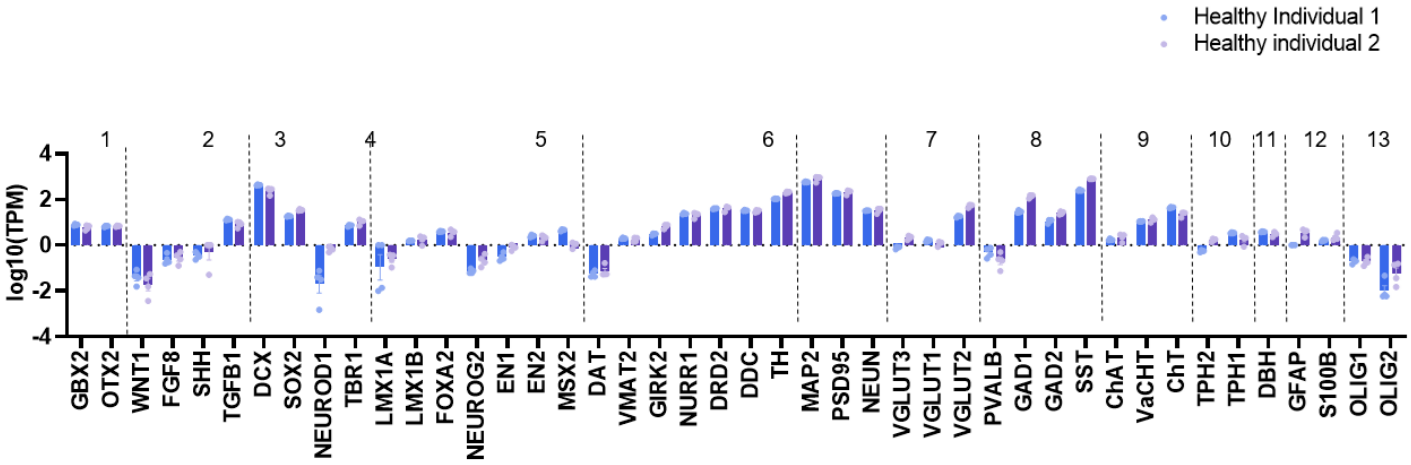

Figure 15. Cellular populations resulting from the forty-day differentiation protocol. *mRNA expression level represented as log10(tpm) of markers of ventral midbrain specification (1), DA differentiation induction (2), immature neurons(3) DA progenitors (4), DA neurons (4), mature neurons (5), Glutamatergic neurons (6), GABAergic neurons (7), cholinergic neurons (9), serotonergic neurons (10), noradrenergic neurons (11), astrocytes (12), and oligodendroctes (13) as collected from RNA-seq data on the differentiated cell pool originating from two healthy individual iPS cell lines.*

Markers associated with ventral midbrain (*GBX2*, *OTX2*, *TGB1*) as well as dopaminergic progenitor (*FOXA2*, *EN2*, *MSX2*) development were also detected. As expected, the differentiated cells exhibited strong expression of DA neuronal markers, such as *TH* and Dopa Decarboxylase (*DDC*), key enzymes for dopamine biosynthesis. Furthermore, the absence of Dopamine Beta Hydroxylase (*DBH*), the downstream enzyme producing noradrenaline from dopamine confirmed that the differentiated cells expressing *TH* were most likely truly dopaminergic. *NURR1*, essential transcription

factor for DA neuron differentiation and maintenance was also robustly expressed. Although the cell culture appeared to contain both progenitors and differentiated neurons, DA progenitor-specific markers showed lower expression levels than differentiated DA neurons suggesting a higher proportion of the later. Overall, these observations indicated a successful DA differentiation using both healthy cell lines.

Our RNA-seq data indicated the presence of different neuronal types including GABAergic (markers: *GAD1, GAD2, SST*), glutamatergic (*VGLUT2*), serotoninergic (*TPH1*) and cholinergic (*ChAT*, *VaCHT* and *ChT*) neurons. Astrocytic markers (*GFAP*, *S100B*) were similarly lowly expressed. To conclude, the differentiated cells originating from healthy iPSCs exhibited coherent cell populations, in line with what is expected in ventral midbrain development (Korotkove *et al*., 2004; La Manno *et al.,* 2016; Jo *et al*., 2016).

3.3. PARKIN loss-of-function appears to impair neuronal identity and maturation

We set out to examine whether the PARKIN loss-of-function mutations affected the differentiation process by inspecting any changes in the mRNA expression of the various cell-type markers previously observed in both patient-derived and *PRKN* KO isogenic line-derived differentiated cells (**Figure 16**).

This analysis revealed distinct changes in expression patterns, including some that appear similar in both patient and isogenic-derived cells. Indeed, both these differentiated cell pools presented a significant decrease in the expression levels of a number of DA progenitor (*EN2* and *MSX2)* and DA neuronal (*NURR1)* markers. In contrast, the early DA differentiation marker *SHH* and the immature neuronal marker *SOX2* were significantly upregulated in both patient-derived and *PRKN* KO isogenic-differentiated cells. Furthermore, we observed an increase in astrocytic (*S100B*) and oligodendrocyte-specific (OLIG2) genes. Overall, these observations may imply a potential delay in the differentiation process as well as a specification shift with a higher yield of glial cells.

It is important to note that although the two *PRKN* KO isogenic lines (KO 1 and KO 2) showed very similar expression patterns for all the genes examined - as expected due to them originating from the same initial cell line (HI2) - the patient cell lines (P 1 and P 2) differed quite clearly for several genes. Patient 1 has a close genetic

background to HI2, as the two individuals are siblings, and is therefore genetically similar to the two isogenic lines as well. Patient 2 has a completely different genetic background and a different *PRKN* mutation, which may explain the differences observed. For example, P2 displayed a much lower expression of mature neuronal (*MAP2*, *PSD95*, *NeuN*), cholinergic (*ChAT*, *VaCHT*, *ChT*), serotonergic (*TPH1*, *TPH2*) and noradrenergic markers (*DBH*) as well as a higher expression of immature neuron

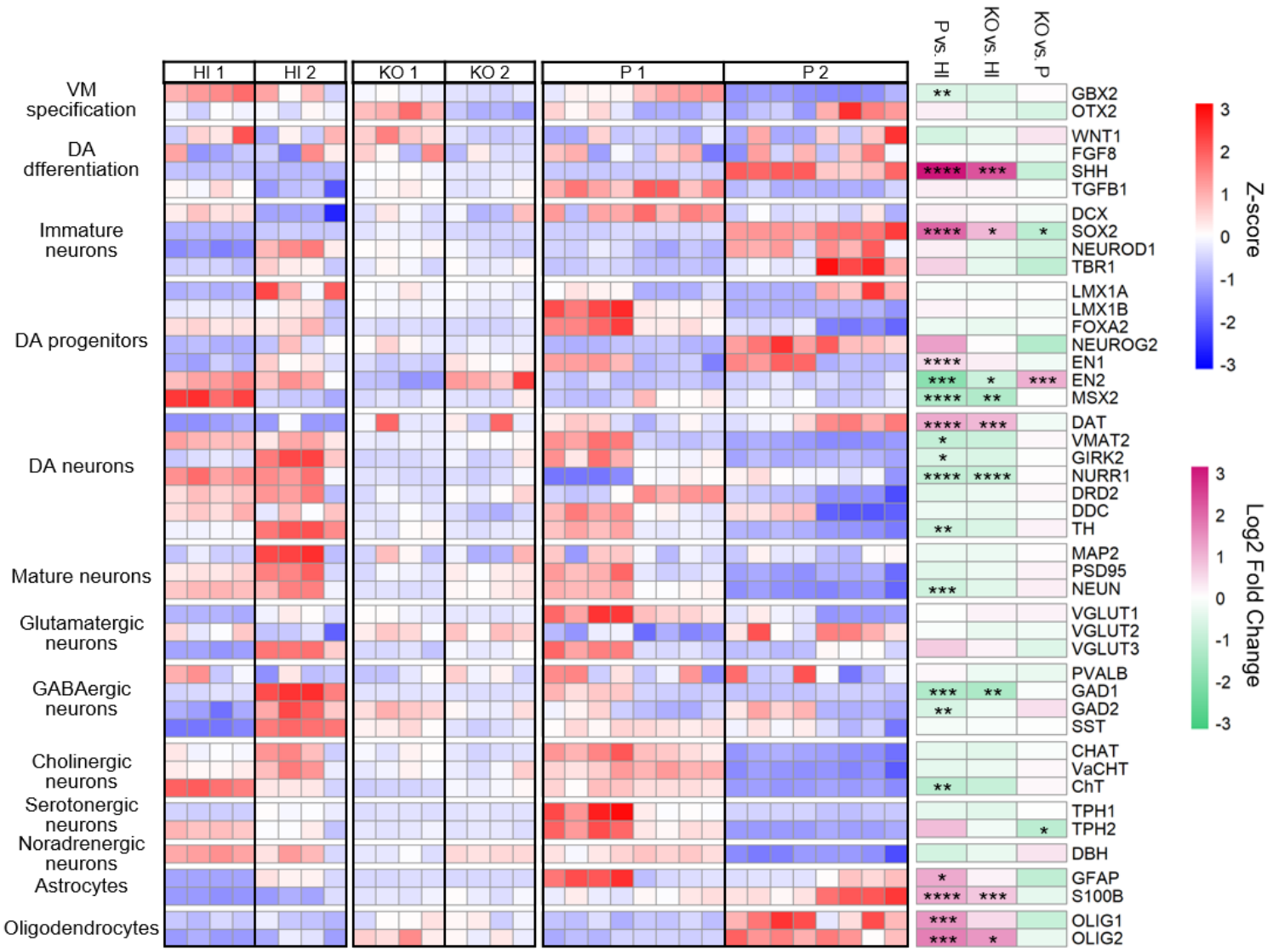

Figure 16. Impact of Parkin loss-of-function on the ventral midbrain-targeted differentiation protocol. *Left heatmap displays the variation of expression levels of a number of neuronal and glial cell type represented as a Z-score in healthy individual (HI1 and HI2), PRKN KO isogenic (KO1 and KO2) and patient (P1 and P2) iPSC-derived differentiated cells. Right-hand heatmap represents the log2 fold change of mRNA expression of the patient or PRKN KO isogenic differentiated cells in comparison to the healthy individual-derived cells (P vs. HI; KO vs. HI) as well as of the PRKN KO isogenic in comparison to the patient differentiated cells (KO vs. P). The observed gene names for both heatmaps are indicated on the right and the cellular identity group they belong to are indicated on the left. Significant change in expression threshold set at log2(fold change) ≥ 0,5 or ≤-0,5. * adjusted p-value ≤ 0.05; ** adjusted p-value ≤ 0.01; *** adjusted p-value ≤ 0.001; **** adjusted p-value ≤ 0.0001.*

(*SOX2*, *NEUROD1*, *TBR1*), oligodendrocyte specific (*OLIG1*, *OLIG2*) and astrocytic (*S100B*) markers. It could be inferred from this that the differentiation in this patient 2 line may be shifted further towards a glial fate than the P1 cell line.

Furthermore, some differences appeared to be due to “batch” effect. The eight P1 samples collected for the RNA-seq experiment were differentiated in two batches at two distinct times (in **Figure 16**, the first 4 columns of P1 correspond to batch 1 and the last 4 to batch 2). There was a noticeable difference in the expression of several genes between these batches. This included a higher level for the first batch of many DA progenitor (*LMX1B*, *FOXA2*), DA neuron (*VMAT2*, *GIRK2*, *DDC*, *TH*), glutamatergic (*VGLUT1*, *VLT3*), serotonergic (*TPH1*, *TPH2*) and astrocytic (GFAP) markers. These results suggest different cell population proportions depending on the batch and more batches will be required to evaluate this effect more thoroughly.

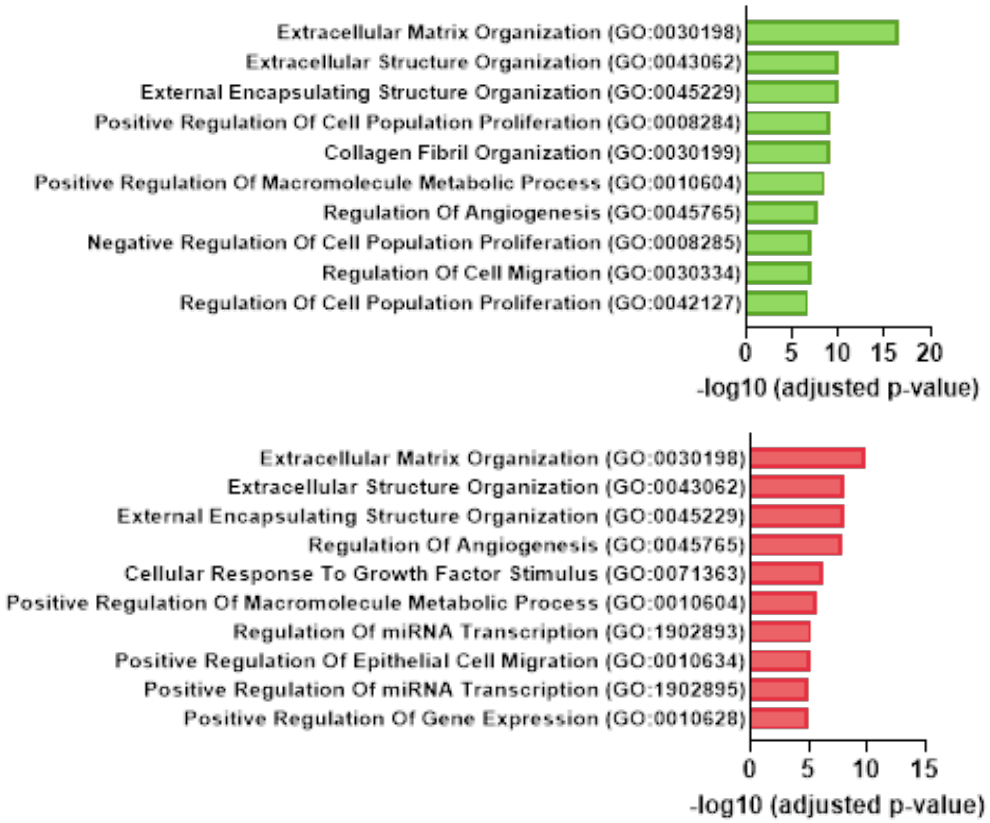

Figure 17. Gene Ontology analysis (Biological Process 2023) on all genes upregulated in the patient- (green; first graph) and PRKN KO isogenic-derived (red; lower graph) cells in comparison with healthy cells *(log (fold change) ≥1). Here showing only the first 10 terms that appeared significantly enriched (Patients: 1149 genes; isogenic PRKN KO: 592 genes).*

We performed pathway enrichment analysis on all the genes whose expression was altered in the patients and *PRKN* KO isogenic cell lines in comparison to the healthy individuals-derived cell lines. *PRKN*-deficient lines displayed similar results. Amongst the genes upregulated in comparison to the healthy individual-derived differentiated cells, we found that in both the patients and isogenic KO cells, there was an enrichment in genes involved in extracellular matrix structural and collagen fibril organization, as well as cell proliferation regulation, which could be linked to the delay in differentiation and maturation previously observed (**Figure 17**).

On the other hand, regarding downregulated genes relative to the healthy individual-originating cells, there appeared to be an enrichment in genes related to GABAergic synapses and receptors for both patients and *PRKN* KO isogenic cell, suggesting altered GABAergic neurotransmission (**Figure 18**).

Altogether, our observations suggested that the *PRKN* loss-of-function may disrupt the differentiation process, possibly by delaying it and causing higher levels of early differentiation markers, as well as by enhancing the production of other cellular subtypes such as glial cells.

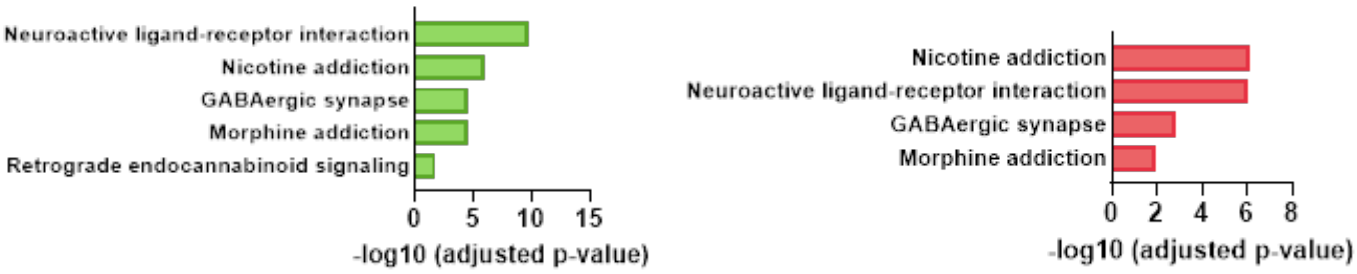

Figure 18. Human pathway enrichment analysis (KEGG 2021) on all genes downregulated in the patient- (green; first graph) and PRKN KO isogenic-derived (red; lower graph) in comparison with healthy individuals-derived cells *(log (fold change) ≤1. Here showing only the first 10 terms that appeared significantly enriched (Patients: 435 genes; isogenic PRKN KO: 203 genes).*

3.4. Mitochondrial stress activates the Endoplasmic Reticulum-dependent Unfolded Protein Response (UPR^{ER}) and the oxidative damage response.

The iPSC-derived differentiated cells were treated with mitochondrial toxins antimycin A and oligomycin for 8 h, a combination known to activate the PINK1/PARKIN-dependent mitophagy (Lazarou *et al.*, 2015) that we previously used on the LUHMES-differentiated DA neurons. We then studied the stress-associated transcriptome alterations to uncover the signaling pathways activated in the differentiated cells in response to this mitochondrial stress protocol.

Principal component analysis revealed that the main factor causing 32.37% of the variance between samples was explained by genetic background (PC#1), as samples clustered depending on the cell lines they were derived from, i.e. healthy individuals, patients, and KO isogenic lines (**Figure 19**). Healthy individual- and patient-derived samples showed slightly more segregation than the *PRKN* KO isogenic cells, linked to the presence of cells originating from two different individuals with distinct genomic backgrounds. Moreover, the two *PRKN* KO isogenic lines were close to the P1 samples, whereas the P2 samples clustered further away. This is likely due to the similar genetic background of the isogenic and P1 cells as they originate from two siblings. On the other hand, the healthy individual-originating samples cluster close to each other even though the two individuals have no genetic link.

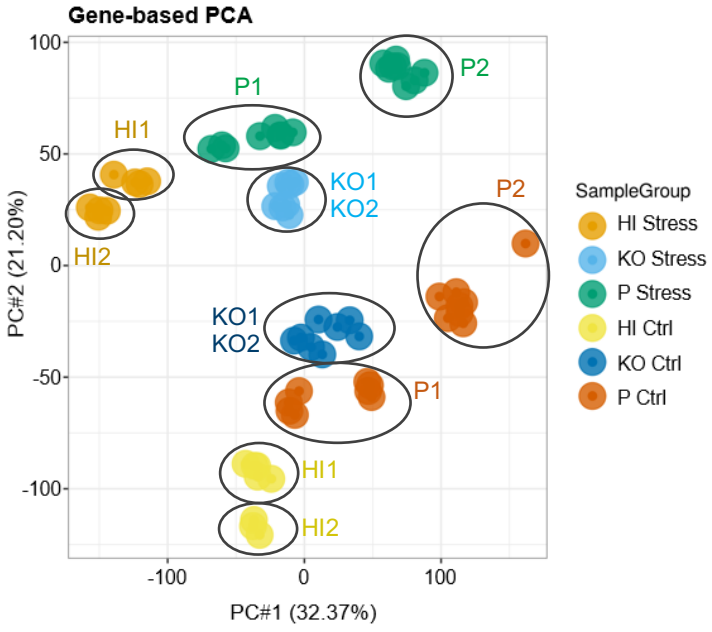

Figure 19. Principal component analysis of RNA-seq datasets. *Data collected from cells treated with mitochondrial toxins (Stress) and originating from healthy individuals (light orange; HI Stress; n=8), PRKN KO isogenic lines (light blue; KO Stress; n=8) and patients (green; P Stress; n=16), as well as cells treated with DMSO only (Ctrl) and originating from healthy individuals (yellow; HI Ctrl; n=8), PRKN KO isogenic lines (dark blue; KO Ctrl; n=8) and patients (dark orange; P Ctrl; n=16).*

Mitochondrial stress protocol accounted for 21% of variance (PC#2), with samples forming two distinct clusters depending on if they were treated with mitochondrial toxins or with DMSO (control group).

To assess which cellular mechanisms were triggered by mitochondrial stress, we subsequently performed gene ontology analysis on genes upregulated or downregulated in response to mitochondrial stress in the cells derived from healthy individuals. Focusing on upregulated genes, we reported the activation of apoptosis regulation pathways as well as endoplasmic reticulum stress response by mitochondrial stress (**Figure 20**). This is very reminiscent of the stress response found in the LUHMES cells (Chapter 1).

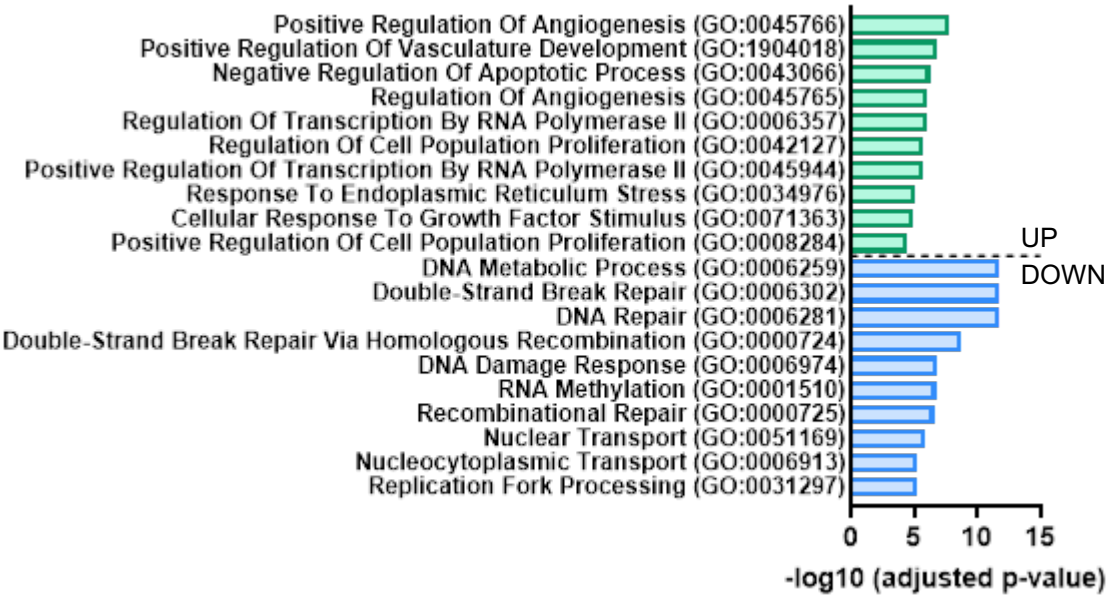

Figure 20. Gene Ontology analysis (Biological Process 2023) on all genes upregulated (green; 717 genes) and downregulated (blue; 477 genes) by mitochondrial stress in the healthy individual-derived differentiated cells compared to control conditions. (log (fold change) ≥1. The first 10 occurrences are shown for each.

Other enriched terms included transcription regulation and angiogenesis regulation with a number of the related genes known to play a role in oxidative stress response (*HMOX1*, *FOXO1*), inflammatory response (*CXCL8*, *IL6*, *ITGAX*), protein refolding (*HSPB1*) as well as cell nervous system development (*FOXC2*, DLL1).

Interestingly, among the genes with upregulated expression following mitochondrial stress, we reported an enrichment in genes involved in cell proliferation processes, indicating that the stress protocol induced a shift towards proliferation as

was previously seen in the *PRKN*-mutated patient and *PRKN* KO isogenic cell lines. Even though this upregulation of proliferation may be linked to neuronal or glial cells, this is reminiscent of the stress response of LUHMES-derived DA neurons where treatment with mitochondrial toxins resulted in a loss of neuronal maturity markers. On the other hand, gene ontology analysis on all the genes downregulated in cells treated with mitochondrial toxins, uncovered strong enrichment in processes involved with DNA repair (**Figure 20**). These results are coherent with observations in neurodegenerative diseases, including PD, that show heightened DNA damage in patients and animal models (Wang *et al.*, 2023). Crosstalks between UPR^{ER} and DNA damage repair pathways have been reported, although studies were conducted mostly in the context of cancer research (Yamamori *et al.*, 2013; Weatherbee, Kraus and Ross, 2016; Liu *et al.*, 2019).

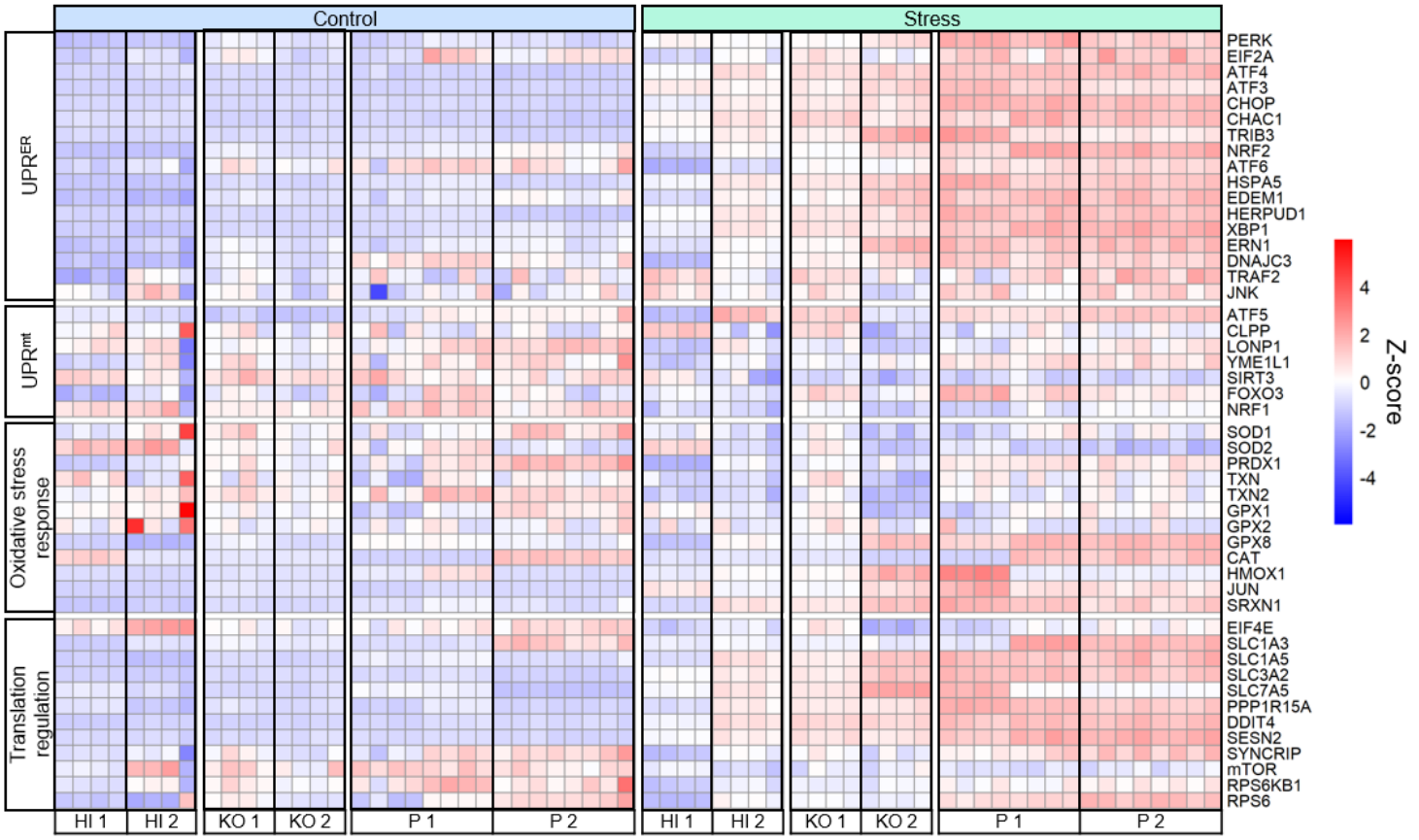

Figure 21. Heatmap of the expression level of UPR^{ER}, UPR^{mt}, oxidative stress response and translation regulation markers in healthy, patient, and isogenic-derived differentiated cells. *Heatmap displays the variation of markers' expression levels (TPM) represented as a Z-score in healthy individual (HI1 and HI2), PRKN KO isogenic (KO1 and KO2) and patient (P1 and P2) iPSC-derived differentiated cells in Control and Stress conditions (as indicated on top of the heatmap). The observed gene names are indicated on the right and the stress response pathway they belong to are indicated on the left.*

Notably, PERK activation upon ER stress has been shown to trigger downregulation of DNA-repair associated genes, impeding cells' ability to resolve DNA damage (Oommen and Prise, 2013). In this study, PERK downregulation was favorable to cell survival.

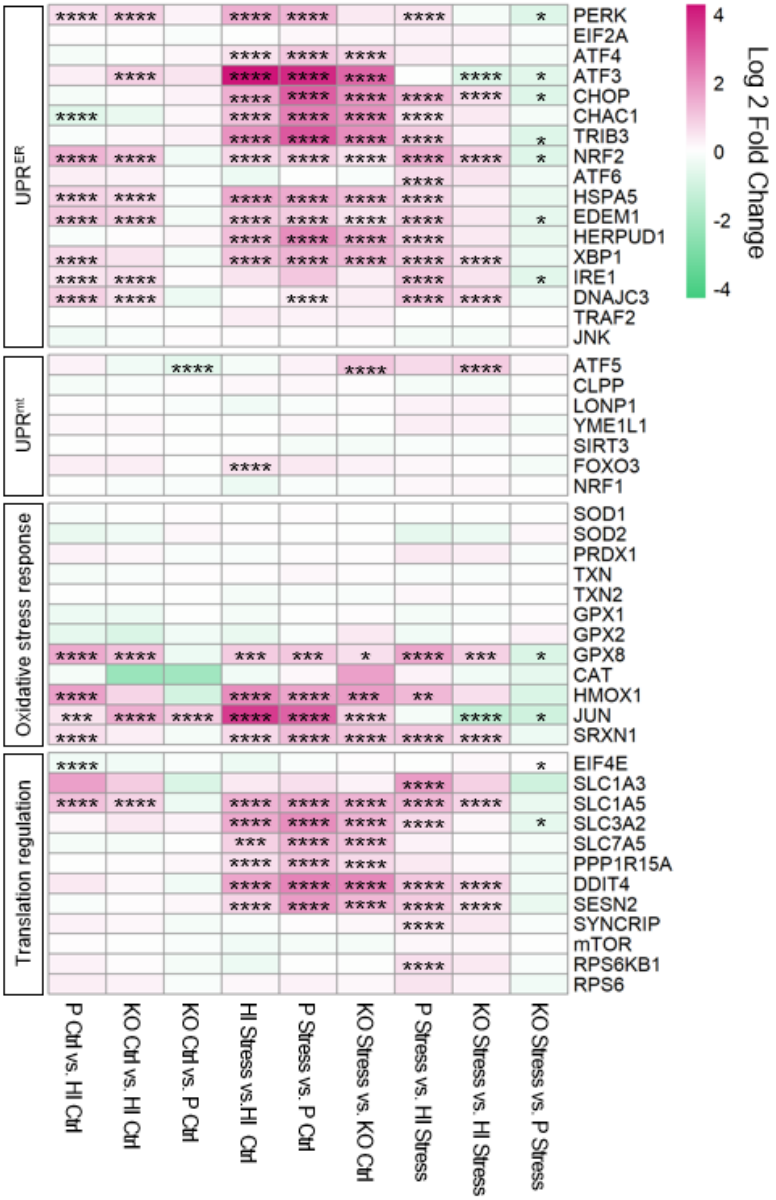

Figure 22. Heatmap showing expression changes of UPR^{ER}, UPR^{mt}, oxidative stress response and translation regulation markers in healthy, patient, and isogenic-derived differentiated. *Color represents log2 fold change of mRNA for 5 different comparisons: patient-derived differentiated cells compared to healthy individual-originating cells (P vs. HI Ctrl), PRKN KO isogenic cells compared to healthy cells (KO vs. HI Ctrl), PRKN KO isogenic cells compared to patient-derived cells (KO vs. P Ctrl), cells treated with mitochondrial toxins compared to control cells in healthy individual-derived cells (HI Stress vs. Ctrl), in patient-derived cells (P Stress vs. Ctrl) and in PRKN KO isogenic cells (KO Stress vs. Ctrl). The genes are indicated on the left of each column and the stress response pathways they belong to are indicated above the heatmap. Significant change in expression threshold set at log2(fold change) ≥ 0,5 or ≤-0,5. * adjusted p-value ≤ 0.05; ** adjusted p-value ≤ 0.01; *** adjusted p-value ≤ 0.001; **** adjusted p-value ≤ 0.0001.*

In our previous work on LUHMES-derived DA neurons, the mitochondrial stress protocol triggered the concomitant activation of the PERK-, IRE1-, and ATF6-mediated UPR^{ER}, with induction of PERK/CHOP-dependent pro-apoptotic signaling. As a result, the integrated stress response led to the downregulation of general translation *via* EIF2α. We also observed alteration in translation initiation, which is dependent on mTOR signaling downregulation by a number of upregulated amino acid transporters.

In contrast, the UPR^{mt} was not induced and some of its main actors were even downregulated. Consequently, we aimed to investigate the contribution of these pathways to the mitochondrial stress response in the iPSC-derived differentiated cells by studying the expression patterns of their main factors in control and stress condition and in all our iPS cell lines (**Figures 21 and 22**).

We also chose to examine a number of factors involved in oxidative stress response as PARKIN loss-of-function has been linked to disrupted oxidoreductive homeostasis in numerous studies (Dorszewska et al., 2021; Surmeier 2018; Barodia et al., 2017). We first studied the stress response of cell derived from healthy individuals. The PERK-, IRE1- and ATF6-mediated UPR^{ER} were concomitantly activated in the LUHMES DA neurons in response to mitochondrial stress, most robustly the PERK-reliant branch. In the differentiated cells derived from healthy individuals, actors of the PERK-mediated UPR^{ER} (*PERK*, *ATF4*, *ATF3*, *CHOP*, *NRF2*) and associated intrinsic apoptotic signaling (*TRIB3*, *CHAC1*) as well as actors of the ATF6-dependent UPR^{ER} (*HSPA5* and *XBP1*) were significantly upregulated by mitochondrial stress treatment (**Figures 21 and 22**). The IRE1-UPR^{ER}'s specific actors (*IRE1* and *DNAJC3*) or the downstream-activated JNK pathway (*TRAF2*, *JNK*) showed unperturbed expression levels in response to mitochondrial stress.

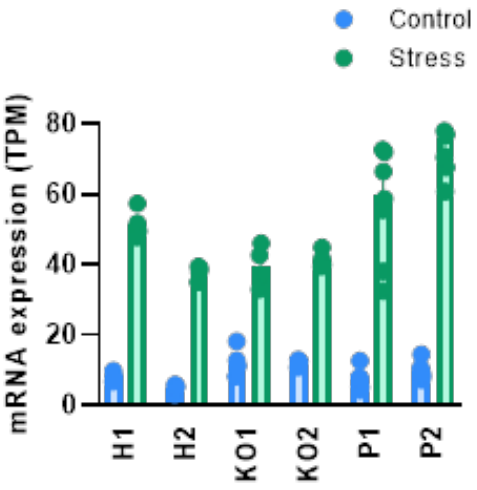

Figure 23. XBP1 spliced isoform mRNA expression (TPM) *in healthy individuals (HI1 and HI2; n=4 for each), PRKN KO isogenic- (KO1 and KO2; n=4 for each) and patient- (P1 and P2; n=8 for each) derived differentiated cells in control (blue) and stress (green) conditions.*

However, it is important to note that the three UPR^{ER} branches, especially the ATF6- and IRE1-reliant pathways, overlap significantly. Two common targets to both branches, *EDEM1* and *HERPUD1* were significantly upregulated by mitochondrial stress. To clearly uncover whether the IRE1-dependent UPR^{ER} was triggered by mitochondrial stress, we looked at the RNA expression level of the spliced isoform of XBP1 (XBP1s), as this splicing event directly results from the activation of the IRE1-UPR^{ER} branch. Our data showed a strong upregulation of the mRNA levels of XBP1s in response to mitochondrial stress in the healthy individual-derived cells, confirming the activation of the IRE1-UPR^{ER} branch (**Figure 23, H1 and H2**).

Regarding the UPR^{mt}, there were no expression changes for its markers upon stress, except for the upregulation of *FOXO3*, suggesting a possible activation for the *SIRT3-FOXO3* branch only (**Figures 21 and 22**).

In parallel, a number of oxidative stress response actors were significantly upregulated in the mitochondrial toxin-treated cells including *JUN* as well as antioxidant genes from the *NRF2*-dependent pathway: *GPX8*, *HMOX1 and SRXN1*. This mechanism is considered to be a protective attempt to relieve the cellular oxidative damage caused by the disrupted mitochondrial electron chain and the subsequent accumulation of Reactive Oxygen Species (ROS).

Translation regulation events also appeared altered in response to mitochondrial stress, in a very similar fashion to what we had observed in the LUHMES-derived DA neurons. Amino acid transporters (*SLC1A5*, *SLC3A2, SLC7A5*), mTOR activators, as well as mTOR inhibitors (*DDIT4*, *SESN2*), were robustly activated by mitochondrial stress, as is often seen as a result of PERK-UPR^{ER} and ISR activation. As all these factors are regulated by ATF4, it could be inferred that these changes in translation may rely on ATF4. It has been well-described that stress induces a shutdown of general translation allowing the cell to focus on the activation of specific pathways directly contributing to managing the occurring cellular stress. This is achieved *via* PERK-mediated phosphorylation of eIF2α (Pakos-Zebrucka *et al.*, 2016; Costa *et al.*, 2020) and via the inhibition of translation initiation complex EIF4E's formation (Yang *et al.*, 2022). The latter mechanism is dependent on mTOR signaling and is modulated by ATF4 (Jang *et al.*, 2021). Mitochondrial toxins treatment on the differentiated cells thus appears to regulate ATF4- and mTOR-dependent translation initiation. Further investigation at the protein level, studying the phosphorylation of the direct mTOR target ribosomal protein S6 will be needed to confirm the modulation of mTOR signaling. *PPP1R15A*, a factor involved in restoring general translation by dephosphorylating eIF2α, was also upregulated as an adaptive response leaning towards cell survival.

In conclusion, our transcriptomic results have shown that the antimycin A and oligomycin combination treatment of the healthy individual-derived differentiated cell pool resulted in a robust activation of all three branches of the UPR^{ER}, with PERK-dependent pro-apoptotic signaling. These observations are strongly reminiscent of the stress response uncovered in LUHMES-derived DA neurons. Furthermore, oxidative stress response signaling appeared triggered by mitochondrial stress, in particular the

NRF2-dependent antioxidant response. Therefore, cytoprotective mechanisms still appear active indicating, thus far, a balance between pro-survival and pro-apoptotic responses within cells.

3.5. Patient-derived and *PRKN* KO isogenic cell lines similarly display activation of the UPR^{ER} and oxidative stress response in basal conditions, compared to healthy individual-derived cells.

Interestingly, we reported differences in the expression levels of several stress response markers in basal conditions in both patient and isogenic-derived differentiated cells in comparison to cells generated from iPSCs of healthy individuals (**Figure 21**). The antioxidant factors *GPX8* and *HMOX1* were upregulated in patient- and isogenic-derived cells relative to healthy individual-derived cells, suggesting that PARKIN deficiency caused oxidative stress even in basal conditions in these cells (**Figure 22**). Under normal physiological conditions, the mitochondrial electron transport chain produces non negligible amounts of ROS through electron leakage that likely accumulates with age as the number of dysfunctional mitochondria also rises (Beal, 2005; Trist, Hare and Double, 2019). In line with our result, it has been shown that deficient PARKIN impairs the mitochondrial quality control mechanisms responsible for mitochondria surveillance and maintaining low levels of ROS, and thus leads to increased ROS accumulation and oxidative stress sensitivity (Barodia, Creed and Goldberg, 2017; Mouton-Liger *et al.*, 2017).

Furthermore, the main actors of the UPR^{ER} were stimulated in the patient and *PRKN* KO isogenic differentiated cells with minor differences between the two populations (**Figure 22**). Most notably, both cell lines exhibit an upregulation of *ATF6*- and *IRE1*-mediated UPR^{ER} markers when compared to the healthy individual-derived cells, including *ERN1*, *XBP1* as well as the heat shock proteins *HSPA5* and *DNAJC3* and the endoplasmic reticulum-associated degradation (ERAD) actor *EDEM1*. The PERK-mediated pathway shows slight changes with increase of *PERK* levels in both patient- and *PRKN* KO isogenic relative to healthy individuals. Links between PARKIN and UPR^{ER} have been described with *PRKN* mutant *Drosophila* exhibiting activation of PERK-UPR^{ER} in basal conditions (Celardo *et al.*, 2016). Interestingly, activation of IRE1-UPR^{ER} appeared neuroprotective against ROS, resulting in *PRKN*-mutant cells being more sensitive to oxidative stress. On the other hand, PERK-UPR^{ER} signaling

was neurotoxic in mutant *Drosophila* as PERK inhibition prevented neuronal loss. Activation of the IRE1-UPR^{ER}, seen even in basal conditions in our *PRKN*-mutant cell lines, may thus be an initial protective response triggered by a heightened oxidative stress state in PARKIN-deficient cells compared to healthy individual-derived cells. Therefore, deficiency in PARKIN appeared to induce increased oxidative stress, sufficient to trigger the UPR^{ER} and oxidative stress response even without mitochondrial toxin treatment. From these observations of the basal stress response levels, we may expect that the patient- and *PRKN* KO isogenic-derived cells could be more sensitive to external stressors.

3.6. Patient-derived and *PRKN* KO isogenic cell lines exhibit similar activation of the UPR^{ER} and oxidative stress response when treated with mitochondrial toxins.

We aimed to investigate whether the mitochondrial stress response was altered in *PRKN*-mutant patient cells and in *PRKN* KO isogenic cells, compared to cultures originating from healthy individuals. To this end, we first assessed changes in the expression patterns of the genes involved in the UPR^{ER}, UPR^{mt} and oxidative stress response after mitochondrial toxin treatment in these cell lines (**Figure 21 and 22**). Although the PARKIN-defective cell lines exhibited similar activation patterns in response to mitochondrial stress to the healthy-derived cells, some discrepancies were still observed.

In both the patient-derived cells and *PRKN* KO isogenic cells, the PERK-mediated (*PERK, ATF4, ATF3, CHOP, CHAC1, TRIB2, NRF2*) and the ATF6-dependent (*HSPA5*, *XBP1*) UPR^{ER} were activated (**Figure 22**). The ATF6- and IRE1-UPR^{ER} common targets *HERPUD1* and *EDEM1* were also upregulated. Moreover, expression of XBP1s was strongly increased by mitochondrial stress in all cell lines (**Figure 23**). Patient cell lines specifically exhibited the upregulation of the IRE1-specific actor *DNAJC3* in stress. Altogether, we reported a concomitant activation of all three branches of the UPR^{ER} in both the differentiated cultures derived from the patients and from the *PRKN* KO isogenic cells in response to mitochondrial stress, in line with what was described for the healthy individual-derived cells.

However, when comparing the stress responses of all three groups to each other, the markers of the UPR^{ER} appear more strongly activated in the patient cells in

stress compared to what was observed in the stressed healthy individual-derived cells. This is also the case in the *PRKN* KO isogenic cells, although more moderately. Indeed, our results show that PERK-downstream pro-apoptotic markers (*CHOP*, *CHAC1*, *TRIB3*) and antioxidant factor *NRF2*, as well as the ATF6- (*ATF6*, *EDEM1*, *XBP1*) and IRE1- (*IRE1*, *DNAJC3*) UPR^{ER} effectors are all upregulated in the patient cells in stress compared to the healthy individual-derived cells in stress (**Figure 22**). This is also the case for the stressed *PRKN* KO isogenic differentiated cells but to a lesser extent, as they display increased expression of *CHOP*, *NRF2*, *XBP1* and *DNAJC3* in comparison to the healthy individual cells exposed to mitochondrial stress. This indicated more exacerbated UPR^{ER} signaling in these cells, which may be due to the fact that they exhibited higher basal level of stress, as observed earlier, caused by PARKIN deficiency and which may lead to a higher sensitivity to stress.

The UPR^{mt}, here as well, was not activated by mitochondrial stress in both patient-derived cells and isogenic cells, except for the upregulation of *ATF5* in the *PRKN* KO isogenic group. The patient and isogenic differentiated cells also displayed strong activation of NRF2-dependent antioxidant actors (*GPX8*, *HMOX1* and *SRXN1*) upon mitochondrial stress and to a significantly higher extent than in the stressed healthy individual-derived cells. This is consistent with our hypothesis that the patient-derived and isogenic cell line present an increased sensitivity to stress and thus, an exacerbated stress response once treated with mitochondrial toxins.

In a similar manner, mTOR signaling appeared altered by mitochondrial stress in both patients and *PRKN* KO isogenic cells with upregulation of mTOR inhibitors (*DDIT4*, *SESN2*) and amino acid transporters (*SLC1A5*, *SLC3A2*, *SLC7A5*). This signaling pathway also appeared further stimulated in the PARKIN-deficient cells treated with mitochondrial stress than in the healthy individual cells with the same treatment.

To conclude, cells originating from the patients and *PRKN* KO isogenic-derived differentiated cells displayed similar activation of the three UPR^{ER} branches, with induced pro-apoptotic signaling, oxidative stress response and regulation of mTOR signaling. Most strikingly, PARKIN deficiency induced more exacerbated cellular stress responses to the mitochondrial toxins, compared to the cells derived from healthy individuals. This suggested increased sensitivity to stress and cytotoxicity susceptibility for cells lacking functional PARKIN.

3.7. Defective PARKIN activates one carbon metabolism processes in response to mitochondrial stress.

We compared the list of genes whose expression was upregulated in all three groups (healthy, patient and *PRKN* KO isogenic cell lines) by mitochondrial stress to examine specific responses (**Figure 24**). In this analysis, we set a more stringent threshold than earlier (**Figure 21 and 22**) whereby for a gene to have increased mRNA expression, the log 2 (Fold Change) had to be equal or higher than 1. This was in line with our previous data showing more enhanced activation of the stress response in PARKIN-deficient cells compared to healthy individual-derived cells.

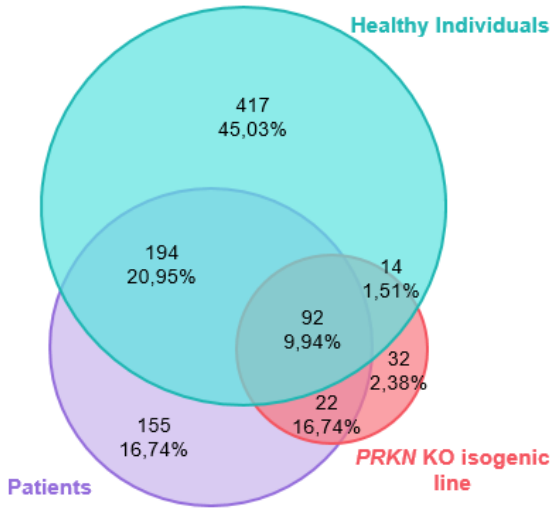

Figure 24. Venn diagram representing all the genes upregulated in response to mitochondrial stress in the healthy (blue) individual-, PRKN mutant patient- (purple) and PRKN KO isogenic (red) - derived differentiated cells. *Within each group the number and the percentage of genes belonging to this category is given. Expression is considered upregulated when log2 FC > 1.*

Interestingly, the expression of 417 genes was further upregulated only in the healthy individual-derived cells, compared to 155 for patient-derived cells and 32 for the KO isogenic cells, suggesting that the *PRKN*-deficient lines may present important differences in their stress responses compared to the healthy controls. Gene ontology analysis on these genes revealed enrichment in genes linked to metal ion transport across plasma membrane (**Figure 25**).

On the other hand, the genes whose expression showed enhanced upregulation in patients-derived cells were strongly linked to inflammatory response pathways, suggesting exacerbated involvement of immune processes in the stress response of the patient-derived cells (**Figure 25**). Gene ontology analysis on the genes specifically upregulated in the *PRKN* KO isogenic line yielded no significant enrichment. However, 22 genes showed enhanced upregulation in both the patient- and *PRKN* KO isogenic

line-derived differentiated cells in comparison to the healthy individual-cells, implying that *PRKN*-deficiency coul trigger a specific stress response. Amongst those genes, we found factors involved in one carbon metabolism (*MTHFD2, SHMT2*), oxidative stress response (*SESN2*, *UCP1*) and amino acid transport (*SLC7A5*, *SLC6A9*).

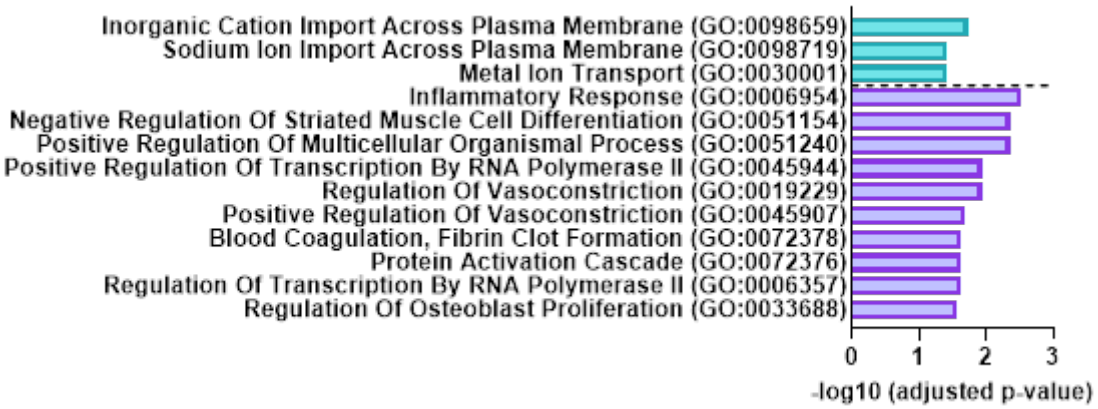

Figure 25. Gene Ontology analysis (Biological Process 2023) on all genes upregulated *(log2 (fold change) ≥1)* ***following mitochondrial stress*** *specific to the healthy individual- (blue, 417 genes), patient- (purple, 155 genes) derived cells.*

Our results are coherent with the PARKIN-deficient cells exhibiting increased oxidative stress sensitivity as was suggested by our previous results. Such enhanced sensitivity has been described in *PRKN* and *LRRK2* mutant iPSC-derived neurons (Nguyen *et al.*, 2011; Chung *et al.*, 2016) and in *PINK1*-mutant mice (Gautier, Kitada and Shen, 2008). It is interesting to note that *SESN2* and the amino acid transporter *SLC7A5,* which are also involved in translation initiation regulation *via* mTOR-modulation as previously described, were both detected as upregulated in healthy individual-derived cells upon mitochondrial stress in our previous analysis where the variation threshold was set at log2 (fold change) higher or equal to 0.5. In the current analysis, with a stricter threshold set at log2(fold change) higher or equal to 1, *SESN2* and *SLC7A5* are exclusively upregulated in *PRKN*-deficient cells. This is in agreement with these cells displaying an exacerbated stress response.

One carbon metabolism has been shown as disrupted by mitochondrial dysfunction in an ATF4-dependent manner (Bao *et al.*, 2016; Quirós *et al.*, 2017), and in PD post-mortem samples (Kalecký, Ashcraft and Bottiglieri, 2022). It has been suggested that upregulation of mitochondrial one-carbon cycle metabolism genes in *PRKN* and *PINK1* mutant *Drosophila*, was driven by ATF4 and acted as potential

compensatory mechanisms to the mitochondria dysfunction caused by defects in the PINK1/PARKIN mitochondrial quality control pathway (Celardo *et al.*, 2016). Blocking the upregulation of *SHMT2* strikingly caused the deterioration of the PD-associated phenotype in the mutant Drosophila. Furthermore, *SESN2* and the amino acid transporters are also ATF4 targets. This suggests that the stress response specific to cells with PARKIN loss-of-function may be dependent on ATF4, a main actor of the PERK-UPR^{ER} that is also activated by mitochondrial stress in healthy individual-derived cells. However, these ATF4-targets appear overstimulated in the PARKIN-deficient cells, likely due to the heightened level of stress and the exacerbated response in these cells.

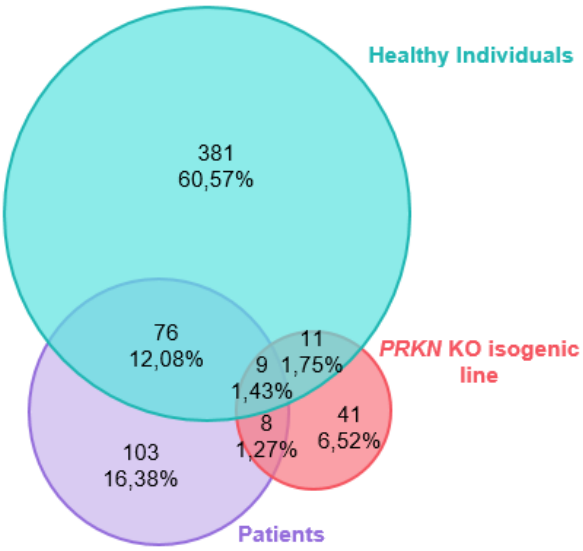

Figure 26. Venn diagram representing all the genes whose expression was downregulated in response to mitochondrial stress in the healthy (blue) individual-, PRKN mutant patient- (purple) and PRKN KO isogenic (red) -derived differentiated cells. *Within each group the number and the percentage of genes belonging to this category is given. Expression is considered downregulated when log2 FC < -1.*

Comparing all downregulated genes in response to mitochondrial stress in differentiated neurons from all cell lines also revealed patterns specific to each (**Figure 26**). Here, we also used a more stringent threshold with the fold change having to be inferior to -2 for a gene to be considered as downregulated. We observed 381 genes that showed enhanced downregulation in the healthy individual-derived cells. Gene ontology analysis linked those genes to regulation of DNA replication, repair and metabolic processes (**Figure 27**). These pathways appear exclusively downregulated in the healthy individual-cells and not in the *PRKN*-mutants, suggesting an alteration of DNA repair mechanisms caused by PARKIN loss-of-function. This could indicate a disrupted cellular stress response and add to the exacerbated state of stress and DNA

damage in PARKIN-deficient cells. As previously mentioned, several studies suggest increased DNA damage and defective DNA repair in PD, especially in the context of *LRRK2* mutations (Wang *et al.*, 2023). Interestingly, PARKIN has been implicated in the regulation of DNA repair not only in the mitochondria (Rothfuss *et al.*, 2009), but also in the nucleus as it can translocate there in the advent of oxidative stress (Kao, 2009; Qin, Geng and Xue, 2022). It appears to play a protective role in maintaining genome integrity. Loss of PARKIN function may therefore induce dysfunctional DNA repair mechanisms. Moreover, 103 genes were specifically downregulated in the patient-derived cells and were associated to the cytokine production regulation involved in immune response processes (**Figure 27**). This is in line with our previous findings, suggesting a disrupted immune response in the patient-derived differentiated cell pool. Only 8 genes were downregulated in both the patient- and *PRKN* KO isogenic line-derived differentiated cells.

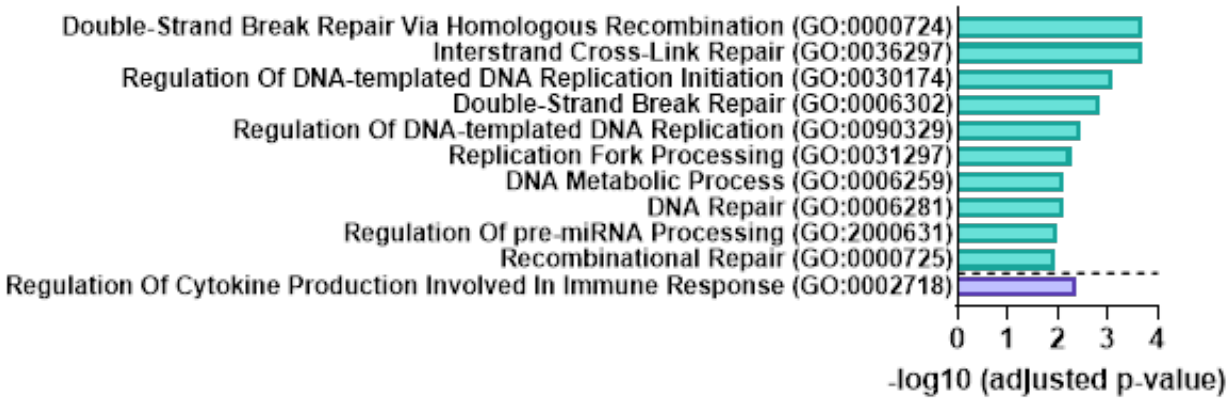

Figure 27. Gene Ontology Biological Process analysis on all genes downregulated *(log2 (fold change) ≤-1)* ***following mitochondrial stress*** *specific to the healthy individual- (blue; 381 genes) or patient- (purple; 103 genes) derived cells.*

3.8. Mitochondrial stress modulates expression of lncRNAs potentially involved in transcription regulation and neuronal system processes.

As part of analyzing the differentiated cells' mitochondrial stress response, we investigated lncRNAs as they are known to be powerful genomic regulators that constitute highly cell- and species-specific signatures. Furthermore, in the previous investigation on LUHMES-derived DA neurons, lncRNAs seemed implicated in distinct stages of the cellular response, notably the regulation of translation initiation (Chapter 1).

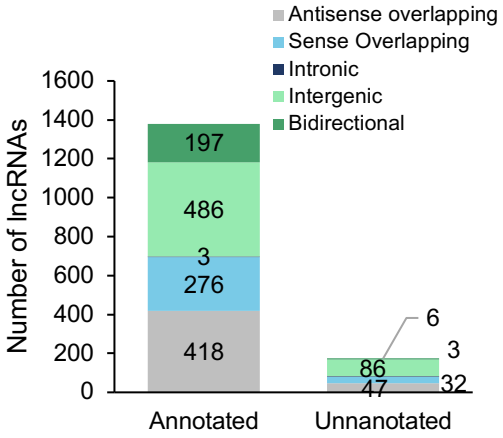

Figure 28. Number of lncRNAs depending on their location-based category in the overall repertoire detected in all our differentiated cell pools. *LncRNAs are divided based on whether they had already been annotated or if they were newly discovered in our study (unannotated). They were also organized based on their location to the nearest protein-coding gene and so if they are bidirectional, intergenic, intronic, sense overlapping or antisense overlaping.*

Through the collected transcriptomic data, we were able to uncover 1554 lncRNAs expressed in the iPSC-derived DA cells when grouping all cell lines. (iPSC from healthy individuals, patients or *PRKN* KO isogenic iPSC). Interestingly, 174 or 11.2% of these lncRNAs had never been sequenced or annotated in existing databases (**Figure 28**). We classified all the lncRNAs according to their position relative to their nearest protein-coding genes and discovered that 13.1% lncRNAs were bidirectional, 36.8% intergenic, 0.4% intronic, 19.8% sense overlapping and 29.9% were antisense overlapping.

Amongst the 1497 lncRNAs identified in basal conditions and the 1504 lncRNAs detected in the mitochondrial stress condition, there also were lncRNAs that were specifically expressed in the healthy individual-, patient- or *PRKN* KO isogenic cells (**Table 5**). For example, among the lncRNAs expressed in basal conditions, 17 lncRNAs were found to be specifically expressed in healthy individual-derived DA cells, 36 were specific to the patient group and 44 to the *PRKN* KO isogenic cell line. This suggests a possible contribution of these lncRNAs to signaling pathways distinctive of each of these cell lines and reinforces the notion of lncRNAs as highly specific molecular signatures.

	Common to all 3 groups	HI Specific	P Specific	KO Specific	HI and P specific	P and KO specific	HI and KO specific
Control	1257	17	36	44	107	15	20
Stress	1236	24	28	30	129	20	37

Table 5. Distribution of lncRNAs in the control and stress condition in the healthy, patient and PRKN KO isogenic differentiated cell pool. *The expression patterns of the lncRNAs are detailed: they can be specific to the healthy individual-derived cells (HI specific), to the patient-derived cells (P specific) or to the PRKN KO isogenic cells (KO specific). LncRNAs may also be present in two groups: HI and P specific, P and KO specific or HI and KO specific.*

Investigating lncRNAs remains challenging, however, as previously explained, a first insight into their function may be obtained by studying their neighboring genes as they constitute highly likely regulatory targets.

Gene ontology analysis on the protein-coding genes adjacent to the lncRNAs identified in healthy-, patient- and *PRKN* KO isogenic-derived cells revealed strong enrichment in transcription regulation-related terms in all three analyses, reflecting the contribution of lncRNAs as genomic regulators (**Figure 29**).

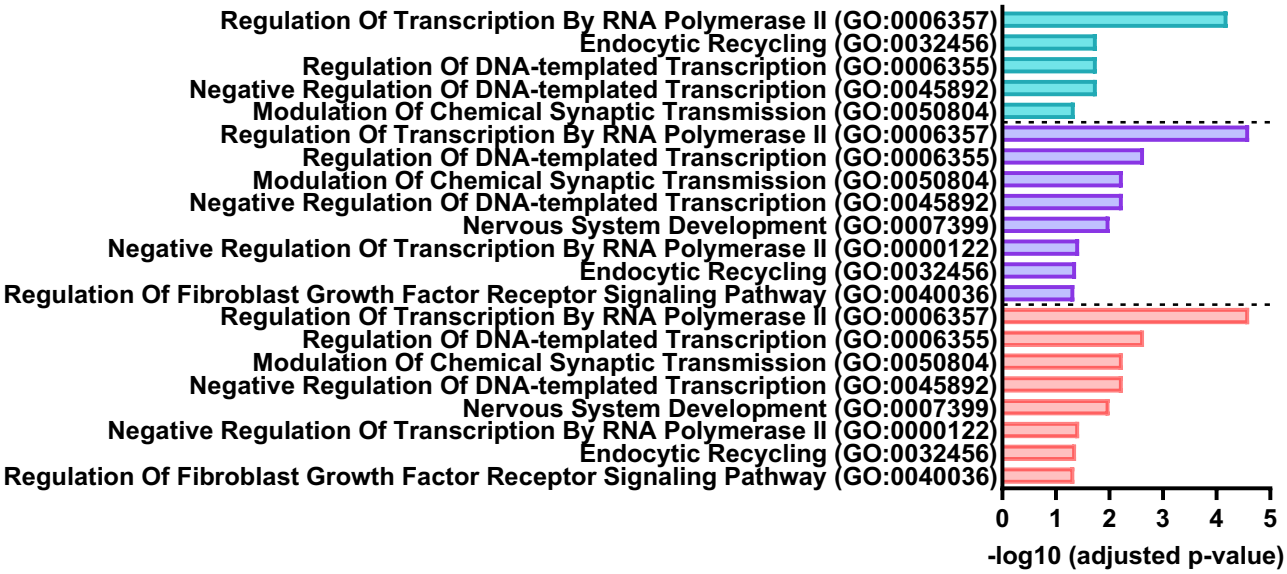

Figure 29. Gene Ontology Biological Process 2023 on adjacent protein-coding genes to all the lncRNAs expressed in differentiated cells *from healthy individual cell lines (blue; 1337 genes), patient cell lines (purple; 1718 genes) and PRKN KO isogenic cell lines (red; 1718 genes).*

Furthermore, the analyses on the patient- and *PRKN* KO isogenic-derived differentiated cells showed an enrichment in lncRNAs neighboring and thus potentially regulating genes involved in nervous system development. These genes are mostly

related to early stages of nervous system development such as axonal guidance factors (*ROBO1*, *SEMA5A*, *SEMA6B*), neural fate specification factors (*SOX11*, *SOX4*, *POU3F3*), or synapse formation factors (*DBNL*).

As described earlier, PARKIN-deficient cell lines exhibited altered cell population identity, with a potential delay in differentiation. Therefore, PARKIN could modulate the expression of a network of lncRNAs that may be contributing to the alteration of differentiation processes as described in the patient- and *PRKN* KO isogenic-derived differentiated cells.

Subsequently, we investigated lncRNAs that displayed altered expression in response to mitochondrial stress to explore their potential contribution the cellular stress response. Pathway analysis on the 111 and 213 lncRNAs downregulated by mitochondrial stress in the healthy and patient cell lines respectively, revealed that their adjacent protein-coding genes were involved in transcription regulation signaling (**Figure 30**). This suggested an attenuation of transcriptional programs, to which these lncRNAs may participate, perhaps to focus on specific signaling pathways involved in managing the response to mitochondrial stress. This analysis on the *PRKN* KO isogenic cells did not show any strong enrichment in particular pathways.

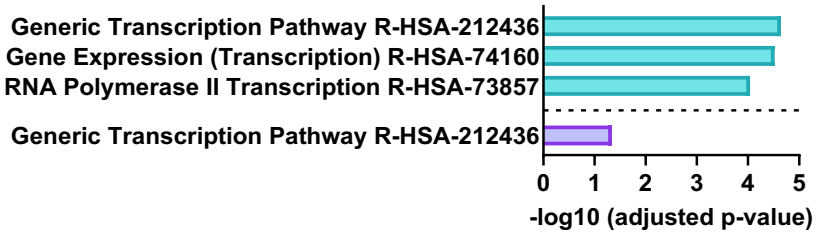

Figure 30. Pathway analysis (Reactome 2022) on all protein-coding genes neighboring lncRNAs that are downregulated following mitochondrial stress treatment *in healthy individual-derived (blue; 242 genes) or patient-derived (purple; 261 genes) differentiated cells.*

Interestingly, the same analysis on lncRNAs with increased expression following mitochondrial toxin treatment only yielded significant results for the 234 stress-upregulated lncRNAs in the patient-derived cells. These lncRNAs appeared to neighbor genes involved in neuronal system processes, reminiscent of the altered neuronal identity previously uncovered in the PARKIN-deficient cell lines (**Figure 31**). In particular, these adjacent protein-coding genes are linked to cholinergic (BCHE, CHRFAM7A), GABAergic (GABRB3) and glutamatergic (GRIN2D, CACNG2) neurotransmission as well as chemical transmission across synapses (SYT7, KCNG1,

KCNH2, KCNH1, DLGAP1). Such lncRNAs may thus be involved in regulating neuronal identity as part of the stress response.

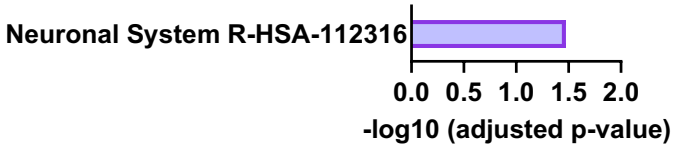

Figure 31. Pathway analysis (Reactome 2022) on all protein-coding genes neighboring lncRNAs that are upregulated following mitochondrial stress treatment *in patient-derived (purple; 286 genes) differentiated cells.*

3.9. LncRNAs upregulated by mitochondrial stress in the LUHMES-derived DA neurons and in patient-derived cells may contribute to mTOR signaling.

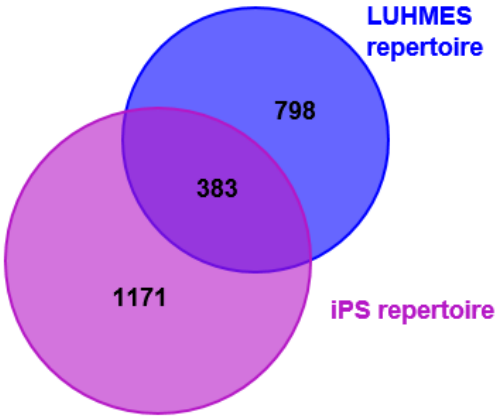

Figure 32. Overlap of lncRNAs that were detected in the LUHMES *(blue; 1181 lncRNAs)* ***and iPS repertoires*** *(purple; 1554 lncRNAs).*

We wanted to examine whether some lncRNAs that we had previously found in our study on LUHMES-derived DA neurons were also detected in the iPSC-derived differentiated ventral midbrain cells. Out of the 1554 lncRNAs of the iPSC-derived cell repertoire, 383 had also been identified in the LUHMES repertoire (**Figure 32**). Therefore, there is a relatively high lncRNA specificity to the model, which is likely due to the fact that the differentiated iPS cell population is quite heterogeneous and does not contain a majority of DA neurons. It could also be explained by differences in the maturity levels of the resulting cell pool and the fact that the LUHMES cells constitute an immortalized cell line, as lncRNAs can be expressed at distinct stages of development.

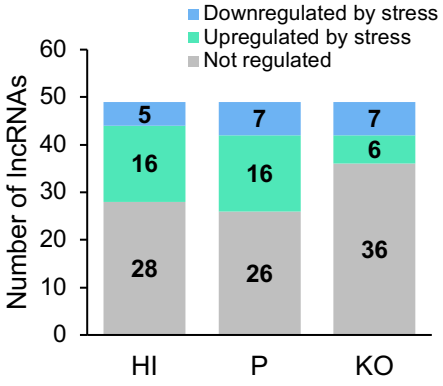

Figure 33. Histogram displaying the lncRNAs upregulated in LUHMES-derived DA neurons by mitochondrial stress that were also detected in the iPSC-differentiated cells. *The number of lncRNAS identified in each group (HI: healthy individuals; P: patients, KO: PRKN KO isogenic lines) is shown.*

We subsequently investigated the expression patterns of lncRNAs previously found to be upregulated by mitochondrial stress in LUHMES-derived DA neurons, in the healthy individual-, patient- and *PRKN* KO isogenic iPSC-derived cells (**Figure 33**). Sixteen of these lncRNAs were also upregulated by mitochondrial stress response in healthy individual and patient differentiated cells, and six in *PRKN* KO isogenic cells. Amongst those, 5 were specifically upregulated by stress in healthy individual-originating cells and another 5 were specifically upregulated in the patient cell line (**Figure 34; left**). The majority of the other lncRNAs were not regulated, with a few being downregulated by mitochondrial stress. Pathway enrichment analysis on the lncRNAs upregulated by mitochondrial stress in both the patient-derived cells and in LUHMES-derived DA neurons, revealed an enrichment in lncRNAs adjacent to genes associated to mTOR signaling (**Figure 34, right**). Among the adjacent genes, the inhibitor of translation initiation *EIF4EBP1* was found, although the lncRNA it is adjacent to is also upregulated in healthy individual-derived cells.

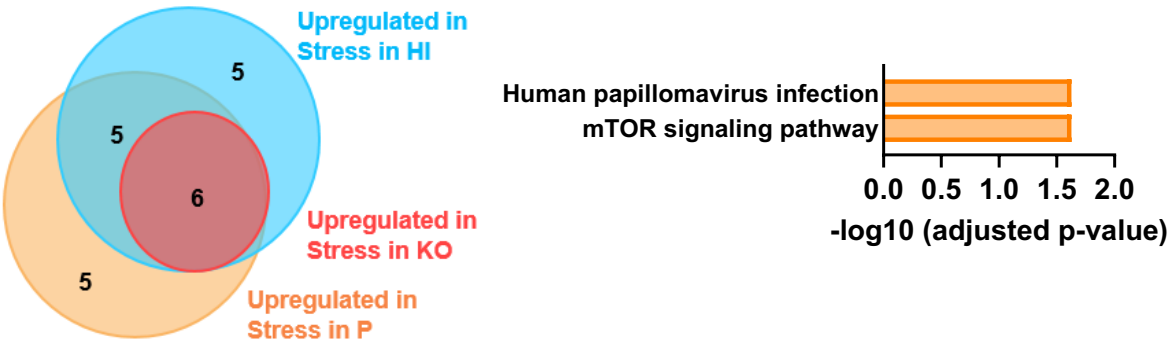

Figure 34. Venn diagram of lncRNAs upregulated by mitochondrial stress response *in LUHMES-originating DA neurons and in healthy individual- (HI), patient (P) and PRKN KO isogenic (KO) derived cells.* ***(left). Pathway analysis (KEGG 2021) on adjacent genes to the lncRNAs upregulated by stress in*** *LUHMES-derived DA neurons and in differentiated cells originating from patients* ***(right).***

Overall, there may be several lncRNAs contributing to mTOR signaling and translation initiation regulation, which would be interesting to study further, given the important role of these pathways in the cellular stress response.

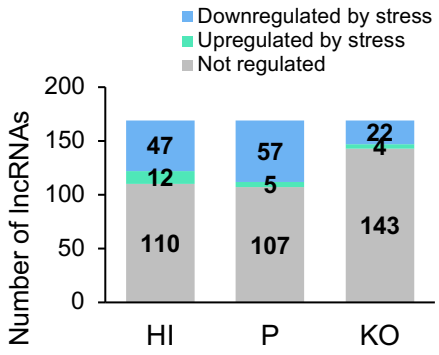

Figure 35. Histogram displaying the lncRNAs downregulated in LUHMES-derived DA neurons by mitochondrial stress that were also detected in the iPSC-differentiated cells. *The number of lncRNAS identified in each group (HI: healthy individuals; P: patients, KO: PRKN KO isogenic lines) is shown.*

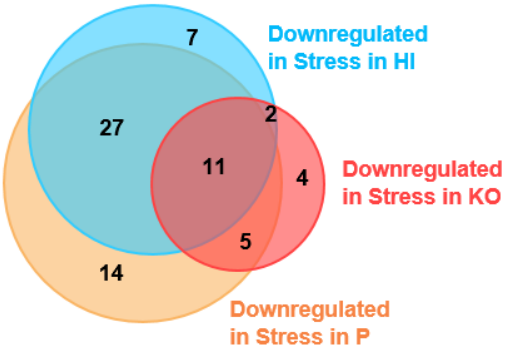

Figure 36. Venn Diagram of lncRNAs downregulated by mitochondrial stress response *in LUHMES-originating DA neurons and in healthy individual- (HI), patient (P) and PRKN KO isogenic (KO) derived cells.*

We also inspected in the iPSC-derived cells, the expression patterns of lncRNAs that were previously found to be downregulated in LUHMES-derived DA neurons (**Figure 35**). A large number of these lncRNAs were downregulated in healthy individual- (47 lncRNAs), patient- (57 lncRNAs) and *PRKN* KO isogenic- (22 lncRNAs) derived cells. Amongst these downregulated lncRNAs in LUHMES DA neurons, 7 were specifically downregulated in healthy individual differentiated cells, 14 in the patient cells and 4 in the *PRKN* KO isogenic line (**Figure 36**). No significant enrichment was found in the adjacent genes of any of these groups of lncRNAs. However, we found that amongst the genes neighboring the lncRNAs only downregulated in the patient and isogenic KO cell lines, a couple were involved in neuronal migration and development (*MEF2C*, *FGFR1*), possibly implicating the related lncRNAs to the neuronal development disruption observed in the PARKIN-deficient cells.

3.10. Expression of candidate lncRNAs potentially implicated in the regulation of the translation initiation and in neuron generation are altered by mitochondrial stress in the IPS-derived cells.

A number of lncRNAs of interest were selected during our study on LUHMES-derived DA neurons treated with the same mitochondrial toxin treatment. These candidates fell within 3 groups: they were either upregulated by mitochondrial stress and associated to translation initiation regulation, downregulated and linked to neuron generation regulation, or associated to PD-linked SNPs. We investigated whether these lncRNAs were also present in the iPSC-derived DA cells. Nine out of 15 candidates were successfully detected and their expression levels in all conditions were evaluated (**Figure 37**).

Within the lncRNAs upregulated by stress in LUHMES cells, *SNHG1* showed equally raised expression following mitochondrial toxin treatment in healthy, patient and *PRKN* KO isogenic differentiated cells. *SNHG1* is a lncRNA of particular interest in the context of PD as it has been described as upregulated in many PD models (Cao *et al.*, 2018; H. Wang *et al.*, 2021) and to promote neuronal injury caused by mitochondrial toxins such as MPP+ (Zhao *et al.*, 2020). Knockdown of *SNHG1* was also shown to be neuroprotective (Xiao *et al.*, 2021; Shen *et al.*, 2023). Therefore, it may be a prime candidate to further characterize in this model.

The lncRNA *VLDLR*-AS1 was interestingly only significantly upregulated by stress in the patient cell line. Not much is known about the function of *VLDLR-AS1*, however, it neighbors the lipoprotein receptor *VLDLR* important for cholesterol metabolism, a disrupted pathway in many neurodegenerative diseases including PD (Jin, Park and Park, 2019).

One lncRNA, *FBXL19-AS1*, containing a PD-associated SNP in its sequence from our list of candidates was detected in the iPSC-derived DA neurons Strikingly, its expression is significantly downregulated by mitochondrial stress only in the patient-derived cell lines, suggesting it could be involved in PARKIN-dependent mechanisms.

Amongst the lncRNAs downregulated by stress in LUHMES-derived DA neurons and associated to neuron generation regulation, two showed similar expression patterns. *NIPBL-DT* and *ZNF778-DT* both shown significantly decreased expression levels following mitochondrial stress in the healthy and patient cell line, as well as the *PRKN* KO isogenic cell line for the later. It would therefore be interesting to

further investigate the function of these candidates and their potential contribution to the cells' stress response.

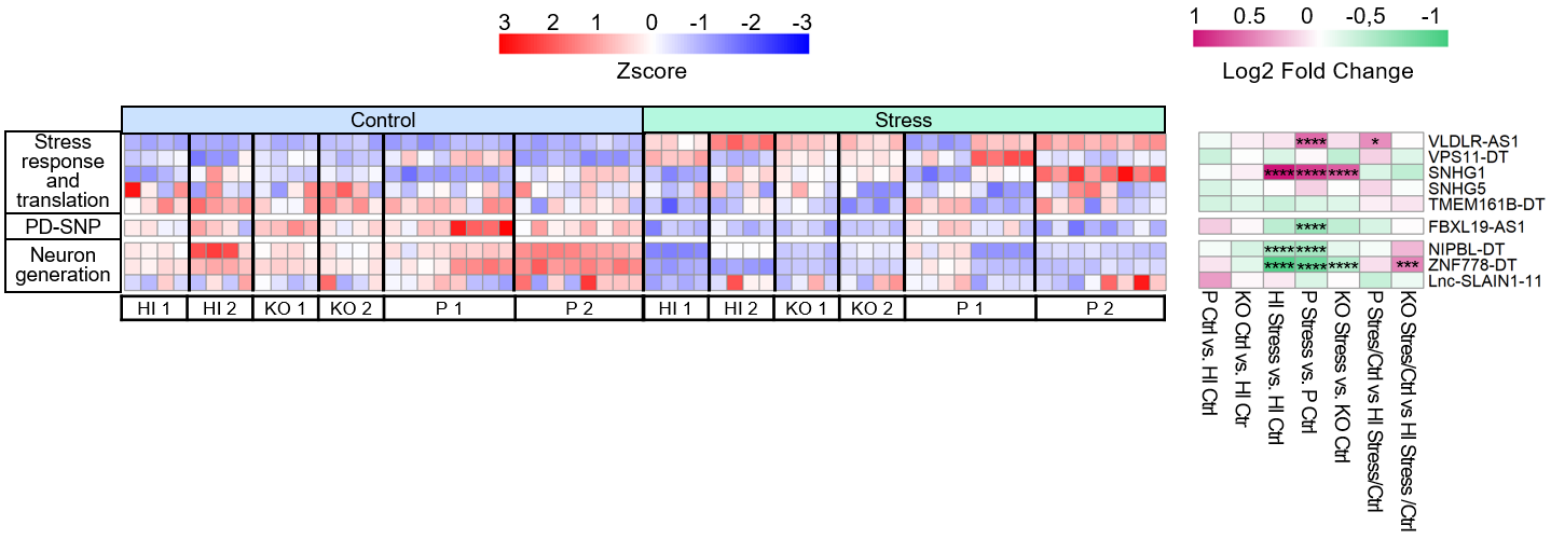

Figure 37. Heatmap of the expression level of candidate lncRNAs in healthy individuals-, patient- and KO isogenic-derived differentiated cells. *Left heatmap displays the variation of markers' expression levels (TPM) represented as a Z-score in healthy individual (HI1 and HI2), PRKN KO isogenic (KO1 and KO2) and patient (P1 and P2) iPSC-derived differentiated cells in Control and Stress conditions (as indicated on top of the heatmap). Right heatmap represents log2 fold change of mRNA for 5 different comparisons: patient-derived differentiated cells compared to healthy individual-originating cells (P Ctrl vs. HI Ctrl), PRKN KO isogenic cells compared to healthy cells (KO Ctrl vs. HI Ctrl), PRKN KO isogenic cells compared to patient-derived cells (KO vs. P Ctrl), cells treated with mitochondrial toxins compared to control cells in healthy individual-derived cells (HI Stress vs. Ctrl), in patient-derived cells (P Stress vs. Ctrl) and in PRKN KO isogenic cells (KO Stress vs. Ctrl) and difference between Stress/Control ratio in patient cells compared to healthy cells (P Stress/Ctrl vs. HI Stress/Ctrl) and in PRKN KO isogenic cells compared to healthy cells (KO Stress/Ctrl vs. HI Stress/Ctrl) . The lncRNAs name are indicated on the right and the pathways they were associated to are indicated on the left. Significant change in expression threshold set at log2(fold change) ≥ 0,5 or ≤-0,5. * adjusted p-value ≤ 0.05; ** adjuster p-value ≤ 0.01; *** adjusted p-value ≤ 0.001; **** adjusted p-value ≤ 0.0001.*

Regarding the candidate that we had selected in our LUHMES-derived DA neuron study, lnc-*SLC6A15*-5, it did not appear in the lncRNA repertoire of the iPSC-derived cells. Looking at the transcript reconstruction data, transcripts corresponding to the annotated isoform ENSG00000289309 of lnc-*SLC6A15*-5 were detected (**Figure 38**). However, they were eliminated from our final lncRNA repertoire in this study due to not surpassing the expression threshold set as part of the lncRNA discovery pipeline. The lower expression levels of the lncRNA in the iPSC-differentiated cells may be due to the heterogeneous cell population and difference in population maturity. It would be interesting to see if the lncRNA is expressed more robustly in differentiated DA neurons amongst the cell pool, by fluorescence in situ hybridization for example.

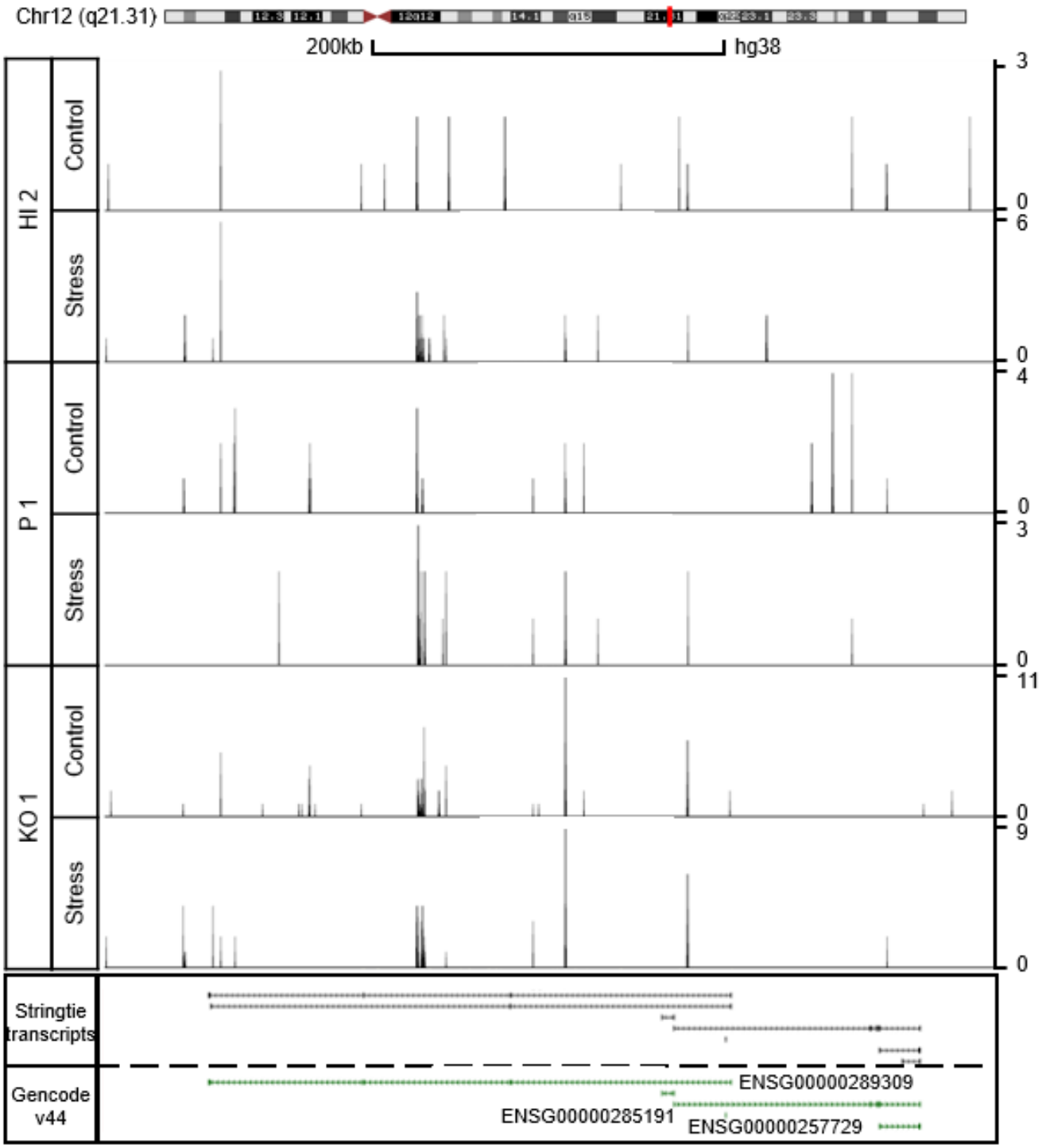

Figure 38. Schematics of the locus of lnc-SLC6A15-6/ENSG00000289309 on chromosome 12. *RNA-seq peaks are depicted in control and stress conditions for the cells derived from healthy individual 2 (HI 2), patient 1 (P 1) and PRKN KO isogenic line 1 (KO 1). Scales represent reads per million (RPM).*

4. Conclusion

Our transcriptomic data suggests alterations in the differentiation status of the iPSC-derived cell lines. The patient-derived and *PRKN* KO isogenic line exhibited a potential delay in maturity and shift in specification with an enhanced glial population in comparison to the healthy group. In basal conditions, the PARKIN-deficient cells displayed increased levels of stress response effectors involved in ATF6- and IRE1-UPR^{ER}, as well as in the NRF2-dependent oxidative stress response. This indicates that these cells are already facing stressful conditions at this stage and these signaling responses may be protective as suggested by previous studies. Mitochondrial toxin treatment expectedly exacerbated these pathways and resulted in more robust activation of the oxidative stress response than in the healthy cells as well as stronger activation of the three branches of the UPR^{ER}. Indeed, in mitochondrial stress condition, the PERK-mediated UPR^{ER} and downstream pro-apoptotic signaling become activated. A potential dysregulation of DNA repair mechanisms was also observed in PARKIN-deficient cells, which may participate to the state of exacerbated stress reported in these cells. Altogether, our data showed that the patient-derived and *PRKN* KO cell cultures appeared more sensitive to mitochondrial dysfunction and oxidative damage due to dysfunctional PARKIN, and displayed potential alterations in differentiation status.

We were also able to compile the lncRNAs repertoires of our cells, revealing a number of never previously sequenced transcripts, which could be specific to mesencephalic cell populations. Some specificity between healthy individual, patients and *PRKN* KO isogenic line was similarly observed, highlighting the specificity of lncRNAs as molecular signatures. Pathway enrichment analysis revealed that a group of upregulated lncRNAs in the patient-derived cells may be involved in neuronal system signaling pathways, which means they could be contributing to the shift in neuronal identity described earlier.

Furthermore, comparison with the LUHMES-DA neuron lncRNA repertoires showed an overlap of a number of lncRNAs in both models, although there also appeared to be a strong lncRNA specificity to the model. This could be explained by the heterogeneity of the cellular population in the iPSC-differentiated cells in comparison to the pure DA population of LUHMES differentiated cells. However, several lncRNAs commonly altered in both models, and thus possibly regulated by

PARKIN, were potentially linked to mTOR signaling and nervous system development. They could be of interest for further investigation.

We also efficiently detected 9 lncRNAs candidates of interest that had been selected in our LUHMES-derived DA neurons exposed to the same mitochondrial stress protocol. Six of these lncRNAs display altered expression patterns in the different cell lines and conditions, making them prime candidates for further functional analysis.

The main candidate of our LUHMES-based study, *lnc-SLC6A15-5*, although not present in the final iPSC-derived differentiated cells lncRNA repertoire, was still detected at very low levels. This could indicate that the conditions here are not optimal for its detection. A perspective would be to attempt detection of this lncRNA in DA neurons present in the cellular population by using techniques such as fluorescence *in situ* hybridization.

V. Discussion

The work in this thesis was centered around investigating the molecular and cellular response to mitochondrial stress of human DA neurons and the contribution of long non-coding RNAs. We present here two complementary studies. The first aimed at studying the mitochondrial stress response in a pure pool of DA neurons and identify elements specific to DA neurons that may underlie their specific vulnerability to mitochondrial stress. For this, we harnessed the LUHMES immortalized mesencephalic precursor cells and were able to generate >80% DA neurons in the total differentiated population, allowing for the direct access to DA specific elements (Lotharius and Brundin, 2002; Lotharius, 2005). The second study aimed to investigate PD-associated alterations of DA neuron's mitochondrial stress response. In this project, we had access to iPS cells originating from *PRKN*-mutant patients and corresponding age matched healthy controls, that we were able to differentiate using a protocol directed towards ventral midbrain fate. Despite the heterogeneity of the resulting population, which nevertheless resembled the global population present in the ventral midbrain, this model was arguably more physiologically relevant and allowed to integrate the Parkinson's Disease component to our analysis.

A central component to this project has been the mitochondrial stress paradigm. As part of our team's ongoing investigation into PARKIN and PINK1-mutant forms of Parkinson's Disease, we have selected a mixture of toxins – the mitochondrial respiratory chain complex III inhibitor antimycin A and the ATP synthase inhibitor oligomycin - that reliably induces PINK1/Parkin-dependent mitophagy (Lazarou *et al.*, 2015; Zachari *et al.*, 2019; Schwartzentruber *et al.*, 2020). The combination of these toxins is known to depolarize the mitochondrial membrane, increases levels of reactive oxygen species and reduces intracellular ATP production (Quirós et al., 2017; Yang et al., 2021; Żuberek et al., 2022). Our stress protocol lasts 8 hours, although we have chosen to explore some cellular mechanisms at earlier timepoints.

In the initial LUHMES-based study, we were able to conduct a comprehensive work based on RNA-seq and ATAC-seq data, which gave an unbiased start point to the investigation. The transcriptome analysis also strongly indicated a central role for the UPR^{ER} to the cellular stress response, with the concomitant activation of all three branches mediated by PERK, ATF6 and IRE1. Interestingly, the PERK-ATF4 axis appeared to be the predominant signaling pathway stimulated by our 8-hour mitochondrial stress protocol, tipping the cellular response towards a pro-apoptotic fate. The PERK-dependent branch triggers the attenuation of translation

phosphorylation of eIF2α by PERK (Pakos-Zebrucka *et al.*, 2016; Hetz, Zhang and Kaufman, 2020). Through this pathway, stress-activated PERK induces the shutdown of general translation, only maintaining translation of selective factors involved in the stress response. Our results are in agreement with previous studies in mammals that showed activation of the ISR under various mitochondrial stress conditions (Michel *et al.*, 2015; Münch and Harper, 2016; Mick *et al.*, 2020; Bilen *et al.*, 2022). In line with this, we showed that mitochondrial damage enhanced eIF2α phosphorylation and efficiently blocked general translation in the LUHMES-derived DA neurons.

Our transcriptomic data additionally showed a downregulation of processes involved in nervous system development. This was complemented by immunofluorescence experiments indicating a decrease in cells expressing the mature DA marker DAT (Article 1, Figure 2). Altogether, this data highlights a potentially altered maturity of the DA neurons subjected to mitochondrial stress. Mitochondrial damage has been shown to hinder differentiation processes but also, differentiated cells have been shown to potentially reenter the cell cycle upon stress or injury, causing a "dedifferentiation"-like process (Ozgen *et al.*, 2021; Li *et al.*, 2023). Interestingly, regulated neuronal death signaling cascades that are highly active during neuronal development - so as to easily discard the surplus of neurons and ensure correct developmental processes - become tightly restricted in mature neurons (Kole, Annis and Deshmukh, 2013; Yamaguchi and Miura, 2015; Hollville, Romero and Deshmukh, 2019). It has therefore been suggested that upon stress and in neurodegeneration contexts, the return to immature neuronal state may be an integrative part of progressive neuronal death (Kole, Annis and Deshmukh, 2013). This process has become increasingly described in the context of Alzheimer's Disease (Caldwell *et al.*, 2020; García-Osta *et al.*, 2022). We could therefore expect that the LUHMES-derived DA neurons are transitioning to this immature neuronal stress as a step of the apoptotic process triggered by persistent unsolvable mitochondrial stress.

The mitochondrial stress protocol appeared to activate PERK-UPR^{ER} at around 2 hours of treatment. Robust activation of effectors of the IRE1- and ATF6-UPR^{ER} occured 4 hours into treatment, with some downstream chaperones upregulated at 6 hours. Although the activation chronology of the three UPR^{ER} branches has been examined in a number of study, contradictory results have been obtained. Some describe IRE1 and ATF6 as the initial rapid stress response, followed by PERK induction in chronic stress circumstances (Rutkowski *et al.*, 2006; Wang and Kaufman,

2016). Others have suggested PERK-UPR^{ER} as the immediate stress response and ATF6-UPR^{ER} as a chronic stress response (Wu *et al.*, 2007; Hetz, Zhang and Kaufman, 2020). Interestingly, studies investigating the interplay between the PERK-, IRE1- and ATF6-UPR^{ER} leading to the modulation of apoptosis, revealed that it may be reliant on the relative dynamics of the UPR^{ER} branches rather than a distinct switch between them (Walter *et al.*, 2015; Chang *et al.*, 2018). It is also important to take into account that the three UPR^{ER} branches do not constitute distinct entities and that there is significant crosstalk between them (Tsuru *et al.*, 2016). Therefore assessing the specific contribution of each of these pathways is difficult. For example, ATF6 activation was shown to modulate IRE1-UPR^{ER} levels and activity of the downstream inflammatory and pro-apoptotic JNK pathway (Walter *et al.*, 2018). On the other hand, interplay between the PERK- and IRE1-UPR^{ER} pathway dictates apoptotic cell fate, with PERK downregulating IRE1 under irresolvable stress, inhibiting its cytoprotective effect and driving apoptosis (Chang *et al.*, 2018). In our model, the predominant activation of the PERK-UPR^{ER} in our model suggests that this branch may be taking over the stress response, driving it towards a commitment to apoptotic processes, corroborated by the observed increase in apoptotic neurons.

The ISR-induced ATF4 has been extensively described as a central regulator of the mitochondrial stress response, interacting and targeting genes of various stress response pathways (Bao *et al.*, 2016; Quirós *et al.*, 2017; X. Guo *et al.*, 2020). For instance, ATF4 and the ISR are necessary for the activation of the UPR^{mt} and interact with ATF5 (Melber and Haynes, 2018; Forsström *et al.*, 2019; D. Jiang *et al.*, 2020; Sayles *et al.*, 2022; Lu *et al.*, 2023). ATF4 is also involved in the regulation of mTOR signaling through modulating the expression of mTORC1 inhibitors SESN2 and DDIT4 (Xu *et al.*, 2020; Jang *et al.*, 2021). Moreover, ATF4 appears to orchestrate the transcriptional activation of the redox regulator NRF2 (Sarcinelli *et al.*, 2020; Kreß *et al.*, 2023), which is upregulating upon stress in the LUHMES-derived DA neurons. One study likewise found that IRE1 could induce the NRF2 antioxidant response (Hourihan *et al.*, 2016). As both the PERK-UPR^{ER} and the IRE1- UPR^{ER} were upregulated in the LUHMES-derived DA neurons following the stress protocol, there could be an interaction between the two pathway leading to the increased levels of NRF2. Our results are in line with was has been previously described in the field, as we demonstrate activation of *SESN2*, *DDIT4* and *NRF2* upon mitochondrial stress.

Further investigation into our data showed no activation of the UPR^{mt}, in contrast to several studies looking at mitochondrial stress response (Houtkooper *et al.*, 2013; Cai *et al.*, 2020; Hu, Liu and Qi, 2021; Uoselis *et al.*, 2023). These disparities are likely due to the use of different types of mitochondria stressors, whether localized and specifically damaging to the mitochondria or not, as well as different treatment length, reproducing a more acute or chronic stress paradigm, as well as the use of various cell types (Lamech and Haynes, 2015; Ko *et al.*, 2020). In the LUHMES-originating DA neurons, we even found inactivation of a number of UPR^{mt} actors following the 8 hour mitochondrial stress protocol. Inhibition of PERK in our study alleviated this downregulation of UPR^{mt}, suggesting that it is reliant on PERK.

At a cellular level, we explored damage to the mitochondrial turnover in response to mitochondrial toxin treatment. Tightly regulated mitochondrial quality mechanisms that maintain mitochondrial homeostasis have been well described. In particular, the coordination between mitophagy and mitochondrial biogenesis is central to adjusting mitochondrial content depending on cellular needs (Ashrafi and Schwarz, 2013; Palikaras, Lionaki and Tavernarakis, 2015; Li *et al.*, 2019; Liu *et al.*, 2023). In healthy cells, damage to the mitochondrial network will result in increased clearance of dysfunctional mitochondria, which is quickly accompanied by an increase in mitochondrial biogenesis to generate new and healthy mitochondria (Palikaras, Lionaki and Tavernarakis, 2015). These mechanisms are essential for cellular survival and stress resistance. Disruption of the balance between mitophagy and mitobiogenesis, as has been uncovered in ageing and in neurodegeneration contexts, results in a dysfunctional mitochondrial network, disturbed cellular energy homeostasis and eventually drives cell death (Markaki and Tavernarakis, 2020). In our project, the mitochondrial stress protocol expectedly triggered mitophagy in the majority of cells. However, mitochondrial biogenesis did not appear to follow this mitophagy increase and instead was diminished in our cells. The uncoordinated action of these two mechanisms may be due to the fact that the cells are already committed to an apoptotic fate and therefore, adaptive survival mechanisms may be halted. The higher energetic needs of dopaminergic neurons (Surmeier, Obeso and Halliday, 2017) may also make them more vulnerable to imbalances in mitochondrial network and ATP production, meaning that they may reach unsurmountable mitochondrial dysfunction more rapidly than other cell types.

We postulated that the PERK-mediated UPR^{ER} may be involved in regulating the mitochondrial homeostasis maintenance processes activated upon mitochondrial stress. To this aim, we used a PERK-specific inhibitor, GSK2606414 to assess the PERK-UPR^{ER} contribution to the cellular changes observed upon stress, in particular regarding mitochondrial turnocver. This experiment demonstrated that mitochondrial quality control processes were similarly regulated by PERK, at least in part. PERK inhibition decreased stress-induced mitophagy levels in the DA neuronal population. To this day, few studies have described such a direct link between PERK activation and mitophagy. A PERK and ATF4-dependent induction of mitophagy was showed following chromium exposure (Dlamini *et al.*, 2021) and *via* PARKIN modulation upon ER stress (Bouman *et al.*, 2011; Zhang *et al.*, 2014). ATF4 was contrastingly shown to block mitophagy in the advent of mitochondrial protein folding stress (Uoselis *et al.*, 2023). Interestingly, basal PERK-levels appeared to play a role in modulating the mitochondrial network as its inhibition instigated mitochondrial fragmentation similar to that observed after cells were incubated with mitochondrial toxins. Mitochondrial biogenesis also was reduced in control conditions by PERK inhibition. Altogether, these observations reveal that PERK activity was necessary for the maintenance of the mitochondrial network and mitochondrial homeostasis in basal conditions, in agreement with previous data (Muñoz *et al.*, 2013; Mesbah Moosavi and Hood, 2017; Kato *et al.*, 2020; Sassano *et al.*, 2023). An interesting point to note is that these studies showed that this link between PERK and mitochondria quality control was independent of the UPR. Some studies have implicated ATF6 in mitochondrial biogenesis regulation through the modulation of the mitochondrial biogenesis master regulator PGC1-α (Wu *et al.*, 2011; Misra *et al.*, 2013). In the LUHMES-derived DA neurons, mitochondrial biogenesis was revealed to be dependent on PERK activity, however, taking into account the possibility of PERK and ATF6 crosstalk, we cannot rule out ATF6 implication.

A main aim to our project was to explore the lncRNA component to the mitochondrial stress response. Although the field of lncRNA research has been exponentially growing in the past decade, most available studies adopt candidate approaches by targeting specific well known and expressed lncRNAs. Others also harness sequencing approaches to identify lncRNAs repertoires in a specific model, however, they mostly do not perform discovery of new transcripts. Here, we wanted to exploit the high specificity of lncRNAs, whether to the cell type, species or

developmental stage, makes them such interesting molecular elements to study in the context of cell type specific processes. Our transcriptomic data allowed the compilation of the lncRNA repertoires in both control and stress conditions, as important differences were uncovered between the two. A large number of identified lncRNAs, representing about 23% of the overall repertoires, had never been sequenced or annotated before, confirming the particularity of lncRNAs as highly specific molecular elements. On top of this, several lncRNAs' expression was regulated by mitochondrial stress. This is promising as it could indicate networks of lncRNAs that are implicated in the cellular stress response. Interestingly, amongst the lncRNAs specific or upregulated in the stress condition, we identified a group of transcripts possibly regulating amino acid transporter involved in the regulation of translation initiation *via* mTOR signaling. As translation modulation is an important component of the cellular stress response, the contribution of lncRNAs may of great interest for further study. Furthermore, linking back to the predominant activation of PERK-UPR^{ER}, we identified groups of lncRNAs that were potentially under the regulation of ATF3 and ATF4, main UPR effectors downstream of PERK. This suggests that some lncRNAs' actions may be directly related to the activation of the UPR^{ER} by the mitochondrial stress response and may contribute to its downstream effects. This is in line with the prominent and well-described particularity of lncRNAs, whereby many exhibit context-specific expression patterns (Morán, Akerman, van de Bunt, *et al.*, 2012; Deveson *et al.*, 2017). We selected a number of promising candidates, possibly linked to the stress responses activated upon stress in the DA neurons or to PD. We identified 15 candidates related to translation regulation or to neuronal generation, as well as several transcripts containing PD-associated SNPs. Many of these candidates exhibited altered expression when the PERK-UPR^{ER} was inhibited, validating their direct link to the stress response. One of these candidates, the lnc-*SLC6A15*-5 was selected for further analysis. This lncRNA neighbors an amino acid transporter and displayed an interesting expression profile: it was not expressed in basal conditions and was switched on by mitochondrial stress. Furthermore, PERK-inhibition restricted the upregulation of lnc-*SLC6A15*-5 upon mitochondrial stress. Our analysis uncovered novel isoforms of this lncRNA that had never been annotated previously. These transcripts could be specific to the cell type or to the stimuli. Functional experiments on lnc-*SLC6A15*-5 revealed that it may contribute to the resumption of translation once mitochondrial stress is resolved. It also appears to modulate the transcription of a

number of ATF4 targets including amino acid transporters and *SESN2*, inhibitor of mTOR signaling. *Lnc-SLC6A15-5* may therefore be part of a feedback loop whereby PERK-UPR^{ER} may boost the upregulation of this lncRNA which can then act upon downstream ATF4 targets and upon translation recovery.

The effects of lnc-SLC6A15-5 inhibition on the DA neurons' mitochondrial stress response discovered here were modest. Nevertheless, this is coherent with the growing literature on lncRNAs that describe subtle and often context-specific functionality, apart for the ubiquitously expressed lncRNAs such as *MALAT1* and *NEAT1* which ultimately do not represent the large majority of lncRNAs (Deveson *et al.*, 2017). This constitutes one of the greatest challenges in lncRNA research that makes strategies used to explore the function of protein-coding genes frequently inapplicable. However, the possible implication of *lnc-SLC6A15-5* in regulating translation resumption following mitochondrial stress could be further validated by allowing for a longer recovery period than the 30 minutes we implemented in our experiments. Given the precise and context-specificity of lncRNA activity (Goff and Rinn, 2015; Liu *et al.*, 2016), it is also possible that *lnc-SLC6A15-5* may have other functions, possibly implicated in the stress response, that our study was not able to elucidate yet.

This study was able to provide important comprehensive observations regarding the mitochondrial stress response of human dopaminergic neurons as well as information regarding lncRNAs' function as highly specific molecular actors. This particularity of lncRNAs is often overlooked in most of the current research pertaining to lncRNAs, as they tend to study ubiquitously expressed lncRNAs. It would be interesting to assess whether the mechanisms triggered by mitochondrial stress here may be specific to DA neurons and if they are altered in other cell types.

In our second study, we were able to use iPSC-derived from two patients and two healthy individuals. One of the patients presented heterozygous composite *PRKN* mutations and was related to one of the healthy individuals who was a carrier for only one of the mutations. Using the iPS cell lines derived from this healthy donor, our team has previously generated two isogenic lines presenting a knockout of *PRKN* to study the specific effects of PARKIN loss of function in cells presenting the same genomics background.

The differentiation using the iPSC cell lines was directed towards the ventral midbrain fate and yielded about 10% of TH-expressing DA neurons relative to the total cell number. Interestingly, PARKIN deficiency seemed to alter the identity of the differentiated cellular population, with a delay in dopaminergic maturity, notably a decrease in the proportion of DA. Further analysis of our data also showed diminished expression of a number of GABAergic receptors and synaptic transmission markers. This was accompanied by an increase in the glial population. Our results are in agreement with studies showing that mutations in *PRKN* hinder the differentiation efficacy of iPSC differentiation, with lower levels of DA neurons achieved in these cell lines compared to healthy controls (Shaltouki *et al.*, 2015). PARKIN loss-of-function also appeared to impair the complexity of neuronal processes, resulting in reduced neurite length, number of terminals and branch points (Ren *et al.*, 2015). Parkin thus appears to play an important role in permitting proper and efficient neuronal differentiation. More experiments are needed to validate these findings, such as targeted immunostaining investigating the proportion of different cell types in the differentiated cell population.

In these cell lines, the mitochondrial stress protocol yielded very similar effects to those observed in the LUHMES-derived DA neurons with the concomitant activation of all three branches of the UPR^{ER} and inactivation of the UPR^{mt}. Mitochondrial stress equally modulated effectors of translation regulation, in particular those targeting translation initiation *via* mTOR signalling. To verify translation shutdown dependent on PERK and eIF2α phosphorylation, quantifications at the protein level will need to be performed. On top of this, we chose to explore oxidative stress response signalling as many studies have shown its implication in the mitochondrial stress response of PD models. A number of effectors of the NRF2-mediated antioxidant pathways were indeed upregulated by the mitochondrial toxins. NRF2 being a direct target of the PERK-UPR^{ER}, it may be that the antioxidant response is modulated by the UPR^{ER} as well. To explore this hypothesis, the expression levels of these factors must be assessed in the stress paradigm when PERK is inhibited, using GSK2606414 as set up in our LUHMES-based study. The stress response in the iPSC-derived differentiated cells originating from healthy individuals also revealed that mitochondrial stress inhibited pathways involved in DNA repair and DNA damage response. These mechanisms appeared to be less downregulated in the PARKIN-deficient cell lines, suggesting disruption of DNA repair in these cells. Activation of the UPR^{ER} has been

shown to interfere with DNA repair processes, mostly in the context of cancer research (Yamamori *et al.*, 2013; Weatherbee, Kraus and Ross, 2016; Liu *et al.*, 2019). Therefore, the robust PERK-UPR^{ER} activation upon stress in the iPSC-differentiated cells may result in impaired DNA repair mechanisms. The increased levels of ROS in PARKIN-deficient neurons cause important DNA damage that could be unresolved due to the disruption in these DNA repair pathways. This was suggested to result in increased neuroinflammation and may be underlying the toxicity observed in PD (Qin, Geng and Xue, 2022).

The PARKIN-deficient cell lines remarkably showed activation of stress response pathways even in basal conditions, most noticeably ATF6- and IRE1-derived UPR^{ER} as well as NRF2-dependent antioxidant response. This suggest that these cells are “pre-stressed” in comparison to the cells derived from healthy individuals, and thus may exhibit enhanced stress sensitivity, in agreement with previous studies (Gautier, Kitada and Shen, 2008; Chung *et al.*, 2016). In line with these findings, the PRKN-mutant cells displayed more exacerbated stress response pathways upon treatment with mitochondrial toxins, in comparison to the healthy individual-originating cells, with higher levels of markers of the three UPR^{ER} branches, NRF2-mediated antioxidant factors, as well as translation initiation modulators. Patient-derived cell lines showed specific activation of an inflammatory response, which could be associated to the boosted presence of astrocytes in the differentiated patient cells in comparison to the healthy individual-derived cells. It has been reported that astrocytes may display neurotoxic activity in PD, favoring the progression of the disease (Brandebura *et al.*, 2023). Moreover, PARKIN was shown to be involved in astrocytes’ inflammatory response and PINK1/PARKIN-mediated mitophagy was able to trigger NLRP3-dependent inflammatory pathways (Khasnavis and Pahan, 2014; Gkikas, Palikaras and Tavernarakis, 2018). An interesting hypothesis is that PARKIN-deficient astrocytes present dysfunctional mitochondria and elevated ROS levels, which could cause sustained NLRP3 inflammasome activity (Kim *et al.*, 2023). Another hypothesis is that the neuron may be source of brain inflammation as recent research surprisingly suggests that upon DNA damage, neurons may also secrete pro-inflammatory cytokines to attract microglia (Welch and Tsai, 2022; Welch *et al.*, 2022). Further investigation would be needed to assess the inflammatory response stimulated by mitochondrial stress in iPSC-differentiated ventral midbrain neurons.

Interestingly, several genes were commonly upregulated by stress in the patient and *PRKN* KO isogenic differentiated cells in contrast to the healthy individual cells, suggesting a possible effect of PARKIN deficiency. Further assessment revealed that some of these genes were involved in one carbon metabolism, which has been reported as regulated by ATF4 and disrupted in PD and Alzheimer's disease post-mortem samples (Celardo *et al.*, 2017; Kalecký, Ashcraft and Bottiglieri, 2022). Several other genes from this list were ATF4 targets and were linked to oxidative stress response, amino acid transport and regulation of mTOR signaling. Mitochondrial stress may therefore trigger a stress response specific to the PARKIN-deficient cells that could rely on ATF4. Understanding whether these pathways are protective or neurotoxic may provide valuable information for PD disease research and may lead to the identification of potential therapeutic targets. This could be done by carrying out pharmacological inhibition of these pathways or targeted knockdowns of their main regulators.

In this study, we were also able to assemble the lncRNA repertoires expressed in the differentiated cells originating from each of the IPSC line. Out of these lncRNAs, 11.2% were never previously annotated, a lower number that what was found in the LUHMES-based lncRNA repertoire. In line with the well-described high context specificity of lncRNAs (Deveson *et al.*, 2017), we identified lncRNAs that were specifically expressed in the patient- cells, the healthy-individual or the PRKN KO isogenic-derived cells. However, the proportion of lncRNAs specific to the cell lines and conditions was significantly lower than that observed LUHMES-derived DA neurons for lncRNAs expressed in either the stress or the control condition specifically. The difference in model, differentiated cell pool identity and maturity level may underly these disparities. Interestingly, amongst the lncRNAs detected in the patient- and *PRKN* KO isogenic-derived cells a number were found to be potentially associated to the regulation of early developmental stages including axonal guidance, which is reminiscent of the altered differentiation status of the PARKIN-deficient cells. These results may suggest a link between PARKIN and regulation of lncRNAs, which participate in the modulation of differentiation processes. In line with these results, analysis of the lncRNAs upregulated in patient-originating cells revealed a network of lncRNAs possibly contributing to synaptic transmission modulation, most notably upon receptors of GABAergic, cholinergic, and glutamatergic transmission.

Altogether, the stress response uncovered during the transcriptomic analysis of protein-coding genes was very similar in both our studies. This is very interesting considering the difference in cellular populations in the two models. On one hand, the LUHMES cells-derived DA neurons provides a pure and mature DA population, albeit not in the most physiological relevant context as they originate from v-myc induced immortalized precursor cells (Lotharius, 2005). On the other hand, the iPSC-derived differentiated cells only produced about 10% of DA neurons. On top of this, the resulting cells exhibited poor expression of the mature DA marker DAT in comparison with the LUHMES-derived cells, suggesting a lower level of DA maturity. This suggests that the stress response characteristics observed may not be specific to DA neurons, but could be a more global response, integrating other neuronal and glial types that are generally present in the ventral midbrain.

On the other hand, overlapping the lncRNA repertoires detected in both studies showed a minority of common transcripts (383 lncRNAs) and a majority of lncRNAs expressed only in one of the models (798 lncRNAs specific to the LUHMES-derived repertoire and 1171 specific to the iPSC-derived repertoire). This could be explained by the difference in cellular populations from which originate the repertoires, with iPSC-based differentiation generating a heterogeneous population, and highlights the high specificity of these molecular elements. The iPSC differentiation generates a cellular population that is, although not entirely DA, coherent with the development of the *Substantia Nigra*. Even though this is the case, there is still a major disparity between the human LUHMES-derived DA neuronal lncRNA repertoire and the ventral midbrain-derived lncRNA repertoire. Furthermore, we identified a smaller proportion of lncRNAs that were specifically expressed in only one of the sample groups: healthy individual-, patient- or *PRKN* KO isogenic-derived differentiated cells. This was also the case for lncRNAs specific to basal or mitochondrial stress contexts. LncRNAs are well-described as highly context-specific transcripts and such cell-type or spatio-temporal specific elements have been hard to detect in bulk transcriptomic analysis as they tend to show low expression levels (Ulitsky, 2016; Deveson *et al.*, 2017). On the other hand, minority of lncRNAs are ubiquitously expressed and robustly detected in bulk RNA-seq, such as *MALAT1* and *NEAT1*. Therefore, due to our study paradigm, we may not be able to detect as many specific lncRNAs in the iPSC-derived cells. This is coherent with the fact that even though lnc-*SLC6A15*-5 was detected in the iPSC-derived differentiated cells, it was eliminated from the final repertoire on the basis of its

expression levels. This is because we set stringent expression criteria in our lncRNA identification pipeline in which transcripts had to exhibit expression levels higher than 1 TPM to be retained in the final repertoire. It could therefore be suitable to use different techniques targeting specific cell types such as fluorescence in situ hybridization or single cell RNA-seq, to possibly detect distinct lncRNAs that may be expressed in a subset of cell types (Liu *et al.*, 2016). For example, lnc-*SLC6A15*-5 may be found as more robustly expressed in DA neurons. Another option that is being set up in our team, is the use of 3D cultures in the form of midbrain organoid that may give access to a physiologically relevant model presenting larger proportions of neuronal, and notably DA neurons. Our current protocol generated about 10-20% of TH-expressing cells relative to the total cell number and exhibited higher levels of DA mature markers such as DAT. We have also successfully derived ventral midbrain organoids from PD patient cell lines. Therefore, using this model may bridge the gap between the LUHMES- and the iPSC-derived neurons, allowing access to mature DA neurons in a physiologically relevant context. Moreover, another incentive to work with organoids is to be able to study the different cell populations generated by ventral midbrain-directed differentiation that develop together within the same structure. For the study of lncRNAs within this model, it would be interesting to harness single cell RNA-seq for the discovery of cell-type specific lncRNAs as has already been done in human neocortex samples (Liu *et al.*, 2016). It is noteworthy that in this study, the use of single cell transcriptomics revealed that lncRNAs usually detected at low levels in bulk tissue analysis, were robustly expressed in individual cells. This technique has already been used on organoids, including midbrain organoids, and described in several studies (Kanton *et al.*, 2019; Fiorenzano *et al.*, 2021; Yin *et al.*, 2021).

Although we may not be in optimal conditions for the identification of cell-type specific lncRNAs in the iPSC-derived cells, we may find transcripts that could be specific to mitochondrial stress response. This could be achieved by selecting candidates that are specifically expressed or regulated upon the mitochondrial stress in both the LUHMES DA neuron- and iPSC-derived repertoires. Most importantly, the iPSC-based model also gave us access to a highly relevant PD context, in which we may be able to uncover lncRNAs specific to the disease. This corresponds to the lncRNAs that are specifically expressed or regulated in the PARKIN-deficient cells. In our team, we have recently collected peripheral blood mononuclear cells (PBMC) from almost a hundred of PD patient blood samples. A perspective here, would be to cross-

analyze the data collected from our ventral midbrain-differentiated iPS cells originating from *PRKN* mutant PD patients, with patient PBMC RNA-seq data. This could allow for the identification of common candidate lncRNAs that constitute molecular signatures of the disease and may be promising novel biomarkers for disease diagnosis.

Altogether, our data provides valuable insights into the mitochondrial stress response of human DA neurons in the aims of uncovering mechanisms specific to these cells that may underlie their selective vulnerability to such mitochondrial stress. We also highlight the importance of highly cell-type and context-specific elements such as lncRNAs that may take part in important stress response pathways.

VI. Bibliography

Aboud, A.A. *et al.* (2015) 'PARK2 patient neuroprogenitors show increased mitochondrial sensitivity to copper', *Neurobiology of Disease*, 73, pp. 204–212. Available at: https://doi.org/10.1016/j.nbd.2014.10.002.

Akerman, I. *et al.* (2017) 'Human Pancreatic β Cell lncRNAs Control Cell-Specific Regulatory Networks', *Cell Metabolism*, 25(2), pp. 400–411. Available at: https://doi.org/10.1016/j.cmet.2016.11.016.

Alam, P. *et al.* (2019) 'α-synuclein oligomers and fibrils: a spectrum of species, a spectrum of toxicities', *Journal of Neurochemistry*, 150(5), pp. 522–534. Available at: https://doi.org/10.1111/jnc.14808.

Alberico, S.L., Cassell, M.D. and Narayanan, N.S. (2015) 'The Vulnerable Ventral Tegmental Area in Parkinson's Disease', *Basal ganglia*, 5(2–3), pp. 51–55. Available at: https://doi.org/10.1016/j.baga.2015.06.001.

Aliperti, V., Skonieczna, J. and Cerase, A. (2021) 'Long Non-Coding RNA (lncRNA) Roles in Cell Biology, Neurodevelopment and Neurological Disorders', *Non-Coding RNA*, 7(2), p. 36. Available at: https://doi.org/10.3390/ncrna7020036.

Altshuler, D., Daly, M.J. and Lander, E.S. (2008) 'Genetic Mapping in Human Disease', *Science*, 322(5903), pp. 881–888. Available at: https://doi.org/10.1126/science.1156409.

Alver, B.H. *et al.* (2017) 'The SWI/SNF chromatin remodelling complex is required for maintenance of lineage specific enhancers', *Nature Communications*, 8, p. 14648. Available at: https://doi.org/10.1038/ncomms14648.

Anderson, N.S. and Haynes, C.M. (2020) 'Folding the Mitochondrial UPR into the Integrated Stress Response', *Trends in Cell Biology*, 30(6), pp. 428–439. Available at: https://doi.org/10.1016/j.tcb.2020.03.001.

Andreev, D.E. *et al.* (2015) 'Translation of 5′ leaders is pervasive in genes resistant to eIF2 repression', *eLife*, 4, p. e03971. Available at: https://doi.org/10.7554/eLife.03971.

Ansorge, O., Daniel, S.E. and Pearce, R.K.B. (1997) 'Neuronal loss and plasticity in the supraoptic nucleus in Parkinson's disease', *Neurology*, 49(2), pp. 610–613. Available at: https://doi.org/10.1212/WNL.49.2.610.

Arena, G. and Valente, E.M. (2017) 'PINK1 in the limelight: multiple functions of an eclectic protein in human health and disease: Functions of PINK1 in human pathology', *The Journal of Pathology*, 241(2), pp. 251–263. Available at: https://doi.org/10.1002/path.4815.

Ariel, F. *et al.* (2020) 'R-Loop Mediated trans Action of the APOLO Long Noncoding RNA', *Molecular Cell*, 77(5), pp. 1055-1065.e4. Available at: https://doi.org/10.1016/j.molcel.2019.12.015.

Armstrong, M.J. and Okun, M.S. (2020) 'Diagnosis and Treatment of Parkinson Disease: A Review', *JAMA*, 323(6), p. 548. Available at: https://doi.org/10.1001/jama.2019.22360.

Arvanitakis, Z., Shah, R.C. and Bennett, D.A. (2019) 'Diagnosis and Management of Dementia: A Review', *JAMA*, 322(16), pp. 1589–1599. Available at: https://doi.org/10.1001/jama.2019.4782.

Ascherio, A. and Schwarzschild, M.A. (2016) 'The epidemiology of Parkinson's disease: risk factors and prevention', *The Lancet Neurology*, 15(12), pp. 1257–1272. Available at: https://doi.org/10.1016/S1474-4422(16)30230-7.

Ashrafi, G. *et al.* (2014) 'Mitophagy of damaged mitochondria occurs locally in distal neuronal axons and requires PINK1 and Parkin', *Journal of Cell Biology*, 206(5), pp. 655–670. Available at: https://doi.org/10.1083/jcb.201401070.

Ashrafi, G. and Schwarz, T.L. (2013) 'The pathways of mitophagy for quality control and clearance of mitochondria', *Cell Death & Differentiation*, 20(1), pp. 31–42. Available at: https://doi.org/10.1038/cdd.2012.81.

Auyeung, V.C. *et al.* (2013) 'Beyond Secondary Structure: Primary-Sequence Determinants License Pri-miRNA Hairpins for Processing', *Cell*, 152(4), pp. 844–858. Available at: https://doi.org/10.1016/j.cell.2013.01.031.

Avazzadeh, S. *et al.* (2021) 'Modelling Parkinson's Disease: iPSCs towards Better Understanding of Human Pathology', *Brain Sciences*, 11(3), p. 373. Available at: https://doi.org/10.3390/brainsci11030373.

Bäckström, D. *et al.* (2018) 'Early predictors of mortality in parkinsonism and Parkinson disease: A population-based study', *Neurology*, 91(22), pp. e2045–e2056. Available at: https://doi.org/10.1212/WNL.0000000000006576.

Baek, J.-H. *et al.* (2016) 'Unfolded protein response is activated in Lewy body dementias', *Neuropathology and Applied Neurobiology*, 42(4), pp. 352–365. Available at: https://doi.org/10.1111/nan.12260.

Baek, J.-H. *et al.* (2019) 'GRP78 Level Is Altered in the Brain, but Not in Plasma or Cerebrospinal Fluid in Parkinson's Disease Patients', *Frontiers in Neuroscience*, 13, p. 697. Available at: https://doi.org/10.3389/fnins.2019.00697.

Bahar Halpern, K. *et al.* (2015) 'Nuclear Retention of mRNA in Mammalian Tissues', *Cell Reports*, 13(12), pp. 2653–2662. Available at: https://doi.org/10.1016/j.celrep.2015.11.036.

Balestrino, R. and Schapira, A.H.V. (2020) 'Parkinson disease', *European Journal of Neurology*, 27(1), pp. 27–42. Available at: https://doi.org/10.1111/ene.14108.

Banani, S.F. *et al.* (2017) 'Biomolecular condensates: organizers of cellular biochemistry', *Nature Reviews Molecular Cell Biology*, 18(5), pp. 285–298. Available at: https://doi.org/10.1038/nrm.2017.7.

Bandres-Ciga, S. *et al.* (2020) 'Genetics of Parkinson's disease: An introspection of its journey towards precision medicine', *Neurobiology of Disease*, 137, p. 104782. Available at: https://doi.org/10.1016/j.nbd.2020.104782.

Bao, X.R. *et al.* (2016) 'Mitochondrial dysfunction remodels one-carbon metabolism in human cells', *eLife*, 5, p. e10575. Available at: https://doi.org/10.7554/eLife.10575.

Barazzuol, L. *et al.* (2020) 'PINK1/Parkin Mediated Mitophagy, Ca2+ Signalling, and ER-Mitochondria Contacts in Parkinson's Disease', *International Journal of Molecular Sciences*, 21(5), p. 1772. Available at: https://doi.org/10.3390/ijms21051772.

Barodia, S.K., Creed, R.B. and Goldberg, M.S. (2017) 'Parkin and PINK1 functions in oxidative stress and neurodegeneration', *Brain research bulletin*, 133, pp. 51–59. Available at: https://doi.org/10.1016/j.brainresbull.2016.12.004.

Barone, P., Erro, R. and Picillo, M. (2017) 'Quality of Life and Nonmotor Symptoms in Parkinson's Disease', in *International Review of Neurobiology*. Elsevier, pp. 499–516. Available at: https://doi.org/10.1016/bs.irn.2017.05.023.

Barsoum, M.J. *et al.* (2006) 'Nitric oxide-induced mitochondrial fission is regulated by dynamin-related GTPases in neurons', *The EMBO Journal*, 25(16), pp. 3900–3911. Available at: https://doi.org/10.1038/sj.emboj.7601253.

Bartel, D.P. (2009) 'MicroRNAs: Target Recognition and Regulatory Functions', *Cell*, 136(2), pp. 215–233. Available at: https://doi.org/10.1016/j.cell.2009.01.002.

B'chir, W. *et al.* (2013) 'The eIF2α/ATF4 pathway is essential for stress-induced autophagy gene expression', *Nucleic Acids Research*, 41(16), pp. 7683–7699. Available at: https://doi.org/10.1093/nar/gkt563.

Beal, M.F. (2005) 'Mitochondria take center stage in aging and neurodegeneration', *Annals of Neurology*, 58(4), pp. 495–505. Available at: https://doi.org/10.1002/ana.20624.

Beilina, A. and Cookson, M.R. (2016) 'Genes associated with Parkinson's disease: regulation of autophagy and beyond', *Journal of Neurochemistry*, 139, pp. 91–107. Available at: https://doi.org/10.1111/jnc.13266.

Bellot, G. *et al.* (2009) 'Hypoxia-Induced Autophagy Is Mediated through Hypoxia-Inducible Factor Induction of BNIP3 and BNIP3L via Their BH3 Domains', *Molecular and Cellular Biology*, 29(10), pp. 2570–2581. Available at: https://doi.org/10.1128/MCB.00166-09.

Bender, A. *et al.* (2008) 'Dopaminergic midbrain neurons are the prime target for mitochondrial DNA deletions', *Journal of Neurology*, 255(8), pp. 1231–1235. Available at: https://doi.org/10.1007/s00415-008-0892-9.

Ben-Zvi, A., Miller, E.A. and Morimoto, R.I. (2009) 'Collapse of proteostasis represents an early molecular event in *Caenorhabditis elegans* aging', *Proceedings of the National Academy of Sciences*, 106(35), pp. 14914–14919. Available at: https://doi.org/10.1073/pnas.0902882106.

Berardelli, A. *et al.* (2013) 'EFNS/MDS-ES recommendations for the diagnosis of Parkinson's disease', *European Journal of Neurology*, 20(1), pp. 16–34. Available at: https://doi.org/10.1111/ene.12022.

Berg, D. *et al.* (2021) 'Prodromal Parkinson disease subtypes - key to understanding heterogeneity', *Nature Reviews. Neurology*, 17(6), pp. 349–361. Available at: https://doi.org/10.1038/s41582-021-00486-9.

Bertholet, A.M. *et al.* (2016) 'Mitochondrial fusion/fission dynamics in neurodegeneration and neuronal plasticity', *Neurobiology of Disease*, 90, pp. 3–19. Available at: https://doi.org/10.1016/j.nbd.2015.10.011.

Bertrand, E. *et al.* (1997) 'Qualitative and quantitative analysis of locus coeruleus neurons in Parkinson's disease', *Folia neuropathologica*, 35(2). Available at: https://pubmed.ncbi.nlm.nih.gov/9377080/ (Accessed: 1 May 2023).

Betarbet, R. *et al.* (2000) 'Chronic systemic pesticide exposure reproduces features of Parkinson's disease', *Nature Neuroscience*, 3(12), pp. 1301–1306. Available at: https://doi.org/10.1038/81834.

Bhan, A. and Mandal, S.S. (2015) 'LncRNA HOTAIR: a master regulator of chromatin dynamics and cancer', *Biochimica et biophysica acta*, 1856(1), pp. 151–164. Available at: https://doi.org/10.1016/j.bbcan.2015.07.001.

Bilen, M. *et al.* (2022) 'The integrated stress response as a key pathway downstream of mitochondrial dysfunction', *Current Opinion in Physiology*, 27, p. 100555. Available at: https://doi.org/10.1016/j.cophys.2022.100555.

Bindoff, L.A. *et al.* (1991) 'Respiratory chain abnormalities in skeletal muscle from patients with Parkinson's disease', *Journal of the Neurological Sciences*, 104(2), pp. 203–208. Available at: https://doi.org/10.1016/0022-510X(91)90311-T.

Bloem, B.R., Okun, M.S. and Klein, C. (2021) 'Parkinson's disease', *The Lancet*, 397(10291), pp. 2284–2303. Available at: https://doi.org/10.1016/S0140-6736(21)00218-X.

Bloemberg, D. and Quadrilatero, J. (2019) 'Autophagy, apoptosis, and mitochondria: molecular integration and physiological relevance in skeletal muscle', *American Journal of Physiology-Cell Physiology*, 317(1), pp. C111–C130. Available at: https://doi.org/10.1152/ajpcell.00261.2018.

Bock, F.J. and Tait, S.W.G. (2020) 'Mitochondria as multifaceted regulators of cell death', *Nature Reviews Molecular Cell Biology*, 21(2), pp. 85–100. Available at: https://doi.org/10.1038/s41580-019-0173-8.

Bommiasamy, H. *et al.* (2009) 'ATF6α induces XBP1-independent expansion of the endoplasmic reticulum', *Journal of Cell Science*, 122(10), pp. 1626–1636. Available at: https://doi.org/10.1242/jcs.045625.

Bond, S. *et al.* (2020) 'The Integrated Stress Response and Phosphorylated Eukaryotic Initiation Factor 2α in Neurodegeneration', *Journal of Neuropathology and Experimental Neurology*, 79(2), pp. 123–143. Available at: https://doi.org/10.1093/jnen/nlz129.

Bonello, F. *et al.* (2019) 'LRRK2 impairs PINK1/Parkin-dependent mitophagy via its kinase activity: pathologic insights into Parkinson's disease', *Human Molecular Genetics*, 28(10), pp. 1645–1660. Available at: https://doi.org/10.1093/hmg/ddz004.

Borsche, M. *et al.* (2021) 'Mitochondria and Parkinson's Disease: Clinical, Molecular, and Translational Aspects', *Journal of Parkinson's Disease*, 11(1), pp. 45–60. Available at: https://doi.org/10.3233/JPD-201981.

Bose, A. and Beal, M.F. (2016) 'Mitochondrial dysfunction in Parkinson's disease', *Journal of Neurochemistry*, 139 Suppl 1, pp. 216–231. Available at: https://doi.org/10.1111/jnc.13731.

Bouman, L. *et al.* (2011) 'Parkin is transcriptionally regulated by ATF4: evidence for an interconnection between mitochondrial stress and ER stress', *Cell Death and Differentiation*, 18(5), pp. 769–782. Available at: https://doi.org/10.1038/cdd.2010.142.

Bower, J.H. *et al.* (2006) 'Immunologic diseases, anti-inflammatory drugs, and Parkinson disease: a case-control study', *Neurology*, 67(3), pp. 494–496. Available at: https://doi.org/10.1212/01.wnl.0000227906.99570.cc.

Braak, H. *et al.* (2003) 'Staging of brain pathology related to sporadic Parkinson's disease', *Neurobiology of Aging*, 24(2), pp. 197–211. Available at: https://doi.org/10.1016/S0197-4580(02)00065-9.

Braak, H. *et al.* (2004) 'Stages in the development of Parkinson's disease-related pathology', *Cell and Tissue Research*, 318(1), pp. 121–134. Available at: https://doi.org/10.1007/s00441-004-0956-9.

Brandebura, A.N. *et al.* (2023) 'Astrocyte contribution to dysfunction, risk and progression in neurodegenerative disorders', *Nature reviews. Neuroscience*, 24(1), pp. 23–39. Available at: https://doi.org/10.1038/s41583-022-00641-1.

Bravo, R. *et al.* (2012) 'Endoplasmic reticulum: ER stress regulates mitochondrial bioenergetics', *The International Journal of Biochemistry & Cell Biology*, 44(1), pp. 16–20. Available at: https://doi.org/10.1016/j.biocel.2011.10.012.

Bridges, M.C., Daulagala, A.C. and Kourtidis, A. (2021) 'LNCcation: lncRNA localization and function', *Journal of Cell Biology*, 220(2), p. e202009045. Available at: https://doi.org/10.1083/jcb.202009045.

Briggs, J.A. *et al.* (2015) 'Mechanisms of Long Non-coding RNAs in Mammalian Nervous System Development, Plasticity, Disease, and Evolution', *Neuron*, 88(5), pp. 861–877. Available at: https://doi.org/10.1016/j.neuron.2015.09.045.

Brissaud, Edouard (1985) *Leçons sur les maladies nerveuses. Salpêtrière, 1893-1894*.

Brodie, A., Azaria, J.R. and Ofran, Y. (2016) 'How far from the SNP may the causative genes be?', *Nucleic Acids Research*, 44(13), pp. 6046–6054. Available at: https://doi.org/10.1093/nar/gkw500.

Bumgarner, S.L. *et al.* (2009) 'Toggle involving cis-interfering noncoding RNAs controls variegated gene expression in yeast', *Proceedings of the National Academy of Sciences of the United States of America*, 106(43), pp. 18321–18326. Available at: https://doi.org/10.1073/pnas.0909641106.

Bumgarner, S.L. *et al.* (2012) 'Single-cell analysis reveals that noncoding RNAs contribute to clonal heterogeneity by modulating transcription factor recruitment', *Molecular Cell*, 45(4), pp. 470–482. Available at: https://doi.org/10.1016/j.molcel.2011.11.029.

Burkewitz, K. *et al.* (2020) 'Atf-6 Regulates Lifespan through ER-Mitochondrial Calcium Homeostasis', *Cell reports*, 32(10), p. 108125. Available at: https://doi.org/10.1016/j.celrep.2020.108125.

Burré, J. (2015) 'The Synaptic Function of α-Synuclein', *Journal of Parkinson's Disease*, 5(4), pp. 699–713. Available at: https://doi.org/10.3233/JPD-150642.

Burré, J., Sharma, M. and Südhof, T.C. (2018) 'Cell Biology and Pathophysiology of α-Synuclein', *Cold Spring Harbor Perspectives in Medicine*, 8(3), p. a024091. Available at: https://doi.org/10.1101/cshperspect.a024091.

Burtscher, J. *et al.* (2023) 'Mitochondrial stress and mitokines in aging', *Aging Cell*, 22(2), p. e13770. Available at: https://doi.org/10.1111/acel.13770.

Bus, C. *et al.* (2020) 'Human Dopaminergic Neurons Lacking PINK1 Exhibit Disrupted Dopamine Metabolism Related to Vitamin B6 Co-Factors', *iScience*, 23(12), p. 101797. Available at: https://doi.org/10.1016/j.isci.2020.101797.

Cabili, M.N. *et al.* (2011) 'Integrative annotation of human large intergenic noncoding RNAs reveals global properties and specific subclasses', *Genes & Development*, 25(18), pp. 1915–1927. Available at: https://doi.org/10.1101/gad.17446611.

Cai, P. *et al.* (2016) 'Inhibition of Endoplasmic Reticulum Stress is Involved in the Neuroprotective Effect of bFGF in the 6-OHDA-Induced Parkinson's Disease Model', *Aging and disease*, 7(4), p. 336. Available at: https://doi.org/10.14336/AD.2016.0117.

Cai, Y. *et al.* (2020) 'Overexpression of PGC-1α influences the mitochondrial unfolded protein response (mtUPR) induced by MPP+ in human SH-SY5Y neuroblastoma cells', *Scientific Reports*, 10(1), p. 10444. Available at: https://doi.org/10.1038/s41598-020-67229-6.

Caldwell, A.B. *et al.* (2020) 'Dedifferentiation and neuronal repression define familial Alzheimer's disease', *Science Advances*, 6(46), p. eaba5933. Available at: https://doi.org/10.1126/sciadv.aba5933.

Calfon, M. *et al.* (2002) 'IRE1 couples endoplasmic reticulum load to secretory capacity by processing the XBP-1 mRNA', *Nature*, 415(6867), pp. 92–96. Available at: https://doi.org/10.1038/415092a.

Camargo, A.P. *et al.* (2020) 'RNAsamba: neural network-based assessment of the protein-coding potential of RNA sequences', *NAR Genomics and Bioinformatics*, 2(1), p. lqz024. Available at: https://doi.org/10.1093/nargab/lqz024.

von Campenhausen, S. *et al.* (2005) 'Prevalence and incidence of Parkinson's disease in Europe', *European Neuropsychopharmacology*, 15(4), pp. 473–490. Available at: https://doi.org/10.1016/j.euroneuro.2005.04.007.

Cao, B. *et al.* (2018) 'Long Noncoding RNA SNHG1 Promotes Neuroinflammation in Parkinson's Disease via Regulating miR-7/NLRP3 Pathway', *Neuroscience*, 388, pp. 118–127. Available at: https://doi.org/10.1016/j.neuroscience.2018.07.019.

Carlsson, Arvid, Lindqvist, Magit, and Magnusson, Tor (1957) '3,4-dihydroxyphenylalanine and 5-hydroxytryptophan as reserpine antagonists', *Nature*, 180, p. 1200.

Carnazza, K.E. *et al.* (2022) 'Synaptic vesicle binding of α-synuclein is modulated by β- and γ-synucleins', *Cell Reports*, 39(2), p. 110675. Available at: https://doi.org/10.1016/j.celrep.2022.110675.

Carreras-Sureda, A. *et al.* (2019) 'Non-canonical function of IRE1α determines mitochondria-associated endoplasmic reticulum composition to control calcium transfer and bioenergetics', *Nature cell biology*, 21(6), pp. 755–767. Available at: https://doi.org/10.1038/s41556-019-0329-y.

Celardo, I. *et al.* (2016) 'Mitofusin-mediated ER stress triggers neurodegeneration in pink1/parkin models of Parkinson's disease', *Cell Death & Disease*, 7(6), p. e2271. Available at: https://doi.org/10.1038/cddis.2016.173.

Celardo, I. *et al.* (2017) 'dATF4 regulation of mitochondrial folate-mediated one-carbon metabolism is neuroprotective', *Cell Death and Differentiation*, 24(4), pp. 638–648. Available at: https://doi.org/10.1038/cdd.2016.158.

Cesana, M. *et al.* (2011) 'A Long Noncoding RNA Controls Muscle Differentiation by Functioning as a Competing Endogenous RNA', *Cell*, 147(2), pp. 358–369. Available at: https://doi.org/10.1016/j.cell.2011.09.028.

Chang, T.-K. *et al.* (2018) 'Coordination between Two Branches of the Unfolded Protein Response Determines Apoptotic Cell Fate', *Molecular Cell*, 71(4), pp. 629-636.e5. Available at: https://doi.org/10.1016/j.molcel.2018.06.038.

Charcot, J.M. (1875) *Lectures on the Diseases of the Nervous System - La Salpêtrière*.

Chen, E.Y. *et al.* (2013) 'Enrichr: interactive and collaborative HTML5 gene list enrichment analysis tool', *BMC bioinformatics*, 14, p. 128. Available at: https://doi.org/10.1186/1471-2105-14-128.

Chen, G., Kroemer, G. and Kepp, O. (2020) 'Mitophagy: An Emerging Role in Aging and Age-Associated Diseases', *Frontiers in Cell and Developmental Biology*, 8. Available at: https://www.frontiersin.org/articles/10.3389/fcell.2020.00200 (Accessed: 17 November 2023).

Chen, H. *et al.* (2003) 'Nonsteroidal anti-inflammatory drugs and the risk of Parkinson disease', *Archives of Neurology*, 60(8), pp. 1059–1064. Available at: https://doi.org/10.1001/archneur.60.8.1059.

Chen, H. *et al.* (2010) 'Smoking duration, intensity, and risk of Parkinson disease', *Neurology*, 74(11), pp. 878–884. Available at: https://doi.org/10.1212/WNL.0b013e3181d55f38.

Chen, Y.G., Satpathy, A.T. and Chang, H.Y. (2017) 'Gene regulation in the immune system by long noncoding RNAs', *Nature Immunology*, 18(9), pp. 962–972. Available at: https://doi.org/10.1038/ni.3771.

Cherra, S.J. *et al.* (2013) 'Mutant LRRK2 Elicits Calcium Imbalance and Depletion of Dendritic Mitochondria in Neurons', *The American Journal of Pathology*, 182(2), pp. 474–484. Available at: https://doi.org/10.1016/j.ajpath.2012.10.027.

Cheshire, P. *et al.* (2015) 'Serotonergic markers in Parkinson's disease and levodopa-induced dyskinesias', *Movement Disorders: Official Journal of the Movement Disorder Society*, 30(6), pp. 796–804. Available at: https://doi.org/10.1002/mds.26144.

Chi *et al.* (2019) 'Long Non-Coding RNA in the Pathogenesis of Cancers', *Cells*, 8(9), p. 1015. Available at: https://doi.org/10.3390/cells8091015.

Cho, S.W. *et al.* (2018) 'Promoter of lncRNA Gene PVT1 Is a Tumor-Suppressor DNA Boundary Element', *Cell*, 173(6), pp. 1398-1412.e22. Available at: https://doi.org/10.1016/j.cell.2018.03.068.

Chowdhary, A., Satagopam, V. and Schneider, R. (2021) 'Long Non-coding RNAs: Mechanisms, Experimental, and Computational Approaches in Identification, Characterization, and Their Biomarker Potential in Cancer', *Frontiers in Genetics*, 12, p. 649619. Available at: https://doi.org/10.3389/fgene.2021.649619.

Chu, C.T. (2019) 'Multiple pathways for mitophagy: A neurodegenerative conundrum for Parkinson's disease', *Neuroscience Letters*, 697, pp. 66–71. Available at: https://doi.org/10.1016/j.neulet.2018.04.004.

Chung, H.K. *et al.* (2017) 'Growth differentiation factor 15 is a myomitokine governing systemic energy homeostasis', *Journal of Cell Biology*, 216(1), pp. 149–165. Available at: https://doi.org/10.1083/jcb.201607110.

Chung, S.Y. *et al.* (2016) 'Parkin and PINK1 Patient iPSC-Derived Midbrain Dopamine Neurons Exhibit Mitochondrial Dysfunction and α-Synuclein Accumulation', *Stem Cell Reports*, 7(4), pp. 664–677. Available at: https://doi.org/10.1016/j.stemcr.2016.08.012.

Clark, B.S. and Blackshaw, S. (2017) 'Understanding the Role of lncRNAs in Nervous System Development', *Advances in experimental medicine and biology*, 1008, pp. 253–282. Available at: https://doi.org/10.1007/978-981-10-5203-3_9.

Clark, M.B. *et al.* (2012) 'Genome-wide analysis of long noncoding RNA stability', *Genome Research*, 22(5), pp. 885–898. Available at: https://doi.org/10.1101/gr.131037.111.

Clemson, C.M. *et al.* (2009) 'An architectural role for a nuclear noncoding RNA: NEAT1 RNA is essential for the structure of paraspeckles', *Molecular Cell*, 33(6), pp. 717–726. Available at: https://doi.org/10.1016/j.molcel.2009.01.026.

Colla, E. *et al.* (2012) 'Endoplasmic Reticulum Stress Is Important for the Manifestations of -Synucleinopathy In Vivo', *Journal of Neuroscience*, 32(10), pp. 3306–3320. Available at: https://doi.org/10.1523/JNEUROSCI.5367-11.2012.

Conway, K.A. *et al.* (2000) 'Acceleration of oligomerization, not fibrillization, is a shared property of both α-synuclein mutations linked to early-onset Parkinson's disease: Implications for pathogenesis and therapy', *Proceedings of the National Academy of Sciences of the United States of America*, 97(2), pp. 571–576.

Cooper, J.F. *et al.* (2017) 'Activation of the mitochondrial unfolded protein response promotes longevity and dopamine neuron survival in Parkinson's disease models', *Scientific Reports*, 7(1), p. 16441. Available at: https://doi.org/10.1038/s41598-017-16637-2.

Corti, O. (2019) 'Neuronal Mitophagy: Lessons from a Pathway Linked to Parkinson's Disease', *Neurotoxicity Research*, 36(2), pp. 292–305. Available at: https://doi.org/10.1007/s12640-019-00060-8.

Costa, C.A. da *et al.* (2020) 'The Endoplasmic Reticulum Stress/Unfolded Protein Response and Their Contributions to Parkinson's Disease Physiopathology', *Cells*, 9(11), p. 2495. Available at: https://doi.org/10.3390/cells9112495.

Coxhead, J. *et al.* (2016) 'Somatic mtDNA variation is an important component of Parkinson's disease', *Neurobiology of Aging*, 38, p. 217.e1-217.e6. Available at: https://doi.org/10.1016/j.neurobiolaging.2015.10.036.

Cremades, N. *et al.* (2012) 'Direct Observation of the Interconversion of Normal and Toxic Forms of α-Synuclein', *Cell*, 149(5), pp. 1048–1059. Available at: https://doi.org/10.1016/j.cell.2012.03.037.

Csordás, G. *et al.* (2006) 'Structural and functional features and significance of the physical linkage between ER and mitochondria', *The Journal of Cell Biology*, 174(7), pp. 915–921. Available at: https://doi.org/10.1083/jcb.200604016.

Damier, P. *et al.* (1999) 'The substantia nigra of the human brain. II. Patterns of loss of dopamine-containing neurons in Parkinson's disease', *Brain : a journal of neurology*, 122 (Pt 8). Available at: https://doi.org/10.1093/brain/122.8.1437.

Danecek, P. *et al.* (2021) 'Twelve years of SAMtools and BCFtools', *GigaScience*, 10(2), p. giab008. Available at: https://doi.org/10.1093/gigascience/giab008.

Danese, A. *et al.* (2021) 'Cell death as a result of calcium signaling modulation: A cancer-centric prospective', *Biochimica et Biophysica Acta (BBA) - Molecular Cell Research*, 1868(8), p. 119061. Available at: https://doi.org/10.1016/j.bbamcr.2021.119061.

Dawson, T.M. and Dawson, V.L. (2010) 'The Role of Parkin in Familial and Sporadic Parkinson's Disease', *Movement disorders : official journal of the Movement Disorder Society*, 25(0 1), pp. S32–S39. Available at: https://doi.org/10.1002/mds.22798.

De Pablo-Fernández, E. *et al.* (2019) 'Prognosis and Neuropathologic Correlation of Clinical Subtypes of Parkinson Disease', *JAMA Neurology*, 76(4), p. 470. Available at: https://doi.org/10.1001/jamaneurol.2018.4377.

Deegan, S. *et al.* (2015) 'A close connection between the PERK and IRE arms of the UPR and the transcriptional regulation of autophagy', *Biochemical and Biophysical Research Communications*, 456(1), pp. 305–311. Available at: https://doi.org/10.1016/j.bbrc.2014.11.076.

Delic, V. *et al.* (2020) 'Biological links between traumatic brain injury and Parkinson's disease', *Acta Neuropathologica Communications*, 8(1), p. 45. Available at: https://doi.org/10.1186/s40478-020-00924-7.

Deng, H., Wang, P. and Jankovic, J. (2018) 'The genetics of Parkinson disease', *Ageing Research Reviews*, 42, pp. 72–85. Available at: https://doi.org/10.1016/j.arr.2017.12.007.

Derrien, T. *et al.* (2012) 'The GENCODE v7 catalog of human long noncoding RNAs: Analysis of their gene structure, evolution, and expression', *Genome Research*, 22(9), pp. 1775–1789. Available at: https://doi.org/10.1101/gr.132159.111.

Deuschl, G. *et al.* (2006) 'A Randomized Trial of Deep-Brain Stimulation for Parkinson's Disease', *n engl j med* [Preprint].

Deveson, I.W. *et al.* (2017) 'The Dimensions, Dynamics, and Relevance of the Mammalian Noncoding Transcriptome', *Trends in genetics: TIG*, 33(7), pp. 464–478. Available at: https://doi.org/10.1016/j.tig.2017.04.004.

Devi, G. *et al.* (2015) 'RNA triplexes: from structural principles to biological and biotech applications', *Wiley interdisciplinary reviews. RNA*, 6(1), pp. 111–128. Available at: https://doi.org/10.1002/wrna.1261.

Diederichs, S. (2014) 'The four dimensions of noncoding RNA conservation', *Trends in Genetics*, 30(4), pp. 121–123. Available at: https://doi.org/10.1016/j.tig.2014.01.004.

Dijkstra, A.A. *et al.* (2014) 'Stage-dependent nigral neuronal loss in incidental Lewy body and Parkinson's disease', *Movement Disorders: Official Journal of the Movement Disorder Society*, 29(10), pp. 1244–1251. Available at: https://doi.org/10.1002/mds.25952.

DiStefano, J.K. (2018) 'The Emerging Role of Long Noncoding RNAs in Human Disease', *Methods in Molecular Biology (Clifton, N.J.)*, 1706, pp. 91–110. Available at: https://doi.org/10.1007/978-1-4939-7471-9_6.

Djebali, S. *et al.* (2012) 'Landscape of transcription in human cells', *Nature*, 489(7414), pp. 101–108. Available at: https://doi.org/10.1038/nature11233.

Dlamini, M.B. *et al.* (2021) 'The crosstalk between mitochondrial dysfunction and endoplasmic reticulum stress promoted ATF4-mediated mitophagy induced by hexavalent chromium', *Environmental Toxicology*, 36(6), pp. 1162–1172. Available at: https://doi.org/10.1002/tox.23115.

Dluzen, D. *et al.* (2011) 'BCL-2 Is a Downstream Target of ATF5 That Mediates the Prosurvival Function of ATF5 in a Cell Type-dependent Manner', *Journal of Biological Chemistry*, 286(9), pp. 7705–7713. Available at: https://doi.org/10.1074/jbc.M110.207639.

Dobin, A. *et al.* (2013) 'STAR: ultrafast universal RNA-seq aligner', *Bioinformatics (Oxford, England)*, 29(1), pp. 15–21. Available at: https://doi.org/10.1093/bioinformatics/bts635.

Dogan, S.A. *et al.* (2014) 'Tissue-Specific Loss of DARS2 Activates Stress Responses Independently of Respiratory Chain Deficiency in the Heart', *Cell Metabolism*, 19(3), pp. 458–469. Available at: https://doi.org/10.1016/j.cmet.2014.02.004.

Dong, Y. *et al.* (2017) 'Long noncoding RNAs coordinate functions between mitochondria and the nucleus', *Epigenetics & Chromatin*, 10(1), p. 41. Available at: https://doi.org/10.1186/s13072-017-0149-x.

Dorsey, E.R., Elbaz, A., *et al.* (2018) 'Global, regional, and national burden of Parkinson's disease, 1990–2016: a systematic analysis for the Global Burden of Disease Study

2016', *The Lancet Neurology*, 17(11), pp. 939–953. Available at: https://doi.org/10.1016/S1474-4422(18)30295-3.

Dorsey, E.R., Sherer, T., *et al.* (2018) 'The Emerging Evidence of the Parkinson Pandemic', *Journal of Parkinson's Disease*, 8(Suppl 1), pp. S3–S8. Available at: https://doi.org/10.3233/JPD-181474.

Driver, J.A. *et al.* (2008) 'Parkinson disease and risk of mortality: A prospective comorbidity-matched cohort study', *Neurology*, 70(Issue 16, Part 2), pp. 1423–1430. Available at: https://doi.org/10.1212/01.wnl.0000310414.85144.ee.

Egawa, N. *et al.* (2011) 'The Endoplasmic Reticulum Stress Sensor, ATF6α, Protects against Neurotoxin-induced Dopaminergic Neuronal Death', *Journal of Biological Chemistry*, 286(10), pp. 7947–7957. Available at: https://doi.org/10.1074/jbc.M110.156430.

Ehringer, H. and Hornykiewicz, O. (1960) '[Distribution of noradrenaline and dopamine (3-hydroxytyramine) in the human brain and their behavior in diseases of the extrapyramidal system]', *Klinische Wochenschrift*, 38, pp. 1236–1239. Available at: https://doi.org/10.1007/BF01485901.

Ehringer, H. and Hornykiewicz, O. (1998) 'Distribution of noradrenaline and dopamine (3-hydroxytyramine) in the human brain and their behavior in diseases of the extrapyramidal system', *Parkinsonism & Related Disorders*, 4(2), pp. 53–57. Available at: https://doi.org/10.1016/s1353-8020(98)00012-1.

Elbaz, A. *et al.* (2016) 'Epidemiology of Parkinson's disease', *Revue Neurologique*, 172(1), pp. 14–26. Available at: https://doi.org/10.1016/j.neurol.2015.09.012.

ENCODE Project Consortium (2012) 'An integrated encyclopedia of DNA elements in the human genome', *Nature*, 489(7414), pp. 57–74. Available at: https://doi.org/10.1038/nature11247.

Engreitz, J.M. *et al.* (2014) 'RNA-RNA Interactions Enable Specific Targeting of Noncoding RNAs to Nascent Pre-mRNAs and Chromatin Sites', *Cell*, 159(1), pp. 188–199. Available at: https://doi.org/10.1016/j.cell.2014.08.018.

Engreitz, J.M. *et al.* (2016) 'Local regulation of gene expression by lncRNA promoters, transcription and splicing', *Nature*, 539(7629), pp. 452–455. Available at: https://doi.org/10.1038/nature20149.

Espay, A.J. *et al.* (2021) 'Rivastigmine in Parkinson's Disease Dementia with Orthostatic Hypotension', *Annals of Neurology*, 89(1), pp. 91–98. Available at: https://doi.org/10.1002/ana.25923.

Esteves, A.R. and Cardoso, S.M. (2020) 'Differential protein expression in diverse brain areas of Parkinson's and Alzheimer's disease patients', *Scientific Reports*, 10(1), p. 13149. Available at: https://doi.org/10.1038/s41598-020-70174-z.

Fabbrini, A. and Guerra, A. (2021) 'Pathophysiological Mechanisms and Experimental Pharmacotherapy for L-Dopa-Induced Dyskinesia', *Journal of Experimental Pharmacology*, Volume 13, pp. 469–485. Available at: https://doi.org/10.2147/JEP.S265282.

Faghihi, M.A. *et al.* (2008) 'Expression of a noncoding RNA is elevated in Alzheimer's disease and drives rapid feed-forward regulation of beta-secretase', *Nature Medicine*, 14(7), pp. 723–730. Available at: https://doi.org/10.1038/nm1784.

Fan, P. and Jordan, V.C. (2022) 'PERK, Beyond an Unfolded Protein Response Sensor in Estrogen-Induced Apoptosis in Endocrine-Resistant Breast Cancer', *Molecular cancer research: MCR*, 20(2), pp. 193–201. Available at: https://doi.org/10.1158/1541-7786.MCR-21-0702.

Fang, F. *et al.* (2012) 'Head injury and Parkinson's disease: a population-based study', *Movement Disorders: Official Journal of the Movement Disorder Society*, 27(13), pp. 1632–1635. Available at: https://doi.org/10.1002/mds.25143.

Fang, M. *et al.* (2017) 'Bioinformatics and co-expression network analysis of differentially expressed lncRNAs and mRNAs in hippocampus of APP/PS1 transgenic mice with Alzheimer disease', *American Journal of Translational Research*, 9(3), pp. 1381–1391.

Fanucchi, S. *et al.* (2019) 'Immune genes are primed for robust transcription by proximal long noncoding RNAs located in nuclear compartments', *Nature Genetics*, 51(1), pp. 138–150. Available at: https://doi.org/10.1038/s41588-018-0298-2.

Fatica, A. and Bozzoni, I. (2014) 'Long non-coding RNAs: new players in cell differentiation and development', *Nature Reviews. Genetics*, 15(1), pp. 7–21. Available at: https://doi.org/10.1038/nrg3606.

Fei, J. *et al.* (2017) 'Quantitative analysis of multilayer organization of proteins and RNA in nuclear speckles at super resolution', *Journal of Cell Science*, p. jcs.206854. Available at: https://doi.org/10.1242/jcs.206854.

Fereshtehnejad, S.-M. *et al.* (2017) 'Clinical criteria for subtyping Parkinson's disease: biomarkers and longitudinal progression', *Brain*, 140(7), pp. 1959–1976. Available at: https://doi.org/10.1093/brain/awx118.

Fernandes, H.J.R. *et al.* (2016) 'ER Stress and Autophagic Perturbations Lead to Elevated Extracellular α-Synuclein in GBA-N370S Parkinson's iPSC-Derived Dopamine Neurons', *Stem Cell Reports*, 6(3), pp. 342–356. Available at: https://doi.org/10.1016/j.stemcr.2016.01.013.

Fickett, J.W. and Tung, C.S. (1992) 'Assessment of protein coding measures', *Nucleic Acids Research*, 20(24), pp. 6441–6450. Available at: https://doi.org/10.1093/nar/20.24.6441.

Fiorenzano, A. *et al.* (2021) 'Single-cell transcriptomics captures features of human midbrain development and dopamine neuron diversity in brain organoids', *Nature Communications*, 12(1), p. 7302. Available at: https://doi.org/10.1038/s41467-021-27464-5.

Fiorese, C.J. *et al.* (2016) 'The Transcription Factor ATF5 Mediates a Mammalian Mitochondrial UPR', *Current Biology*, 26(15), pp. 2037–2043. Available at: https://doi.org/10.1016/j.cub.2016.06.002.

Flippo, K.H. and Strack, S. (2017) 'Mitochondrial dynamics in neuronal injury, development and plasticity', *Journal of Cell Science*, p. jcs.171017. Available at: https://doi.org/10.1242/jcs.171017.

Foehring, R.C. *et al.* (2009) 'Endogenous Calcium Buffering Capacity of Substantia Nigral Dopamine Neurons', *Journal of Neurophysiology*, 102(4), pp. 2326–2333. Available at: https://doi.org/10.1152/jn.00038.2009.

Forsaa, E.B. *et al.* (2010) 'What predicts mortality in Parkinson disease?: A prospective population-based long-term study', *Neurology*, 75(14), pp. 1270–1276. Available at: https://doi.org/10.1212/WNL.0b013e3181f61311.

Forsström, S. *et al.* (2019) 'Fibroblast Growth Factor 21 Drives Dynamics of Local and Systemic Stress Responses in Mitochondrial Myopathy with mtDNA Deletions', *Cell Metabolism*, 30(6), pp. 1040-1054.e7. Available at: https://doi.org/10.1016/j.cmet.2019.08.019.

Franco, A. *et al.* (2022) 'Mitochondrial Dysfunction and Pharmacodynamics of Mitofusin Activation in Murine Charcot-Marie-Tooth Disease Type 2A', *Journal of Pharmacology and Experimental Therapeutics*, 383(2), pp. 137–148. Available at: https://doi.org/10.1124/jpet.122.001332.

Gai, W. *et al.* (1991) 'Substance P-containing neurons in the mesopontine tegmentum are severely affected in Parkinson's disease', *Brain : a journal of neurology*, 114 (Pt 5). Available at: https://doi.org/10.1093/brain/114.5.2253.

Gai, W.P. *et al.* (1992) 'Age-related loss of dorsal vagal neurons in Parkinson's disease', *Neurology*, 42(11), pp. 2106–2111. Available at: https://doi.org/10.1212/wnl.42.11.2106.

Galbiati, A. *et al.* (2019) 'The risk of neurodegeneration in REM sleep behavior disorder: A systematic review and meta-analysis of longitudinal studies', *Sleep Medicine Reviews*, 43, pp. 37–46. Available at: https://doi.org/10.1016/j.smrv.2018.09.008.

Gamber, K.M. (2016) 'Animal Models of Parkinson's Disease: New models provide greater translational and predictive value', *BioTechniques*, 61(4), pp. 210–211. Available at: https://doi.org/10.2144/000114463.

Gao, X. *et al.* (2011) 'Use of ibuprofen and risk of Parkinson disease', *Neurology*, 76(10), pp. 863–869. Available at: https://doi.org/10.1212/WNL.0b013e31820f2d79.

Gao, X.-Y. *et al.* (2022) 'Mitochondrial Dysfunction in Parkinson's Disease: From Mechanistic Insights to Therapy', *Frontiers in Aging Neuroscience*, 14. Available at: https://www.frontiersin.org/articles/10.3389/fnagi.2022.885500 (Accessed: 16 November 2023).

García-Osta, A. *et al.* (2022) 'p27, The Cell Cycle and Alzheimer´s Disease', *International Journal of Molecular Sciences*, 23(3), p. 1211. Available at: https://doi.org/10.3390/ijms23031211.

Gash, D.M. *et al.* (2008) 'Trichloroethylene: Parkinsonism and complex 1 mitochondrial neurotoxicity', *Annals of Neurology*, 63(2), pp. 184–192. Available at: https://doi.org/10.1002/ana.21288.

Gatica, D., Lahiri, V. and Klionsky, D.J. (2018) 'Cargo Recognition and Degradation by Selective Autophagy', *Nature cell biology*, 20(3), pp. 233–242. Available at: https://doi.org/10.1038/s41556-018-0037-z.

Gautier, C.A. *et al.* (2016) 'The endoplasmic reticulum-mitochondria interface is perturbed in PARK2 knockout mice and patients with PARK2 mutations', *Human Molecular Genetics*, 25(14), pp. 2972–2984. Available at: https://doi.org/10.1093/hmg/ddw148.

Gautier, C.A., Kitada, T. and Shen, J. (2008) 'Loss of PINK1 causes mitochondrial functional defects and increased sensitivity to oxidative stress', *Proceedings of the National Academy of Sciences of the United States of America*, 105(32), pp. 11364–11369. Available at: https://doi.org/10.1073/pnas.0802076105.

Ge, Y. *et al.* (2020) 'Two forms of Opa1 cooperate to complete fusion of the mitochondrial inner-membrane', *eLife*, 9, p. e50973. Available at: https://doi.org/10.7554/eLife.50973.

Gendron, J. *et al.* (2019) 'Long non-coding RNA repertoire and open chromatin regions constitute midbrain dopaminergic neuron - specific molecular signatures', *Scientific Reports*, 9(1), p. 1409. Available at: https://doi.org/10.1038/s41598-018-37872-1.

Georgakopoulos, N.D., Wells, G. and Campanella, M. (2017) 'The pharmacological regulation of cellular mitophagy', *Nature Chemical Biology*, 13(2), pp. 136–146. Available at: https://doi.org/10.1038/nchembio.2287.

George, J.M. *et al.* (1995) 'Characterization of a novel protein regulated during the critical period for song learning in the zebra finch', *Neuron*, 15(2), pp. 361–372. Available at: https://doi.org/10.1016/0896-6273(95)90040-3.

German, D.C. *et al.* (1992) 'Disease-specific patterns of locus coeruleus cell loss', *Annals of neurology*, 32(5). Available at: https://doi.org/10.1002/ana.410320510.

Ghribi, O. *et al.* (2003) 'MPP+ induces the endoplasmic reticulum stress response in rabbit brain involving activation of the ATF-6 and NF-kappaB signaling pathways', *Journal of Neuropathology and Experimental Neurology*, 62(11), pp. 1144–1153. Available at: https://doi.org/10.1093/jnen/62.11.1144.

Giacomello, M. and Pellegrini, L. (2016) 'The coming of age of the mitochondria-ER contact: a matter of thickness', *Cell Death and Differentiation*, 23(9), pp. 1417–1427. Available at: https://doi.org/10.1038/cdd.2016.52.

Giannakakis, A. *et al.* (2015) 'Contrasting expression patterns of coding and noncoding parts of the human genome upon oxidative stress', *Scientific Reports*, 5(1), p. 9737. Available at: https://doi.org/10.1038/srep09737.

Giasson, B.I. *et al.* (2001) 'A hydrophobic stretch of 12 amino acid residues in the middle of alpha-synuclein is essential for filament assembly', *The Journal of Biological Chemistry*, 276(4), pp. 2380–2386. Available at: https://doi.org/10.1074/jbc.M008919200.

Giguère, N., Burke Nanni, S. and Trudeau, L.-E. (2018) 'On Cell Loss and Selective Vulnerability of Neuronal Populations in Parkinson's Disease', *Frontiers in Neurology*, 9, p. 455. Available at: https://doi.org/10.3389/fneur.2018.00455.

Gil, N. and Ulitsky, I. (2020) 'Regulation of gene expression by cis-acting long non-coding RNAs', *Nature Reviews Genetics*, 21(2), pp. 102–117. Available at: https://doi.org/10.1038/s41576-019-0184-5.

Gillespie, M. *et al.* (2022) 'The reactome pathway knowledgebase 2022', *Nucleic Acids Research*, 50(D1), pp. D687–D692. Available at: https://doi.org/10.1093/nar/gkab1028.

Gillies, G.E. *et al.* (2014) 'Sex differences in Parkinson's disease', *Frontiers in Neuroendocrinology*, 35(3), pp. 370–384. Available at: https://doi.org/10.1016/j.yfrne.2014.02.002.

Gkikas, I., Palikaras, K. and Tavernarakis, N. (2018) 'The Role of Mitophagy in Innate Immunity', *Frontiers in Immunology*, 9, p. 1283. Available at: https://doi.org/10.3389/fimmu.2018.01283.

de Goede, O.M. *et al.* (2021) 'Population-scale tissue transcriptomics maps long non-coding RNAs to complex disease', *Cell*, 184(10), pp. 2633-2648.e19. Available at: https://doi.org/10.1016/j.cell.2021.03.050.

Goff, L.A. and Rinn, J.L. (2015) 'Linking RNA biology to lncRNAs', *Genome Research*, 25(10), pp. 1456–1465. Available at: https://doi.org/10.1101/gr.191122.115.

Gomez-Lazaro, M. *et al.* (2008) '6-Hydroxydopamine (6-OHDA) induces Drp1-dependent mitochondrial fragmentation in SH-SY5Y cells', *Free Radical Biology and Medicine*, 44(11), pp. 1960–1969. Available at: https://doi.org/10.1016/j.freeradbiomed.2008.03.009.

Gong, C. and Maquat, L.E. (2011) 'lncRNAs transactivate STAU1-mediated mRNA decay by duplexing with 3′ UTRs via Alu elements', *Nature*, 470(7333), pp. 284–288. Available at: https://doi.org/10.1038/nature09701.

Gowers, W.R. (1888) 'A manual of diseases of the nervous system'.

Grassi, D. *et al.* (2018) 'Identification of a highly neurotoxic α-synuclein species inducing mitochondrial damage and mitophagy in Parkinson's disease', *Proceedings of the National Academy of Sciences*, 115(11). Available at: https://doi.org/10.1073/pnas.1713849115.

Grossi, E. *et al.* (2020) 'A lncRNA-SWI/SNF complex crosstalk controls transcriptional activation at specific promoter regions', *Nature Communications*, 11(1), p. 936. Available at: https://doi.org/10.1038/s41467-020-14623-3.

Grünewald, A. *et al.* (2014) 'Does Uncoupling Protein 2 Expression Qualify as Marker of Disease Status in LRRK2-Associated Parkinson's Disease?', *Antioxidants & Redox Signaling*, 20(13), pp. 1955–1960. Available at: https://doi.org/10.1089/ars.2013.5737.

Grünewald, A., Kumar, K.R. and Sue, C.M. (2019) 'New insights into the complex role of mitochondria in Parkinson's disease', *Progress in Neurobiology*, 177, pp. 73–93. Available at: https://doi.org/10.1016/j.pneurobio.2018.09.003.

Guo, C. *et al.* (2020) 'Pathophysiological Functions of the lncRNA TUG1', *Current Pharmaceutical Design*, 26(6), pp. 688–700. Available at: https://doi.org/10.2174/1381612826666191227154009.

Guo, C.-J. *et al.* (2020) 'Distinct Processing of lncRNAs Contributes to Non-conserved Functions in Stem Cells', *Cell*, 181(3), pp. 621-636.e22. Available at: https://doi.org/10.1016/j.cell.2020.03.006.

Guo, F. *et al.* (2015) 'Regulation of MALAT1 expression by TDP43 controls the migration and invasion of non-small cell lung cancer cells in vitro', *Biochemical and Biophysical Research Communications*, 465(2), pp. 293–298. Available at: https://doi.org/10.1016/j.bbrc.2015.08.027.

Guo, J.-C. *et al.* (2019) 'CNIT: a fast and accurate web tool for identifying protein-coding and long non-coding transcripts based on intrinsic sequence composition', *Nucleic Acids Research*, 47(W1), pp. W516–W522. Available at: https://doi.org/10.1093/nar/gkz400.

Guo, K. *et al.* (2021) 'LncRNA-MIAT promotes thyroid cancer progression and function as ceRNA to target EZH2 by sponging miR-150-5p', *Cell Death & Disease*, 12(12), p. 1097. Available at: https://doi.org/10.1038/s41419-021-04386-0.

Guo, X. *et al.* (2020) 'Mitochondrial stress is relayed to the cytosol by an OMA1-DELE1-HRI pathway', *Nature*, 579(7799), pp. 427–432. Available at: https://doi.org/10.1038/s41586-020-2078-2.

Guttman, M. *et al.* (2009) 'Chromatin signature reveals over a thousand highly conserved large non-coding RNAs in mammals', *Nature*, 458(7235), pp. 223–227. Available at: https://doi.org/10.1038/nature07672.

Guzman, J.N. *et al.* (2010) 'Oxidant stress evoked by pacemaking in dopaminergic neurons is attenuated by DJ-1', *Nature*, 468(7324), pp. 696–700. Available at: https://doi.org/10.1038/nature09536.

Hacisuleyman, E. *et al.* (2014) 'Topological organization of multichromosomal regions by the long intergenic noncoding RNA Firre', *Nature Structural & Molecular Biology*, 21(2), pp. 198–206. Available at: https://doi.org/10.1038/nsmb.2764.

Hall, H. *et al.* (2014) 'Hippocampal Lewy pathology and cholinergic dysfunction are associated with dementia in Parkinson's disease', *Brain*, 137(9), pp. 2493–2508. Available at: https://doi.org/10.1093/brain/awu193.

Hanss, Z. *et al.* (2021) 'Mitochondrial and Clearance Impairment in p. D620N VPS35 Patient-Derived Neurons', *Movement Disorders*, 36(3), pp. 704–715. Available at: https://doi.org/10.1002/mds.28365.

Hashida, K. *et al.* (2012) 'ATF6alpha Promotes Astroglial Activation and Neuronal Survival in a Chronic Mouse Model of Parkinson's Disease', *PLoS ONE*. Edited by M. Asanuma, 7(10), p. e47950. Available at: https://doi.org/10.1371/journal.pone.0047950.

Hawkes, C.H., Del Tredici, K. and Braak, H. (2007) 'Parkinson's disease: a dual-hit hypothesis', *Neuropathology and Applied Neurobiology*, 33(6), pp. 599–614. Available at: https://doi.org/10.1111/j.1365-2990.2007.00874.x.

Haze, K. *et al.* (1999) 'Mammalian Transcription Factor ATF6 Is Synthesized as a Transmembrane Protein and Activated by Proteolysis in Response to Endoplasmic Reticulum Stress', *Molecular Biology of the Cell*. Edited by P. Silver, 10(11), pp. 3787–3799. Available at: https://doi.org/10.1091/mbc.10.11.3787.

Hebert, A.S. *et al.* (2013) 'Calorie Restriction and SIRT3 Trigger Global Reprogramming of the Mitochondrial Protein Acetylome', *Molecular Cell*, 49(1), pp. 186–199. Available at: https://doi.org/10.1016/j.molcel.2012.10.024.

Heger, L.M. *et al.* (2021) 'Mitochondrial Phenotypes in Parkinson's Diseases—A Focus on Human iPSC-Derived Dopaminergic Neurons', *Cells*, 10(12), p. 3436. Available at: https://doi.org/10.3390/cells10123436.

Heinz, S. *et al.* (2018) 'Transcription Elongation Can Affect Genome 3D Structure', *Cell*, 174(6), pp. 1522-1536.e22. Available at: https://doi.org/10.1016/j.cell.2018.07.047.

Heman-Ackah, S.M. *et al.* (2017) 'Alpha-synuclein induces the unfolded protein response in Parkinson's disease SNCA triplication iPSC-derived neurons', *Human Molecular Genetics*, 26(22), pp. 4441–4450. Available at: https://doi.org/10.1093/hmg/ddx331.

Henderson, M.X., Trojanowski, J.Q. and Lee, V.M.-Y. (2019) 'α-Synuclein pathology in Parkinson's disease and related α-synucleinopathies', *Neuroscience Letters*, 709, p. 134316. Available at: https://doi.org/10.1016/j.neulet.2019.134316.

Henis-Korenblit, S. *et al.* (2010) 'Insulin/IGF-1 signaling mutants reprogram ER stress response regulators to promote longevity', *Proceedings of the National Academy of*

Sciences, 107(21), pp. 9730–9735. Available at: https://doi.org/10.1073/pnas.1002575107.

Henrich, M.T. *et al.* (2023) 'Mitochondrial dysfunction in Parkinson's disease – a key disease hallmark with therapeutic potential', *Molecular Neurodegeneration*, 18(1), p. 83. Available at: https://doi.org/10.1186/s13024-023-00676-7.

Hepp, D.H. *et al.* (2013) 'Pedunculopontine cholinergic cell loss in hallucinating Parkinson disease patients but not in dementia with Lewy bodies patients', *Journal of Neuropathology and Experimental Neurology*, 72(12), pp. 1162–1170. Available at: https://doi.org/10.1097/NEN.0000000000000014.

Hernán, M.A. *et al.* (2001) 'Cigarette smoking and the incidence of Parkinson's disease in two prospective studies', *Annals of Neurology*, 50(6), pp. 780–786. Available at: https://doi.org/10.1002/ana.10028.

Hernán, M.A., Logroscino, G. and García Rodríguez, L.A. (2006) 'Nonsteroidal anti-inflammatory drugs and the incidence of Parkinson disease', *Neurology*, 66(7), pp. 1097–1099. Available at: https://doi.org/10.1212/01.wnl.0000204446.82823.28.

Hetz, C., Zhang, K. and Kaufman, R.J. (2020) 'Mechanisms, regulation and functions of the unfolded protein response', *Nature Reviews Molecular Cell Biology*, 21(8), pp. 421–438. Available at: https://doi.org/10.1038/s41580-020-0250-z.

Hezroni, H. *et al.* (2015) 'Principles of Long Noncoding RNA Evolution Derived from Direct Comparison of Transcriptomes in 17 Species', *Cell Reports*, 11(7), pp. 1110–1122. Available at: https://doi.org/10.1016/j.celrep.2015.04.023.

Hinnebusch, A.G., Ivanov, I.P. and Sonenberg, N. (2016) 'Translational control by 5′-untranslated regions of eukaryotic mRNAs', *Science*, 352(6292), pp. 1413–1416. Available at: https://doi.org/10.1126/science.aad9868.

Hirsch, E.C. and Hunot, S. (2009) 'Neuroinflammation in Parkinson's disease: a target for neuroprotection?', *The Lancet. Neurology*, 8(4), pp. 382–397. Available at: https://doi.org/10.1016/S1474-4422(09)70062-6.

Hirsch, E.C., Vyas, S. and Hunot, S. (2012) 'Neuroinflammation in Parkinson's disease', *Parkinsonism & Related Disorders*, 18 Suppl 1, pp. S210-212. Available at: https://doi.org/10.1016/S1353-8020(11)70065-7.

Holdt, L.M. *et al.* (2013) 'Alu Elements in ANRIL Non-Coding RNA at Chromosome 9p21 Modulate Atherogenic Cell Functions through Trans-Regulation of Gene Networks', *PLoS Genetics*. Edited by M.I. McCarthy, 9(7), p. e1003588. Available at: https://doi.org/10.1371/journal.pgen.1003588.

Hollville, E., Romero, S.E. and Deshmukh, M. (2019) 'Apoptotic Cell Death Regulation in Neurons', *The FEBS journal*, 286(17), pp. 3276–3298. Available at: https://doi.org/10.1111/febs.14970.

Hoozemans, J.J.M. *et al.* (2007) 'Activation of the unfolded protein response in Parkinson's disease', *Biochemical and Biophysical Research Communications*, 354(3), pp. 707–711. Available at: https://doi.org/10.1016/j.bbrc.2007.01.043.

Hornykiewicz, O. (1998) 'Biochemical aspects of Parkinson's disease', *Neurology*, 51(2 Suppl 2), pp. S2-9. Available at: https://doi.org/10.1212/wnl.51.2_suppl_2.s2.

Hornykiewicz, O. (2002) 'Dopamine miracle: From brain homogenate to dopamine replacement', *Movement Disorders*, 17(3), pp. 501–508. Available at: https://doi.org/10.1002/mds.10115.

Hou, X. *et al.* (2018) 'Age- and disease-dependent increase of the mitophagy marker phospho-ubiquitin in normal aging and Lewy body disease', *Autophagy*, 14(8), pp. 1404–1418. Available at: https://doi.org/10.1080/15548627.2018.1461294.

Hourihan, J.M. *et al.* (2016) 'Cysteine sulfenylation directs IRE-1 to activate the SKN-1/Nrf2 antioxidant response', *Molecular cell*, 63(4), pp. 553–566. Available at: https://doi.org/10.1016/j.molcel.2016.07.019.

Houtkooper, R.H. *et al.* (2013) 'Mitonuclear protein imbalance as a conserved longevity mechanism', *Nature*, 497(7450), pp. 451–457. Available at: https://doi.org/10.1038/nature12188.

Hsieh, C.-H. *et al.* (2016) 'Functional Impairment in Miro Degradation and Mitophagy Is a Shared Feature in Familial and Sporadic Parkinson's Disease', *Cell Stem Cell*, 19(6), pp. 709–724. Available at: https://doi.org/10.1016/j.stem.2016.08.002.

Hsieh, T.-H.S. *et al.* (2020) 'Resolving the 3D Landscape of Transcription-Linked Mammalian Chromatin Folding', *Molecular Cell*, 78(3), pp. 539-553.e8. Available at: https://doi.org/10.1016/j.molcel.2020.03.002.

Hu, D. *et al.* (2019) 'Alpha-synuclein suppresses mitochondrial protease ClpP to trigger mitochondrial oxidative damage and neurotoxicity', *Acta Neuropathologica*, 137(6), pp. 939–960. Available at: https://doi.org/10.1007/s00401-019-01993-2.

Hu, D., Liu, Z. and Qi, X. (2021) 'UPRmt activation protects against MPP+-induced toxicity in a cell culture model of Parkinson's disease', *Biochemical and Biophysical Research Communications*, 569, pp. 17–22. Available at: https://doi.org/10.1016/j.bbrc.2021.06.079.

Hu, Gang *et al.* (2007) 'Coffee and tea consumption and the risk of Parkinson's disease - PubMed', *Movement disorders : official journal of the Movement Disorder Society*, 22(15), pp. 2242–2248. Available at: https://doi.org/10.1002/mds.21706.

Huarte, M. *et al.* (2010) 'A Large Intergenic Noncoding RNA Induced by p53 Mediates Global Gene Repression in the p53 Response', *Cell*, 142(3), pp. 409–419. Available at: https://doi.org/10.1016/j.cell.2010.06.040.

Hughes, D. and Mallucci, G.R. (2019) 'The unfolded protein response in neurodegenerative disorders – therapeutic modulation of the PERK pathway', *The FEBS Journal*, 286(2), pp. 342–355. Available at: https://doi.org/10.1111/febs.14422.

Hutchinson, J.N. *et al.* (2007) 'A screen for nuclear transcripts identifies two linked noncoding RNAs associated with SC35 splicing domains', *BMC Genomics*, 8(1), p. 39. Available at: https://doi.org/10.1186/1471-2164-8-39.

Hwang, J. and Qi, L. (2018) 'Quality Control in the Endoplasmic Reticulum: Crosstalk between ERAD and UPR pathways', *Trends in Biochemical Sciences*, 43(8), pp. 593–605. Available at: https://doi.org/10.1016/j.tibs.2018.06.005.

Iljina, M. *et al.* (2016) 'Kinetic model of the aggregation of alpha-synuclein provides insights into prion-like spreading', *Proceedings of the National Academy of Sciences*, 113(9). Available at: https://doi.org/10.1073/pnas.1524128113.

Imai, Y. *et al.* (2001) 'An unfolded putative transmembrane polypeptide, which can lead to endoplasmic reticulum stress, is a substrate of Parkin', *Cell*, 105(7), pp. 891–902. Available at: https://doi.org/10.1016/s0092-8674(01)00407-x.

Imai, Y., Soda, M. and Takahashi, R. (2000) 'Parkin suppresses unfolded protein stress-induced cell death through its E3 ubiquitin-protein ligase activity', *The Journal of*

Biological Chemistry, 275(46), pp. 35661–35664. Available at: https://doi.org/10.1074/jbc.C000447200.

Ishii, N. *et al.* (2006) 'Identification of a novel non-coding RNA, MIAT, that confers risk of myocardial infarction', *Journal of Human Genetics*, 51(12), pp. 1087–1099. Available at: https://doi.org/10.1007/s10038-006-0070-9.

Ivanes, F. *et al.* (2014) 'The compound BTB06584 is an IF $_1$ -dependent selective inhibitor of the mitochondrial F $_1$ Fo-ATPase: Pharmacological regulation of the F $_1$ Fo-ATPase', *British Journal of Pharmacology*, 171(18), pp. 4193–4206. Available at: https://doi.org/10.1111/bph.12638.

Iwai, A. *et al.* (1995) 'The precursor protein of non-A beta component of Alzheimer's disease amyloid is a presynaptic protein of the central nervous system', *Neuron*, 14(2), pp. 467–475. Available at: https://doi.org/10.1016/0896-6273(95)90302-x.

Iyer, M.K. *et al.* (2015) 'The landscape of long noncoding RNAs in the human transcriptome', *Nature Genetics*, 47(3), pp. 199–208. Available at: https://doi.org/10.1038/ng.3192.

Jain, A.K. *et al.* (2016) 'LncPRESS1 Is a p53-Regulated LncRNA that Safeguards Pluripotency by Disrupting SIRT6-Mediated De-acetylation of Histone H3K56', *Molecular Cell*, 64(5), pp. 967–981. Available at: https://doi.org/10.1016/j.molcel.2016.10.039.

Jalali, S. *et al.* (2015) 'Computational approaches towards understanding human long non-coding RNA biology', *Bioinformatics (Oxford, England)*, 31(14), pp. 2241–2251. Available at: https://doi.org/10.1093/bioinformatics/btv148.

Jang, S.-K. *et al.* (2021) 'Inhibition of mTORC1 through ATF4-induced REDD1 and Sestrin2 expression by Metformin', *BMC Cancer*, 21(1), p. 803. Available at: https://doi.org/10.1186/s12885-021-08346-x.

Jarroux, J., Morillon, A. and Pinskaya, M. (2017) 'History, Discovery, and Classification of lncRNAs', in M.R.S. Rao (ed.) *Long Non Coding RNA Biology*. Singapore: Springer Singapore (Advances in Experimental Medicine and Biology), pp. 1–46. Available at: https://doi.org/10.1007/978-981-10-5203-3_1.

Jia, F., Fellner, A. and Kumar, K.R. (2022) 'Monogenic Parkinson's Disease: Genotype, Phenotype, Pathophysiology, and Genetic Testing', *Genes*, 13(3), p. 471. Available at: https://doi.org/10.3390/genes13030471.

Jiang, C. *et al.* (2016) 'Identifying and functionally characterizing tissue-specific and ubiquitously expressed human lncRNAs', *Oncotarget*, 7(6), pp. 7120–7133. Available at: https://doi.org/10.18632/oncotarget.6859.

Jiang, D. *et al.* (2020) 'ATF4 Mediates Mitochondrial Unfolded Protein Response in Alveolar Epithelial Cells', *American Journal of Respiratory Cell and Molecular Biology*, 63(4), pp. 478–489. Available at: https://doi.org/10.1165/rcmb.2020-0107OC.

Jiang, J. *et al.* (2020) 'LncRNA H19 diminishes dopaminergic neuron loss by mediating microRNA-301b-3p in Parkinson's disease via the HPRT1-mediated Wnt/β-catenin signaling pathway', *Aging*, 12(10), pp. 8820–8836. Available at: https://doi.org/10.18632/aging.102877.

Jiao, F.-J. *et al.* (2017) 'CDK5-mediated phosphorylation of XBP1s contributes to its nuclear translocation and activation in MPP+-induced Parkinson's disease model',

Scientific Reports, 7, p. 5622. Available at: https://doi.org/10.1038/s41598-017-06012-6.

Jin, S.M. *et al.* (2010) 'Mitochondrial membrane potential regulates PINK1 import and proteolytic destabilization by PARL', *Journal of Cell Biology*, 191(5), pp. 933–942. Available at: https://doi.org/10.1083/jcb.201008084.

Jin, U., Park, S.J. and Park, S.M. (2019) 'Cholesterol Metabolism in the Brain and Its Association with Parkinson's Disease', *Experimental Neurobiology*, 28(5), pp. 554–567. Available at: https://doi.org/10.5607/en.2019.28.5.554.

Julienne, H. *et al.* (2017) 'Drosophila PINK1 and parkin loss-of-function mutants display a range of non-motor Parkinson's disease phenotypes', *Neurobiology of Disease*, 104, pp. 15–23. Available at: https://doi.org/10.1016/j.nbd.2017.04.014.

Kachroo, A., Irizarry, M.C. and Schwarzschild, M.A. (2010) 'Caffeine protects against combined paraquat and maneb-induced dopaminergic neuron degeneration', *Experimental Neurology*, 223(2), pp. 657–661. Available at: https://doi.org/10.1016/j.expneurol.2010.02.007.

Kalecký, K., Ashcraft, P. and Bottiglieri, T. (2022) 'One-Carbon Metabolism in Alzheimer's Disease and Parkinson's Disease Brain Tissue', *Nutrients*, 14(3). Available at: https://doi.org/10.3390/nu14030599.

Kalinderi, K., Bostantjopoulou, S. and Fidani, L. (2016) 'The genetic background of Parkinson's disease: current progress and future prospects', *Acta Neurologica Scandinavica*, 134(5), pp. 314–326. Available at: https://doi.org/10.1111/ane.12563.

Kamienieva, I., Duszyński, J. and Szczepanowska, J. (2021) 'Multitasking guardian of mitochondrial quality: Parkin function and Parkinson's disease', *Translational Neurodegeneration*, 10(1), p. 5. Available at: https://doi.org/10.1186/s40035-020-00229-8.

Kanehisa, M. *et al.* (2023) 'KEGG for taxonomy-based analysis of pathways and genomes', *Nucleic Acids Research*, 51(D1), pp. D587–D592. Available at: https://doi.org/10.1093/nar/gkac963.

Kang, Y.-J. *et al.* (2017a) 'CPC2: a fast and accurate coding potential calculator based on sequence intrinsic features', *Nucleic Acids Research*, 45(W1), pp. W12–W16. Available at: https://doi.org/10.1093/nar/gkx428.

Kang, Y.-J. *et al.* (2017b) 'CPC2: a fast and accurate coding potential calculator based on sequence intrinsic features', *Nucleic Acids Research*, 45(W1), pp. W12–W16. Available at: https://doi.org/10.1093/nar/gkx428.

Kanitz, A. *et al.* (2015) 'Comparative assessment of methods for the computational inference of transcript isoform abundance from RNA-seq data', *Genome Biology*, 16(1), p. 150. Available at: https://doi.org/10.1186/s13059-015-0702-5.

Kanton, S. *et al.* (2019) 'Organoid single-cell genomic atlas uncovers human-specific features of brain development', *Nature*, 574(7778), pp. 418–422. Available at: https://doi.org/10.1038/s41586-019-1654-9.

Kao, S.-Y. (2009) 'DNA damage induces nuclear translocation of parkin', *Journal of Biomedical Science*, 16(1), p. 67. Available at: https://doi.org/10.1186/1423-0127-16-67.

Karachi, C. *et al.* (2010) 'Cholinergic mesencephalic neurons are involved in gait and postural disorders in Parkinson disease', *The Journal of Clinical Investigation*, 120(8), pp. 2745–2754. Available at: https://doi.org/10.1172/JCI42642.

Kartha, R.V. and Subramanian, S. (2014) 'Competing endogenous RNAs (ceRNAs): new entrants to the intricacies of gene regulation', *Frontiers in Genetics*, 5. Available at: https://doi.org/10.3389/fgene.2014.00008.

Kato, H. *et al.* (2020) 'ER-resident sensor PERK is essential for mitochondrial thermogenesis in brown adipose tissue', *Life Science Alliance*, 3(3), p. e201900576. Available at: https://doi.org/10.26508/lsa.201900576.

Kaufman, R.J. (2002) 'Orchestrating the unfolded protein response in health and disease', *Journal of Clinical Investigation*, 110(10), pp. 1389–1398. Available at: https://doi.org/10.1172/JCI0216886.

Khasnavis, S. and Pahan, K. (2014) 'Cinnamon Treatment Upregulates Neuroprotective Proteins Parkin and DJ-1 and Protects Dopaminergic Neurons in a Mouse Model of Parkinson's Disease', *Journal of neuroimmune pharmacology : the official journal of the Society on NeuroImmune Pharmacology*, 9(4), pp. 569–581. Available at: https://doi.org/10.1007/s11481-014-9552-2.

Kiferle, L. *et al.* (2014) 'Caudate dopaminergic denervation and visual hallucinations: evidence from a ^{123}I-FP-CIT SPECT study', *Parkinsonism & Related Disorders*, 20(7), pp. 761–765. Available at: https://doi.org/10.1016/j.parkreldis.2014.04.006.

Kim, D. *et al.* (2019) 'Graph-based genome alignment and genotyping with HISAT2 and HISAT-genotype', *Nature Biotechnology*, 37(8), pp. 907–915. Available at: https://doi.org/10.1038/s41587-019-0201-4.

Kim, S. *et al.* (2023) 'Role of Astrocytes in Parkinson's Disease Associated with Genetic Mutations and Neurotoxicants', *Cells*, 12(4), p. 622. Available at: https://doi.org/10.3390/cells12040622.

Kirkeby, A. *et al.* (2017) 'Predictive Markers Guide Differentiation to Improve Graft Outcome in Clinical Translation of hESC-Based Therapy for Parkinson's Disease', *Cell Stem Cell*, 20(1), pp. 135–148. Available at: https://doi.org/10.1016/j.stem.2016.09.004.

Kish, S.J. *et al.* (2008) 'Preferential loss of serotonin markers in caudate versus putamen in Parkinson's disease', *Brain: A Journal of Neurology*, 131(Pt 1), pp. 120–131. Available at: https://doi.org/10.1093/brain/awm239.

Kish, S.J., Shannak, K. and Hornykiewicz, O. (1988) 'Uneven pattern of dopamine loss in the striatum of patients with idiopathic Parkinson's disease. Pathophysiologic and clinical implications', *The New England Journal of Medicine*, 318(14), pp. 876–880. Available at: https://doi.org/10.1056/NEJM198804073181402.

Kitada, T. *et al.* (1998) 'Mutations in the parkin gene cause autosomal recessive juvenile parkinsonism', *Nature*, 392(6676), pp. 605–608. Available at: https://doi.org/10.1038/33416.

Kitada, T. *et al.* (2007) 'Impaired dopamine release and synaptic plasticity in the striatum of PINK1-deficient mice', *Proceedings of the National Academy of Sciences of the United States of America*, 104(27), pp. 11441–11446. Available at: https://doi.org/10.1073/pnas.0702717104.

Ko, K.R. *et al.* (2020) 'SH-SY5Y and LUHMES cells display differential sensitivity to MPP+, tunicamycin, and epoxomicin in 2D and 3D cell culture', *Biotechnology Progress*, 36(2), p. e2942. Available at: https://doi.org/10.1002/btpr.2942.

Kodroń, A. *et al.* (2021) 'The ubiquitin-proteasome system and its crosstalk with mitochondria as therapeutic targets in medicine', *Pharmacological Research*, 163, p. 105248. Available at: https://doi.org/10.1016/j.phrs.2020.105248.

Kogan, M., McGuire, M. and Riley, J. (2019) 'Deep Brain Stimulation for Parkinson Disease', *Neurosurgery Clinics of North America*, 30(2), pp. 137–146. Available at: https://doi.org/10.1016/j.nec.2019.01.001.

Kole, A.J., Annis, R.P. and Deshmukh, M. (2013) 'Mature neurons: equipped for survival', *Cell Death & Disease*, 4(6), p. e689. Available at: https://doi.org/10.1038/cddis.2013.220.

Kong, Y., Hsieh, C.-H. and Alonso, L.C. (2018) 'ANRIL: A lncRNA at the CDKN2A/B Locus With Roles in Cancer and Metabolic Disease', *Frontiers in Endocrinology*, 9, p. 405. Available at: https://doi.org/10.3389/fendo.2018.00405.

Kopp, F. (2019) 'Molecular functions and biological roles of long non-coding RNAs in human physiology and disease', *The Journal of Gene Medicine*, 21(8). Available at: https://doi.org/10.1002/jgm.3104.

Kopp, F. and Mendell, J.T. (2018) 'Functional Classification and Experimental Dissection of Long Noncoding RNAs', *Cell*, 172(3), pp. 393–407. Available at: https://doi.org/10.1016/j.cell.2018.01.011.

Kordower, J.H. *et al.* (2008) 'Transplanted dopaminergic neurons develop PD pathologic changes: A second case report', *Movement Disorders*, 23(16), pp. 2303–2306. Available at: https://doi.org/10.1002/mds.22369.

Kornienko, A.E. *et al.* (2013) 'Gene regulation by the act of long non-coding RNA transcription', *BMC Biology*, 11(1), p. 59. Available at: https://doi.org/10.1186/1741-7007-11-59.

Kramer, M.L. and Schulz-Schaeffer, W.J. (2007) 'Presynaptic α-Synuclein Aggregates, Not Lewy Bodies, Cause Neurodegeneration in Dementia with Lewy Bodies', *The Journal of Neuroscience*, 27(6), pp. 1405–1410. Available at: https://doi.org/10.1523/JNEUROSCI.4564-06.2007.

Kraus, T.F.J. *et al.* (2017) 'Altered Long Noncoding RNA Expression Precedes the Course of Parkinson's Disease—a Preliminary Report', *Molecular Neurobiology*, 54(4), pp. 2869–2877. Available at: https://doi.org/10.1007/s12035-016-9854-x.

Kreß, J.K.C. *et al.* (2023) 'The integrated stress response effector ATF4 is an obligatory metabolic activator of NRF2', *Cell Reports*, 42(7), p. 112724. Available at: https://doi.org/10.1016/j.celrep.2023.112724.

Kretz, M. *et al.* (2013) 'Control of somatic tissue differentiation by the long non-coding RNA TINCR', *Nature*, 493(7431), pp. 231–235. Available at: https://doi.org/10.1038/nature11661.

Krige, D. *et al.* (1992) 'Platelet mitochondria function in Parkinson's disease', *Annals of Neurology*, 32(6), pp. 782–788. Available at: https://doi.org/10.1002/ana.410320612.

Kuleshov, M.V. *et al.* (2016) 'Enrichr: a comprehensive gene set enrichment analysis web server 2016 update', *Nucleic Acids Research*, 44(W1), pp. W90-97. Available at: https://doi.org/10.1093/nar/gkw377.

Kuo, M.-C. *et al.* (2021) 'The role of noncoding RNAs in Parkinson's disease: biomarkers and associations with pathogenic pathways', *Journal of Biomedical Science*, 28(1), p. 78. Available at: https://doi.org/10.1186/s12929-021-00775-x.

Kutter, C. *et al.* (2012) 'Rapid Turnover of Long Noncoding RNAs and the Evolution of Gene Expression', *PLoS Genetics*. Edited by D.P. Bartel, 8(7), p. e1002841. Available at: https://doi.org/10.1371/journal.pgen.1002841.

Labunskyy, V.M. *et al.* (2014) 'Lifespan Extension Conferred by Endoplasmic Reticulum Secretory Pathway Deficiency Requires Induction of the Unfolded Protein Response', *PLoS Genetics*. Edited by S.K. Kim, 10(1), p. e1004019. Available at: https://doi.org/10.1371/journal.pgen.1004019.

Lai, F. *et al.* (2013) 'Activating RNAs associate with Mediator to enhance chromatin architecture and transcription', *Nature*, 494(7438), pp. 497–501. Available at: https://doi.org/10.1038/nature11884.

Lamech, L.T. and Haynes, C.M. (2015) 'The unpredictability of prolonged activation of stress response pathways', *The Journal of Cell Biology*, 209(6), pp. 781–787. Available at: https://doi.org/10.1083/jcb.201503107.

Langston, J.W. *et al.* (1983) 'Chronic Parkinsonism in Humans Due to a Product of Meperidine-Analog Synthesis', *Science*, 219(4587), pp. 979–980. Available at: https://doi.org/10.1126/science.6823561.

Langston, J.W. *et al.* (1984) '1-Methyl-4-phenylpyridinium ion (MPP+): Identification of a metabolite of MPTP, a toxin selective to the substantia nigra', *Neuroscience Letters*, 48(1), pp. 87–92. Available at: https://doi.org/10.1016/0304-3940(84)90293-3.

Latos, P.A. *et al.* (2012) '*Airn* Transcriptional Overlap, But Not Its lncRNA Products, Induces Imprinted *Igf2r* Silencing', *Science*, 338(6113), pp. 1469–1472. Available at: https://doi.org/10.1126/science.1228110.

Lawton, M. *et al.* (2018) 'Developing and validating Parkinson's disease subtypes and their motor and cognitive progression', *Journal of Neurology, Neurosurgery & Psychiatry*, 89(12), pp. 1279–1287. Available at: https://doi.org/10.1136/jnnp-2018-318337.

Lazarou, M. *et al.* (2015) 'The ubiquitin kinase PINK1 recruits autophagy receptors to induce mitophagy', *Nature*, 524(7565), pp. 309–314. Available at: https://doi.org/10.1038/nature14893.

Lebeau, J. *et al.* (2018) 'The PERK Arm of the Unfolded Protein Response Regulates Mitochondrial Morphology during Acute Endoplasmic Reticulum Stress', *Cell Reports*, 22(11), pp. 2827–2836. Available at: https://doi.org/10.1016/j.celrep.2018.02.055.

Lee, J.E. *et al.* (2016) 'Multiple dynamin family members collaborate to drive mitochondrial division', *Nature*, 540(7631), pp. 139–143. Available at: https://doi.org/10.1038/nature20555.

Lenain, C. *et al.* (2017) 'Massive reshaping of genome–nuclear lamina interactions during oncogene-induced senescence', *Genome Research*, 27(10), pp. 1634–1644. Available at: https://doi.org/10.1101/gr.225763.117.

Lesage, S. and Brice, A. (2009) 'Parkinson's disease: from monogenic forms to genetic susceptibility factors', *Human Molecular Genetics*, 18(R1), pp. R48–R59. Available at: https://doi.org/10.1093/hmg/ddp012.

Lewandowski, J.P. *et al.* (2019) 'The Firre locus produces a trans-acting RNA molecule that functions in hematopoiesis', *Nature Communications*, 10(1), p. 5137. Available at: https://doi.org/10.1038/s41467-019-12970-4.

Li, A., Zhang, J. and Zhou, Z. (2014) 'PLEK: a tool for predicting long non-coding RNAs and messenger RNAs based on an improved k-mer scheme', *BMC Bioinformatics*, 15(1), p. 311. Available at: https://doi.org/10.1186/1471-2105-15-311.

Li, F. *et al.* (2015) 'Spatiotemporal-specific lncRNAs in the brain, colon, liver and lung of macaque during development', *Molecular BioSystems*, 11(12), pp. 3253–3263. Available at: https://doi.org/10.1039/C5MB00474H.

Li, H. *et al.* (2019) 'Mitochondrial dysfunction and mitophagy defect triggered by heterozygous *GBA* mutations', *Autophagy*, 15(1), pp. 113–130. Available at: https://doi.org/10.1080/15548627.2018.1509818.

Li, J., Zhang, X. and Liu, C. (2020) 'The computational approaches of lncRNA identification based on coding potential: Status quo and challenges', *Computational and Structural Biotechnology Journal*, 18, pp. 3666–3677. Available at: https://doi.org/10.1016/j.csbj.2020.11.030.

Li, J.-Y. *et al.* (2008) 'Lewy bodies in grafted neurons in subjects with Parkinson's disease suggest host-to-graft disease propagation', *Nature Medicine*, 14(5), pp. 501–503. Available at: https://doi.org/10.1038/nm1746.

Li, Y. *et al.* (2023) 'ROS signaling–induced mitochondrial Sgk1 expression regulates epithelial cell renewal', *Proceedings of the National Academy of Sciences*, 120(24), p. e2216310120. Available at: https://doi.org/10.1073/pnas.2216310120.

Liang, Y. *et al.* (2022) 'The IRE1/JNK signaling pathway regulates inflammation cytokines and production of glomerular extracellular matrix in the acute kidney injury to chronic kidney disease transition', *Molecular Biology Reports*, 49(8), pp. 7709–7718. Available at: https://doi.org/10.1007/s11033-022-07588-7.

Lin, J.H. *et al.* (2007) 'IRE1 Signaling Affects Cell Fate During the Unfolded Protein Response', *Science*, 318(5852), pp. 944–949. Available at: https://doi.org/10.1126/science.1146361.

Lin, M.T. *et al.* (2012) 'Somatic mitochondrial DNA mutations in early parkinson and incidental lewy body disease', *Annals of Neurology*, 71(6), pp. 850–854. Available at: https://doi.org/10.1002/ana.23568.

Lin, Q. *et al.* (2019) 'LncRNA HOTAIR targets miR-126-5p to promote the progression of Parkinson's disease through RAB3IP', *Biological Chemistry*, 400(9), pp. 1217–1228. Available at: https://doi.org/10.1515/hsz-2018-0431.

Lin, Y. *et al.* (2018) 'Structural analyses of NEAT1 lncRNAs suggest long-range RNA interactions that may contribute to paraspeckle architecture', *Nucleic Acids Research*, 46(7), pp. 3742–3752. Available at: https://doi.org/10.1093/nar/gky046.

Liu, G., Mattick, J. and Taft, R.J. (2013) 'A meta-analysis of the genomic and transcriptomic composition of complex life', *Cell Cycle*, 12(13), pp. 2061–2072. Available at: https://doi.org/10.4161/cc.25134.

Liu, L. *et al.* (2023) 'Crosstalk between mitochondrial biogenesis and mitophagy to maintain mitochondrial homeostasis', *Journal of Biomedical Science*, 30(1), p. 86. Available at: https://doi.org/10.1186/s12929-023-00975-7.

Liu, R. *et al.* (2012) 'Caffeine Intake, Smoking, and Risk of Parkinson Disease in Men and Women', *American Journal of Epidemiology*, 175(11), pp. 1200–1207. Available at: https://doi.org/10.1093/aje/kwr451.

Liu, R., Li, F. and Zhao, W. (2020) 'Long noncoding RNA NEAT1 knockdown inhibits MPP+-induced apoptosis, inflammation and cytotoxicity in SK-N-SH cells by regulating miR-212-5p/RAB3IP axis', *Neuroscience Letters*, 731, p. 135060. Available at: https://doi.org/10.1016/j.neulet.2020.135060.

Liu, S.J. *et al.* (2016) 'Single-cell analysis of long non-coding RNAs in the developing human neocortex', *Genome Biology*, 17(1), p. 67. Available at: https://doi.org/10.1186/s13059-016-0932-1.

Liu, T. *et al.* (2014) 'Attenuated ability of BACE1 to cleave the amyloid precursor protein via silencing long noncoding RNA BACE1-AS expression', *Molecular Medicine Reports*, 10(3), pp. 1275–1281. Available at: https://doi.org/10.3892/mmr.2014.2351.

Liu, Y. *et al.* (2019) 'Activation of the Unfolded Protein Response via Inhibition of Protein Disulfide Isomerase Decreases the Capacity for DNA Repair to Sensitize Glioblastoma to Radiotherapy', *Cancer Research*, 79(11), pp. 2923–2932. Available at: https://doi.org/10.1158/0008-5472.CAN-18-2540.

Liu, Y.J. *et al.* (2020) 'Mitochondrial fission and fusion: A dynamic role in aging and potential target for age-related disease', *Mechanisms of Ageing and Development*, 186, p. 111212. Available at: https://doi.org/10.1016/j.mad.2020.111212.

Liu, Z.-W. *et al.* (2013) 'Protein kinase RNA- like endoplasmic reticulum kinase (PERK) signaling pathway plays a major role in reactive oxygen species (ROS)- mediated endoplasmic reticulum stress- induced apoptosis in diabetic cardiomyopathy', *Cardiovascular Diabetology*, 12(1), p. 158. Available at: https://doi.org/10.1186/1475-2840-12-158.

Longo, F. *et al.* (2021) 'Cell-type-specific disruption of PERK-eIF2α signaling in dopaminergic neurons alters motor and cognitive function', *Molecular Psychiatry*, 26(11), pp. 6427–6450. Available at: https://doi.org/10.1038/s41380-021-01099-w.

Lotharius, J. (2005) 'Progressive Degeneration of Human Mesencephalic Neuron-Derived Cells Triggered by Dopamine-Dependent Oxidative Stress Is Dependent on the Mixed-Lineage Kinase Pathway', *Journal of Neuroscience*, 25(27), pp. 6329–6342. Available at: https://doi.org/10.1523/JNEUROSCI.1746-05.2005.

Lotharius, J. and Brundin, P. (2002) 'Impaired dopamine storage resulting from alpha-synuclein mutations may contribute to the pathogenesis of Parkinson's disease', *Human Molecular Genetics*, 11(20), pp. 2395–2407. Available at: https://doi.org/10.1093/hmg/11.20.2395.

Lu, H. *et al.* (2023) 'Mitochondrial Unfolded Protein Response and Integrated Stress Response as Promising Therapeutic Targets for Mitochondrial Diseases', *Cells*, 12(1), p. 20. Available at: https://doi.org/10.3390/cells12010020.

Lu, M. *et al.* (2018) 'LncRNA-UCA1 promotes PD development by upregulating SNCA', *European Review for Medical and Pharmacological Sciences*, 22(22), pp. 7908–7915. Available at: https://doi.org/10.26355/eurrev_201811_16417.

Lu, P.D., Harding, H.P. and Ron, D. (2004) 'Translation reinitiation at alternative open reading frames regulates gene expression in an integrated stress response', *Journal of Cell Biology*, 167(1), pp. 27–33. Available at: https://doi.org/10.1083/jcb.200408003.

Lubelsky, Y. and Ulitsky, I. (2018) ‘Sequences enriched in Alu repeats drive nuclear localization of long RNAs in human cells’, *Nature*, 555(7694), pp. 107–111. Available at: https://doi.org/10.1038/nature25757.

Luo, Y. *et al.* (2020) ‘New developments on the Encyclopedia of DNA Elements (ENCODE) data portal’, *Nucleic Acids Research*, 48(D1), pp. D882–D889. Available at: https://doi.org/10.1093/nar/gkz1062.

Lyu, Y., Bai, L. and Qin, C. (2019) ‘Long noncoding RNAs in neurodevelopment and Parkinson’s disease’, *Animal Models and Experimental Medicine*, 2(4), pp. 239–251. Available at: https://doi.org/10.1002/ame2.12093.

Macleod, A.D., Taylor, K.S.M. and Counsell, C.E. (2014) ‘Mortality in Parkinson’s disease: A systematic review and meta-analysis’, *Movement Disorders*, 29(13), pp. 1615–1622. Available at: https://doi.org/10.1002/mds.25898.

Mahlknecht, P., Seppi, K. and Poewe, W. (2015) ‘The Concept of Prodromal Parkinson’s Disease’, *Journal of Parkinson’s Disease*, 5(4), pp. 681–697. Available at: https://doi.org/10.3233/JPD-150685.

Malakar, P. *et al.* (2019) ‘Long Noncoding RNA MALAT1 Regulates Cancer Glucose Metabolism by Enhancing mTOR-Mediated Translation of TCF7L2’, *Cancer Research*, 79(10), pp. 2480–2493. Available at: https://doi.org/10.1158/0008-5472.CAN-18-1432.

Managadze, D. *et al.* (2011) ‘Negative Correlation between Expression Level and Evolutionary Rate of Long Intergenic Noncoding RNAs’, *Genome Biology and Evolution*, 3, pp. 1390–1404. Available at: https://doi.org/10.1093/gbe/evr116.

Mann, V.M. *et al.* (1992) ‘BRAIN, SKELETAL MUSCLE AND PLATELET HOMOGENATE MITOCHONDRIAL FUNCTION IN PARKINSON’S DISEASE’, *Brain*, 115(2), pp. 333–342. Available at: https://doi.org/10.1093/brain/115.2.333.

Marchi, S., Patergnani, S. and Pinton, P. (2014) ‘The endoplasmic reticulum–mitochondria connection: One touch, multiple functions’, *Biochimica et Biophysica Acta (BBA) - Bioenergetics*, 1837(4), pp. 461–469. Available at: https://doi.org/10.1016/j.bbabio.2013.10.015.

Marcus, J.M. and Andrabi, S.A. (2018) ‘SIRT3 Regulation Under Cellular Stress: Making Sense of the Ups and Downs’, *Frontiers in Neuroscience*, 12, p. 799. Available at: https://doi.org/10.3389/fnins.2018.00799.

Markaki, M. and Tavernarakis, N. (2020) ‘Mitochondrial turnover and homeostasis in ageing and neurodegeneration’, *FEBS Letters*, 594(15), pp. 2370–2379. Available at: https://doi.org/10.1002/1873-3468.13802.

Markesbery, W.R. *et al.* (2009) ‘Lewy Body Pathology in Normal Elderly Subjects’, *Journal of Neuropathology & Experimental Neurology*, 68(7), pp. 816–822. Available at: https://doi.org/10.1097/NEN.0b013e3181ac10a7.

Markey, S.P. *et al.* (1984) ‘Intraneuronal generation of a pyridinium metabolite may cause drug-induced parkinsonism’, *Nature*, 311.

Maroteaux, L., Campanelli, J. and Scheller, R. (1988) ‘Synuclein: a neuron-specific protein localized to the nucleus and presynaptic nerve terminal’, *The Journal of Neuroscience*, 8(8), pp. 2804–2815. Available at: https://doi.org/10.1523/JNEUROSCI.08-08-02804.1988.

Marras, C. *et al.* (2014) 'Systematic Review of the Risk of Parkinson's Disease After Mild Traumatic Brain Injury: Results of the International Collaboration on Mild Traumatic Brain Injury Prognosis', *Archives of Physical Medicine and Rehabilitation*, 95(3), pp. S238–S244. Available at: https://doi.org/10.1016/j.apmr.2013.08.298.

Martinez, B.A. *et al.* (2017) 'Dysregulation of the Mitochondrial Unfolded Protein Response Induces Non-Apoptotic Dopaminergic Neurodegeneration in *C. elegans* Models of Parkinson's Disease', *The Journal of Neuroscience*, 37(46), pp. 11085–11100. Available at: https://doi.org/10.1523/JNEUROSCI.1294-17.2017.

Martinus, R.D. *et al.* (1996) 'Selective Induction of Mitochondrial Chaperones in Response to Loss of the Mitochondrial Genome', *European Journal of Biochemistry*, 240(1), pp. 98–103. Available at: https://doi.org/10.1111/j.1432-1033.1996.0098h.x.

Marzluff, W.F. (2012) 'Novel 3′ ends that support translation', *Genes & Development*, 26(22), pp. 2457–2460. Available at: https://doi.org/10.1101/gad.207233.112.

Matai, L. *et al.* (2019) 'Dietary restriction improves proteostasis and increases life span through endoplasmic reticulum hormesis', *Proceedings of the National Academy of Sciences*, 116(35), pp. 17383–17392. Available at: https://doi.org/10.1073/pnas.1900055116.

Matsuda, W. *et al.* (2009) 'Single Nigrostriatal Dopaminergic Neurons Form Widely Spread and Highly Dense Axonal Arborizations in the Neostriatum', *Journal of Neuroscience*, 29(2), pp. 444–453. Available at: https://doi.org/10.1523/JNEUROSCI.4029-08.2009.

Maurel, M. *et al.* (2014) 'Getting RIDD of RNA: IRE1 in cell fate regulation', *Trends in Biochemical Sciences*, 39(5), pp. 245–254. Available at: https://doi.org/10.1016/j.tibs.2014.02.008.

McCluggage, F. and Fox, A.H. (2021) 'Paraspeckle nuclear condensates: Global sensors of cell stress?', *BioEssays*, 43(5), p. 2000245. Available at: https://doi.org/10.1002/bies.202000245.

McCown, P.J. *et al.* (2019) 'Secondary Structural Model of Human MALAT1 Reveals Multiple Structure–Function Relationships', *International Journal of Molecular Sciences*, 20(22), p. 5610. Available at: https://doi.org/10.3390/ijms20225610.

McGregor, M.M. and Nelson, A.B. (2019) 'Circuit Mechanisms of Parkinson's Disease', *Neuron*, 101(6), pp. 1042–1056. Available at: https://doi.org/10.1016/j.neuron.2019.03.004.

Melber, A. and Haynes, C.M. (2018) 'UPRmt regulation and output: a stress response mediated by mitochondrial-nuclear communication', *Cell Research*, 28(3), pp. 281–295. Available at: https://doi.org/10.1038/cr.2018.16.

Melé, M. *et al.* (2017) 'Chromatin environment, transcriptional regulation, and splicing distinguish lincRNAs and mRNAs', *Genome Research*, 27(1), pp. 27–37. Available at: https://doi.org/10.1101/gr.214205.116.

Mesbah Moosavi, Z.S. and Hood, D.A. (2017) 'The unfolded protein response in relation to mitochondrial biogenesis in skeletal muscle cells', *American Journal of Physiology. Cell Physiology*, 312(5), pp. C583–C594. Available at: https://doi.org/10.1152/ajpcell.00320.2016.

Mesmin, B. (2016) 'Mitochondrial lipid transport and biosynthesis: A complex balance', *Journal of Cell Biology*, 214(1), pp. 9–11. Available at: https://doi.org/10.1083/jcb.201606069.

Michel, P.P., Hirsch, E.C. and Hunot, S. (2016) 'Understanding Dopaminergic Cell Death Pathways in Parkinson Disease', *Neuron*, 90(4), pp. 675–691. Available at: https://doi.org/10.1016/j.neuron.2016.03.038.

Michel, S. *et al.* (2015) 'Inhibition of mitochondrial genome expression triggers the activation of CHOP-10 by a cell signaling dependent on the integrated stress response but not the mitochondrial unfolded protein response', *Mitochondrion*, 21, pp. 58–68. Available at: https://doi.org/10.1016/j.mito.2015.01.005.

Michely, J. *et al.* (2015) 'Dopaminergic modulation of motor network dynamics in Parkinson's disease', *Brain*, 138(3), pp. 664–678. Available at: https://doi.org/10.1093/brain/awu381.

Mick, E. *et al.* (2020) 'Distinct mitochondrial defects trigger the integrated stress response depending on the metabolic state of the cell', *eLife*, 9, p. e49178. Available at: https://doi.org/10.7554/eLife.49178.

Mills, J.D. *et al.* (2013) 'Unique Transcriptome Patterns of the White and Grey Matter Corroborate Structural and Functional Heterogeneity in the Human Frontal Lobe', *PLoS ONE*. Edited by T. Preiss, 8(10), p. e78480. Available at: https://doi.org/10.1371/journal.pone.0078480.

Misko, A.L. *et al.* (2012) 'Mitofusin2 Mutations Disrupt Axonal Mitochondrial Positioning and Promote Axon Degeneration', *Journal of Neuroscience*, 32(12), pp. 4145–4155. Available at: https://doi.org/10.1523/JNEUROSCI.6338-11.2012.

Misra, J. *et al.* (2013) 'Transcriptional cross talk between orphan nuclear receptor ERRγ and transmembrane transcription factor ATF6α coordinates endoplasmic reticulum stress response', *Nucleic Acids Research*, 41(14), pp. 6960–6974. Available at: https://doi.org/10.1093/nar/gkt429.

Mohammadin, S. *et al.* (2015) 'Positionally-conserved but sequence-diverged: identification of long non-coding RNAs in the Brassicaceae and Cleomaceae', *BMC Plant Biology*, 15(1), p. 217. Available at: https://doi.org/10.1186/s12870-015-0603-5.

Monroy-Eklund, A. *et al.* (2022) *Structural conservation of MALAT1 long non-coding RNA in cells and in evolution*. preprint. Molecular Biology. Available at: https://doi.org/10.1101/2022.07.29.502018.

Monteiro, J.P. *et al.* (2019) 'Endothelial function and dysfunction in the cardiovascular system: the long non-coding road', *Cardiovascular Research*, 115(12), pp. 1692–1704. Available at: https://doi.org/10.1093/cvr/cvz154.

Morán, I., Akerman, İ., van de Bunt, M., *et al.* (2012) 'Human β Cell Transcriptome Analysis Uncovers lncRNAs That Are Tissue-Specific, Dynamically Regulated, and Abnormally Expressed in Type 2 Diabetes', *Cell Metabolism*, 16(4), pp. 435–448. Available at: https://doi.org/10.1016/j.cmet.2012.08.010.

Morán, I., Akerman, İ., van de Bunt, M., *et al.* (2012) 'Human β Cell Transcriptome Analysis Uncovers lncRNAs That Are Tissue-Specific, Dynamically Regulated, and Abnormally Expressed in Type 2 Diabetes', *Cell metabolism*, 16(4), pp. 435–448. Available at: https://doi.org/10.1016/j.cmet.2012.08.010.

Morikawa, H. and Paladini, C.A. (2011) 'Dynamic regulation of midbrain dopamine neuron activity: intrinsic, synaptic, and plasticity mechanisms', *Neuroscience*, 198, pp. 95–111. Available at: https://doi.org/10.1016/j.neuroscience.2011.08.023.

Mouton-Liger, F. *et al.* (2017) 'PINK1/Parkin-Dependent Mitochondrial Surveillance: From Pleiotropy to Parkinson's Disease', *Frontiers in Molecular Neuroscience*, 10, p. 120. Available at: https://doi.org/10.3389/fnmol.2017.00120.

Münch, C. and Harper, J.W. (2016) 'Mitochondrial unfolded protein response controls matrix pre-RNA processing and translation', *Nature*, 534(7609), pp. 710–713. Available at: https://doi.org/10.1038/nature18302.

Muñoz, J.P. *et al.* (2013) 'Mfn2 modulates the UPR and mitochondrial function via repression of PERK', *The EMBO journal*, 32(17), pp. 2348–2361. Available at: https://doi.org/10.1038/emboj.2013.168.

Naidoo, N. *et al.* (2011) 'Endoplasmic reticulum stress in wake-active neurons progresses with aging: Aging of wake neurons: ER stress', *Aging Cell*, 10(4), pp. 640–649. Available at: https://doi.org/10.1111/j.1474-9726.2011.00699.x.

Nakaya, H.I. *et al.* (2007) 'Genome mapping and expression analyses of human intronic noncoding RNAs reveal tissue-specific patterns and enrichment in genes related to regulation of transcription', *Genome Biology*, 8(3), p. R43. Available at: https://doi.org/10.1186/gb-2007-8-3-r43.

Nalls, M.A. *et al.* (2019) 'Identification of novel risk loci, causal insights, and heritable risk for Parkinson's disease: a meta-analysis of genome-wide association studies', *The Lancet. Neurology*, 18(12), pp. 1091–1102. Available at: https://doi.org/10.1016/S1474-4422(19)30320-5.

Narendra, D. *et al.* (2008) 'Parkin is recruited selectively to impaired mitochondria and promotes their autophagy', *Journal of Cell Biology*, 183(5), pp. 795–803. Available at: https://doi.org/10.1083/jcb.200809125.

Nargund, A.M. *et al.* (2012) 'Mitochondrial Import Efficiency of ATFS-1 Regulates Mitochondrial UPR Activation', *Science*, 337(6094), pp. 587–590. Available at: https://doi.org/10.1126/science.1223560.

Nargund, A.M. *et al.* (2015) 'Mitochondrial and Nuclear Accumulation of the Transcription Factor ATFS-1 Promotes OXPHOS Recovery during the UPRmt', *Molecular Cell*, 58(1), pp. 123–133. Available at: https://doi.org/10.1016/j.molcel.2015.02.008.

Nguyen, H.N. *et al.* (2011) 'LRRK2 Mutant iPSC-Derived DA Neurons Demonstrate Increased Susceptibility to Oxidative Stress', *Cell stem cell*, 8(3), pp. 267–280. Available at: https://doi.org/10.1016/j.stem.2011.01.013.

Nicoletti, A. *et al.* (2017) 'Gender effect on non-motor symptoms in Parkinson's disease: are men more at risk?', *Parkinsonism & Related Disorders*, 35, pp. 69–74. Available at: https://doi.org/10.1016/j.parkreldis.2016.12.008.

O'Callaghan, B., Hardy, J. and Plun-Favreau, H. (2023) 'PINK1: From Parkinson's disease to mitophagy and back again', *PLoS biology*, 21(6), p. e3002196. Available at: https://doi.org/10.1371/journal.pbio.3002196.

Oertel, W. and Schulz, J.B. (2016) 'Current and experimental treatments of Parkinson disease: A guide for neuroscientists', *Journal of Neurochemistry*, 139, pp. 325–337. Available at: https://doi.org/10.1111/jnc.13750.

Oh, C.-K. *et al.* (2017) 'S-Nitrosylation of PINK1 Attenuates PINK1/Parkin-Dependent Mitophagy in hiPSC-Based Parkinson's Disease Models', *Cell Reports*, 21(8), pp. 2171–2182. Available at: https://doi.org/10.1016/j.celrep.2017.10.068.

Oommen, D. and Prise, K.M. (2013) 'Down-regulation of PERK enhances resistance to ionizing radiation', *Biochemical and Biophysical Research Communications*, 441(1), pp. 31–35. Available at: https://doi.org/10.1016/j.bbrc.2013.09.129.

O'Reilly, E.J. *et al.* (2005) 'Smokeless tobacco use and the risk of Parkinson's disease mortality', *Movement Disorders: Official Journal of the Movement Disorder Society*, 20(10), pp. 1383–1384. Available at: https://doi.org/10.1002/mds.20587.

Ozgen, S. *et al.* (2021) 'Significance of mitochondrial activity in neurogenesis and neurodegenerative diseases', *Neural Regeneration Research*, 17(4), pp. 741–747. Available at: https://doi.org/10.4103/1673-5374.322429.

Ozkurede, U. and Miller, R.A. (2019) 'Improved mitochondrial stress response in long-lived Snell dwarf mice', *Aging Cell*, 18(6). Available at: https://doi.org/10.1111/acel.13030.

Pacelli, C. *et al.* (2015) 'Elevated Mitochondrial Bioenergetics and Axonal Arborization Size Are Key Contributors to the Vulnerability of Dopamine Neurons', *Current Biology*, 25(18), pp. 2349–2360. Available at: https://doi.org/10.1016/j.cub.2015.07.050.

Padman, B.S. *et al.* (2013) 'The protonophore CCCP interferes with lysosomal degradation of autophagic cargo in yeast and mammalian cells', *Autophagy*, 9(11), pp. 1862–1875. Available at: https://doi.org/10.4161/auto.26557.

Pakos-Zebrucka, K. *et al.* (2016) 'The integrated stress response', *EMBO reports*, 17(10), pp. 1374–1395. Available at: https://doi.org/10.15252/embr.201642195.

Pal, G.D. *et al.* (2015) 'The Core Assessment Program for Surgical Interventional Therapies in Parkinson's Disease (CAPSIT-PD): Tolerability of Preoperative Neuropsychological Testing for Deep Brain Stimulation in Parkinson's Disease', *Movement Disorders Clinical Practice*, 2(4), pp. 379–383. Available at: https://doi.org/10.1002/mdc3.12213.

Palam, L.R., Baird, T.D. and Wek, R.C. (2011) 'Phosphorylation of eIF2 Facilitates Ribosomal Bypass of an Inhibitory Upstream ORF to Enhance CHOP Translation', *Journal of Biological Chemistry*, 286(13), pp. 10939–10949. Available at: https://doi.org/10.1074/jbc.M110.216093.

Palazzo, A.F. and Lee, E.S. (2015) 'Non-coding RNA: what is functional and what is junk?', *Frontiers in Genetics*, 6. Available at: https://doi.org/10.3389/fgene.2015.00002.

Palikaras, K., Lionaki, E. and Tavernarakis, N. (2015) 'Balancing mitochondrial biogenesis and mitophagy to maintain energy metabolism homeostasis', *Cell Death & Differentiation*, 22(9), pp. 1399–1401. Available at: https://doi.org/10.1038/cdd.2015.86.

Pan, H. *et al.* (2023) 'Genome-wide association study using whole-genome sequencing identifies risk loci for Parkinson's disease in Chinese population', *npj Parkinson's Disease*, 9(1), pp. 1–11. Available at: https://doi.org/10.1038/s41531-023-00456-6.

Papa, L. and Germain, D. (2011) 'Estrogen receptor mediates a distinct mitochondrial unfolded protein response', *Journal of Cell Science*, 124(9), pp. 1396–1402. Available at: https://doi.org/10.1242/jcs.078220.

Papa, L. and Germain, D. (2014) 'SirT3 Regulates the Mitochondrial Unfolded Protein Response', *Molecular and Cellular Biology*, 34(4), pp. 699–710. Available at: https://doi.org/10.1128/MCB.01337-13.

Paralkar, V.R. *et al.* (2016) 'Unlinking an lncRNA from Its Associated cis Element', *Molecular Cell*, 62(1), pp. 104–110. Available at: https://doi.org/10.1016/j.molcel.2016.02.029.

Parkinson, J. (2002) 'An Essay on the Shaking Palsy', *J Neuropsychiatry Clin Neurosci* [Preprint].

Parkkinen, L., Pirttilä, T. and Alafuzoff, I. (2008) 'Applicability of current staging/categorization of α-synuclein pathology and their clinical relevance', *Acta Neuropathologica*, 115(4), pp. 399–407. Available at: https://doi.org/10.1007/s00401-008-0346-6.

Pasmant, E. *et al.* (2007) 'Characterization of a germ-line deletion, including the entire INK4/ARF locus, in a melanoma-neural system tumor family: identification of ANRIL, an antisense noncoding RNA whose expression coclusters with ARF', *Cancer Research*, 67(8), pp. 3963–3969. Available at: https://doi.org/10.1158/0008-5472.CAN-06-2004.

Patergnani, S. *et al.* (2021) 'Mitochondrial Oxidative Stress and "Mito-Inflammation": Actors in the Diseases', *Biomedicines*, 9(2), p. 216. Available at: https://doi.org/10.3390/biomedicines9020216.

Patergnani, S. *et al.* (2022) 'The "mitochondrial stress responses": the "Dr. Jekyll and Mr. Hyde" of neuronal disorders', *Neural Regeneration Research*, 17(12), p. 2563. Available at: https://doi.org/10.4103/1673-5374.339473.

Paupe, V. and Prudent, J. (2018) 'New insights into the role of mitochondrial calcium homeostasis in cell migration', *Biochemical and Biophysical Research Communications*, 500(1), pp. 75–86. Available at: https://doi.org/10.1016/j.bbrc.2017.05.039.

Pavese, N. *et al.* (2010) 'Fatigue in Parkinson's disease is linked to striatal and limbic serotonergic dysfunction', *Brain: A Journal of Neurology*, 133(11), pp. 3434–3443. Available at: https://doi.org/10.1093/brain/awq268.

Peelaerts, W. *et al.* (2015) 'α-Synuclein strains cause distinct synucleinopathies after local and systemic administration', *Nature*, 522(7556), pp. 340–344. Available at: https://doi.org/10.1038/nature14547.

Pellegrino, M.W. and Haynes, C.M. (2015) 'Mitophagy and the mitochondrial unfolded protein response in neurodegeneration and bacterial infection', *BMC Biology*, 13(1), p. 22. Available at: https://doi.org/10.1186/s12915-015-0129-1.

Perez, F.A. and Palmiter, R.D. (2005) 'Parkin-deficient mice are not a robust model of parkinsonism', *Proceedings of the National Academy of Sciences of the United States of America*, 102(6), pp. 2174–2179. Available at: https://doi.org/10.1073/pnas.0409598102.

Pertea, G. and Pertea, M. (2020) 'GFF Utilities: GffRead and GffCompare', *F1000Research*, 9, p. ISCB Comm J-304. Available at: https://doi.org/10.12688/f1000research.23297.2.

Pertea, M. *et al.* (2015) 'StringTie enables improved reconstruction of a transcriptome from RNA-seq reads', *Nature Biotechnology*, 33(3), pp. 290–295. Available at: https://doi.org/10.1038/nbt.3122.

Pezzoli, G. and Cereda, E. (2013) ‘Exposure to pesticides or solvents and risk of Parkinson disease’, *Neurology*, 80(22), pp. 2035–2041. Available at: https://doi.org/10.1212/WNL.0b013e318294b3c8.

Picca, A. *et al.* (2021) ‘Mitochondrial Dysfunction, Protein Misfolding and Neuroinflammation in Parkinson’s Disease: Roads to Biomarker Discovery’, *Biomolecules*, 11(10), p. 1508. Available at: https://doi.org/10.3390/biom11101508.

Pickles, S., Vigié, P. and Youle, R.J. (2018) ‘Mitophagy and Quality Control Mechanisms in Mitochondrial Maintenance’, *Current Biology*, 28(4), pp. R170–R185. Available at: https://doi.org/10.1016/j.cub.2018.01.004.

Pickrell, A.M. *et al.* (2015) ‘Endogenous Parkin Preserves Dopaminergic Substantia Nigral Neurons following Mitochondrial DNA Mutagenic Stress’, *Neuron*, 87(2), pp. 371–381. Available at: https://doi.org/10.1016/j.neuron.2015.06.034.

Pimenta de Castro, I. *et al.* (2012) ‘Genetic analysis of mitochondrial protein misfolding in Drosophila melanogaster’, *Cell Death & Differentiation*, 19(8), pp. 1308–1316. Available at: https://doi.org/10.1038/cdd.2012.5.

Pingale, T. and Gupta, G.L. (2020) ‘Classic and evolving animal models in Parkinson’s disease’, *Pharmacology Biochemistry and Behavior*, 199, p. 173060. Available at: https://doi.org/10.1016/j.pbb.2020.173060.

Politis, M. and Niccolini, F. (2015) ‘Serotonin in Parkinson’s disease’, *Behavioural Brain Research*, 277, pp. 136–145. Available at: https://doi.org/10.1016/j.bbr.2014.07.037.

Poller, W. *et al.* (2018) ‘Non-coding RNAs in cardiovascular diseases: diagnostic and therapeutic perspectives’, *European Heart Journal*, 39(29), pp. 2704–2716. Available at: https://doi.org/10.1093/eurheartj/ehx165.

Polymeropoulos, M.H. *et al.* (1997) ‘Mutation in the α-Synuclein Gene Identified in Families with Parkinson’s Disease’, *Science*, 276(5321), pp. 2045–2047. Available at: https://doi.org/10.1126/science.276.5321.2045.

Postuma, R.B. *et al.* (2015) ‘MDS clinical diagnostic criteria for Parkinson’s disease’, *Movement Disorders: Official Journal of the Movement Disorder Society*, 30(12), pp. 1591–1601. Available at: https://doi.org/10.1002/mds.26424.

Poulopoulos, M., Levy, O.A. and Alcalay, R.N. (2012) ‘The neuropathology of genetic Parkinson’s disease’, *Movement Disorders*, 27(7), pp. 831–842. Available at: https://doi.org/10.1002/mds.24962.

Pringsheim, T. *et al.* (2014) ‘The prevalence of Parkinson’s disease: A systematic review and meta-analysis: PD PREVALENCE’, *Movement Disorders*, 29(13), pp. 1583–1590. Available at: https://doi.org/10.1002/mds.25945.

Przedborski, S. (2017) ‘The two-century journey of Parkinson disease research’, *Nature Reviews Neuroscience*, 18(4), pp. 251–259. Available at: https://doi.org/10.1038/nrn.2017.25.

Puschmann, A. *et al.* (2017) ‘Heterozygous PINK1 p.G411S increases risk of Parkinson’s disease via a dominant-negative mechanism’, *Brain*, 140(1), pp. 98–117. Available at: https://doi.org/10.1093/brain/aww261.

Pyakurel, A. *et al.* (2015) ‘Extracellular Regulated Kinase Phosphorylates Mitofusin 1 to Control Mitochondrial Morphology and Apoptosis’, *Molecular Cell*, 58(2), pp. 244–254. Available at: https://doi.org/10.1016/j.molcel.2015.02.021.

Qamhawi, Z. *et al.* (2015) 'Clinical correlates of raphe serotonergic dysfunction in early Parkinson's disease', *Brain: A Journal of Neurology*, 138(Pt 10), pp. 2964–2973. Available at: https://doi.org/10.1093/brain/awv215.

Qian, C. *et al.* (2019) 'Downregulated lncRNA-SNHG1 enhances autophagy and prevents cell death through the miR-221/222 /p27/mTOR pathway in Parkinson's disease', *Experimental Cell Research*, 384(1), p. 111614. Available at: https://doi.org/10.1016/j.yexcr.2019.111614.

Qin, N., Geng, A. and Xue, R. (2022) 'Activated or Impaired: An Overview of DNA Repair in Neurodegenerative Diseases', *Aging and Disease*, 13(4), pp. 987–1004. Available at: https://doi.org/10.14336/AD.2021.1212.

Quinn, J.J. *et al.* (2016) 'Rapid evolutionary turnover underlies conserved lncRNA–genome interactions', *Genes & Development*, 30(2), pp. 191–207. Available at: https://doi.org/10.1101/gad.272187.115.

Quinn, J.J. and Chang, H.Y. (2016) 'Unique features of long non-coding RNA biogenesis and function', *Nature Reviews Genetics*, 17(1), pp. 47–62. Available at: https://doi.org/10.1038/nrg.2015.10.

Quinn, P.M.J. *et al.* (2020) 'PINK1/PARKIN signalling in neurodegeneration and neuroinflammation', *Acta Neuropathologica Communications*, 8(1), p. 189. Available at: https://doi.org/10.1186/s40478-020-01062-w.

Quirós, P.M. *et al.* (2017) 'Multi-omics analysis identifies ATF4 as a key regulator of the mitochondrial stress response in mammals', *The Journal of Cell Biology*, 216(7), pp. 2027–2045. Available at: https://doi.org/10.1083/jcb.201702058.

Rackham, O. *et al.* (2011) 'Long noncoding RNAs are generated from the mitochondrial genome and regulated by nuclear-encoded proteins', *RNA*, 17(12), pp. 2085–2093. Available at: https://doi.org/10.1261/rna.029405.111.

Rakovic, A. *et al.* (2019) 'PINK1-dependent mitophagy is driven by the UPS and can occur independently of LC3 conversion', *Cell Death & Differentiation*, 26(8), pp. 1428–1441. Available at: https://doi.org/10.1038/s41418-018-0219-z.

Ramsay, R.R. *et al.* (1986) 'Energy-driven uptake of N-methyl-4-phenylpyridine by brain mitochondria mediates the neurotoxicity of MPTP', *Life Sciences*, 39(7), pp. 581–588. Available at: https://doi.org/10.1016/0024-3205(86)90037-8.

Ransohoff, J.D., Wei, Y. and Khavari, P.A. (2018) 'The functions and unique features of long intergenic non-coding RNA', *Nature Reviews Molecular Cell Biology*, 19(3), pp. 143–157. Available at: https://doi.org/10.1038/nrm.2017.104.

Rao, S.-Q. *et al.* (2015) 'Genetic variants in long non-coding RNA MIAT contribute to risk of paranoid schizophrenia in a Chinese Han population', *Schizophrenia Research*, 166(1–3), pp. 125–130. Available at: https://doi.org/10.1016/j.schres.2015.04.032.

Rappold, P.M. *et al.* (2014) 'Drp1 inhibition attenuates neurotoxicity and dopamine release deficits in vivo', *Nature Communications*, 5, p. 5244. Available at: https://doi.org/10.1038/ncomms6244.

Ratti, A. and Buratti, E. (2016) 'Physiological functions and pathobiology of TDP-43 and FUS/TLS proteins', *Journal of Neurochemistry*, 138 Suppl 1, pp. 95–111. Available at: https://doi.org/10.1111/jnc.13625.

Remy, P. *et al.* (2005) 'Depression in Parkinson's disease: loss of dopamine and noradrenaline innervation in the limbic system', *Brain: A Journal of Neurology*, 128(Pt 6), pp. 1314–1322. Available at: https://doi.org/10.1093/brain/awh445.

Ren, L. *et al.* (2018) 'Nonsteroidal anti-inflammatory drugs use and risk of Parkinson disease', *Medicine*, 97(37), p. e12172. Available at: https://doi.org/10.1097/MD.0000000000012172.

Ren, Y. *et al.* (2015) 'Parkin Mutations Reduce the Complexity of Neuronal Processes in iPSC-derived Human Neurons', *Stem cells (Dayton, Ohio)*, 33(1), pp. 68–78. Available at: https://doi.org/10.1002/stem.1854.

Reyes, S. *et al.* (2012) 'GIRK2 expression in dopamine neurons of the substantia nigra and ventral tegmental area', *The Journal of Comparative Neurology*, 520(12), pp. 2591–2607. Available at: https://doi.org/10.1002/cne.23051.

Riaz, T.A. *et al.* (2020) 'Role of Endoplasmic Reticulum Stress Sensor IRE1α in Cellular Physiology, Calcium, ROS Signaling, and Metaflammation', *Cells*, 9(5), p. 1160. Available at: https://doi.org/10.3390/cells9051160.

Rinne, J.O. *et al.* (2008) 'Loss of cholinergic neurons in the pedunculopontine nucleus in Parkinson's disease is related to disability of the patients', *Parkinsonism & Related Disorders*, 14(7), pp. 553–557. Available at: https://doi.org/10.1016/j.parkreldis.2008.01.006.

Ritz, B. *et al.* (2014) 'Parkinson disease and smoking revisited: ease of quitting is an early sign of the disease', *Neurology*, 83(16), pp. 1396–1402. Available at: https://doi.org/10.1212/WNL.0000000000000879.

Romero-Barrios, N. *et al.* (2018) 'Splicing regulation by long noncoding RNAs', *Nucleic Acids Research*, 46(5), pp. 2169–2184. Available at: https://doi.org/10.1093/nar/gky095.

Ron, D. and Walter, P. (2007) 'Signal integration in the endoplasmic reticulum unfolded protein response', *Nature Reviews Molecular Cell Biology*, 8(7), pp. 519–529. Available at: https://doi.org/10.1038/nrm2199.

Rong, S. *et al.* (2021) 'Meynert nucleus-related cortical thinning in Parkinson's disease with mild cognitive impairment', *Quantitative Imaging in Medicine and Surgery*, 11(4), pp. 1554–1566. Available at: https://doi.org/10.21037/qims-20-444.

Ross, O.A. *et al.* (2008) 'Genetic variation of Omi/HtrA2 and Parkinson's disease', *Parkinsonism & related disorders*, 14(7), pp. 539–543. Available at: https://doi.org/10.1016/j.parkreldis.2008.08.003.

Rothfuss, O. *et al.* (2009) 'Parkin protects mitochondrial genome integrity and supports mitochondrial DNA repair', *Human Molecular Genetics*, 18(20), pp. 3832–3850. Available at: https://doi.org/10.1093/hmg/ddp327.

Rugbjerg, K. *et al.* (2008) 'Risk of Parkinson's disease after hospital contact for head injury: population based case-control study', *BMJ (Clinical research ed.)*, 337, p. a2494. Available at: https://doi.org/10.1136/bmj.a2494.

Rutkowski, D.T. *et al.* (2006) 'Adaptation to ER Stress Is Mediated by Differential Stabilities of Pro-Survival and Pro-Apoptotic mRNAs and Proteins', *PLoS Biology*. Edited by J.S. Weissman, 4(11), p. e374. Available at: https://doi.org/10.1371/journal.pbio.0040374.

Ryan, E. *et al.* (2019) 'GBA1-associated parkinsonism: new insights and therapeutic opportunities', *Current Opinion in Neurology*, 32(4), pp. 589–596. Available at: https://doi.org/10.1097/WCO.0000000000000715.

Rzymski, T. *et al.* (2010) 'Regulation of autophagy by ATF4 in response to severe hypoxia', *Oncogene*, 29(31), pp. 4424–4435. Available at: https://doi.org/10.1038/onc.2010.191.

Sääksjärvi, K. *et al.* (2008) 'Prospective study of coffee consumption and risk of Parkinson's disease', *European Journal of Clinical Nutrition*, 62(7), pp. 908–915. Available at: https://doi.org/10.1038/sj.ejcn.1602788.

Sabath, N. *et al.* (2020) 'Cellular proteostasis decline in human senescence', *Proceedings of the National Academy of Sciences*, 117(50), pp. 31902–31913. Available at: https://doi.org/10.1073/pnas.2018138117.

Sado, M. *et al.* (2009) 'Protective effect against Parkinson's disease-related insults through the activation of XBP1', *Brain Research*, 1257, pp. 16–24. Available at: https://doi.org/10.1016/j.brainres.2008.11.104.

Saez-Atienzar, S. *et al.* (2014) 'The LRRK2 inhibitor GSK2578215A induces protective autophagy in SH-SY5Y cells: involvement of Drp-1-mediated mitochondrial fission and mitochondrial-derived ROS signaling', *Cell Death & Disease*, 5(8), p. e1368. Available at: https://doi.org/10.1038/cddis.2014.320.

Safarpour, D. *et al.* (2015) 'Nursing home and end-of-life care in Parkinson disease', *Neurology*, 85(5), pp. 413–419. Available at: https://doi.org/10.1212/WNL.0000000000001715.

Salmena, L. *et al.* (2011) 'A ceRNA Hypothesis: The Rosetta Stone of a Hidden RNA Language?', *Cell*, 146(3), pp. 353–358. Available at: https://doi.org/10.1016/j.cell.2011.07.014.

Salvatori, B., Biscarini, S. and Morlando, M. (2020) 'Non-coding RNAs in Nervous System Development and Disease', *Frontiers in Cell and Developmental Biology*, 8, p. 273. Available at: https://doi.org/10.3389/fcell.2020.00273.

Sanchez, S.E. *et al.* (2021) 'Alpha Synuclein only Forms Fibrils In Vitro when Larger than its Critical Size of 70 Monomers', *Chembiochem*, 22(19), pp. 2867–2871. Available at: https://doi.org/10.1002/cbic.202100285.

Sanchez-Alvarez, M., del Pozo, M.A. and Bakal, C. (2017) 'AKT-mTOR signaling modulates the dynamics of IRE1 RNAse activity by regulating ER-mitochondria contacts', *Scientific Reports*, 7(1), p. 16497. Available at: https://doi.org/10.1038/s41598-017-16662-1.

Sandoval, H. *et al.* (2008) 'Essential role for Nix in autophagic maturation of erythroid cells', *Nature*, 454(7201), pp. 232–235. Available at: https://doi.org/10.1038/nature07006.

Santos, D. *et al.* (2015) 'The Impact of Mitochondrial Fusion and Fission Modulation in Sporadic Parkinson's Disease', *Molecular Neurobiology*, 52(1), pp. 573–586. Available at: https://doi.org/10.1007/s12035-014-8893-4.

Sarcinelli, C. *et al.* (2020) 'ATF4-Dependent NRF2 Transcriptional Regulation Promotes Antioxidant Protection during Endoplasmic Reticulum Stress', *Cancers*, 12(3), p. 569. Available at: https://doi.org/10.3390/cancers12030569.

Sasaki, Y.T.F. *et al.* (2007) 'Identification and characterization of human non-coding RNAs with tissue-specific expression', *Biochemical and Biophysical Research*

Communications, 357(4), pp. 991–996. Available at: https://doi.org/10.1016/j.bbrc.2007.04.034.

Sassano, M.L. *et al.* (2023) 'PERK recruits E-Syt1 at ER-mitochondria contacts for mitochondrial lipid transport and respiration', *The Journal of Cell Biology*, 222(3), p. e202206008. Available at: https://doi.org/10.1083/jcb.202206008.

Sauvageau, M. *et al.* (2013) 'Multiple knockout mouse models reveal lincRNAs are required for life and brain development', *eLife*, 2, p. e01749. Available at: https://doi.org/10.7554/eLife.01749.

Savica, R. *et al.* (2016) 'Time Trends in the Incidence of Parkinson Disease', *JAMA Neurology*, 73(8), p. 981. Available at: https://doi.org/10.1001/jamaneurol.2016.0947.

Sayles, N.M. *et al.* (2022) 'Mutant CHCHD10 causes an extensive metabolic rewiring that precedes OXPHOS dysfunction in a murine model of mitochondrial cardiomyopathy', *Cell reports*, 38(10), p. 110475. Available at: https://doi.org/10.1016/j.celrep.2022.110475.

Scatton, B. *et al.* (1983) 'Reduction of cortical dopamine, noradrenaline, serotonin and their metabolites in Parkinson's disease', *Brain Research*, 275(2), pp. 321–328. Available at: https://doi.org/10.1016/0006-8993(83)90993-9.

Schapira, A.H. *et al.* (1990) 'Mitochondrial complex I deficiency in Parkinson's disease', *Journal of Neurochemistry*, 54(3), pp. 823–827. Available at: https://doi.org/10.1111/j.1471-4159.1990.tb02325.x.

Schapira, A.H.V., Chaudhuri, K.R. and Jenner, P. (2017) 'Non-motor features of Parkinson disease', *Nature Reviews Neuroscience*, 18(7), pp. 435–450. Available at: https://doi.org/10.1038/nrn.2017.62.

Schertzer, M.D. *et al.* (2019) 'lncRNA-Induced Spread of Polycomb Controlled by Genome Architecture, RNA Abundance, and CpG Island DNA', *Molecular Cell*, 75(3), pp. 523-537.e10. Available at: https://doi.org/10.1016/j.molcel.2019.05.028.

Schöndorf, D.C. *et al.* (2018) 'The NAD+ Precursor Nicotinamide Riboside Rescues Mitochondrial Defects and Neuronal Loss in iPSC and Fly Models of Parkinson's Disease', *Cell Reports*, 23(10), pp. 2976–2988. Available at: https://doi.org/10.1016/j.celrep.2018.05.009.

Schulz, A.M. and Haynes, C.M. (2015) 'UPRmt-mediated cytoprotection and organismal aging', *Biochimica et Biophysica Acta (BBA) - Bioenergetics*, 1847(11), pp. 1448–1456. Available at: https://doi.org/10.1016/j.bbabio.2015.03.008.

Schulz, J. *et al.* (2018) 'Nucleus basalis of Meynert degeneration precedes and predicts cognitive impairment in Parkinson's disease', *Brain: A Journal of Neurology*, 141(5), pp. 1501–1516. Available at: https://doi.org/10.1093/brain/awy072.

Schwartzentruber, A. *et al.* (2020) 'Oxidative switch drives mitophagy defects in dopaminergic parkin mutant patient neurons', *Scientific Reports*, 10(1), p. 15485. Available at: https://doi.org/10.1038/s41598-020-72345-4.

Scorziello, A. *et al.* (2020) 'Mitochondrial Homeostasis and Signaling in Parkinson's Disease', *Frontiers in Aging Neuroscience*, 12, p. 100. Available at: https://doi.org/10.3389/fnagi.2020.00100.

Seibler, P. *et al.* (2011) 'Mitochondrial Parkin Recruitment Is Impaired in Neurons Derived from Mutant PINK1 Induced Pluripotent Stem Cells', *Journal of Neuroscience*, 31(16), pp. 5970–5976. Available at: https://doi.org/10.1523/JNEUROSCI.4441-10.2011.

Selvaraj, S. *et al.* (2012) 'Neurotoxin-induced ER stress in mouse dopaminergic neurons involves downregulation of TRPC1 and inhibition of AKT/mTOR signaling', *Journal of Clinical Investigation*, 122(4), pp. 1354–1367. Available at: https://doi.org/10.1172/JCI61332.

Shahmoradian, S.H. *et al.* (2019) 'Lewy pathology in Parkinson's disease consists of crowded organelles and lipid membranes', *Nature Neuroscience*, 22(7), pp. 1099–1109. Available at: https://doi.org/10.1038/s41593-019-0423-2.

Shaltouki, A. *et al.* (2015) 'Mitochondrial Alterations by PARKIN in Dopaminergic Neurons Using PARK2 Patient-Specific and PARK2 Knockout Isogenic iPSC Lines', *Stem Cell Reports*, 4(5), pp. 847–859. Available at: https://doi.org/10.1016/j.stemcr.2015.02.019.

Shaltouki, A. *et al.* (2018) 'Alpha-synuclein delays mitophagy and targeting Miro rescues neuron loss in Parkinson's models', *Acta Neuropathologica*, 136(4), pp. 607–620. Available at: https://doi.org/10.1007/s00401-018-1873-4.

Sharma, V. *et al.* (2018) 'Local Inhibition of PERK Enhances Memory and Reverses Age-Related Deterioration of Cognitive and Neuronal Properties', *The Journal of Neuroscience*, 38(3), pp. 648–658. Available at: https://doi.org/10.1523/JNEUROSCI.0628-17.2017.

Shen, D.-F. *et al.* (2023) 'Resveratrol Promotes Autophagy to Improve neuronal Injury in Parkinson's Disease by Regulating SNHG1/miR-128-3p/SNCA Axis', *Brain Sciences*, 13(8), p. 1124. Available at: https://doi.org/10.3390/brainsci13081124.

Shen, R.-S. *et al.* (1985) 'Serotonergic conversion of MPTP and dopaminergic accumulation of MPP^{+}', *FEBS Letters*, 189(2), pp. 225–230. Available at: https://doi.org/10.1016/0014-5793(85)81028-0.

Sheng, Y. *et al.* (2021) 'Distinct temporal actions of different types of unfolded protein responses during aging', *Journal of Cellular Physiology*, 236(7), pp. 5069–5079. Available at: https://doi.org/10.1002/jcp.30215.

Sherstyuk, V.V., Medvedev, S.P. and Zakian, S.M. (2018) 'Noncoding RNAs in the Regulation of Pluripotency and Reprogramming', *Stem Cell Reviews and Reports*, 14(1), pp. 58–70. Available at: https://doi.org/10.1007/s12015-017-9782-9.

Shiba-Fukushima, K. *et al.* (2017) 'Evidence that phosphorylated ubiquitin signaling is involved in the etiology of Parkinson's disease', *Human Molecular Genetics*, 26(16), pp. 3172–3185. Available at: https://doi.org/10.1093/hmg/ddx201.

Shoulders, M.D. *et al.* (2013) 'Stress-Independent Activation of XBP1s and/or ATF6 Reveals Three Functionally Diverse ER Proteostasis Environments', *Cell Reports*, 3(4), pp. 1279–1292. Available at: https://doi.org/10.1016/j.celrep.2013.03.024.

Shpilka, T. and Haynes, C.M. (2018) 'The mitochondrial UPR: mechanisms, physiological functions and implications in ageing', *Nature Reviews Molecular Cell Biology*, 19(2), pp. 109–120. Available at: https://doi.org/10.1038/nrm.2017.110.

Shukla, C.J. *et al.* (2018) 'High-throughput identification of RNA nuclear enrichment sequences', *The EMBO Journal*, 37(6). Available at: https://doi.org/10.15252/embj.201798452.

Silva, R.M. *et al.* (2005) 'CHOP/GADD153 is a mediator of apoptotic death in substantia nigra dopamine neurons in an in vivo neurotoxin model of parkinsonism', *Journal of*

Neurochemistry, 95(4), pp. 974–986. Available at: https://doi.org/10.1111/j.1471-4159.2005.03428.x.

Sims, R.J., Belotserkovskaya, R. and Reinberg, D. (2004) 'Elongation by RNA polymerase II: the short and long of it', *Genes & Development*, 18(20), pp. 2437–2468. Available at: https://doi.org/10.1101/gad.1235904.

Simuni, T. *et al.* (2016) 'Predictors of time to initiation of symptomatic therapy in early Parkinson's disease', *Annals of Clinical and Translational Neurology*, 3(7), pp. 482–494. Available at: https://doi.org/10.1002/acn3.317.

Singh, F. *et al.* (2021) 'Pharmacological rescue of impaired mitophagy in Parkinson's disease-related LRRK2 G2019S knock-in mice', *eLife*, 10, p. e67604. Available at: https://doi.org/10.7554/eLife.67604.

Sison, S.L. *et al.* (2018) 'Using Patient-Derived Induced Pluripotent Stem Cells to Identify Parkinson's Disease-Relevant Phenotypes', *Current Neurology and Neuroscience Reports*, 18(12), p. 84. Available at: https://doi.org/10.1007/s11910-018-0893-8.

Sliter, D.A. *et al.* (2018) 'Parkin and PINK1 mitigate STING-induced inflammation', *Nature*, 561(7722), pp. 258–262. Available at: https://doi.org/10.1038/s41586-018-0448-9.

Soutar, M.P.M. *et al.* (2018) 'AKT signalling selectively regulates PINK1 mitophagy in SHSY5Y cells and human iPSC-derived neurons', *Scientific Reports*, 8(1), p. 8855. Available at: https://doi.org/10.1038/s41598-018-26949-6.

Sozen, E. *et al.* (2020) 'Cholesterol induced autophagy via IRE1/JNK pathway promotes autophagic cell death in heart tissue', *Metabolism*, 106, p. 154205. Available at: https://doi.org/10.1016/j.metabol.2020.154205.

Spillantini, M.G. *et al.* (1998) 'Filamentous alpha-synuclein inclusions link multiple system atrophy with Parkinson's disease and dementia with Lewy bodies', *Neuroscience Letters*, 251(3), pp. 205–208. Available at: https://doi.org/10.1016/s0304-3940(98)00504-7.

Spinelli, J.B. and Haigis, M.C. (2018) 'The multifaceted contributions of mitochondria to cellular metabolism', *Nature Cell Biology*, 20(7), pp. 745–754. Available at: https://doi.org/10.1038/s41556-018-0124-1.

Spitale, R.C. *et al.* (2015) 'Structural imprints in vivo decode RNA regulatory mechanisms', *Nature*, 519(7544), pp. 486–490. Available at: https://doi.org/10.1038/nature14263.

Statello, L. *et al.* (2021) 'Gene regulation by long non-coding RNAs and its biological functions', *Nature Reviews Molecular Cell Biology*, 22(2), pp. 96–118. Available at: https://doi.org/10.1038/s41580-020-00315-9.

Strauss, K.M. *et al.* (2005) 'Loss of function mutations in the gene encoding Omi/HtrA2 in Parkinson's disease', *Human Molecular Genetics*, 14(15), pp. 2099–2111. Available at: https://doi.org/10.1093/hmg/ddi215.

Strecker, K. *et al.* (2011) 'Preserved serotonin transporter binding in de novo Parkinson's disease: negative correlation with the dopamine transporter', *Journal of Neurology*, 258(1), pp. 19–26. Available at: https://doi.org/10.1007/s00415-010-5666-5.

Su, Y.-C. and Qi, X. (2013) 'Inhibition of excessive mitochondrial fission reduced aberrant autophagy and neuronal damage caused by LRRK2 G2019S mutation', *Human Molecular Genetics*, 22(22), pp. 4545–4561. Available at: https://doi.org/10.1093/hmg/ddt301.

Sun, X. *et al.* (2013) 'ATF4 Protects Against Neuronal Death in Cellular Parkinson's Disease Models by Maintaining Levels of Parkin', *The Journal of Neuroscience*, 33(6), pp. 2398–2407. Available at: https://doi.org/10.1523/JNEUROSCI.2292-12.2013.

Sunwoo, H. *et al.* (2009) '*MEN ε/β* nuclear-retained non-coding RNAs are up-regulated upon muscle differentiation and are essential components of paraspeckles', *Genome Research*, 19(3), pp. 347–359. Available at: https://doi.org/10.1101/gr.087775.108.

Suomalainen, A. and Battersby, B.J. (2018) 'Mitochondrial diseases: the contribution of organelle stress responses to pathology', *Nature Reviews Molecular Cell Biology*, 19(2), pp. 77–92. Available at: https://doi.org/10.1038/nrm.2017.66.

Surmeier, D.J. (2018) 'Determinants of dopaminergic neuron loss in Parkinson's disease', *The FEBS Journal*, 285(19), pp. 3657–3668. Available at: https://doi.org/10.1111/febs.14607.

Surmeier, D.J., Obeso, J.A. and Halliday, G.M. (2017) 'Selective neuronal vulnerability in Parkinson disease', *Nature Reviews Neuroscience*, 18(2), pp. 101–113. Available at: https://doi.org/10.1038/nrn.2016.178.

Suzuki, S. *et al.* (2017) 'Efficient induction of dopaminergic neuron differentiation from induced pluripotent stem cells reveals impaired mitophagy in PARK2 neurons', *Biochemical and Biophysical Research Communications*, 483(1), pp. 88–93. Available at: https://doi.org/10.1016/j.bbrc.2016.12.188.

Swatek, K.N. *et al.* (2019) 'Insights into ubiquitin chain architecture using Ub-clipping', *Nature*, 572(7770), pp. 533–537. Available at: https://doi.org/10.1038/s41586-019-1482-y.

Szcześniak, M.W. *et al.* (2021) 'Comparative genomics in the search for conserved long noncoding RNAs', *Essays in Biochemistry*, 65(4), pp. 741–749. Available at: https://doi.org/10.1042/EBC20200069.

Tang, F.-L. *et al.* (2015) 'VPS35 deficiency or mutation causes dopaminergic neuronal loss by impairing mitochondrial fusion and function', *Cell reports*, 12(10), pp. 1631–1643. Available at: https://doi.org/10.1016/j.celrep.2015.08.001.

Tanner, C.M. *et al.* (2002) 'Smoking and Parkinson's disease in twins', *Neurology*, 58(4), pp. 581–588. Available at: https://doi.org/10.1212/wnl.58.4.581.

Taylor, D.J. *et al.* (1994) 'A 31P magnetic resonance spectroscopy study of mitochondrial function in skeletal muscle of patients with Parkinson's disease', *Journal of the Neurological Sciences*, 125(1), pp. 77–81. Available at: https://doi.org/10.1016/0022-510X(94)90245-3.

Taylor, R.C. and Dillin, A. (2013) 'XBP-1 Is a Cell-Nonautonomous Regulator of Stress Resistance and Longevity', *Cell*, 153(7), pp. 1435–1447. Available at: https://doi.org/10.1016/j.cell.2013.05.042.

Thacker, E.L. *et al.* (2007) 'Temporal relationship between cigarette smoking and risk of Parkinson disease', *Neurology*, 68(10), pp. 764–768. Available at: https://doi.org/10.1212/01.wnl.0000256374.50227.4b.

Thenganatt, M.A. and Jankovic, J. (2014) 'Parkinson Disease Subtypes', *JAMA Neurology*, 71(4), p. 499. Available at: https://doi.org/10.1001/jamaneurol.2013.6233.

Tilokani, L. *et al.* (2018) 'Mitochondrial dynamics: overview of molecular mechanisms', *Essays in Biochemistry*. Edited by C. Garone and M. Minczuk, 62(3), pp. 341–360. Available at: https://doi.org/10.1042/EBC20170104.

Tofaris, G.K. (2022) ‘Initiation and progression of α-synuclein pathology in Parkinson’s disease’, *Cellular and Molecular Life Sciences*, 79(4), p. 210. Available at: https://doi.org/10.1007/s00018-022-04240-2.

Tofaris, G.K., Goedert, M. and Spillantini, M.G. (2017) ‘The Transcellular Propagation and Intracellular Trafficking of α-Synuclein’, *Cold Spring Harbor Perspectives in Medicine*, 7(9), p. a024380. Available at: https://doi.org/10.1101/cshperspect.a024380.

Tolosa, E. *et al.* (2021) ‘Challenges in the diagnosis of Parkinson’s disease’, *The Lancet. Neurology*, 20(5), pp. 385–397. Available at: https://doi.org/10.1016/S1474-4422(21)00030-2.

Ton, T.G. *et al.* (2006) ‘Nonsteroidal anti-inflammatory drugs and risk of Parkinson’s disease’, *Movement Disorders: Official Journal of the Movement Disorder Society*, 21(7), pp. 964–969. Available at: https://doi.org/10.1002/mds.20856.

Tonelli, C., Chio, I.I.C. and Tuveson, D.A. (2018) ‘Transcriptional Regulation by Nrf2’, *Antioxidants & Redox Signaling*, 29(17), pp. 1727–1745. Available at: https://doi.org/10.1089/ars.2017.7342.

Tong, Q. *et al.* (2016) ‘Inhibition of endoplasmic reticulum stress-activated IRE1α-TRAF2-caspase-12 apoptotic pathway is involved in the neuroprotective effects of telmisartan in the rotenone rat model of Parkinson’s disease’, *European Journal of Pharmacology*, 776, pp. 106–115. Available at: https://doi.org/10.1016/j.ejphar.2016.02.042.

Tosserams, A. *et al.* (2018) ‘Underrepresentation of women in Parkinson’s disease trials: Underrepresentation Of Women In Pd Trials’, *Movement Disorders*, 33(11), pp. 1825–1826. Available at: https://doi.org/10.1002/mds.27505.

Trétiakoff, C. (1919) *Contribution a l’etude l’anatomie pathologique du locus Niger de soemmering: avec quelques déductions relatives à la pathogénie des troubles du tonus musculaire et de la maladie de Parkinson*. Jouve.

Trist, B.G., Hare, D.J. and Double, K.L. (2019) ‘Oxidative stress in the aging substantia nigra and the etiology of Parkinson’s disease’, *Aging Cell*, 18(6), p. e13031. Available at: https://doi.org/10.1111/acel.13031.

Tsuru, A. *et al.* (2016) ‘Novel mechanism of enhancing IRE1α-XBP1 signalling via the PERK-ATF4 pathway’, *Scientific Reports*, 6, p. 24217. Available at: https://doi.org/10.1038/srep24217.

Ulitsky, I. (2016) ‘Evolution to the rescue: using comparative genomics to understand long non-coding RNAs’, *Nature Reviews Genetics*, 17(10), pp. 601–614. Available at: https://doi.org/10.1038/nrg.2016.85.

Ulitsky, I. and Bartel, D.P. (2013) ‘lincRNAs: Genomics, Evolution, and Mechanisms’, *Cell*, 154(1), pp. 26–46. Available at: https://doi.org/10.1016/j.cell.2013.06.020.

Unal Gulsuner, H. *et al.* (2014) ‘Mitochondrial serine protease HTRA2 p.G399S in a kindred with essential tremor and Parkinson disease’, *Proceedings of the National Academy of Sciences*, 111(51), pp. 18285–18290. Available at: https://doi.org/10.1073/pnas.1419581111.

Uoselis, L. *et al.* (2023) ‘Temporal landscape of mitochondrial proteostasis governed by the UPRmt’, *Science Advances*, 9(38), p. eadh8228. Available at: https://doi.org/10.1126/sciadv.adh8228.

Upton, J.-P. *et al.* (2012) 'IRE1α Cleaves Select microRNAs During ER Stress to Derepress Translation of Proapoptotic Caspase-2', *Science*, 338(6108), pp. 818–822. Available at: https://doi.org/10.1126/science.1226191.

Urano, F. *et al.* (2000) 'Coupling of stress in the ER to activation of JNK protein kinases by transmembrane protein kinase IRE1', *Science (New York, N.Y.)*, 287(5453), pp. 664–666. Available at: https://doi.org/10.1126/science.287.5453.664.

Valdés, P. *et al.* (2014) 'Control of dopaminergic neuron survival by the unfolded protein response transcription factor XBP1', *Proceedings of the National Academy of Sciences*, 111(18), pp. 6804–6809. Available at: https://doi.org/10.1073/pnas.1321845111.

Valente, E.M. *et al.* (2004) 'Hereditary Early-Onset Parkinson's Disease Caused by Mutations in *PINK1*', *Science*, 304(5674), pp. 1158–1160. Available at: https://doi.org/10.1126/science.1096284.

Van Laar, V.S. *et al.* (2015) 'Glutamate excitotoxicity in neurons triggers mitochondrial and endoplasmic reticulum accumulation of Parkin, and, in the presence of N-acetyl cysteine, mitophagy', *Neurobiology of Disease*, 74, pp. 180–193. Available at: https://doi.org/10.1016/j.nbd.2014.11.015.

Vattem, K.M. and Wek, R.C. (2004) 'Reinitiation involving upstream ORFs regulates *ATF4* mRNA translation in mammalian cells', *Proceedings of the National Academy of Sciences*, 101(31), pp. 11269–11274. Available at: https://doi.org/10.1073/pnas.0400541101.

Verfaillie, T. *et al.* (2012) 'PERK is required at the ER-mitochondrial contact sites to convey apoptosis after ROS-based ER stress', *Cell Death & Differentiation*, 19(11), pp. 1880–1891. Available at: https://doi.org/10.1038/cdd.2012.74.

Vidal, R.L. *et al.* (2021) 'Enforced dimerization between XBP1s and ATF6f enhances the protective effects of the UPR in models of neurodegeneration', *Molecular Therapy*, 29(5), pp. 1862–1882. Available at: https://doi.org/10.1016/j.ymthe.2021.01.033.

Vielhaber, S. *et al.* (2013) 'Mitofusin 2 mutations affect mitochondrial function by mitochondrial DNA depletion', *Acta Neuropathologica*, 125(2), pp. 245–256. Available at: https://doi.org/10.1007/s00401-012-1036-y.

Villa, E. *et al.* (2017) 'Parkin-Independent Mitophagy Controls Chemotherapeutic Response in Cancer Cells', *Cell Reports*, 20(12), pp. 2846–2859. Available at: https://doi.org/10.1016/j.celrep.2017.08.087.

van Vliet, A.R. and Agostinis, P. (2018) 'Mitochondria-Associated Membranes and ER Stress', *Current Topics in Microbiology and Immunology*, 414, pp. 73–102. Available at: https://doi.org/10.1007/82_2017_2.

Wakabayashi, K. *et al.* (2013) 'The Lewy body in Parkinson's disease and related neurodegenerative disorders', *Molecular neurobiology*, 47(2). Available at: https://doi.org/10.1007/s12035-012-8280-y.

Walter, F. *et al.* (2015) 'Imaging of single cell responses to ER stress indicates that the relative dynamics of IRE1/XBP1 and PERK/ATF4 signalling rather than a switch between signalling branches determine cell survival', *Cell Death and Differentiation*, 22(9), pp. 1502–1516. Available at: https://doi.org/10.1038/cdd.2014.241.

Walter, F. *et al.* (2018) 'ER stress signaling has an activating transcription factor 6α (ATF6)-dependent "off-switch"', *The Journal of Biological Chemistry*, 293(47), pp. 18270–18284. Available at: https://doi.org/10.1074/jbc.RA118.002121.

Wang, H. *et al.* (2021) 'LncRNA SNHG1 promotes neuronal injury in Parkinson's disease cell model by miR-181a-5p/CXCL12 axis', *Journal of Molecular Histology*, 52(2), pp. 153–163. Available at: https://doi.org/10.1007/s10735-020-09931-3.

Wang, L. *et al.* (2013a) 'CPAT: Coding-Potential Assessment Tool using an alignment-free logistic regression model', *Nucleic Acids Research*, 41(6), p. e74. Available at: https://doi.org/10.1093/nar/gkt006.

Wang, L. *et al.* (2013b) 'CPAT: Coding-Potential Assessment Tool using an alignment-free logistic regression model', *Nucleic Acids Research*, 41(6), p. e74. Available at: https://doi.org/10.1093/nar/gkt006.

Wang, L. *et al.* (2015) 'PERK Limits Drosophila Lifespan by Promoting Intestinal Stem Cell Proliferation in Response to ER Stress', *PLOS Genetics*. Edited by G.P. Copenhaver, 11(5), p. e1005220. Available at: https://doi.org/10.1371/journal.pgen.1005220.

Wang, M. and Kaufman, R.J. (2016) 'Protein misfolding in the endoplasmic reticulum as a conduit to human disease', *Nature*, 529(7586), pp. 326–335. Available at: https://doi.org/10.1038/nature17041.

Wang, S.-H. *et al.* (2021) 'LncRNA H19 governs mitophagy and restores mitochondrial respiration in the heart through Pink1/Parkin signaling during obesity', *Cell Death & Disease*, 12(6), p. 557. Available at: https://doi.org/10.1038/s41419-021-03821-6.

Wang, W. *et al.* (2016) 'Parkinson's disease-associated mutant VPS35 causes mitochondrial dysfunction by recycling DLP1 complexes', *Nature medicine*, 22(1), pp. 54–63. Available at: https://doi.org/10.1038/nm.3983.

Wang, W. *et al.* (2021) 'Biological Function of Long Non-coding RNA (LncRNA) Xist', *Frontiers in Cell and Developmental Biology*, 9, p. 645647. Available at: https://doi.org/10.3389/fcell.2021.645647.

Wang, X. *et al.* (2011) 'DLP1-dependent mitochondrial fragmentation mediates 1-methyl-4-phenylpyridinium toxicity in neurons: implications for Parkinson's disease: MPP^+ induces mitochondrial fragmentation', *Aging Cell*, 10(5), pp. 807–823. Available at: https://doi.org/10.1111/j.1474-9726.2011.00721.x.

Wang, X. *et al.* (2012) 'LRRK2 regulates mitochondrial dynamics and function through direct interaction with DLP1', *Human Molecular Genetics*, 21(9), pp. 1931–1944. Available at: https://doi.org/10.1093/hmg/dds003.

Wang, Y. *et al.* (2019) 'Mitochondrial dysfunction in neurodegenerative diseases and the potential countermeasure', *CNS neuroscience & therapeutics*, 25(7), pp. 816–824. Available at: https://doi.org/10.1111/cns.13116.

Wang, Y. *et al.* (2021) 'Mitophagy coordinates the mitochondrial unfolded protein response to attenuate inflammation-mediated myocardial injury', *Redox Biology*, 45, p. 102049. Available at: https://doi.org/10.1016/j.redox.2021.102049.

Wang, Z., Li, K. and Huang, W. (2020) 'Long non-coding RNA NEAT1-centric gene regulation', *Cellular and molecular life sciences: CMLS*, 77(19), pp. 3769–3779. Available at: https://doi.org/10.1007/s00018-020-03503-0.

Wang, Z.-X. *et al.* (2023) 'DNA Damage-Mediated Neurotoxicity in Parkinson's Disease', *International Journal of Molecular Sciences*, 24(7), p. 6313. Available at: https://doi.org/10.3390/ijms24076313.

Ward, M. *et al.* (2015) 'Conservation and tissue-specific transcription patterns of long noncoding RNAs', *Journal of Human Transcriptome*, 1(1), pp. 2–9. Available at: https://doi.org/10.3109/23324015.2015.1077591.

Washietl, S., Kellis, M. and Garber, M. (2014) 'Evolutionary dynamics and tissue specificity of human long noncoding RNAs in six mammals', *Genome Research*, 24(4), pp. 616–628. Available at: https://doi.org/10.1101/gr.165035.113.

Watatani, Y. *et al.* (2008) 'Stress-induced Translation of ATF5 mRNA Is Regulated by the 5′-Untranslated Region', *Journal of Biological Chemistry*, 283(5), pp. 2543–2553. Available at: https://doi.org/10.1074/jbc.M707781200.

Wauer, T. *et al.* (2015) 'Mechanism of phospho-ubiquitin-induced PARKIN activation', *Nature*, 524(7565), pp. 370–374. Available at: https://doi.org/10.1038/nature14879.

Weatherbee, J.L., Kraus, J.-L. and Ross, A.H. (2016) 'ER stress in temozolomide-treated glioblastomas interferes with DNA repair and induces apoptosis', *Oncotarget*, 7(28), pp. 43820–43834. Available at: https://doi.org/10.18632/oncotarget.9907.

Wei, C.-W. *et al.* (2018) 'The Role of Long Noncoding RNAs in Central Nervous System and Neurodegenerative Diseases', *Frontiers in Behavioral Neuroscience*, 12. Available at: https://doi.org/10.3389/fnbeh.2018.00175.

Welch, G. and Tsai, L. (2022) 'Mechanisms of DNA damage-mediated neurotoxicity in neurodegenerative disease', *EMBO Reports*, 23(6), p. e54217. Available at: https://doi.org/10.15252/embr.202154217.

Welch, G.M. *et al.* (2022) 'Neurons burdened by DNA double-strand breaks incite microglia activation through antiviral-like signaling in neurodegeneration', *Science Advances*, 8(39), p. eabo4662. Available at: https://doi.org/10.1126/sciadv.abo4662.

Werner, M.S. *et al.* (2017) 'Chromatin-enriched lncRNAs can act as cell-type specific activators of proximal gene transcription', *Nature Structural & Molecular Biology*, 24(7), pp. 596–603. Available at: https://doi.org/10.1038/nsmb.3424.

Werner, M.S. and Ruthenburg, A.J. (2015) 'Nuclear Fractionation Reveals Thousands of Chromatin-Tethered Noncoding RNAs Adjacent to Active Genes', *Cell Reports*, 12(7), pp. 1089–1098. Available at: https://doi.org/10.1016/j.celrep.2015.07.033.

West, J.A. *et al.* (2014) 'The Long Noncoding RNAs NEAT1 and MALAT1 Bind Active Chromatin Sites', *Molecular Cell*, 55(5), pp. 791–802. Available at: https://doi.org/10.1016/j.molcel.2014.07.012.

West, J.A. *et al.* (2016) 'Structural, super-resolution microscopy analysis of paraspeckle nuclear body organization', *Journal of Cell Biology*, 214(7), pp. 817–830. Available at: https://doi.org/10.1083/jcb.201601071.

Westermann, B. (2010) 'Mitochondrial fusion and fission in cell life and death', *Nature Reviews Molecular Cell Biology*, 11(12), pp. 872–884. Available at: https://doi.org/10.1038/nrm3013.

Wilson, H., de Natale, E.R. and Politis, M. (2021) 'Nucleus basalis of Meynert degeneration predicts cognitive impairment in Parkinson's disease', *Handbook of Clinical Neurology*, 179, pp. 189–205. Available at: https://doi.org/10.1016/B978-0-12-819975-6.00010-8.

Wilusz, J.E. *et al.* (2012) 'A triple helix stabilizes the 3' ends of long noncoding RNAs that lack poly(A) tails', *Genes & Development*, 26(21), pp. 2392–2407. Available at: https://doi.org/10.1101/gad.204438.112.

Winner, B. *et al.* (2011) 'In vivo demonstration that α-synuclein oligomers are toxic', *Proceedings of the National Academy of Sciences of the United States of America*, 108(10), pp. 4194–4199. Available at: https://doi.org/10.1073/pnas.1100976108.

Wirdefeldt, K. *et al.* (2005) 'Risk and protective factors for Parkinson's disease: a study in Swedish twins', *Annals of Neurology*, 57(1), pp. 27–33. Available at: https://doi.org/10.1002/ana.20307.

Wodrich, A.P.K. *et al.* (2022) 'The Unfolded Protein Responses in Health, Aging, and Neurodegeneration: Recent Advances and Future Considerations', *Frontiers in Molecular Neuroscience*, 15, p. 831116. Available at: https://doi.org/10.3389/fnmol.2022.831116.

Wu, J. *et al.* (2007) 'ATF6α Optimizes Long-Term Endoplasmic Reticulum Function to Protect Cells from Chronic Stress', *Developmental Cell*, 13(3), pp. 351–364. Available at: https://doi.org/10.1016/j.devcel.2007.07.005.

Wu, J. *et al.* (2011) 'The unfolded protein response mediates adaptation to exercise in skeletal muscle through a PGC-1α/ATF6α complex', *Cell Metabolism*, 13(2), pp. 160–169. Available at: https://doi.org/10.1016/j.cmet.2011.01.003.

Xia, M. *et al.* (2019) 'Communication between mitochondria and other organelles: a brand-new perspective on mitochondria in cancer', *Cell & Bioscience*, 9(1), p. 27. Available at: https://doi.org/10.1186/s13578-019-0289-8.

Xiao, X. *et al.* (2021) 'Long Noncoding RNA SNHG1 Knockdown Ameliorates Apoptosis, Oxidative Stress and Inflammation in Models of Parkinson's Disease by Inhibiting the miR-125b-5p/MAPK1 Axis', *Neuropsychiatric Disease and Treatment*, 17, pp. 1153–1163. Available at: https://doi.org/10.2147/NDT.S286778.

Xie, Z. *et al.* (2021) 'Gene Set Knowledge Discovery with Enrichr', *Current Protocols*, 1(3), p. e90. Available at: https://doi.org/10.1002/cpz1.90.

Xu, D. *et al.* (2020) 'ATF4-Mediated Upregulation of REDD1 and Sestrin2 Suppresses mTORC1 Activity during Prolonged Leucine Deprivation', *The Journal of Nutrition*, 150(5), pp. 1022–1030. Available at: https://doi.org/10.1093/jn/nxz309.

Xu, K. *et al.* (2010) 'Neuroprotection by caffeine: Time course and role of its metabolites in the MPTP model of Parkinson Disease', *Neuroscience*, 167(2), pp. 475–481. Available at: https://doi.org/10.1016/j.neuroscience.2010.02.020.

Yamaguchi, Y. and Miura, M. (2015) 'Programmed cell death in neurodevelopment', *Developmental Cell*, 32(4), pp. 478–490. Available at: https://doi.org/10.1016/j.devcel.2015.01.019.

Yamamori, T. *et al.* (2013) 'ER stress suppresses DNA double-strand break repair and sensitizes tumor cells to ionizing radiation by stimulating proteasomal degradation of Rad51', *FEBS letters*, 587(20), pp. 3348–3353. Available at: https://doi.org/10.1016/j.febslet.2013.08.030.

Yamamoto, K. *et al.* (2007) 'Transcriptional Induction of Mammalian ER Quality Control Proteins Is Mediated by Single or Combined Action of ATF6α and XBP1', *Developmental Cell*, 13(3), pp. 365–376. Available at: https://doi.org/10.1016/j.devcel.2007.07.018.

Yamazaki, T. *et al.* (2018) 'Functional Domains of NEAT1 Architectural lncRNA Induce Paraspeckle Assembly through Phase Separation', *Molecular Cell*, 70(6), pp. 1038-1053.e7. Available at: https://doi.org/10.1016/j.molcel.2018.05.019.

Yan, C. *et al.* (2019) 'IRE1 promotes neurodegeneration through autophagy-dependent neuron death in the Drosophila model of Parkinson's disease', *Cell Death & Disease*, 10(11), p. 800. Available at: https://doi.org/10.1038/s41419-019-2039-6.

Yan, M.H., Wang, X. and Zhu, X. (2013) 'Mitochondrial defects and oxidative stress in Alzheimer disease and Parkinson disease', *Free radical biology & medicine*, 62, pp. 90–101. Available at: https://doi.org/10.1016/j.freeradbiomed.2012.11.014.

Yan, W. *et al.* (2018) 'LncRNA NEAT1 promotes autophagy in MPTP-induced Parkinson's disease through stabilizing PINK1 protein', *Biochemical and Biophysical Research Communications*, 496(4), pp. 1019–1024. Available at: https://doi.org/10.1016/j.bbrc.2017.12.149.

Yang, H. *et al.* (2021) 'Dynamic Modeling of Mitochondrial Membrane Potential Upon Exposure to Mitochondrial Inhibitors', *Frontiers in Pharmacology*, 12, p. 679407. Available at: https://doi.org/10.3389/fphar.2021.679407.

Yang, M. *et al.* (2020) 'Mitochondria-Associated ER Membranes – The Origin Site of Autophagy', *Frontiers in Cell and Developmental Biology*, 8. Available at: https://www.frontiersin.org/articles/10.3389/fcell.2020.00595 (Accessed: 17 November 2023).

Yang, M. *et al.* (2022) 'The Translational Regulation in mTOR Pathway', *Biomolecules*, 12(6), p. 802. Available at: https://doi.org/10.3390/biom12060802.

Yang, W. *et al.* (2009) 'Paraquat activates the IRE1/ASK1/JNK cascade associated with apoptosis in human neuroblastoma SH-SY5Y cells', *Toxicology Letters*, 191(2–3), pp. 203–210. Available at: https://doi.org/10.1016/j.toxlet.2009.08.024.

Yao, R.-Q. *et al.* (2021) 'Organelle-specific autophagy in inflammatory diseases: a potential therapeutic target underlying the quality control of multiple organelles', *Autophagy*, 17(2), pp. 385–401. Available at: https://doi.org/10.1080/15548627.2020.1725377.

Yap, K.L. *et al.* (2010) 'Molecular Interplay of the Noncoding RNA ANRIL and Methylated Histone H3 Lysine 27 by Polycomb CBX7 in Transcriptional Silencing of INK4a', *Molecular Cell*, 38(5), pp. 662–674. Available at: https://doi.org/10.1016/j.molcel.2010.03.021.

Yapa, N.M.B. *et al.* (2021) 'Mitochondrial dynamics in health and disease', *FEBS Letters*, 595(8), pp. 1184–1204. Available at: https://doi.org/10.1002/1873-3468.14077.

Ye, J. *et al.* (2000) 'ER Stress Induces Cleavage of Membrane-Bound ATF6 by the Same Proteases that Process SREBPs', *Molecular Cell*, 6(6), pp. 1355–1364. Available at: https://doi.org/10.1016/S1097-2765(00)00133-7.

Yin, Y. *et al.* (2021) 'Single-Cell Sequencing and Organoids: A Powerful Combination for Modelling Organ Development and Diseases', *Reviews of Physiology, Biochemistry and Pharmacology*, 179, pp. 189–210. Available at: https://doi.org/10.1007/112_2020_47.

Yokota, M. *et al.* (2021) 'Establishment of an in vitro model for analyzing mitochondrial ultrastructure in PRKN-mutated patient iPSC-derived dopaminergic neurons',

Molecular Brain, 14(1), p. 58. Available at: https://doi.org/10.1186/s13041-021-00771-0.

Yoshida, H. *et al.* (2001) 'XBP1 mRNA Is Induced by ATF6 and Spliced by IRE1 in Response to ER Stress to Produce a Highly Active Transcription Factor', *Cell*, 107(7), pp. 881–891. Available at: https://doi.org/10.1016/S0092-8674(01)00611-0.

Young, S.K. and Wek, R.C. (2016) 'Upstream Open Reading Frames Differentially Regulate Gene-specific Translation in the Integrated Stress Response', *Journal of Biological Chemistry*, 291(33), pp. 16927–16935. Available at: https://doi.org/10.1074/jbc.R116.733899.

Yu, R. *et al.* (2020) 'Regulation of Mammalian Mitochondrial Dynamics: Opportunities and Challenges', *Frontiers in Endocrinology*, 11, p. 374. Available at: https://doi.org/10.3389/fendo.2020.00374.

Yue, F. *et al.* (2014) 'A comparative encyclopedia of DNA elements in the mouse genome', *Nature*, 515(7527), pp. 355–364. Available at: https://doi.org/10.1038/nature13992.

Yue, W. *et al.* (2014) 'A small natural molecule promotes mitochondrial fusion through inhibition of the deubiquitinase USP30', *Cell Research*, 24(4), pp. 482–496. Available at: https://doi.org/10.1038/cr.2014.20.

Zachari, M. *et al.* (2019) 'Selective Autophagy of Mitochondria on a Ubiquitin-Endoplasmic-Reticulum Platform', *Developmental Cell*, 50(5), pp. 627-643.e5. Available at: https://doi.org/10.1016/j.devcel.2019.06.016.

Zambon, F. *et al.* (2019) 'Cellular α-synuclein pathology is associated with bioenergetic dysfunction in Parkinson's iPSC-derived dopamine neurons', *Human Molecular Genetics*, 28(12), pp. 2001–2013. Available at: https://doi.org/10.1093/hmg/ddz038.

Zeng, K.-W. *et al.* (2021) 'Small molecule induces mitochondrial fusion for neuroprotection via targeting CK2 without affecting its conventional kinase activity', *Signal Transduction and Targeted Therapy*, 6(1), p. 71. Available at: https://doi.org/10.1038/s41392-020-00447-6.

Zhang, G. *et al.* (2022) 'The integrated stress response in ischemic diseases', *Cell Death & Differentiation*, 29(4), pp. 750–757. Available at: https://doi.org/10.1038/s41418-021-00889-7.

Zhang, M., He, P. and Bian, Z. (2021) 'Long Noncoding RNAs in Neurodegenerative Diseases: Pathogenesis and Potential Implications as Clinical Biomarkers', *Frontiers in Molecular Neuroscience*, 14, p. 685143. Available at: https://doi.org/10.3389/fnmol.2021.685143.

Zhang, Q. *et al.* (2021) 'The memory of neuronal mitochondrial stress is inherited transgenerationally via elevated mitochondrial DNA levels', *Nature Cell Biology*, 23(8), pp. 870–880. Available at: https://doi.org/10.1038/s41556-021-00724-8.

Zhang, S., Ma, Y. and Feng, J. (2020) 'Neuroprotective mechanisms of ε-viniferin in a rotenone-induced cell model of Parkinson's disease: significance of SIRT3-mediated FOXO3 deacetylation', *Neural Regeneration Research*, 15(11), p. 2143. Available at: https://doi.org/10.4103/1673-5374.282264.

Zhang, W. *et al.* (2018) 'Knockdown of BACE1-AS by siRNA improves memory and learning behaviors in Alzheimer's disease animal model', *Experimental and Therapeutic Medicine*, 16(3), pp. 2080–2086. Available at: https://doi.org/10.3892/etm.2018.6359.

Zhang, X. *et al.* (2014) 'Endoplasmic reticulum stress induced by tunicamycin and thapsigargin protects against transient ischemic brain injury: Involvement of PARK2-dependent mitophagy', *Autophagy*, 10(10), pp. 1801–1813. Available at: https://doi.org/10.4161/auto.32136.

Zhang, X. *et al.* (2019) 'Role of GTPases in the regulation of mitochondrial dynamics in Parkinson's disease', *Experimental Cell Research*, 382(1), p. 111460. Available at: https://doi.org/10.1016/j.yexcr.2019.06.005.

Zhang, X., Hamblin, M.H. and Yin, K.-J. (2017) 'The long noncoding RNA Malat1: Its physiological and pathophysiological functions', *RNA Biology*, 14(12), pp. 1705–1714. Available at: https://doi.org/10.1080/15476286.2017.1358347.

Zhang, Y., Xia, Q. and Lin, J. (2020) 'LncRNA H19 Attenuates Apoptosis in MPTP-Induced Parkinson's Disease Through Regulating miR-585-3p/PIK3R3', *Neurochemical Research*, 45(7), pp. 1700–1710. Available at: https://doi.org/10.1007/s11064-020-03035-w.

Zhao, J. *et al.* (2020) 'SNHG1 promotes MPP+-induced cytotoxicity by regulating PTEN/AKT/mTOR signaling pathway in SH-SY5Y cells via sponging miR-153-3p', *Biological Research*, 53(1), p. 1. Available at: https://doi.org/10.1186/s40659-019-0267-y.

Zhao, Q. *et al.* (2002) 'A mitochondrial specific stress response in mammalian cells', *The EMBO journal*, 21(17), pp. 4411–4419. Available at: https://doi.org/10.1093/emboj/cdf445.

Zhao, Y. *et al.* (2019) 'Aberrant shuttling of long noncoding RNAs during the mitochondria-nuclear crosstalk in hepatocellular carcinoma cells', *American Journal of Cancer Research*, 9(5), pp. 999–1008.

Zharikov, A.D. *et al.* (2015) 'shRNA targeting α-synuclein prevents neurodegeneration in a Parkinson's disease model', *Journal of Clinical Investigation*, 125(7), pp. 2721–2735. Available at: https://doi.org/10.1172/JCI64502.

Zhou, J. *et al.* (2006) 'The crystal structure of human IRE1 luminal domain reveals a conserved dimerization interface required for activation of the unfolded protein response', *Proceedings of the National Academy of Sciences*, 103(39), pp. 14343–14348. Available at: https://doi.org/10.1073/pnas.0606480103.

Zhou, S. *et al.* (2021) 'Long Non-coding RNAs in Pathogenesis of Neurodegenerative Diseases', *Frontiers in Cell and Developmental Biology*, 9. Available at: https://www.frontiersin.org/articles/10.3389/fcell.2021.719247 (Accessed: 17 November 2023).

Zhu, C. *et al.* (2021) 'Mechanism of Mitophagy and Its Role in Sepsis Induced Organ Dysfunction: A Review', *Frontiers in Cell and Developmental Biology*, 9, p. 664896. Available at: https://doi.org/10.3389/fcell.2021.664896.

Zhu, J.-H. *et al.* (2003) 'Localization of phosphorylated ERK/MAP kinases to mitochondria and autophagosomes in Lewy body diseases', *Brain Pathology (Zurich, Switzerland)*, 13(4), pp. 473–481. Available at: https://doi.org/10.1111/j.1750-3639.2003.tb00478.x.

van Ziel, A.M. and Scheper, W. (2020) 'The UPR in Neurodegenerative Disease: Not Just an Inside Job', *Biomolecules*, 10(8), p. 1090. Available at: https://doi.org/10.3390/biom10081090.

Żuberek, M. *et al.* (2022) ‘How to Use Respiratory Chain Inhibitors in Toxicology Studies—Whole-Cell Measurements’, *International Journal of Molecular Sciences*, 23(16), p. 9076. Available at: https://doi.org/10.3390/ijms23169076.

Zuckerman, B. *et al.* (2020) ‘Gene Architecture and Sequence Composition Underpin Selective Dependency of Nuclear Export of Long RNAs on NXF1 and the TREX Complex’, *Molecular Cell*, 79(2), pp. 251-267.e6. Available at: https://doi.org/10.1016/j.molcel.2020.05.013.

Zuckerman, B. and Ulitsky, I. (2019) ‘Predictive models of subcellular localization of long RNAs’, *RNA*, 25(5), pp. 557–572. Available at: https://doi.org/10.1261/rna.068288.118.

VII. Appendices

1. List of figures

2. List of tables

3. List of abbreviations

ATF3: Activating Transcription Factor 3

ATF4: Activating Transcription Factor 4

ATF5: Activating Transcription Factor 5

ATF6: Activating Transcription Factor 6

ATP: adenosine 5'-triphosphate

BBB: Blood-Brain Barrier

BMP: Bone morphogenetic protein

CASP3: Caspase 3

CAT: Catalase

cCASP4: cleaved Caspase 3

CCCP: Carbonyl cyanide m-chlorophenyl hydrazine

CHAC1: ChaC Glutathione Specific Gamma-Glutamylcyclotransferase 1

ChAT: Choline O-Acetyltransferase

CHOP: C/EBP Homologous Protein

CLPP : Caseinolytic Mitochondrial Matrix Peptidase Proteolytic Subunit

DA: Dopaminergic

DAT: Dopamine transporter

DBH: Dopamine Beta-Hydroxylase

DCX: Doublecortin

DDC: Dopa Decarboxylase

DDIT4: DNA Damage Inducible Transcript 4

dMSN: direct pathway Medium Spiny Neuron

DBS: Deep-brain stimulation

DNAJC3: DnaJ Heat Shock Protein Family (Hsp40) Member C3

DRD2: Dopamine receptor D2

DRP1: dynamin-related protein-1

EDEM1: ER Degradation-Enhancing Alpha-Mannosidase-Like Protein 1

EIF2A: Eukaryotic translation initiation factor 2A

EN1: Engrailed Homeobox 1

EN2: Engrailed Homeobox 2

ER: endoplasmic reticulum

ERN1: Endoplasmic Reticulum To Nucleus Signaling 1

ETC: Electron transport chain
FGF8: Fibroblast Growth Factor 8
FIS1: mitochondria fission 1
FOXA2: Forkhead box protein A2
FOXO3: Forkhead box O3
GAD1: Glutamate Decarboxylase 1
GAD2: Glutamate Decarboxylase 2
GBA: Glucosylceramidase Beta 1
GBX2: Gastrulation Brain Homeobox 2
GFAP: Glial Fibrillary Acidic Protein
GIRK2: G-protein-regulated inward-rectifier potassium channel 2
GPe: Globus pallidus pars externa
GPi : Globus pallidus pars interna
GPX1: Glutathione Peroxidase 1
GPX2: Glutathione Peroxidase 2
GPX8: Glutathione Peroxidase 8
HERPUD1: Homocysteine Inducible ER Protein With Ubiquitin Like Domain 1
HI: healthy individual
HMOX1: Heme Oxygenase 1
HSPA5: Heat Shock Protein Family A (Hsp70) Member 5
IMM: Inner Mitochondrial Membrane
IMS: mitochondrial inner membrane space
iMSN: Indirect pathway Medium Spiny Neuron
iPSC: induced pluripotent stem cells
IRE1: Inositol-Requiring Enzyme 1
JNK: JUN N-Terminal Kinase
JUN: Jun Proto-Oncogene, AP-1 Transcription Factor Subunit
KO: knockout
LB: Lewy Body
L-DOPA: Levodopa
LMX1A: LIM Homeobox Transcription Factor 1 Alpha
LMX1B: LIM Homeobox Transcription Factor 1 Beta
LncRNA: long non-coding RNA
LONP1: Lon Peptidase 1, Mitochondrial

LRRK2: Leucine Rich Repeat Kinase 2

LUHMES: Lund Human Mesencephalic

MAO-B: monoamine oxidase-B

MAP2: Microtubule-associated protein 2

MAPT: Microtubule Associated Protein Tau

MFF: Mitochondrial Fission Factor

MFN1: Mitofusin-1

MFN2: Mitofusin-2

MiD49: Mitochondrial Dynamics proteins of 49 kDa

MiD51: Mitochondrial Dynamics proteins of 51 kDa

MPTP: 1-methyl-4-phenyl-1,2,3,6-tetrahydropyridine

MSN: Medium Spiny Neurons

MSX2: Msh Homeobox 2

MUL1: mitochondrial E3 ubiquitin ligase-1

mtDNA: Mitochondrial DNA

mTOR: mammalian target of rapamycin

NcRNA: non-coding RNA

NDD: Neurodegenerative disorders

NeuN : Neuronal Nuclei

NEUROD1 : Neuronal Differentiation 1

NEUROG2 : Neurogenin 2

NMS: Non-motor symptoms

NRF1: Nuclear Respiratory Factor 1

NRF2: Nuclear Factor (Erythroid-Derived 2)-Like 2

NSAID: Non-steroidal anti-inflammatory drugs

NURR1 : Nuclear Receptor Subfamily 4 Group A Member 2

OLIG1 : Oligodendrocyte Transcription Factor 1

OLIG2 : Oligodendrocyte Transcription Factor 2

OMM: Outer Mitochondrial Membrane

OPA1: dynamin-like GTPase protein optic atrophy 1

ORF: Open Reading Frame

OTX2 : Orthodenticle Homeobox 2

P: patient

PCG: protein-coding gene

PD: Parkinson’s Disease

PERK: PRKR-Like Endoplasmic Reticulum Kinase

PKR: Protein kinase R

PRDX1: Peroxiredoxin 1

PSD95: Postsynaptic density protein 95

PVALB: Parvalbumin

RBD: REM sleep behavior disorder

S100B: S100 Calcium Binding Protein B

SESN2: Sestrin 2

SHH: Sonig hedgehog

SIRT3: Sirtuin 3

SLC1A3: Solute Carrier Family 1 Member 3

SLC1A5: Solute Carrier Family 1 Member 5

SLC3A2: Solute Carrier Family 3 Member 2

SLC7A5: Solute Carrier Family 7 Member 5

SNCA: Synuclein Alpha

SNpc : *Substantia Nigra pars compacta*

SNpr: Substantia Nigra pars reticulate

SNRI: Serotonin–norepinephrine reuptake inhibitor

SOD1: Superoxide dismutase 1

SOD2: Superoxide dismutase 2

SOX2: SRY-Box Transcription Factor 2

SRXN1: Sulfiredoxin 1

SSRI: Selective serotonin reuptake inhibitor

SST: Somatostatin

STN: Subthalamic nucleus

SYNCRIP: Synaptotagmin Binding Cytoplasmic RNA Interacting Protein

TBI: Traumatic Brain Injury

TBR1: T-Box Brain Transcription Factor 1

TGFB1: Transforming Growth Factor Beta 1

TH: Tyrosine hydroxylase

TIMM: Translocase Of Inner Mitochondrial Membrane

TOMM: Translocase Of Outer Mitochondrial Membrane

TPH1: Tryptophan Hydroxylase 1

TPH2: Tryptophan Hydroxylase 2

TRAF2: Tumor Necrosis Factor Type 2 Receptor-Associated Protein 3

TRIB3: Tribbles Pseudokinase 3

TXN: Thioredoxin

TXN2: Thioredoxin 2

uORF: upstream open reading frame

UPR^{ER}: unfolded protein response from the endoplasmic reticulum

UPR^{mt}: mitochondrial unfolded protein response

VaCHT: Vesicular Acetylcholine Transporter

VGLUT1: Vesicular Glutamate Transporter 1

VGLUT2: Vesicular Glutamate Transporter 2

VGLUT3: Vesicular Glutamate Transporter 3

VPS35: Vacuolar Protein Sorting-Associated Protein 35

VMAT2: Vesicular Amine Transporter 2

WNT1: Wingless-Type MMTV Integration Site Family, Member 1

YME1L1: YME1-Like 1 ATPase

XBP1: X-Box Binding Protein 1

XBP1: spliced X-Box Binding Protein 1

VIII. Résumé français

Il est aujourd'hui admis que le dysfonctionnement mitochondrial joue un rôle central dans la physiopathologie de la maladie de Parkinson (MP). Les neurones dopaminergiques (DA) de la substance noire sont particulièrement sensibles au stress mitochondrial, entraînant leur dégénérescence massive et l'apparition de symptômes moteurs. Les mécanismes moléculaires sous-jacents à cette vulnérabilité sélective des neurones DA humains restent largement méconnus. De plus, l'étude des éléments moléculaires propres aux neurones DA s'est, jusqu'à présent, concentrée principalement sur les gènes codant pour des protéines. Cependant, il y a un intérêt croissant pour les éléments non-codants du génome, tels que les longs ARN non codants (lncRNA), régulateurs génomiques puissants présentant une spécificité élevée selon le type cellulaire et le contexte. Ainsi, notre étude s'est focalisée sur la réponse au stress mitochondrial des neurones DA humains et sur la possible contribution des lncRNAs à cette réponse.

Nous avons d'abord utilisé des neurones DA dérivés de cellules LUHMES pour élucider la réponse spécifique des neurones DA humains au stress mitochondrial. L'inhibition de la chaîne respiratoire mitochondriale a entraîné une perturbation significative de l'homéostasie mitochondriale, induisant la mitophagie et réduisant la biogenèse mitochondriale. De plus, le stress a induit un déclin du statut de maturation des neurones DA et une élévation de la proportion de cellules apoptotiques, révélant des dommages cellulaires au-delà du réseau mitochondrial. La réponse au protéines malformées du réticulum endoplasmique (UPRER) dépendante de PERK se révèle être un coordinateur central de la réponse au stress, modulant l'inactivation de l'UPR mitochondriale (UPRmt) et l'expression des lncRNAs. L'identification de nouveaux lncRNAs spécifiquement exprimés dans les neurones DA humains exposés au stress suggère fortement leur implication dans les mécanismes moléculaires intrinsèques à la réponse au stress des neurones DA. De plus, nous avons identifié un lncRNA spécifique au stress, lnc-SLC6A15-5, qui régule la reprise de la traduction après un stress mitochondrial, potentiellement en modulant l'expression des gènes cibles d'ATF4 impliqués dans la régulation de la voie mTOR.

Dans une seconde partie, nous avons évalué si cette réponse au stress mitochondrial était altérée dans le contexte de la MP, en particulier liée aux mutations PRKN. Nous avons recueilli des données transcriptomiques à partir de cellules dérivées de cellules souches pluripotentes induites (iPSC) de patients atteints de la MP porteurs de mutations PRKN et de sujets sains. Nos résultats suggèrent que l'invalidation de PARKIN altère la différenciation cellulaire, entraînant un éventuel retard de maturité et une augmentation de la population gliale. Les cellules PRKN-mutantes semblent également être "pré-stressées" en condition basale, avec activation des voies de l'UPRER dépendantes d'ATF6 et d'IRE1, ainsi que de la réponse antioxydante régulée par NRF2. L'incubation avec des toxines mitochondriales a intensifié ces réponses, avec une activation accrue des trois branches de l'UPRER, l'induction de l'apoptose UPRER-dépendante et une potentielle dérégulation des mécanismes de réparation de l'ADN chez les mutants PRKN. De plus, nous avons identifié des lncRNAs potentiellement régulés par PARKIN et impliqués dans les voies de signalisation du développement neuronal ou de la voie mTOR. Des expériences fonctionnelles supplémentaires seront nécessaires pour évaluer leur participation aux altérations de la différenciation et de la réponse au stress résultant de la perte de PARKIN. Notre travail a ainsi amélioré notre compréhension de la réponse spécifique des neurones DA humains au dysfonctionnement mitochondrial dans le contexte de la MP,

présentant également des informations précieuses sur le rôle potentiel des lncRNAs dans les mécanismes liés au stress et à la maladie.

IX. Summary

Mitochondrial dysfunction is known to play a central role in the pathophysiology of Parkinson's disease. Dopaminergic (DA) neurons of the *substantia nigra pars compacta* appear particularly vulnerable to mitochondrial stress, leading to their massive degeneration and the occurrence of motor symptoms. The molecular mechanisms underlying this selective susceptibility of human DA neurons remain poorly understood. Furthermore, the search for molecular elements intrinsic to DA neurons has been largely focused on protein-coding genes as of yet. However, there is growing interest in the study of non-coding elements of the genome such as long non-coding RNAs (lncRNAs), potent genomic regulator that display high cell type-and context-specificity. This work centered on the study of the mitochondrial stress response of human DA neurons and the potential contribution of lncRNAs to this response.

We first used LUHMES-derived DA neurons to elucidate the specific response of human DA neurons to mitochondrial stress. We demonstrated that inhibiting the mitochondrial electron transport chain led to a significant disruption of mitochondrial homeostasis, resulting in mitochondrial loss. This is supported by a robust induction of mitophagy and a reduction in mitochondrial biogenesis. In addition to these mitochondrial impairments, we observed a stress-induced decline in the maturation status of the DA population and an elevated proportion of apoptotic cells, indicating cellular damage beyond the mitochondrial network. PERK-dependent Unfolded Protein Response of the Endoplasmic Reticulum (UPR^{ER}), emerged as a central coordinator of the stress response. It appeared to modulate the inactivation of the mitochondrial UPR (UPR^{mt}) and the cell-specific expression of lncRNAs. The identification of novel lncRNAs, specifically expressed in human DA neurons upon stress, strongly suggests their involvement in the intrinsic molecular mechanisms underlying the DA stress response. We highlight the discovery of a stress-specific lncRNA, lnc-SLC6A15-5, which regulated translation resumption after mitochondrial stress potentially through modulating the expression of ATF4 target genes involved in the mTOR signaling regulation.

In a second part, we wished to assess whether this mitochondrial stress response was altered in a PD context, in particular linked to *PRKN* mutations. For this, we collected transcriptomic data from induced pluripotent stem cells (iPSC)-derived cells from PD patients carrying *PRKN* mutations and age-matched healthy individuals. Our results suggest that PARKIN deficiency altered cells' differentiation status, displaying a potential delay in maturity and increase in glial population. The *PRKN*-mutant cells also appeared "pre-stressed" in basal conditions, as they exhibited activation of effectors of the ATF6- and IRE1-UPR^{ER}, as well as the NRF2-dependent antioxidant response. Incubation with mitochondrial toxins expectedly exacerbated these responses, with stronger activation of the three UPR^{ER} branches, downstream pro-apoptotic signaling and potential dysregulation of DNA repair mechanisms in *PRKN*-mutants. Furthermore, we uncovered lncRNAs possibly regulated by PARKIN and potentially involved in neuronal system signaling pathways or mTOR signaling. Further functional experiments will be required to assess whether they may participate to the alterations in differentiation and stress response resulting from PARKIN loss. Our work improved our understanding of the human DA neuron-specific response to mitochondrial dysfunction in the context of PD. We also report valuable information on the potential role of lncRNAs in stress- and disease-associated processes.